SISSA, Via Bonomea 265, 34136, Trieste, Italy

Doctorate in Theoretical Particle Physics

Presented by

Marina Moleti

String Theory on Non-Toric Singularities: D-brane Probes, Quivers, and Five-Dimensional SCFTs

Supervised by Roberto Valandro

Publicly defended on May 11th, 2026

Acknowledgements

"So long, and thanks for all the fish."

I would like to thank my supervisor, the academic staff, and all collaborators involved in this work for their support, guidance, and contribution throughout the development of this thesis.

Most of what I have learned and achieved throughout these years, I owe to them. They helped me grow professionally and taught me what it truly means to do research. Beyond the physics I had the privilege to discover thanks to them, I am especially grateful for the hours we spent together in pursuit of understanding.

I always fail when I try to express in words the ecstatic joy and wide-eyed wonder that take hold of me whenever I am gifted an epiphany of clarity.

The academic environment has allowed this side of me to burst forth and thrive, and I will never cease to be grateful for that.

When I started my PhD, I was strongly convinced that it would be only the beginning of a very long journey toward self-realization; a first clumsy step toward intellectual independence. I came to Trieste carrying a stifling sense of incompleteness and the dread of not being worthy of my dream. And then, I met the people who are now my pride and my strength: the friends I will always carry in my heart, and to whom I owe the best years of my youth.

Alfredo, you were the first person I saw on that awkward first day of school. Looking at you has never ceased to soothe me and make me feel at home, just as it did that very first time. I am deeply grateful to have you in my life, and not only because you have been the most effective Cupid. You are a person of extraordinary intelligence, kindness, and vitality. To me, you are and always will be the boss of the TPPs.

Shre, I cannot find a better way to say this: you are like a brother to me. I have always felt a blissful connection with you, a sentiment so deep and effortless that it seems to transcend time and consequence. You possess the purest, most disarming sensitivity I could imagine in a human being. You are one of those rare people who naturally express beauty through both their countenance and their personality.

Benni, when I think of you, the first thing that comes to my mind is a kaleidoscope. Your personality is a maze of colour and form: overwhelmingly complex and alive, always burning and simmering with creativity. What I miss most are our passionate, stupendously articulate, and implacably studious conversations. I have always felt that we shared a kind of luxurious proclivity for details and their meaning.

Giulio, time has never been our friend, and yet you have always been present in my life, since the day we met. You were the first person I felt seen by. Your genuine curiosity and stark directness tore through the layers of insecurity and self-deprivation in which I was suffocating. I cherish those moments of mutual, uncontaminated scrutiny.

Lodo, words feel poor knowing that we share a far more powerful language: music. Music is the channel that reaches deepest into my being, my greatest companion, and my obsession. Of all the people I have tormented with this passion, you are the one who has always responded to it and resonated with me in a way that transcends rationality and verbal expression.

Neurofra, with your peaceful and grounded attitude, you awakened the rebellious, spoiled baby warrior inhabiting my spirit, who conceives his dictatorship only as a path toward cosmic equilibrium. I will deeply miss our incessant, pointless, and garrulous arguments.

Anant, you have become a vital source of support and equilibrium in my life, and I will never stop being grateful for all the care you put into our friendship. Your commitment to the people you love is almost superhuman in its constancy and spontaneity, and your infallibly hilarious jokes never fail to cheer me up.

Amartya, no one has ever left me as amazed and enthralled as you did with the stories from your shockingly adventurous past. Talking to you has always been the most pleasant discovery.

Baso, I wish I could say this while looking at you. No matter what will be, I will never forget what we have shared throughout these years. You have brought so much happiness, euphoria, and energy into my life. You have a piece of my heart.

Mich, knowing you has been magical and overwhelming. I am deeply grateful for the time we shared. Whenever I wish to feel at peace, I follow the erratic silvery ripples we observed upon the sentient vastness of the Croatian sea.

To all those who shared fragments of their lives with me throughout these years, and who together gave life to the most formidable group — Kendall, Astrofra, Cecilia, Clemente, Mina, Cristiano, Anna, Freya, Alessandro, Claudia, Alessio, Fra Gentile, Paso, Vincenzo, and Mavi — my deepest thanks.

And now it comes to you, Albe. How do I thank the person to whom I owe my life? These three years have seen us change, grow, and gradually mold into a single being, one that you have never failed to nurture and sustain. We have both given so much to it, and received just as much in return. But this is not what I value most in our relationship. What I value most is that we never lost each other within it. You have never failed to understand my contradictions, and you never stopped believing in me. I owe you the person I am today.

My final and deepest thanks go to my family: Mom, Dad, Francesco, Federico, Zia Luisa, Zia Marina, Nonna Titina, Aglaja, Georgina, and our lord and saviour, Keiko.

Abstract

This thesis investigates the interplay between geometry and supersymmetric quantum field theory, intending to develop a systematic framework for constructing and analyzing field theories associated with non-toric singular geometries. A central role is played by quiver gauge theories, which provide a bridge between geometric data and field-theoretic structures, both in the context of probe brane dynamics and in geometrically engineered theories.

The first approach developed in this work examines D2-branes probing twofold and threefold geometries characterized by a background adjoint scalar field Φ. This field couples to the probe via superpotential deformations of the worldvolume theory, providing a framework for the systematic derivation of three-dimensional $\mathcal{N} = 2$ quiver gauge theories associated with compound Du Val (cDV) singularities—a class of non-toric geometries that arise naturally in the Higgs field construction.

The second approach that we apply to these geometries is studying the five-dimensional superconformal field theories arising from M-theory reduced on these geometries. In particular, new infinite families of SCFTs are constructed from abelian orbifolds of the Reid Pagoda singularity. These constructions give rise to theories of arbitrary rank, including an infinite class of rank-one theories that can be understood as non-toric deformations of local $\mathbb{F}_2$. A distinctive feature of these models is the presence of an additional matter sector, referred to as Pagoda matter, whose vacuum expectation values obstruct the resolution of the underlying geometry. This obstruction is shown to correspond, from the field-theoretic perspective, to a mechanism termed the freezing of the gauge coupling: the Kähler modulus controlling the inverse gauge coupling is dynamically forced to vanish, preventing access to a weakly-coupled regime and rendering the theory intrinsically strongly coupled. The origin of this phenomenon is traced to the interplay between Higgs field backgrounds and dynamical geometric deformations.

More broadly, the results of this thesis suggest that non-toric geometries support a richer structure of quantum field theories than previously understood, and that additional geometric data, not captured by the naive local description, may play a role in determining the physical content of the theory.

Contents

Introduction

In the past three decades, string theory has provided a natural and mathematically controlled framework for defining and investigating quantum field theories. A decisive development in this direction was the introduction of D-branes by Polchinski [1], which opened the way to the realization of a vast landscape of supersymmetric quantum field theories (QFTs), including many that do not admit a conventional Lagrangian description. The success of this framework lies in the interplay between geometry and field theory: when quantum field theories are embedded in string theory, their properties are tightly constrained by the underlying geometric structure. In this context, D-branes—viewed as submanifolds of the target space supporting their own worldvolume dynamics—provide a natural bridge between geometric data and field-theoretic observables.

A particularly fruitful setting arises when D-branes probe singular Calabi–Yau geometries. In such configurations, the low-energy dynamics on the brane worldvolume are governed by supersymmetric gauge theories whose structure is encoded by the geometry of the singularity. A seminal example is provided by the work of Douglas and Moore [2], where D-branes probing ALE spaces give rise to quiver gauge theories. These constructions reveal that singularities are loci where the dynamics of the worldvolume theory become especially rich, leading to enhanced symmetries and novel degrees of freedom.

Quivers naturally emerge in this context as combinatorial structures encoding the gauge group and matter content of the theory. However, their significance goes well beyond this initial interpretation. In an appropriate regime, D-branes can be described as objects in the derived category of coherent sheaves supported on compact cycles of the Calabi–Yau geometry. From this perspective, there exists an equivalence between such sheaves and finite-dimensional modules over the path algebra of the associated quiver. As a result, quivers provide an algebraic encoding of the geometry itself. From a physical viewpoint, this correspondence is reflected in the spectrum of BPS states of the geometrically engineered theory: stable sheaves correspond to BPS configurations, and their classification is mapped to the study of stable representations of the quiver algebra.

Complementary insights arise from brane engineering constructions. In the Hanany–Witten setup [3], supersymmetric gauge theories are realized using configurations of branes, where gauge and matter content can be directly read off from the brane arrangement. These methods have proven particularly effective in the study of D-branes probing toric Calabi–Yau threefold singularities, where brane configurations provide a systematic way to extract the associated quiver data

even in geometries of considerable complexity.

These ideas admit a particularly powerful realization in the framework of brane tilings, or dimer models, which provide a unified description of quiver gauge theories associated with toric Calabi–Yau threefolds [4–11]. In this approach, the gauge theory data are encoded in a bipartite graph on a two-dimensional torus, from which both the quiver and the superpotential can be systematically derived. Brane tilings thus offer a complementary perspective to both direct brane probing and geometric engineering, making explicit the relation between field-theoretic data and the underlying toric geometry.

A key feature underlying the effectiveness of these constructions is the toric nature of the geometry, which guarantees the existence of dual descriptions in terms of brane tilings and (p, q) five-brane webs. These provide powerful combinatorial tools to extract the associated gauge theories. Although various extensions of this framework allow one to move partially beyond the toric setting [12–22], no general construction is currently known that applies to arbitrary non-toric Calabi–Yau singularities. Importantly, however, the absence of a brane realization does not imply the absence of an associated quiver description. Quivers arise from intrinsic geometric and algebraic structures and therefore persist even when a direct brane-engineering picture is not available.

Toric geometries thus provide a fundamental testing ground for field theory–geometry correspondences, enabling the derivation of highly nontrivial and often exact results. At the same time, the class of geometries of physical interest extends far beyond the toric regime. A prominent example is given by five-dimensional superconformal field theories engineered from canonical singularities, many of which are non-toric. In these cases, the lack of a combinatorial framework significantly limits our ability to extract detailed information about the corresponding field theories. Developing systematic tools to study such theories—particularly to determine their BPS spectra and associated quiver structures—therefore constitutes an important open problem. A remarkable step in this direction was recently made with the formulation of a generalised version of toric polygons (GTP), in which a specific class of non-toric deformations of the CY geometry is incorporated in 5-brane webs with 7-branes [13–15].

Among canonical Calabi–Yau singularities, compound du Val (cDV) singularities form a particularly important and tractable subclass [23]. The most well-known example is the Conifold singularity. Contrary to the Conifold, most of them are non-toric. However, they retain enough structure to allow for explicit analysis. Moreover, cDV singularities arise naturally in partial

crepant resolutions of canonical singularities, and thus play a central role in the geometric transitions underlying many constructions in string theory. For these reasons, they offer an ideal setting in which to investigate the extension of field theory–geometry correspondences beyond the toric regime.

The primary goal of this thesis is to develop a systematic framework to derive the quiver associated with cDV singularities. To this end, we exploit their interpretation as fibrations of ADE surface singularities over a complex curve. This allows us to build on the well-understood case of D-branes probing ADE singularities, where the corresponding quiver gauge theories are known. A key ingredient in our construction is an M-theory (Type IIA) realization of such fibrations, in which nontrivial geometry is engineered by turning on position-dependent Higgs field vevs in a seven(six)-dimensional gauge theory associated with the ADE singularity[19, 24–27]. These Higgs fields parametrize complex deformations of the surface geometry, and their dependence on a complex coordinate encodes the nontrivial fibration structure of the cDV threefold.

We probe these backgrounds with a $D2$-brane. The three-dimensional worldvolume theory flows in the infrared to a supersymmetric gauge theory whose moduli space reproduces the geometry of the singularity. This provides a direct and physically motivated procedure to determine the associated quiver and its path algebra. The three-dimensional probe theories that arise in this construction belong to the class of 3d $\mathcal{N} = 2$ and $\mathcal{N} = 4$ supersymmetric gauge theories, whose infrared dynamics have been the subject of extensive study over the past two decades. A central tool in this context is three-dimensional mirror symmetry [3, 28, 29], an infrared duality that exchanges Higgs and Coulomb branches of the moduli space and maps classical data of one theory to quantum-corrected data of its dual. More recently, the systematic understanding of monopole operators—local disorder operators carrying topological charge [30, 31]—has led to powerful techniques for computing Coulomb branches as algebraic varieties [32–34] and for analyzing the effects of monopole superpotentials on the vacuum structure of 3d theories [31, 35].

In this thesis, these field-theoretic tools are employed in a novel way: rather than studying 3d theories as objects of interest in their own right, we use them as probes of higher-dimensional geometry. The key observation is that Higgs field backgrounds, which engineer non-trivial ADE fibrations in M-theory, induce monopole superpotential deformations on the worldvolume theory of the $D2$-brane probe. The presence of such terms breaks the enhanced $\mathcal{N} = 4$ supersymmetry to $\mathcal{N} = 2$ and triggers a non-trivial RG flow. Tracking this flow—by combining mirror symmetry, integrating out massive fields, and matching monopole and meson operators across dualities—allows us to reconstruct the effective infrared theory and to extract the geometry of the

probed singularity from the moduli space of the resulting quiver.

This approach builds on a well-established tradition of employing 3d dualities and brane dynamics to extract geometric information [3, 28, 29, 36, 37]. The contribution of this work is to develop it into a systematic method that applies to geometries beyond the reach of toric techniques. In particular, the monopole superpotentials that arise in our construction are not introduced as abstract deformations: their structure is entirely dictated by the Lie-algebraic data of the ADE fibration, and the resulting RG flow can be tracked explicitly using mirror symmetry. This provides, as a byproduct, new families of 3d $\mathcal{N} = 2$ theories with monopole superpotentials whose moduli spaces are exactly computable and admit a direct geometric interpretation as compound Du Val singularities.

A notable outcome of this construction is that the quivers obtained from the probe analysis suggest a richer structure for the five-dimensional theories engineered on cDV singularities. Focusing on the class of Reid's Pagoda singularities, we find that the departure from toricity is encoded in specific superpotential terms, which render the moduli space of quiver representations non-reduced. From the perspective of the five-dimensional theory, these representations are expected to correspond to hypermultiplet states; however, this identification appears to be incomplete, as the standard notion of quantization does not readily extend to non-reduced schemes.

These results acquire particular significance when viewed in the context of the classification of 5d SCFTs via M-theory compactifications on singular Calabi–Yau threefolds [22, 38–52]. A guiding principle in this program is that the local geometry of the singularity should be sufficient to determine the interacting fixed point. This expectation is well supported in the toric regime, where the technology of (p, q) brane webs provides a systematic and combinatorially controlled framework.

The cDV singularities studied in this thesis offer a concrete testing ground for this expectation beyond the toric class. In particular, by considering abelian orbifolds of the Reid Pagoda geometry, we construct infinite families of 5d SCFTs of arbitrary rank, whose BPS quivers and superpotentials we determine explicitly. In the rank-one case, the resulting theories closely resemble those associated with the local Hirzebruch surface $\mathbb{F}_2$, a well-studied toric geometry. However, the non-toric deformation inherited from the Pagoda parent introduces an additional matter sector—which we call Pagoda matter—that has no counterpart in the toric model.

The vacuum expectation values of this matter sector obstruct the small resolution of the exceptional curve, dynamically forcing the Kähler modulus controlling the inverse gauge coupling

to vanish. We refer to this phenomenon as the freezing of the gauge coupling. Its physical consequence is that the five-dimensional theory cannot be deformed to a weakly coupled gauge theory regime: it is intrinsically strongly coupled, in a manner that is qualitatively distinct from the familiar toric examples.

From a conceptual standpoint, this mechanism points to a tension with the locality assumption underlying current classification schemes. The Pagoda and the conifold share the same local geometry near the exceptional curve, yet they give rise to physically distinct five-dimensional theories. The difference is traced to an obstruction in the global structure of the normal bundle, which is invisible to the standard local analysis but has direct consequences for the spectrum and dynamics of the theory. This observation suggests that the geometric data required to fully characterize a 5d SCFT may be richer than what is captured by the local singularity type alone, and that non-toric geometries may harbour physical phenomena not accessible within the current classification paradigm.

Content organization

This thesis is organized into two main parts. The first part develops the physical and mathematical framework underlying the correspondence between geometry and quantum field theory. The second part contains the original results of this work, where this framework is applied to the study of non-toric Calabi-Yau singularities, in particular compound Du Val (cDV) threefolds.

Chapter 1. The chapter is devoted to establishing the physical background. We begin by reviewing string compactifications and geometric engineering, emphasizing how gauge theories arise from singular Calabi-Yau spaces. In 1.2 we then analyze M-theory compactifications on ALE spaces, where the correspondence between geometry and gauge theory can be made fully explicit. In 2 follows a discussion on $D3$ and $D2$-branes probing ALE surfaces and the description of their worldvolume dynamics in terms of quiver gauge theories. Particular attention is given to the role of Higgs field backgrounds and T-branes, which provide a mechanism for constructing non-trivially fibered geometries and play a central role in the extension beyond the toric setting. Section 3.1 reviews general features of M-theory geometric engineering on Calabi-Yau threefolds, with focus on the classification of BPS states and moduli spaces of Kähler and complex structure deformations. Section 3.2 is a brief review of BPS spectra of geometrically engineered 5d SCFTs and the technology of BPS quivers.

Chapter 4. This chapter develops the mathematical tools used throughout the thesis. We introduce the language of algebraic varieties and singularities, together with the basic operations of resolution and deformation. We then focus on ADE surface singularities and their rich structure, including their resolutions, root lattice description, and semiuniversal deformations, in 4.2. Building on this framework, we introduce compound Du Val singularities as higher-dimensional generalizations and place them within the classification of threefold singularities (Sections 4.2.4 and 4.3). Finally, in 4.3.1, we review simple flops, their classification, and their algebraic description in terms of quivers and universal flopping algebras. This material provides the geometric backbone for the constructions developed in the subsequent chapters.

Chapter 5. We develop a D2-brane probe description of families of deformed ADE surface singularities and their relation to universal flops. In particular, we show how universal flops of increasing length can be realized and studied using probe branes, and we analyze the role of the Higgs field in generating the corresponding deformations. This provides a first bridge between the

geometric/M-theoretic constructions reviewed in the introduction and three-dimensional gauge dynamics.

Chapter 6. We extend this framework to the study of D2-branes probing non-toric Calabi-Yau threefold singularities. After comparing D3- and D2-brane probes, we analyze three-dimensional $\mathcal{N} = 2$ gauge theories and the role of monopole superpotentials. We then apply these tools to cDV singularities, both in monodromic and non-monodromic cases, and derive the corresponding probe theories. Particular attention is given to Reid's Pagoda geometries and to examples of length 2 flops and non-resolvable D-type singularities.

Chapter 7. We discuss geometric engineering on a specific example of a simple flop, that is, the Reid Pagoda. We present its noncommutative resolution in the form of a quiver path algebra and recover the singular geometry from the moduli space of a $D0$-brane representation. From the analysis of the semistable quiver representations, we identify the presence of nonreduced moduli spaces and discuss their implications for the interpretation of BPS states in the associated five-dimensional theories. In order to include gauge interactions in the 5d theory, we consider abelian orbifolds of Pagoda geometries. The construction leads to an infinite class of new non-toric BPS quivers. In this context, we uncover a novel phenomenon, which we refer to as the *freezing of the gauge coupling*. We discuss its physical significance and identify a possible origin by exploiting the knowledge acquired with the $D2$-probe analysis of chapters 5 and 6.

Conclusions. We end with a summary of the main results and a discussion of possible directions for future research.

Appendices. In A.1, we summarize the main features of supersymmetry with 8 real supercharges in dimensions 3, 4, and 5. In A.2, we integrate the discussion on the classification of canonical singularity with a review of the Minimal Model Program in the sense of Reid [53] and in its modern formulation. In B, we develop in more detail some of the computations of Chapter 5. In C we provide a practical definition of Levi subalgebras of Lie algebras. In D we discuss the representation theory of quiver path algebra following [54] and [55]. We present two examples: the 2-Kronecker quiver and the Pagoda quiver.

Original contributions This thesis is based on original research results obtained by the author and presented in three works, one published, one currently under review and available on `arXiv`,

and one completed and ready for submission. The material has been organized and adapted to form a coherent narrative. The introductory chapters provide the necessary information to contextualise our work and produce a self-contained analysis.

Chapter 5 is extensively based on the work *"Universal flops of length 1 and 2 from D2-branes at surface singularities"* [56], where the physical interpretation of universal flops in terms of probe D2-brane dynamics is developed, together with the identification of the corresponding quiver gauge theories and their moduli spaces.

Chapter 6 is based on the project *"D2-brane probes of non-toric cDV threefolds via monopole superpotentials"*, which has been completed and is currently being prepared for submission [57]. In this work, a systematic framework is developed for deriving three-dimensional $\mathcal{N} = 2$ quiver gauge theories associated with compound Du Val singularities, including both monodromic and non-monodromic configurations.

Chapter 7 is based on the work *"Non-toric 5d SCFTs from Reid's Pagoda"*, currently under review and available on `arXiv` at [58]. In this work, new classes of five-dimensional superconformal field theories are constructed from orbifolds of the non-toric singularity known as Reid Pagoda, and novel physical phenomena are identified.

The results presented in this thesis are, to the best of the author's knowledge, original, unless otherwise stated.

Part I

QFT engineering in String Theory

Chapter 1

From String Compactifications to Geometric Engineering

The development of string theory as a candidate framework for a unified description of gravitational and gauge interactions can be broadly divided into two phases. The first phase, which took place during the early development of superstring theory, was characterized by the emergence of five apparently distinct consistent theories in ten spacetime dimensions: Type I, Type IIA, Type IIB, and the two heterotic theories with gauge groups $E_8 \times E_8$ and $SO(32)$. A crucial milestone in establishing their consistency was the demonstration of anomaly cancellation in ten dimensions by Green and Schwarz, who showed that gauge and gravitational anomalies cancel in certain supersymmetric ten-dimensional theories through what is now known as the Green–Schwarz mechanism [59].

All five theories are superstring theories, meaning that supersymmetry relates bosonic and fermionic degrees of freedom in the string spectrum. In the present work we will primarily focus on the theories with maximal supersymmetry in ten dimensions, namely Type IIA and Type IIB string theory, both of which possess 32 supercharges.

Since their discovery, considerable effort has been devoted to identifying whether one of these theories could provide a consistent ultraviolet completion of the Standard Model. A central challenge arises from the mismatch between the ten-dimensional nature of string theory and the observed four-dimensional structure of spacetime. This motivates the introduction of the mechanism known as *compactification*.

The basic idea of compactification is to consider one of the consistent ten-dimensional string theories on a background of the form

$$\mathbb{R}^{1,d-1} \times \mathcal{M}, \tag{1.1}$$

where $\mathbb{R}^{1,d-1}$ describes a non–compact d–dimensional spacetime and $\mathcal{M}$ is a compact internal manifold of dimension $10 - d$. In the limit in which the characteristic length scale of the compact space becomes much smaller than the scales accessible to low-energy observers, the theory becomes effectively d–dimensional.

The geometry of the internal manifold $\mathcal{M}$ plays a crucial role in determining the structure of the resulting effective quantum field theory. In particular, it controls properties such as the particle spectrum, gauge symmetries, moduli fields, and the structure of the vacuum. Conversely, phenomenological requirements and internal consistency conditions of the low-energy quantum field theory impose strong constraints on the admissible geometries for $\mathcal{M}$.

One of the most important ingredients for maintaining theoretical control over the resulting quantum field theory is supersymmetry. In particular, it is often desirable that the compactification preserves at least a portion of the supersymmetry of the original ten-dimensional theory. This requirement is closely related to the structure of the theory's vacuum. A vacuum configuration preserves supersymmetry if the supersymmetry variation of all fermionic fields vanishes when evaluated on the background.

In supergravity, which describes the low-energy limit of string theory, the relevant condition arises from the supersymmetry variation of the gravitino. For vanishing background fermionic fields, this variation takes schematically the form

$$\delta\psi_M = \nabla_M \epsilon + \ldots, \tag{1.2}$$

where ψ_M is the gravitino and ϵ is the parameter of the supersymmetry transformation. Preserving supersymmetry in a given background, therefore requires the existence of a spinor field ϵ satisfying

$$\nabla_M \epsilon = 0. \tag{1.3}$$

When the spacetime geometry is assumed to factorize as $\mathbb{R}^{1,d-1} \times \mathcal{M}$, the supersymmetry parameter decomposes accordingly, and the condition above implies that the internal manifold

$\mathcal{M}$ must admit a covariantly constant spinor. The existence of such spinors imposes strong constraints on the geometry of $\mathcal{M}$. In particular, the integrability condition of the Killing spinor equation implies that the manifold must be Ricci–flat [60]. Moreover, for a simply connected $2n$–dimensional Riemannian manifold, covariantly constant spinors exist if and only if the holonomy group is a subgroup of $U(n)$. Manifolds satisfying such conditions belong to the class of special holonomy manifolds classified by Berger. In particular, those manifolds whose holonomy lies in $SU(n)$ are known as Calabi-Yau. In this thesis, we will be mostly concerned with Calabi-Yau manifolds of complex dimension 2, the so-called K3 manifolds, and 3, namely Calabi-Yau threefolds (CY3).

A second major phase in the development of string theory, often referred to as the *second superstring revolution*, began in the mid–1990s and was largely triggered by the work of Polchinski. In a seminal paper, Polchinski showed that the solitonic objects that had previously appeared as classical solutions of supergravity, known as p–branes, admit a natural interpretation within perturbative string theory as hypersurfaces on which open strings can end with Dirichlet boundary conditions [1, 61]. These objects are now known as D_p–branes, where p denotes the number of spatial dimensions of the brane.

This insight had far-reaching consequences. In particular, it led to the realization that many string theory vacua can be described in terms of stable configurations of D-branes embedded in the ten-dimensional spacetime. Open strings whose endpoints lie on a stack of D–branes give rise to massless excitations that propagate along the $(p+1)$–dimensional worldvolume of the branes. These modes organize themselves into the fields of a quantum field theory localized on the brane worldvolume.

As in the case of traditional string compactifications, the properties of the resulting quantum field theories are deeply influenced by the geometry of the underlying string background. In particular, gauge groups, coupling constants, vacuum moduli, and global symmetries can often be inferred from the type of D–branes present and from the way they are arranged in the ten–dimensional spacetime.[1]

At the same time, the discovery of a network of strong–weak coupling dualities revealed that the five superstring theories are related and should be viewed as different limits of a single non-perturbative framework, commonly referred to as M-theory [62].

[1] In appropriate limits, D–branes admit a purely geometric description. In particular, in Calabi-Yau compactifications, they can be interpreted mathematically as stable objects in the derived category of coherent sheaves.

A striking consequence of these developments was the realization that branes wrapped on special cycles of a Calabi-Yau manifold behave as particle states in the non-compact spacetime directions. These states carry gauge charges and can become massless at special loci in the moduli space of the Calabi-Yau geometry, leading to an enhancement of the gauge symmetry.

The first clear indication of this phenomenon appeared in [62, 63]. In the context of the conjectured duality between heterotic compactified on T^4 and Type IIA on a K3 surface, consistency of the dual description requires the appearance of enhanced non-abelian gauge symmetries at special points in the moduli space. On the Type IIA side, these enhanced symmetries arise when the K3 surface develops ADE singularities. At such loci, D2–branes wrapping vanishing two–cycles of the singular geometry become massless and behave as charged particle states in the remaining spacetime dimensions, giving rise to the corresponding non-abelian gauge bosons.

This idea was subsequently generalized by Vafa and collaborators [64], who showed that similar mechanisms can be used to engineer supersymmetric gauge theories from Type IIA string theory on Calabi–Yau threefolds. In particular, the first constructions involved Calabi-Yau threefolds that are K3 fibrations over a compact curve of genus g. At singular loci of the threefold, configurations of vanishing cycles in the K3 fiber reproduce the structure of ADE Lie algebras, and wrapped D-branes behave as massless representations of $\mathcal{N} = 2$ supersymmetry. This program, now known as *geometric engineering*, provides a powerful framework in which properties of quantum field theories can be extracted from the geometry of the underlying string compactification.

A crucial observation underlying geometric engineering is that the physics of the light states is entirely determined by the local geometry near the singularity. This becomes precise in a decoupling limit in which gravity is removed while the singular structure is kept fixed. Indeed, upon compactification of Type IIA string theory on a Calabi–Yau threefold X, the four–dimensional Einstein–Hilbert term takes the form

$$S_4 \sim M_{\mathrm{Pl},4}^2 \int d^4x \, \sqrt{-g}\, \mathcal{R}^{(4)}, \qquad M_{\mathrm{Pl},4}^2 \sim \frac{Vol(X)}{\ell_s^8 g_s^2}. \tag{1.4}$$

Hence, by taking the limit $Vol(X) \to \infty$ while keeping fixed the local data of the singularity, one obtains $M_{\mathrm{Pl},4} \to \infty$, so that gravitational interactions decouple. The resulting theory is therefore a pure quantum field theory for the localized modes associated with the singular locus. This justifies replacing the compact Calabi–Yau by a non-compact local model capturing only the neighbourhood of the singularity.

1.1 M-theory/Type IIA duality

Shortly before the development of geometric engineering, an important insight concerning the non-perturbative structure of string theory was obtained. It was discovered that the strong coupling limit of $10d$ Type IIA string theory is $11d$ supergravity [62]. Eleven-dimensional supergravity is also the low-energy limit of M-theory, whose microscopic nature is unknown. In this paragraph, we briefly review the duality between M-theory and Type IIA string theory. This discussion will serve as a starting point for the study of M-theory compactifications and will emphasize the relation between brane configurations and geometry.

The bosonic field content of 11d supergravity consists of the metric G_{MN} and a three-form gauge potential C_3 with field strength $G_4 = dC_3$. The corresponding action takes the schematic form

$$S_{11} \sim \frac{1}{\ell_p^9} \int d^{11}x \sqrt{-G}\, R - \frac{1}{2} \int G_4 \wedge \star G_4 - \frac{1}{6} \int C_3 \wedge G_4 \wedge G_4. \tag{1.5}$$

The relation between M-theory and Type IIA string theory becomes manifest when the former is compactified on a circle [65]. Let x^{11} denote the coordinate along the circle S^1 of radius R_{11}. The 11d metric can then be written in Kaluza–Klein form as

$$ds_{11}^2 = e^{-2\phi/3} ds_{10,\text{str}}^2 + \alpha' e^{4\phi/3} \left(dx^{11} + C_\mu dx^\mu\right)^2, \tag{1.6}$$

where $ds_{10}^2 = g_{\mu\nu}^{(10)} dx^\mu dx^\nu$ is the ten–dimensional string–frame metric, ϕ is the dilaton, and C_μ is a one–form gauge field that corresponds to the connection of the S^1 bundle.

Under this dimensional reduction, the massless Kaluza–Klein modes of eleven-dimensional supergravity reproduce the bosonic spectrum of Type IIA supergravity. In particular, the fields $g_{\mu\nu}^{(10)}$, ϕ, and the Ramond–Ramond one–form $C_1 = C_\mu dx^\mu$ arise from the components of the eleven–dimensional metric, while the eleven–dimensional three–form decomposes as

$$C_3^{(11)} = C_3 + B_2 \wedge dx^{11}, \tag{1.7}$$

giving rise to the Ramond–Ramond three–form C_3 and the Neveu–Schwarz two–form B_2. The resulting massless bosonic fields

$$g_{\mu\nu}, \qquad \phi, \qquad B_2, \qquad C_1, \qquad C_3 \tag{1.8}$$

coincide precisely with the bosonic spectrum of Type IIA supergravity.

The asymptotic value of the dilaton determines the Type IIA string coupling,

$$g_s = e^{2\phi_\infty/3}, \tag{1.9}$$

and is related to the radius of the M-theory circle by

$$R_{11} = g_s \ell_s. \tag{1.10}$$

Thus, the weak coupling limit of Type IIA corresponds to a small M-theory circle, while in the strong coupling regime, the eleventh dimension becomes large. An important observation is that a solution of the equations of motion for $g^{(10)}_{\mu\nu}$, ϕ, and C_1 uplifts to pure geometry in 11d.

1.1.1 $D6$-branes and the Taub-NUT solution

Among the possible solutions of Type IIA SUGRA, we find $D6$-branes, which are sources for the three fields $g^{(10)}_{\mu\nu}$, ϕ. The uplift of n parallel $D6$-branes in 11d SUGRA is a geometric background of the form:

$$ds^2_{11} = ds^2_7 + V d\vec{x}^2 + \alpha' V^{-1} \left(dx^{11} + w_j dx^j\right)^2, \tag{1.11}$$

with:

$$V = 1 + \sum_{i=1}^{n} \frac{R_{11}}{|\vec{x} - \vec{x}_i|}, \qquad \nabla \times \vec{w} = -\nabla V \tag{1.12}$$

The $10d$ metric splits into a $7d$ Minkowski component and $\mathbb{R}^3$, the latter parametrized by (x_1, x_2, x_3). The M-theory circle is non-trivially fibered over the $\mathbb{R}^3$ component. The four-dimensional space with this fibration structure is known as the Taub-NUT manifold[2]. The space is smooth, and the metric is endowed with a hyperKahler structure (See Section 4.2). The metric has three associated Kahler forms, which are the w_j. The $\vec{x}_i$ are points at which the S^1 fiber degenerates (said centers of the Taub-NUT). These points are identified with the positions of the $D6$ branes in the transverse space. When two or more $D6$-branes come together, or equivalently, when some of the centers of the Taub-NUT collide, the space develops a singularity. Suppose that we collide all of the n centers. Then, in the limit of $R_{11} \to \infty$, the metric becomes ALE (asymptotically locally euclidean)

[2]This is an example of ALF space.

and the singular space is isomorphic to the abelian orbifold $\mathbb{C}^2/\mathbb{Z}_n$.[3] This surface singularity is known as A_{n-1} and belongs to the famous ADE classification of the singular K3 degenerations. We review the topic in more detail in Section 4. The classification arises from a correspondence between the structure of the root spaces of simply-laced Lie algebras (the families A_n, D_n, and E_6, E_7, E_8) and the intersection theory of local K3 surfaces (local means non-compact here). To visualise this correspondence in the simple case of A_{n-1}[4], let us choose a complex structure on the Taub–NUT space such that

$$z = x_1 + ix_2, \qquad s = x_3 + ix_{11}. \tag{1.13}$$

Since $x_3 \in \mathbb{R}$ and $x_{11} \sim x_{11} + 2\pi R$, the pair (x_3, x_{11}) parametrizes a cylinder $\mathbb{R} \times S^1$, which is naturally identified with $\mathbb{C}^*$ by exponentiation:

$$t = e^{-s/R} = e^{-(x_3+ix_{11})/R}. \tag{1.14}$$

Thus, asymptotically, Taub–NUT is described as a $\mathbb{C}^*$ fibration over the complex z–plane. To take into account the degeneration of the S^1 fiber at the centers of the Taub-NUT, we need to refine the change of coordinates.

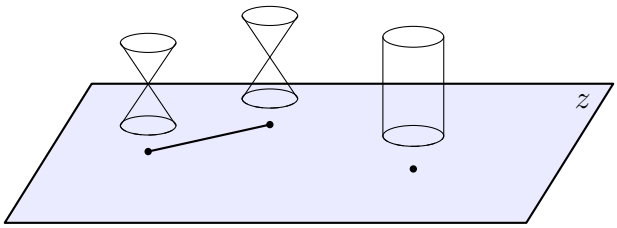

Figure 1.1: Multi-centered Taub-NUT, seen as a cylinder fibration over the z-plane. The degenerate fibers correspond to the centers of the Taub-NUT. The fibration of the S^1 in the fiber over the line connecting distinct centers defines a non-trivial 2-cycle.

Let us distinguish two cases:

[3] Note that in this limit a term ndx^{11} appears in the metric. This signals the presence of a $\mathbb{Z}_n$ quotient acting on the angular coordinate x^{11}. Asymptotically, the space looks like $S^3/\mathbb{Z}_n$.

[4] Here we limit ourselves to considering the simplest case. However, the discussion can be generalised to all ALE spaces [65, 66]

Deformation Suppose that the centers of the Taub-NUT are located at distinct points along the z plane, namely, $\vec{x}_i = (c_i^1, c_i^2, 0)$. Then, let us introduce the holomorphic coordinates:

$$y = e^{-(x_3+ix_{11})/R} \prod_{i=1}^{n} \sqrt{r_i - x_3}, \qquad x = e^{(x_3+ix_{11})/R} \prod_{i=1}^{n} \sqrt{r_i + x_3}, \tag{1.15}$$

Where

$$r_i = \sqrt{|z + t_i|^2 + x_3^2}, \qquad t_i = -(c_i^1 + ic_i^2). \tag{1.16}$$

In these variables, the space takes the algebraic form

$$xy = \prod_{i=1}^{n} (z + t_i). \tag{1.17}$$

For fixed z away from the degeneration points $-t_i$, the fiber is $\mathbb{C}^*$.[5]. When $z + t_i = 0$ for some i the $\mathbb{C}^*$ fiber degenerates to the union of two $\mathbb{C}$-planes, intersecting at $x = y = 0$.

As we said, the singularity is generated by the collision of two or more centers. In particular, when all t_i coincide, for simplicity let us consider the case $t_i = 0 \, \forall \, i$, one recovers the surface

$$xy = z^n, \tag{1.18}$$

which is one of the presentations of the A_{n-1} singularity. So, separating the centers amounts to smoothing out the singularity. So far, we have considered the separation of the centers along the base of the $\mathbb{C}^*$ fibration. This process is called deformation (See 4). For local K3 surfaces, this amounts to blowing up a set of S^2 spheres. Without loss of generality, we can impose:

$$|t_1| > |t_2| > ... > |t_n| \,, \qquad \sum_i t_i = 0. \tag{1.19}$$

Taking a path in the z–plane between two neighboring degeneration points t_i and t_{i+1} and fibering over it the $S^1 \subset \mathbb{C}^*$ that collapses at the endpoints, we get a two-sphere S_i.[6] As a result, we have $n - 1$ independent S^2 cycles, whose arrangement reproduces the Dynkin diagram of A_{n-1}. There is, in fact, a one-to-one correspondence between the S_i and the simple roots of the

[5] In the patch $x \neq 0$ we can solve the algebraic equation for y. Vice versa, when $y \neq 0$ we can solve for x. Both patches are copies of $\mathbb{C}^*$.

[6] The S^1 fibration along paths connecting any of the t_i is a two-sphere but it can be decomposed into a sum of generators of the second homology of the Taub-NUT.

A_{n-1} algebra. The parameters t_i, called complex structure deformations, parametrize the space of cohomology classes of holomorphic $(2,0)$ forms $\Omega^{2,0}$.[7] Differences $t_i - t_{i+1}$ correspond to the size (or holomorphic volume) of the S_i spheres. We will make this statement more precise in Section 2. For now, let us conclude by considering a different situation, that is, the resolution of the singularity.

Resolution Let the centers be localised at distinct points along x_3, $\vec{x}_i = (0,0,c_i^3)$. Now, the globally defined coordinates of the $\mathbb{C}^*$ fiber become:

$$y = e^{-(x_3+ix_{11})/R}\prod_{i=1}^{n}\sqrt{r_i-(x_3+\theta_i)}, \qquad x = e^{(x_3+ix_{11})/R}\prod_{i=1}^{n}\sqrt{r_i+(x_3+\theta_i)}, \tag{1.20}$$

Where

$$r_i = \sqrt{|z|^2+(x_3+\theta_i)^2}, \qquad \theta_i = -c_i^3. \tag{1.21}$$

The equation relating variables x, y, z is now

$$xy = z^n,$$

which is the singular equation defining A_{n-1}. The displacement along the x_3 direction does not affect the holomorphic structure of the singularity, but modifies what is called the Kähler structure 4. For simplicity, let us impose:

$$|\theta_1| > ... > |\theta_n|\,. \tag{1.22}$$

This time, the S^1 fibration over each line segment $[\theta_i, \theta_{i+1}] \in \mathbb{R}_{x_3}$ is a 2-cycle $\tilde{S}_i$, entirely contained in the $\mathbb{C}^*$ fiber over $z=0$. Again, the space is smooth and the $\tilde{S}_i$ intersect in the same way as the non-holomorphic spheres S_i, generated in the deformation. The volumes of the $\tilde{S}_i$ are the relative displacements $\theta_i - \theta_{i+1}$. The real parameters θ_i[8] parametrize the space of Kähler classes of the Taub-NUT, namely the cohomology classes of $(1,1)$ forms $\Omega^{1,1}$. This situation is a resolution of the singularity. In this case, the 2-cycles that are blown-up have zero holomorphic volume and non-trivial Kähler volume, so they correspond to a different choice of Kähler class. Before proceeding towards the description of the spectrum of the theory localised at the singularity, let us make

[7] The metric of the $\mathbb{C}*$ fibration induces a holomorphic $(2,0)$ form ω and a Kähler $(1,1)$ form ω_3.

[8] The number of independent parameters is $n-1$, the same as the rank of the Lie algebra, due to a relation $\sum_{a=1}^{n}\theta_a = 0$. If we displace all the centers by the same amount, the Kähler form remains unchanged. Only relative displacements matter.

one comment. We have presented deformations and resolutions as different types of smoothings. However, a very special property of K3 is being HyperKähler. This means that the compatible complex structures form a triplet of $SO(3)$. Our choice of complex structure has explicitly broken this symmetry. For example, we can change our choice so that the S_i are holomorphic with respect to the new complex structure (they sit in the $\mathbb{C}^*$ fiber) and the $\tilde{S}_i$ become non-holomorphic. In other words, we can always trade deformations for resolutions and vice versa.

1.2 M-theory on local $K3$ manifolds

In this section, we review the geometric engineering of M-theory on local $K3$ surfaces. We begin by describing the worldvolume QFT of the dual configuration of $D6$-branes in Type IIA, where the phenomenon of gauge symmetry enhancement is well understood. Our goal is to show that the physics of the $D6$-brane system is fully encoded in the geometry of its M-theory uplift.

1.2.1 The $D6$-brane worldvolume theory and its M-theory dual

We have just seen that, upon reduction on the M-theory circle, M-theory on the ALE space A_{n-1} is equivalent to Type IIA with a stack of parallel $D6$ branes. The branes are localised at the singularity, conventionally, the origin of $\mathbb{R}^3$ where the M-theory circle degenerates. The open string modes localised on the $D6$ brane stack give rise to a $7d$ QFT with 16 real supercharges.[9] The theory is pure gauge, and the spectrum contains a $U(n)$ vector multiplet.[10] The bosonic sector consists of:

$$A_\mu, \qquad \Phi, \qquad \varphi_3. \tag{1.23}$$

The index μ refers to the 7d Minkowski directions. The complex scalar Φ and the real one φ_3 are in the adjoint of $U(n)$. However, since the diagonal $U(1)$ eventually decouples from the spectrum, we will henceforth restrict our representation to the adjoint of $SU(n)$. The complex and real vevs of the scalars parametrize the positions of the $D6$-branes along the z-plane (base of the $\mathbb{C}^*$ fibration described before) and the x_3 direction (coordinate along the fiber). The configuration in

[9] $D6$ branes are $1/2$-BPS states from the point of view of the 10d string theory. A configuration of parallel D_p branes preserves half of the supersymmetry. Note that 16 real supercharges is the same number as in $\mathcal{N} = 4$ susy in 4d.

[10] The diagonal $U(1)$, whose scalars account for the center of mass positions of the brane stack, decouples from the interacting theory and becomes mere background in the IR. That leaves a $SU(n)$ SYM theory.

which the $D6$ are separated along the z-plane corresponds to a diagonal vev for Φ

$$\langle \Phi \rangle = \text{diag}(\phi_1, ..., \phi_n), \qquad \phi_1 \neq \phi_2 \neq ... \neq \phi_n, \qquad \sum_{i=1}^{n} \phi_i = 0. \tag{1.24}$$

This uplifts to the fully deformed A_{n-1} singularity. The separations between consecutive $D6$ branes $\phi_i - \phi_{i+1}$ correspond to the holomorphic volumes of the two spheres S_i. The last relation implies that $\langle \Phi \rangle$ lies in the Cartan subalgebra of A_{n-1}. Similarly, a diagonal vev for φ_3 with distinct eigenvalues corresponds to the resolution phase of the singularity. The quantities $\varphi_3^i - \varphi_3^{i+1}$, are the Kähler volumes of the $\tilde{S}_i$. The singular limit corresponds to the configuration in which the $D6$-branes become coincident. In this limit, gauge symmetry enhancement occurs. The mechanism is well understood: when the branes coincide, open strings stretching between distinct branes become massless. The low-energy excitations of these strings correspond to the W-bosons, which enhance the gauge symmetry from $U(1)^{n-1}$ to $SU(n)$.

This observation indicates that a corresponding enhancement of gauge symmetry should also arise in the M-theory description when the ALE space degenerates. Indeed, this is the case, as we are going to argue. We have to look for the string modes whose dynamics are localised at the singularity. First of all, we have to consider the modes that descend from the Kaluza-Klein reduction of elementary fields of 11d supergravity. Massless modes are associated with harmonic two forms on K3.

For the ALE space X resolving the A_{n-1} singularity, there exist $(n-1)$ L^2-normalizable harmonic two-forms ω_i. These forms are supported on the curves $S_i \simeq \mathbb{P}^1$ and generate the compactly supported cohomology

$$H_c^2(X) \cong \mathbb{Z}^{n-1}.$$

For noncompact manifolds, compactly supported cohomology is naturally isomorphic to relative cohomology with respect to the boundary at infinity,

$$H_c^2(X) \cong H^2(X, \partial X),$$

where $\partial X \simeq S^3/\mathbb{Z}_n$ is the asymptotic boundary of the ALE space.

Relative cohomology is defined for a pair (X, A), where $A \subset X$ is a subspace. Intuitively, it describes cohomology classes on X modulo those that become trivial when restricted to A. It is naturally associated with relative homology groups $H_k(X, A)$ through the usual pairing between

homology and cohomology. Relative homology is generated by *relative cycles*, namely chains in X whose boundary lies entirely in A.

In addition to these normalizable modes, the geometry admits a harmonic two-form ω_n that is not L^2-normalizable. The origin of this mode can be understood from the long exact sequence of the pair $(X, \partial X)$,

$$0 \to H^1(\partial X) \to H^2(X, \partial X) \to H^2(X) \to H^2(\partial X) \to 0.$$

Since $\partial X = S^3/\mathbb{Z}_n$, $H^1(\partial X) = 0$ and $H^2(\partial X, \mathbb{Z}) \cong \mathbb{Z}_n$. Eventually, the sequence reduces to:

$$0 \to \mathbb{Z}^{n-1} \to \mathbb{Z}^{n-1} \to \mathbb{Z}_n \to 0,$$

which defines an extension of the free abelian group $H^2(X, \partial X)$ by a pure torsion term $\mathbb{Z}_n$. In other words, the real cohomology classes are just those corresponding to the compactly supported two-forms. However, there is an extra non-normalizable form constructed out of the ALE metric, which is the extension in the bulk of a boundary two-form that is non-trivial in the boundary cohomology. The latter is the curvature of the S^1 bundle or Hopf fibration

$$S^1 \to S^3/\mathbb{Z}_n \to S^2,$$

determined by the asymptotic behavior of the metric at the boundary. Since ω_n is non-trivial on the asymptotic boundary, the integral

$$||\omega_n||_{L^2} = \int_X \omega_n \wedge *\omega_n = \infty.$$

By decomposing the C_3 form field along these cocycles, we obtain

$$C_3 = \sum_{i=1}^{n-1} A_i \wedge \omega_i + A^b \wedge \omega_n.$$

[11] The A_i are 7d abelian gauge fields, all of them dynamical. A^b is a 7d vector field, but a back-

[11] ω_n is dual to a non-compact divisor D_n given by

$$D_n = \sum_i S_i + \Sigma_- + \Sigma_+$$

ground one, as it corresponds to the non-normalizable node.[12] The internal components of the metric tensor induce a Kähler $(1,1)$-form J_3 and a holomorphic $(2,0)$-form Ω. The 7d modes along them are scalars, defined by the period integrals

$$\varphi_3^i - \varphi_3^{i+1} = \int_{S_i} J_3, \qquad \Phi^i - \Phi^{i+1} = \int_{S_i} \Omega,$$

Together, these fields form (the bosonic sector of) n 7d abelian vector multiplets. Their vevs parametrize Kähler and complex structure deformations of the ALE surface. We have chosen the same names as in 1.23 to highlight the correspondence with the Cartan torus of the $U(n)$ generated on the dual $D6$-brane stack.

At this point, only the W bosons are missing. The solution was found to lie in the non-perturbative sector of the 11d spectrum[67, 68]. It was argued that the states responsible for the enhancement of gauge symmetry at the ALE singularity are solitonic states wrapping the S^2 cycles of the geometry. The masses of these states are proportional to the volumes of the wrapped sphere, so that they become light in the singular limit. [13] In M-theory, these correspond to wrapped $M2$-branes. Along with the $M5$-brane (six-dimensional), the $M2$-brane (three-dimensional) is the only solitonic solution of 11d SUGRA. The latter is electrically charged under the C_3-form, while the former is a magnetic source. In this case, we have only $M2$-branes. The mass is proportional to the Khäler and holomorphic volume of the wrapped cycle. The gauge charges are given by

$$q^i(M2_j) = \int_{S_j} \omega_i = S_i \cdot S_j = -\alpha_i \cdot \alpha_j, \qquad i,j = 1,...,n-1.$$

These integrals reproduce the root vectors of the $su(n)$ algebra (non-simple roots are just $M2$ branes wrapped on composite cycles). Indeed, as we anticipated, the cycles S_i are associated with the simple roots. Here, we have chosen the Poincaré duals to the S_i as a basis for the normalizable two forms, so that the charge vectors reproduce the rows of the Cartan matrix. This means that the ω_i are one-to-one with the generators of the Cartan subalgebra in the Chevalley basis.

Finally, to recover the Type IIA picture, we have to reduce the theory on the S^1 fiber. Then,

$\Sigma_\pm$ are non-compact two-cycles, originating from the S^1 fibration on segments $[z_1,\infty)$ and $[z_n,\infty)$.

[12] The kinetic term for the gauge field in the action is proportional to the L^2-norm of the corresponding harmonic two-form.

[13] Strominger argued that these should be wrapped D-branes. In [68], he analysed the low-energy limit of Type II compactifications on the singular Conifold, and showed that the consistency of the field theory is tied to the emergence of non-perturbative massless RR black holes, which smooth out the classical singularity.

the geometry projects down to the $D6$-brane stack, and the $M2$ wrapping S_i becomes a fundamental string stretching between the i-th and $i+1$-th $D6$-brane. The masses of these strings are consistently proportional to the separation between the $D6$-branes (that is, the mass of the W bosons).

The analysis presented above illustrates the power of the correspondence between the geometric description in M-theory and the D6-brane picture. The agreement between the two suggests that the field-theoretic phenomena associated with brane systems should admit a geometric interpretation in M-theory. One might therefore expect such a correspondence to hold quite generally. In the next section, however, we describe a phenomenon that appears to contradict this expectation.

1.3 The Higgs field formalism: M-theory on deformed ALE surfaces

In the previous section, we established a duality between M-theory on an ALE space of type A_{n-1} and systems of parallel $D6$-branes in Type IIA string theory. Within the family of ALE surfaces, only the non-exceptional cases, A_n and D_n, admit a dual description in terms of perturbative $D6$-branes. The D_n family arises as the M-theory uplift of a stack of n $D6$-branes coincident with an $O6^-$-plane. The enhancement of gauge symmetry to SO and Sp groups is a well-known effect associated with orientifold planes. We will return to this case later.

Deformed A_n as a Φ-dependent $\mathbb{C}^*$ fibration For now, let us go back to A_{n-1} and the dual $D6$-branes. The singular limit of the ALE space corresponds to the situation in which all of the $D6$ are at the same point. Then, the brane locus is described by

$$\delta = z^n = 0, \tag{1.25}$$

and the equation for the singularity is

$$xy = z^n, \tag{1.26}$$

The latter is invariant under the rescaling $(x, y) \to (\lambda x, \lambda^{-1} y)$, with $\lambda \in \mathbb{C}^*$. Indeed, this geometry can be seen as a $\mathbb{C}^*$ fibration over the z-plane. We now turn on a diagonal vev for the complex

scalar Φ, which we will often call the *Higgs field*, to separate the branes

$$\delta = \prod_i (z - \phi_i) = 0, \tag{1.27}$$

which can be rewritten as [19, 24, 25]

$$\delta = \det(z\mathbb{1} - \Phi), \tag{1.28}$$

The corresponding geometry is the $\mathbb{C}^*$ fibration

$$xy = \det(z\mathbb{1} - \Phi). \tag{1.29}$$

Here we drop the symbol $\langle\cdot\rangle$ for the vacuum expectation value of Φ to simplify the notation.

Writing the brane locus in this form makes manifest a key fact: the fibration is completely determined by the Casimirs of Φ, which appear as the coefficients of its characteristic polynomial.[14] This may seem natural, since vacua are characterized by gauge-invariant quantities. However, the Casimirs of Φ do not encode all the information specifying the brane configuration. This can already be seen in the simplest example, namely a stack of two parallel $D6$-branes. In this case, Φ takes values in $\mathrm{SU}(2)$, and at a generic point in the moduli space it can be written as

$$\Phi = \begin{pmatrix} t & 0 \\ 0 & -t \end{pmatrix}. \tag{1.30}$$

So that the A_1 equation gets deformed to:

$$xy = (z + t)(z - t). \tag{1.31}$$

[14] Given a Lie algebra $\mathfrak{g}$, the Casimirs of $\mathfrak{g}$ are the $Ad_{\mathfrak{g}}$-invariant functions:

$$f(Ad_{\mathfrak{g}}(A)) = f(A), \quad A \in \mathfrak{g}$$

. For A_{n-1}, the Casimirs form the polynomial ring of Weyl invariants $\mathbb{C}[t_1, ..., t_n]^{S_n}/\langle t_1 + ... + t_n\rangle$, with S_n the Weyl group, and t_n the coordinates on the Cartan subalgebra. Given a generic matrix representative A in A_{n-1}, the Casimir generators can be expressed as $u_i = \mathrm{Tr}(A^i), \quad i = 2, ..., n$.

The Higgs field as a T-brane background We are always allowed to act on Φ with a conjugation by a group element and turn it into

$$\Phi = \begin{pmatrix} 0 & 1 \\ -t^2 & 0 \end{pmatrix}. \tag{1.32}$$

Obviously, this won't affect the equation for the deformed A_1. But now let us consider the limit $t \to 0$. In this limit, the first gauge choice goes to the zero matrix, faithfully reproducing the situation of $SU(2)$ enhancement that we expected. The second matrix, instead, becomes a nilpotent element of the algebra. It is not diagonalizable, and its stabilizer is merely the identity element. From the point of view of the gauge theory, this means that the vacuum breaks all of $SU(2)$. In this context, nilpotent Higgs vevs are called T-branes, with the T referring to the triangular structure of the matrix[15]. The admissibility of nilpotent vevs for the scalars on 7-branes is not immediately obvious. The consistency conditions that allow such configurations were first discussed in [84, 85]. In [85], the authors explored the possibility of describing D-branes as coherent sheaves and interpreted the role of the Higgs field from this perspective. Their analysis considers branes wrapping a complex subvariety S of the spacetime manifold X, such that the splitting

$$TX = TS \oplus N_{S/X}$$

is holomorphic. This condition is necessary to identify the Higgs field with a holomorphic section of the normal bundle $N_{S/X}$ tensored with the adjoint representation of the gauge group. Physically, this requires that the Higgs background satisfies the equations of a Hitchin system, involving a non-trivial F_2 (gauge field strength along S) flux on S [16, 86]. Throughout this work, we only consider cases where this condition is satisfied.

An interesting observation made by Donagi et al. is that, whereas diagonal vevs describe deformations that move the support of the corresponding sheaves inside X, nilpotent vevs exhibit a much subtler behaviour. In particular, both nilpotent and vanishing vev appear to correspond to structure sheaves of non-reduced schemes.[16] From the physics side, the resulting sheaves are interpreted as bound states of branes, but the massless spectrum of open string modes is different

[15] The literature on T-branes is vast. Here we mention some important contributions: [14, 16, 37, 69–83]

[16] A scheme is non-reduced when its structure sheaf contains nilpotents. A trivial example is the fat point $Spec(\mathbb{C}[x]/\langle x^2\rangle)$. The situation in which all eigenvalues of Φ are zero is associated with a non-reduced scheme because it corresponds to the collision of the curves supporting each sheaf. This signals the generation of a bound state, but the associated gauge bundle is known to be a rank 2 $SU(n)$ bundle.

in the two cases. Moreover, there is a tension between this physical distinction and the holomorphic structure of the A_1, which appears the same. The tension is solved if we take into account the resolution maps allowed by the two choices of Higgs vev. There is indeed a deep connection between the structure of the Higgs field living in a Lie algebra $\mathfrak{g}$ and the partial simultaneous resolutions of the associated ADE surface, which will be covered more systematically in the following sections. Here, we give a first physical explanation. As we said, the $D6$-branes carry a vector multiplet with a complex scalar Φ and a real one φ_3, both in the adjoint of the gauge group.[17] It is easy to see that the D-terms of the 7d theory impose:

$$[\varphi_3, \Phi] = 0 \tag{1.33}$$

We recall that Φ and φ_3 control the deformations and the resolutions of the singular ADE surface. We can always fix a gauge in which φ_3 takes values in the Cartan subalgebra $\mathfrak{h}$ [18].This condition forces Φ to lie in the Levi subalgebra associated to φ_3, that is, the centralizer of φ_3. In the example that we have just described, the first choice of Higgs field 1.30 commutes with the only Cartan element of A_1. In particular, when $t = 0$, φ_3 can assume any value in the Cartan algebra and give a non-trivial volume to the resolution two-cycle. The second case 1.32 does not differ from the first as long as we keep $t \neq 0$, since we can always apply a gauge transformation to put Φ in diagonal form. The difference occurs at $t = 0$, namely in the presence of a T-brane. Now φ_3 cannot have non-zero eigenvalues. This tells us that all resolution parameters are frozen at zero due to this deformation.

Deformed D_n as a Φ-dependent $\mathbb{C}^*$ fibration In general, a configuration of $D6$-branes uplifts in M-theory to a $\mathbb{C}^*$ fibration that degenerates along the brane locus. In the former case, the connection between the brane locus and the equation of the A_{n-1} singularity is rather straightforward. In the case of D_n, the equation can be written as a $\mathbb{C}^*$ fibration, but the existence of a $\mathbb{Z}_2$ quotient due to the orientifold projection makes the derivation more involved. For the detailed derivation, we refer to [19, 24, 25]. Here, we will be very brief. This $O6^-$ plane action on the superstring worldsheet is combined with the reflection of the transverse directions to the O-plane.

[17] With this choice we have hidden the $SU(2)$ R-symmetry that rotates the three real scalars corresponding to Φ and φ_3.

[18] φ_3 is a real adjoint scalar. This means

$$\varphi_3^\dagger = \varphi_3, \qquad \varphi_3 = \varphi_3^a g^a, \quad g_a \in \mathfrak{g}_\mathbb{R} \tag{1.34}$$

, where $\mathfrak{g}_\mathbb{R}$ is the real Lie algebra

The defining equation for a D_n singularity is:

$$F_{D_n} : x^2 + zy^2 + z^{n-1} = 0. \tag{1.35}$$

And its generic deformation can be written as:

$$F^{def}_{D_n} : x^2 + zy^2 + z^{n-1} - \tilde{P}(z; \{u_i\}) + 2yQ(z; \{u_i\}) = 0, \tag{1.36}$$

where P and Q are polynomials that are parametric in the complex deformation constants $\{u_i\}_{i=1,..,n}$, which are the Casimirs of Φ.[19]In this case Φ is an antisymmetric $2n \times 2n$ matrix (as it lives in the adjoint of $SO(2n)$ Lie algebra), so the Casimirs are:

$$u_a = \text{Tr}(\Phi^{2a}), \quad u_n = \text{Pfaff}(\Phi), \quad a = 1, ..., n-1 \tag{1.38}$$

Where $textPfaff$ denotes the Pfaffian of the matrix.

For simplicity, we inglobe the factor z^{n-1} into $\tilde{P}$, defining $P = \tilde{P} - z^{n-1}$.

Let us call η the complex spacetime coordinate transverse to the O-plane, which will correspond to the double cover of the coordinate z in 1.35:

$$\eta^2 = z \tag{1.39}$$

The action of $O6^-$ is:

$$O6^- : \quad \eta \mapsto -\eta \tag{1.40}$$

The locus of the $D6$ branes, in presence of a deformation induced by Φ, is expressed as:

$$\delta = \det(\eta \mathbb{1} + \Phi) = 0. \tag{1.41}$$

The goal of the game is to rewrite 1.36 as a $\mathbb{C}^*$ fibration that degenerates on the $\mathbb{Z}_2$ quotient of

[19] $\tilde{P}$ and Q belong to the ring of versal deformationsof the surface:

$$\mathcal{R}_{def} = \frac{\mathbb{H}[x, y, z]}{\langle \nabla F_{D_n} \rangle}, \quad \mathbb{H} = \mathbb{C}[u_1, ..., u_n] \tag{1.37}$$

. For details see 4.

this locus. Let us consider the rewriting of 1.36 in the double cover:

$$\tilde{F}^{def}_{D_n} = XY + \eta^{2(n-1)} - P(\eta^2;\{u_i\}) + 2yQ(\eta^2;\{u_i\}), \quad X = x + i\eta y, \;\; Y = x - i\eta y. \tag{1.42}$$

Note that:

$$\eta \mapsto -\eta \quad \longrightarrow \quad X \leftrightarrow Y. \tag{1.43}$$

This exchange is consistent with the fact that the orientifold acts as an inversion on the M-theory S^1. So, X, Y can be consistently identified as the local $\mathbb{C}^*$ coordinates.The points where the fiber collapses are given by zeros of the discriminant of the polynomial $zy^2 - P + 2yQ$ with respect to y:

$$\Delta = P^2 + \eta^2 Q, \tag{1.44}$$

[20] Finally, imposing $\delta = \Delta$ one can find the expressions for P and Q in terms of Φ:

$$P(\eta^2) = \frac{\det(\eta\mathbb{1} + \Phi) - \text{Pfaff}^2(\Phi)}{\eta^2}, \quad Q(\eta^2) = \text{Pfaff}(\Phi). \tag{1.45}$$

We can now use 1.45 to rewrite 1.36 as:

$$x^2 + zy^2 - \frac{\det(z\mathbb{1} + \Phi^2) - \text{Pfaff}^2(\Phi)}{z} + 2y\text{Pfaff}(\Phi) = 0. \tag{1.46}$$

To avoid repeating ourselves, we will refrain from considering specific examples for this case.
Let us summarize what we did. In this section, we have reviewed two results from the literature that will be relevant for the development of this work:

- The local geometry of ALE spaces of A_n and D_n type can be reconstructed from a $\mathbb{C}^*$-fibration degenerating over the locus of the $D6$-branes that uplift to that geometry in M-theory. Crucially, both families can be described via algebraic equations where the dependence on the Higgs field profile is manifest. E_6, E_7 and E_8 do not possess a $\mathbb{C}^*$-fibered structure. If they had one, there would be an associated perturbative $D6$ brane solution. [12, 19]

- Field theory contains information beyond that captured by the holomorphic geometry. In particular, nilpotent Higgs vevs — the so-called T-branes — are invisible to the holomorphic

[20] It is easy to check that, with a simple change of coordinates, the equation 1.42 reduces to a form $\tilde{X}\tilde{Y} = 0$ when $\Delta = 0$.

geometric description [16, 86]. The geometric effect of T-branes is an obstruction to resolutions. The physical implications of this are best understood from the theory of a probe $D2$-brane [37, 77]

1.4 Non-constant Higgs vevs: geometric engineering of rank 0 5d SCFTs

In this section, we review a construction introduced in [19, 25–27] which is central to our work. This is a physics-based method to engineer Calabi-Yau threefolds of a very special kind, the so-called *compound Du Val* singularities, reviewed in the second chapter. These geometries have proven to develop interesting physics both in the context of geometric engineering and the brane probe theories. Our contributions to both approaches will be the object of Chapters 5, 6, 7.

We have just seen an example of how different vevs for the adjoint scalar Φ control the complex deformations of the background geometry. Actually, the amount of information that it provides is more than that, as its profile is tied to the resolution structure. To unravel the full potential of this construction, we consider a more general kind of situation. Instead of switching on a constant vev, we are allowed to choose a vacuum in which Φ is a holomorphic function of a complex coordinate w. In the $D6$-brane picture, w parametrizes a complex plane wrapped by the $D6$-branes. In the dual M-theory setup, w is a plane along which the ALE surface is trivially fibered. Then, in the former case, a non-constant $\Phi(w)$ will correspond to the bending of the $D6$. In the latter, the geometry will become a non-trivially fibered ALE surface.

1.4.1 The Conifold

Let us consider A_1 again. Now, take

$$\Phi = \begin{pmatrix} w & 0 \\ 0 & -w \end{pmatrix}, \tag{1.47}$$

for which the brane locus is promoted to

$$\delta = (z + w)(z - w) = 0, \tag{1.48}$$

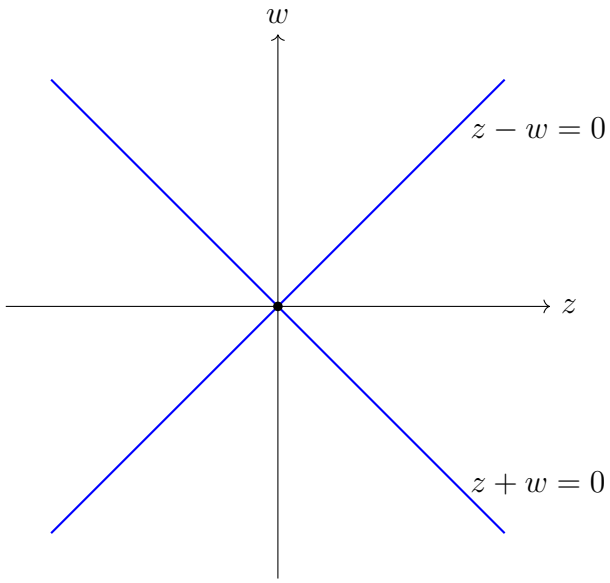

Figure 1.2: The reducible $D6$-brane locus $(z+w)(z-w)=0$ in the (z,w)-plane.

The two branes intersect at the origin of the $\mathbb{C}^2$ parametrized by (z,w) and occupy distinct curves as can be seen in Figure 1.2. In the present case, the bending of the branes is such as to preserve half of the supercharges of the original theory. Moreover, it can be shown [24] that the light degrees of freedom are now open strings localized at the intersection $w=z=0$. These modes are identified with hypermultiplets propagating in the transverse five directions along the branes. The dual geometry is now an equation in $\mathbb{C}^4$

$$xy=(z+w)(z-w), \tag{1.49}$$

This is a well-known example of a toric threefold, universally named Conifold. It is the only toric example in the class that we are focusing on. This makes the analysis of the associated physics more accessible. There are plenty of approaches to the study of this geometry and the associated 5d SCFT, all of them in agreement [86–89]. We refrain from reviewing all of them and limit ourselves to making a few observations. First, let us consider the original framework as a compactification on the threefold $\mathbb{C}^2/\mathbb{Z}_2\times\mathbb{C}_w$. The singularity covers the entire w-plane invariably. $M2$-branes wrap the 2-cycles of the resolution fibered along the complex curve $\mathbb{C}_w$. These states correspond to the W bosons of the 7d $SU(2)$ vector multiplet. When 1.47 is turned on, it breaks the $SU(2)$ symmetry down to $U(1)$ for every $w\neq 0$. This signals that the A_1

singularity is now isolated at $w = 0$. All the other ALE fibers are deformed and correspond to smooth points on the threefold. As opposed to the trivially fibered K3, this space preserves half of the supercharges. Indeed, the theory localised at the singularity corresponds to a 5d $\mathcal{N} = 1$ SCFT. We will discuss the features of geometric engineering on CY3 in a greater generality (See chapter 3.1). For now, let us describe what happens in this very simple but special case. In the previous sections, we have described how resolving a singularity in a local K3 manifold, namely a CY surface, amounts to extracting 2-cycles. In three dimensions, the mechanism is more complicated, because there are more ways of resolving. In 3d, a resolution extracts a locus, said the exceptional locus, which can contain curves and divisors (codimension 1 subvarieties). In our case, the resolution is a blow-up that inflates the 2-cycle of the A_1 fiber at $w = 0$ without extracting new divisors.[21] This is an example of small resolution (see chapter 2), which gives rise to substantially different physics than the divisorial case.

The 2-cycle of the resolution has a non-trivial intersection with a non-compact divisor E, which signals the presence of a global symmetry. The reduction of the C_3 form on the Poincaré dual of E produces an abelian gauge field indeed. This is the 7d gauge field, which becomes a background for the 5d field theory. The $U(1)$ symmetry carried by the background corresponds to the commutant (or centralizer) of the Higgs field profile 1.47, which is the Cartan of A_1. The $M2$-branes wrapping the resolution curve are the charged states under the flavor symmetry. In the trivially fibered case, these were identified with the W-bosons of $SU(2)$. Since there are no compact divisors, there can't be dynamical gauge interactions, so the Coulomb Branch of the theory contains only a non-dynamical deformation, that is, the mass of the $M2$ wrapped states. From the point of view of the 5d theory, the $M2$ states are just hypermultiplets. This is not obvious from what we stated. A way to check that we have hypers and count their number is to describe the space of complex structure deformations of the threefold (a very hard problem in general!). For the Conifold, there is only one dynamical deformation:

$$F_{def} \; : \quad xy = z^2 - w^2 + \mu, \quad \mu \in Spec\big(\frac{\mathbb{C}[x,y,z,w]}{\langle \nabla F \rangle}\big). \tag{1.50}$$

The complex parameter μ is the holomorphic volume of an S^3-cycle A that appears in the deformed geometry

$$\mu = \int_A \Omega_3. \tag{1.51}$$

[21] The process involves blowing up a non-Cartier Weyl divisor that contains the singular point. In the resolution, the divisor becomes Cartier and contains the blown-up $\mathbb{P}^1$, but no new divisor is generated.

Ω_3 is the holomorphic volume 3-form of the CY3. The cycle A is unpaired, or paired with a non-compact 3-cycle B, namely $\exists B$ such that $B \cdot A = 1$. The reduction of C_3 on A determines a $\mathbb{C}^*$ fibered over the μ-plane. This fibration defines the moduli of a hypermultiplet. The Higgs branch is indeed the quaternionic space $\mathbb{C}^2$ (which is a $\mathbb{C}^*$ fibration). We refer to [26, 39, 51, 90, 91] for a more rigorous treatment.

1.4.2 $\mathbb{C}^3$

Let us consider a non-constant Higgs of the form

$$\Phi = \begin{pmatrix} 0 & 1 \\ -w & 0 \end{pmatrix}. \tag{1.52}$$

The corresponding brane locus is

$$\delta = z^2 - w = 0. \tag{1.53}$$

As opposed to the previous case, the support of the $D6$-branes is now an irreducible variety, since it cannot be factorized holomorphically. Only if we go to the double cover of the w-plane, that is, we make the change $w = t^2$, we recover the previous situation. So, when the Casimir of Φ is linear in the base coordinate w, we cannot diagonalize the Higgs field. This means that the $SU(2)$ symmetry is fully broken, and the resolution is obstructed in a similar way to what we saw in the presence of the T-brane. We can think of it as a situation in which the two branes are glued into a bound state by the T-brane and then bent by the w-dependent factor. On the geometry side, we have the threefold

$$xy = z^2 - w. \tag{1.54}$$

The A_1 fiber is singular only at $w = 0$. If we look at the origin of the w-plane, though, Φ becomes a T-brane and obstructs turning on non-trivial vevs for φ_3. So, in this case, there is no residual symmetry from 7d. The theory is actually empty, since the threefold is globally smooth and its homology groups are trivial.

To wrap up, let us list what we have observed:

- Allowing the adjoint scalar Φ to depend holomorphically on w corresponds to bending $D6$-branes and, in M-theory, to non-trivial fibrations of ALE surfaces over the w-plane. The resulting physics is controlled by the holomorphic behaviour of the eigenvalues of $\Phi(w)$.

When the eigenvalues are holomorphic functions of w, the Higgs field can be diagonalized, and the brane locus is reducible.

- In this case (e.g. $\Phi = \mathrm{diag}(w, -w)$), the geometry is the conifold, with an isolated A_1 singularity at $w = 0$. Its small resolution introduces a compact $\mathbb{P}^1$, and $M2$-branes wrapping this curve give a hypermultiplet charged under a $U(1)$ flavor symmetry that propagates in 5d.

- When the eigenvalues do not depend holomorphically on w (the Higgs field is non-diagonalizable, as in $\Phi = \begin{pmatrix} 0 & 1 \\ -w & 0 \end{pmatrix}$), the branes form an irreducible bound state, the resolution is obstructed, and the threefold is smooth. Consequently, no localized degrees of freedom arise.

1.4.3 ADE-families, Φ and the partial simultaneous resolutions

The relation between Higgs backgrounds and the resolution structure of ADE-fibered threefolds can be understood systematically in the framework of Grothendieck–Springer resolutions. In this context, one studies the minimal resolutions of ADE surface singularities across their versal deformation space. The K3-fibered threefolds generated by holomorphic Higgs vevs naturally arise within this framework, as their crepant resolutions are small. In particular, small resolutions of the threefold are in one-to-one correspondence with minimal resolutions of the ADE surface fibers.

From the physical perspective, the resolution data is encoded in the group-theoretic structure of the Higgs field Φ. More precisely, Φ is interpreted as a representative element of a Levi subalgebra of the Lie algebra $\mathfrak{g}$. The Levi subalgebra is defined as the commutant of a subset of Cartan generators and geometrically corresponds to selecting a subset of the 2-cycles in the second homology of the ADE fiber. These are precisely the cycles that remain unobstructed in the presence of the Higgs background.

Consistency of the construction requires the Casimir invariants of Φ to depend linearly on the base coordinate w and vanish at $w = 0$. This ensures that the eigenvalues of Φ—which geometrically correspond to the volumes of the unobstructed 2-cycles—vary holomorphically along the base. In this way, the Higgs background determines both the deformation of the ALE fiber and the structure of the simultaneous resolution.

Analogous to the A_1 case studied above, the various possible (partial) simultaneous resolutions of a family of ADE surfaces can be encoded in the different forms of the field Φ. This was first described in [19]. Given a choice of partial resolution, the corresponding field Φ is determined in the following way:

- Choose the subset of simple roots $\alpha_1, ...\alpha_\kappa$ ($\kappa \leq r$) that are blown up at the origin.[22]
- Take the abelian subalgebra of $\mathfrak{g}$ generated by

$$\mathcal{H} = \langle \alpha_1^*, ...\alpha_\ell^* \rangle \,, \tag{1.55}$$

  where $\alpha_1^*, ..., \alpha_r^*$ is a basis of the Cartan subalgebra dual to the set of simple roots.
- The commutant of $\mathcal{H}$ in $\mathfrak{g}$ is a Levi subalgebra $\mathcal{L}$ of $\mathfrak{g}$ that takes the form

$$\mathcal{L} = \bigoplus_h \mathcal{L}_h \oplus \mathcal{H} \,, \tag{1.56}$$

  with $\mathcal{L}_h$ simple Lie algebras.
- Φ must be a generic element of $\mathcal{L}$.[23]
- The choice of Levi determines the good coordinates on the space of deformations of the ALE fiber. The good coordinates are the Casimirs of Φ, ϱ_i ($i = 1, ..., r$), which parametrize the space $\mathfrak{h}/\mathcal{W}'$. Here, $\mathfrak{h}$ is the Cartan subalgebra, and $\mathcal{W}'$ is the Weyl group of the Levi (in general, a subgroup of the Weyl group of $\mathfrak{g}$).[24]

[22] In the A_1 case, the only options are either to resolve the single simple root or to resolve none. In the A_2 case, for example, one has the following three choices: 1) resolve both the simple roots, 2) resolve one of the simple roots, and 3) resolve none.

[23] This can be understood in the type IIA picture with D6-branes [25]: the resolution corresponds here to the motion of the D6-branes along the direction $\mathbb{R}$ in $\mathbb{R}^{1,5} \times S^1 \times \mathbb{C} \times \mathbb{R}$ and is then a Cartan vev for a real adjoint field $\phi \in \mathcal{H}$. The equations of motion impose ϕ to commute with Φ. Hence Φ must live in the commutant of $\mathcal{H}$.

[24] In the Grotendieck-Springer construction, the curves preserved by the partial simultaneous resolution are one-to-one with the group quotients

$$L_x/P_{\mathcal{L}} \tag{1.57}$$

Here, we have $x \in \mathfrak{g}$, an element of the Slodowy slice through the subregular nilpotent orbit of $\mathfrak{g}$. We conjecture that this may be our Higgs field. L_x is the Levi subgroup generated by the commutant of the diagonalizable component of x (with a gauge transformation, x can always be decomposed into a diagonal plus a nilpotent part). $\mathcal{L}$ is the Levi subalgebra that determines the partial resolution. Finally, $P_{\mathcal{L}}$ is a parabolic subgroup of G. It is generated by the

- From the Casimir invariants of Φ, we can read how the ALE fiber is deformed.[25] Since at the origin of $\mathfrak{h}/\mathcal{W}'$ the fiber presents the full ADE singularity, all the Casimir invariants of Φ must vanish when $\varrho_i = 0$ $(i = 1, ..., r)$, i.e. $\Phi(\varrho = 0)$ should be a nilpotent element of $\mathcal{L}$. In particular, when restricted to each summand $\mathcal{L}_h$ of the Levi subalgebra, Φ must be in the corresponding principal nilpotent orbit [19].[26]

- The Higgs field $\Phi(\varrho)$ must deform the singularity outside the origin. The coordinates $\boldsymbol{\varrho}$ should parametrize a transverse direction to the nilpotent orbit (that includes $\Phi(0)$) in $\mathfrak{g}$. This is achieved by taking $\Phi(\varrho)$ in the Slodowy slice[27] in $\mathfrak{g}$ that passes through $\Phi(0)$. This provides a canonical form for the Higgs field $\Phi(\varrho)$.

The discussion above shows that Higgs backgrounds provide a systematic way to construct families of ADE-fibered threefolds with simultaneous partial resolutions. Within the Grothendieck–Springer framework, the resolution structure is completely encoded in the group-theoretic data of the Higgs field: the choice of Levi subalgebra determines which 2-cycles of the ADE fiber remain unobstructed, while the Casimir invariants of Φ control the deformation of the singularity along the base. In this way, the geometry of the Calabi-Yau threefold and its resolution are directly dictated by the structure of the Higgs background.

This mathematical framework turns out to be extremely efficient in constructively deriving the homological structure of ALE fibrations. As we will review in the mathematical part of this thesis (see Chapter 2), Grothendieck–Springer resolutions allow one to describe the full space of Calabi–Yau threefold singularities that admit small crepant resolutions. On the physics side, this construction provides a classification of rank-zero five-dimensional SCFTs, namely theories with no dynamical gauge interactions. Moreover, the Higgs field gives direct access to the spectrum and global symmetries of these theories: the physical states can be extracted by counting the five-dimensional localized fluctuations of Φ around its background value, following the method developed in [16].

---

algebra

$$\mathcal{P}_{\mathcal{L}} = \mathfrak{b} + \sum_i e_{-\alpha_i} \tag{1.58}$$

, where $\mathfrak{b}$ is the maximal borel subalgebra of $\mathfrak{g}$, and the additional factors are the negative root generators contained in $\mathcal{L}$.

[25] Since the preserved 2-cycles are holomorphic in the ϱ_i, the ϱ_i must be holomorphic in w.

[26] This prevents the family from developing singularities that cannot be resolved. In the A and D cases, this requirement translates to asking that $\Phi(\varrho)$ is a reconstructible Higgs [16], i.e., it is written in terms of the Casimir invariants of the $\mathcal{L}_h$'s.

[27] See for example, Appendix B of [26] for a definition of the Slodowy slice.

From our perspective, this framework provides a concrete and constructive approach to the study of non-toric Calabi-Yau geometries and can be regarded as a first step toward understanding geometric engineering beyond the toric regime. Even the simplest examples exhibit physical properties that remain poorly understood and appear to be related to the scheme-theoretic structure of the moduli spaces of these manifolds. One of the aims of this work is to stimulate further interest in this direction and highlight connections with recent developments at the interface between physics and mathematics. Among the most promising advances toward generalizing toric geometric engineering is the Generalized Toric Polygon approach, which may ultimately prove complementary to the perspective adopted here.

In this thesis, we restrict our attention to the most mathematically controlled class of K3-fibered geometries within this framework, namely the so-called *simple flops*. These correspond to ADE fibrations in which all but one of the fiber 2-cycles are obstructed by the Higgs background. Geometrically, they can be regarded as the simplest non-toric generalizations of the conifold geometry discussed above.

While the geometric construction described above provides a powerful way to characterize these backgrounds, the perspective adopted in our first work (content of chapters 5 and 6) differs from the original Higgs-field approach. In particular, we have seen that a crucial ingredient in generating obstructed cycles in the threefold geometry is the presence of T-brane backgrounds. At present, the most concrete understanding of T-branes arises from studying their effects on the worldvolume theory of probe branes.

To this end, we consider a probe $D2$-brane extending along the directions transverse to the Calabi-Yau threefold. The worldvolume theory on the probe is a three-dimensional $\mathcal{N} = 2$ supersymmetric quantum field theory in which the degrees of freedom of the higher-dimensional theory appear as background fields. When the five- or seven-dimensional modes acquire vacuum expectation values, the probe theory is correspondingly deformed. In general, this triggers a non-trivial RG flow whose infrared dynamics can be difficult to determine directly. However, string dualities provide powerful tools to reconstruct the IR physics of the probe.

In particular, we will see that the moduli space of the $D2$-brane theory reproduces the Calabi-Yau threefold geometry induced by the Higgs background. Moreover, the low-energy dynamics of the probe capture the dynamics of the BPS particles on the Coulomb branch of the geometrically engineered five-dimensional theory. This reflects the deep connection between D-branes and BPS states in geometric engineering, whereby wrapped branes provide a microscopic realization of the

BPS spectrum of the effective field theory.

Chapter 2

D-brane probes and quiver gauge theories

To introduce our method and place our analysis within the broader framework of worldvolume supersymmetric quantum field theories, we begin by reviewing the seminal work of Douglas and Moore [2] on $D3$-branes probing ADE orbifold singularities. Their analysis revealed that the low-energy dynamics of the probe branes are described by a class of supersymmetric gauge theories whose matter content and interactions can be encoded in directed graphs, the so-called *quiver gauge theories*. This construction established a deep connection between the geometry of singular spaces and the structure of supersymmetric gauge theories, and will provide the conceptual starting point for the probe-brane approach developed in the following.

2.1 D3-branes probing ADE orbifold singularities

D-branes provide a powerful tool for probing the local structure of string theory backgrounds. A D-brane that extends along the non-compact Minkowski directions while remaining localized in the internal space behaves, at low energies, as a dynamical probe of the ambient geometry. When the number of probe branes is small, their backreaction on the bulk fields can be neglected, and the probe approximation is valid. In this regime, the worldvolume theory on the brane captures information about the local structure of the string vacuum. In particular, the scalar fields of the probe gauge theory parameterize the motion of the brane in the transverse space, so that the moduli space of vacua of the worldvolume theory reproduces the geometry of the internal space.

A prototypical example of this correspondence arises when a D3-brane probes an orbifold

singularity. Consider Type IIB string theory on a background of the form

$$\mathbb{R}^{1,3} \times \mathbb{C}^2/\Gamma \times \mathbb{C}, \tag{2.1}$$

where Γ is a finite subgroup of $SU(2)$. The quotient $\mathbb{C}^2/\Gamma$ provides an orbifold presentation of the ADE singularities introduced in the previous sections. Far from the singularity, the theory that localises on the probe is a $\mathcal{N} = 4$ supersymmetric QFT with a single vector multiplet carrying a $U(1)$ gauge symmetry.

To understand qualitatively what happens at the singularity, it is useful to recall the meaning of taking an orbifold quotient. When a portion of spacetime is quotiented by a discrete group Γ, the effect at the level of field theory (and string theory) is to project the Hilbert space onto states that are invariant under the action of Γ. Concretely, this can be viewed as an averaging procedure over the images of states under the elements of the orbifold group.

In string theory, this structure appears naturally in the partition function, which decomposes into a sum over the untwisted sector, corresponding to the identity element of Γ, and the twisted sectors associated with the non-trivial elements of the group. This sum implements a projection onto Γ-invariant combinations of states.

From the point of view of D-branes, the effect of the orbifold depends crucially on the position of the brane with respect to the fixed locus of the group action. If a D-brane sits away from the fixed point, its images under the action of Γ are located at distinct points in spacetime. After performing the quotient, the brane together with all of its images becomes a single brane whose worldvolume theory is identical to that of a brane probing flat space.

The situation is qualitatively different when the brane sits at a fixed point of the orbifold action. In this case, the images of the brane coincide in spacetime but remain distinct as objects carrying an equivariant action of the orbifold group Γ. From this perspective, the quotient behaves more naturally as a stack quotient: the resulting geometry retains a Γ-equivariant structure that remembers the quotient symmetry.[1] The Γ-equivariant D-brane states are said *fractional branes*. Being only defined at the singular point, they form a new set of localised states. Moreover, at the singular point, half of the supersymmetry is broken. Hence, the worldvolume dynamics of the branes form a 4d $\mathcal{N} = 2$ susy QFT. The degrees of freedom are vector multiplets and hypermultiplets. The first is generated by open strings ending on the same fractional brane, the second by

[1] Isometry quotients with non-trivial stabilizers are mathematically described by stacks. When the stabilizer group is finite the resulting objects are Deligne–Mumford stacks, while more general stabilizers give rise to Artin stacks.

open strings connecting different Γ-images. The spectrum can be derived in the following way.

Let $\{\rho_i\}$ be the irreducible representations of Γ with dimensions $d_i = \dim(\rho_i)$.

Chan–Paton space. The Chan–Paton space associated with the stack of fractional branes is taken to be

$$\mathbb{C}^{|\Gamma|}.$$

Before the orbifold projection, the gauge symmetry of the system is therefore

$$U(|\Gamma|).$$

Orbifold action. The orbifold group acts on the Chan–Paton indices through the regular embedding

$$\gamma : \Gamma \to U(|\Gamma|),$$

defined by the regular representation R of Γ. The regular representation decomposes into irreducible representations as

$$R = \bigoplus_i d_i \, \rho_i.$$

The orbifold projection requires physical open-string states to be invariant under the simultaneous action of Γ on spacetime coordinates and Chan–Paton factors. In particular the gauge generators λ must satisfy

$$\lambda = \gamma(g)\lambda\gamma(g)^{-1}, \qquad g \in \Gamma.$$

The surviving gauge symmetry is therefore the commutant of $\gamma(\Gamma)$ in $U(|\Gamma|)$, which yields

$$\prod_i U(d_i).$$

Open-string spectrum. To determine the invariant spectrum, we consider the transformation properties of open string states. Since open strings carry one fundamental and one antifundamental Chan–Paton index, the Chan–Paton part transforms in

$$R^\dagger \otimes R.$$

For the orbifold $\mathbb{C}^2/\Gamma$, the geometric action of Γ acts on the coordinates of $\mathbb{C}^2$ in the two-dimensional representation

$$V \simeq \mathbf{2},$$

while the remaining complex direction $\mathbb{C}$ transforms trivially. The open string states, therefore, transform in

$$R^\dagger \otimes R \otimes (\mathbf{2}, \mathbf{1}).$$

The orbifold group must be embedded in $SU(2)$ so that the action on $\mathbb{C}^2$ preserves the holomorphic two-form, ensuring that the quotient space is a Calabi–Yau twofold.

Projecting onto the Γ-invariant subspace and using Schur's lemma, the spectrum is determined by the decomposition

$$\rho_i \otimes \mathbf{2} = \bigoplus_j a_{ij}\rho_j.$$

The coefficients a_{ij} determine the number of bifundamental fields transforming in

$$(d_i, \overline{d_j})$$

under the gauge group $\prod_i U(d_i)$.

Example: $\mathbb{C}^2/\mathbb{Z}_n$**.** The group $\mathbb{Z}_n$ has n one-dimensional irreducible representations ρ_i, with $i = 0, \ldots, n-1$. The regular representation, therefore, decomposes as

$$R = \bigoplus_{i=0}^{n-1} \rho_i.$$

The surviving gauge group is

$$\prod_{i=0}^{n-1} U(1)_i.$$

The action of the two-dimensional representation $\mathbf{2} = \rho_0 \oplus \rho_1$ gives

$$\rho_i \otimes \mathbf{2} = \rho_{i+1} \oplus \rho_{i-1},$$

with indices understood modulo n. Hence, bifundamental fields connect neighbouring gauge

factors. This structure can be represented by a quiver diagram (See Figure 2.1) in which nodes correspond to gauge factors and arrows represent bifundamental matter fields. The resulting quiver coincides with the affine A_{n-1} Dynkin diagram, illustrating the McKay correspondence between finite subgroups of $SU(2)$ and ADE Dynkin diagrams. To be more explicit, let us define the orbifold invariant chiral superfields:

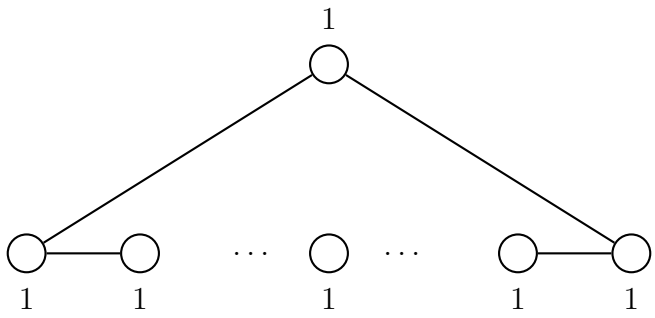

Figure 2.1: A_n Dynkin diagram

$$\hat{Z}_1 = \begin{pmatrix} 0 & Z_1^{(01)} & 0 & \cdots & 0 \\ 0 & 0 & Z_1^{(12)} & \cdots & 0 \\ \vdots & \vdots & \ddots & \ddots & \vdots \\ 0 & 0 & \cdots & 0 & Z_1^{(n-2,n-1)} \\ Z_1^{(n-1,0)} & 0 & \cdots & 0 & 0 \end{pmatrix}, \qquad \hat{Z}_2 = \begin{pmatrix} 0 & 0 & \cdots & 0 & Z_2^{(0n-1)} \\ Z_2^{(10)} & 0 & \cdots & 0 & 0 \\ 0 & Z_2^{(21)} & \ddots & \vdots & \vdots \\ \vdots & \ddots & \ddots & 0 & 0 \\ 0 & \cdots & 0 & Z_2^{(n-1,n-2)} & 0 \end{pmatrix},$$

$$\hat{W} = \begin{pmatrix} W_0 & 0 & 0 & \cdots & 0 \\ 0 & W_1 & 0 & \cdots & 0 \\ \vdots & \vdots & W_2 & \ddots & \vdots \\ 0 & 0 & \cdots & W_{n-2} & 0 \\ 0 & 0 & \cdots & 0 & W_{n-1} \end{pmatrix}.$$

Here, $(\hat{Z}_1, \hat{Z}_2)$ are the hypermultiplets and $\hat{W}$ is the set of chirals in the $\mathcal{N} = 2$ vector multiplets. Our convention is that the map $Z^{(ij)}$ goes from node j to node i. The theory inherits a superpotential from the original (pre-orbifold) $\mathcal{N} = 4$ theory:

$$\mathcal{W}_{\mathcal{N}=2} = \mathrm{Tr}(\hat{W}[\hat{Z}_1, \hat{Z}_2]). \tag{2.2}$$

The corresponding F-terms, $(\partial_{\hat{Z}_1}\mathcal{W}_{\mathcal{N}=2}, \partial_{\hat{Z}_2}\mathcal{W}_{\mathcal{N}=2}, \partial_{\hat{W}}\mathcal{W}_{\mathcal{N}=2})$, determine the vacua of the theory, defined modulo complex gauge transformations [2, 92]. Seen in more abstract terms, the set of operators $(\hat{Z}_1, \hat{Z}_2, \hat{W})$ together with the F-term conditions, defines a representation of a non-commutative algebra associated with the quiver (the so-called non-commutative crepant resolution of $\mathbb{C}\times\mathbb{C}^2/\mathbb{Z}_n$). The center of the algebra reproduces the probed ALE geometry (See Appendix D). Note that

$$\hat{Z}_1^n = Z_1^{(01)} Z_1^{(12)} \cdots Z_1^{(n-2,n-1)} Z_1^{(n-1,0)} \mathbb{1}, \quad \hat{Z}_2^n = Z_2^{(0n-1)} Z_2^{(n-1n-2)} \cdots Z_2^{(21)} Z_2^{(10)} \mathbb{1}, \tag{2.3}$$

$$\hat{Z}_1\hat{Z}_2 = \begin{pmatrix} Z_1^{(01)}Z_2^{(10)} & 0 & 0 & \cdots & 0 \\ 0 & Z_1^{(12)}Z_2^{(21)} & 0 & \cdots & 0 \\ \vdots & \vdots & \ddots & \ddots & \vdots \\ 0 & 0 & \cdots & Z_1^{(n-2n-1)}Z_2^{(n-1n-2)} & 0 \\ 0 & 0 & \cdots & 0 & Z_1^{(n-10)}Z_2^{(0n-1)} \end{pmatrix}. \tag{2.4}$$

The F-term $\partial_{\hat{W}}\mathcal{W}_{\mathcal{N}=2} = 0$ implies $\det(\hat{Z}_1\hat{Z}_2) = (Z_1^{(01)}Z_2^{(10)})^n$.

$$\hat{Z}_1^n\hat{Z}_2^n = (\hat{Z}_1\hat{Z}_2)^n, \tag{2.5}$$

Since the three factors $\hat{Z}_1^n, \hat{Z}_2^n, \hat{Z}_1\hat{Z}_2$ are central elements of the representation, 2.5 becomes a scalar relation:

$$xy = z^n, \quad x = 1/n\mathrm{Tr}(\hat{Z}_1^n), \quad y = 1/n\mathrm{Tr}(\hat{Z}_2^n), \quad z = \hat{Z}_1\hat{Z}_2. \tag{2.6}$$

From the geometric point of view, the algebra governs the structure of the minimal resolution of the orbifold singularity $\mathbb{C}^2/\Gamma$. The resolution replaces the singular point with a collection of exceptional $\mathbb{P}^1$ curves whose intersection matrix is given by minus the Cartan matrix of the corresponding ADE Lie algebra. Let us see how the $\mathbb{P}^1$ emerges in a simple case.

$n = 2$ **case** Now we have

$$\hat{Z}_1 = \begin{pmatrix} 0 & Z_1^{(01)} \\ Z_1^{(10)} & 0 \end{pmatrix}, \qquad \hat{Z}_2 = \begin{pmatrix} 0 & Z_2^{(01)} \\ Z_2^{(10)} & 0 \end{pmatrix}.$$

We can see that setting $Z_1^{(10)}$ and $Z_2^{(10)}$ to zero is sufficient to restrict ourselves to the singular locus:

$$Z_1^{(10)} = Z_1^{(10)} = 0 \quad \rightarrow \quad x = 1/2\mathrm{Tr}(\hat{Z}_1^2) = 0, \quad y = 1/2\mathrm{Tr}(\hat{Z}_2^2) = 0, \quad z = \hat{Z}_1\hat{Z}_2 = 0. \tag{2.7}$$

So, both $\hat{Z}_1$ and $\hat{Z}_2$ are now nilpotent $\mathfrak{sl}_2$ matrices which gauge fix most of the $\mathfrak{sl}_2$ up to a $\mathbb{C}^*$ action:

$$\begin{array}{ccc} & Z_1^{(01)} & Z_2^{(01)} \\ \mathbb{C}^* & 1 & 1 \end{array}. \tag{2.8}$$

This is the $\mathbb{P}^1$ of the resolution of A_1. The fact that fractional brane vacua reproduce the probed geometry suggests the existence of a relation between fractional branes and branes wrapped on vanishing two-cycles. Indeed, the correct description of these localised solitonic states is given in terms of wrapped higher-dimensional D-branes. In general, these are not elementary branes, but bound states of branes of different dimensions (in this case, bound states of $D5$ and $D3$)[12].

We have seen that the probed geometry determines the vacua of the brane system worldvolume theory. Additionally, the geometric picture provides an interpretation of the couplings of the quiver gauge theory. The gauge coupling associated with each node is controlled by the effective Khäler volume of the corresponding exceptional two-cycle ξ. Roughly

$$1/g_i^2 \sim \xi_i \tag{2.9}$$

. The effective volumes arise in the IR from blow-up modes of the singularity, which correspond to twisted-sector states of the closed string localized at the orbifold fixed point. The existence of these modes is what makes the effective theory consistent even in the orbifold limit, that is, when the bare Khäler moduli tend to zero. In this limit he closed string background effectively resolves the singularity. In the gauge theory of the probe, this means that the inverse couplings $1/g_i^2$ are kept finite. Complex-structure deformations appear as complex Fayet-Iliopulos terms in the superpotential. As any $\mathcal{N} = 2$ susy qft, the moduli space of the theory splits into two branches, namely Coulomb branch (CB) and Higgs branch (HB). On the CB the $U(1)_R$ factor of the R-symmetry acts as an isometry. On the HB the $SU(2)_R$ factor does. The CB describes the relative motion of the fractional branes along the singular locus. In this example, it corresponds to the differences $W_i - W_{i+1}$ in the eigenvalues of the operator $\hat{W}$. On the HB the branes form a bound state that reproduces the integral brane moving along $(\mathbb{C}^2/\Gamma)\backslash\{(0,0)\}$. The bound state is represented by the collective coordinates x, y, z satisfying equation 2.6. Consistently, Fayet-

Iliopulos terms deform the HB and eventually, excise the singularity (lift the CB).

2.2 D2-branes probing ADE fibrations

In this section, we review the main aspects of the worldvolume dynamics of a $D2$-brane probing ALE surfaces in Type IIA string theory. This will serve us as a starting point for introducing our approach to the study of Higgs field backgrounds in chapters 1 and 2. We will see that $D2$-branes constitute the natural probe in the context developed in [19, 25–27] and reviewed in the previous sections. We will briefly go through the generalities of 3d qfts with 8 supercharges: supersymmetry multiplets, moduli spaces, monopole operators. Then, we will present a 3d IR duality known as 3d mirror symmetry and relate it to string dualities. We will discuss examples of mirror pairs that will be our building blocks for the contents of Chapters 5 and 6. Finally, we will compare this approach with $D3$-brane probes in type IIB.

Let us consider once more the setup of M-theory compactified on ALE spaces. So far, we have analysed in detail the duality:

$$\text{M-theory on} \quad \mathbb{R}^{1,5} \times A_r \quad \Leftrightarrow \quad \text{r+1 D6 branes in Type IIA on} \quad \mathbb{R}^{1,6} \times \mathbb{R}^3 \tag{2.10}$$

We remind that this also holds for singularities of type D_r, with the complication of having an orientifold $O6^-$ plane on top of the $r+1$ $D6$-branes.

We consider the following situation. The $D6$ branes wrap coordinates $x_0, ..., x_6$, where x_4 is compactified to a circle of radius R. Accordingly, M-theory is now defined on $\mathbb{R}^{1,3} \times S^1_R \times \mathbb{C} \times \mathbb{C}^2/\mathbb{Z}_n$. Now we can reduce M-theory on S^1_R and obtain Type IIA string theory[2] on the background $\mathbb{R}^{1,3} \times \mathbb{C} \times \mathbb{C}^2/\mathbb{Z}_n$. So, now we have a duality of two distinct Type IIA configurations realized through the M-theory uplift:

$$\text{r+1 D6 branes in Type IIA on} \quad \mathbb{R}^{1,3}\times S^1_R\times\mathbb{C}\times\mathbb{R}^3 \quad \Leftrightarrow \quad \text{Type IIA on} \quad \mathbb{R}^{1,3}\times\mathbb{C}\times\mathbb{C}^2/\mathbb{Z}_n \tag{2.11}$$

We can start from M-theory and either reduce on the circle fibration of the ALE space, which would give the right-hand result, or reduce on the S^1_R and obtain the one on the left-hand. This duality is often called the 9-11 flip (x_9 and x_{11} were the coordinates parametrizing the two circles). In fact, the transition from one theory to the other can equivalently be obtained with the com-

[2]The low energy limit of Type IIA is the $g_s \to 0$ limit of 11d SUGRA compactified on a circle

position of T and S dualities: TST. When we reduce to S^1_R, the geometrically engineered theory becomes a 6d SYM gauge theory with 16 supercharges. The Higgs field Φ controlling complex deformations of the ALE is the massless mode of the KK reduction along S^1_R.

Now, if we add an $M2$-brane stretched along x_0, x_1, x_2 in M-theory, this will descend to a $D2$-brane probing the stack of $D6$ branes in one case, and the space $\mathbb{R} \times \mathbb{C} \times \mathbb{C}^2/\mathbb{Z}_{r+1}$ in the second.

At the singularity, the $D2$ will experience a similar fate to the $D3$, forming a stack of fractional states associated with the irreducible representations of the orbifold group $\mathbb{Z}_{r+1}$. The effective low-energy theory is a 3d quiver gauge theory with 8 supercharges, i.e., $\mathcal{N} = 4$ supersymmetry. Gauge and matter multiplets can be read from the dimensional reduction of 4d $\mathcal{N} = 2$ supersymmetry. We list here the bosonic components of vector multiplets and hypermultiplets in 3d.

$$\begin{array}{lllll} \text{Vector} & A_\mu & \sigma & \varphi \\ \text{Hyper} & & q & \tilde{q} \end{array} \tag{2.12}$$

The fourth component of the 4d vector is now a real scalar σ parametrizing the position of the $D2$ brane along S^1_R. φ is a complex scalar parametrizing motion along the $\mathbb{C}$-plane transverse to the $D2$ and the orbifold. q and $\tilde{q}$ are complex scalars in conjugate representations of the gauge group.

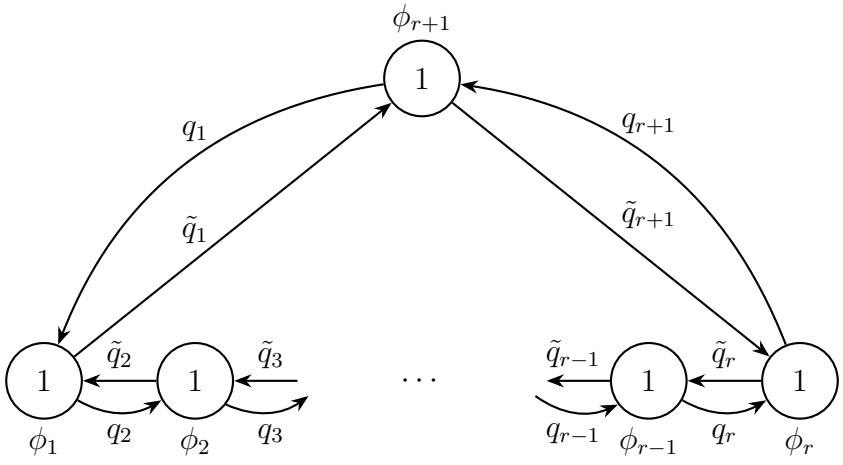

Figure 2.2: A_r theory. For each node i, $i = 1, ..., r+1$, there is a $\mathcal{N} = 4$ $U(1)$ vector multiplet V_i containing a $\mathcal{N} = 2$ vector multiplet and an adjoint chiral ϕ_i. Pairs of oriented lines between adjacent nodes represent bifundamental hypermultiplets $(q_i, \tilde{q}_i)$.

The quiver has the shape of the affine Dynkin diagram of the corresponding ADE Lie algebra [2]. Its nodes correspond to fractional D2-branes, and each node carries an $\mathcal{N}=4$ vector multiplet with gauge group $U(n_i)$, where n_i is the dual Coxeter label of the i-th node in the associated Dynkin diagram. Bifundamental hypermultiplets are represented in the quiver by pairs of arrows connecting adjacent nodes. Figure 6.2 illustrates the case of the A_r quiver.

For the A_r theory, the gauge group is

$$\left(\prod_{i=0}^{r} U(1)\right)/U(1)\,.$$

The vector multiplet chiral fields ϕ_i couple to the hypermultiplets $(q_i, \tilde{q}_i)$ through the $\mathcal{N}=4$ superpotential

$$W=\sum_{i=1}^{r+1}(\phi_i-\phi_{i-1})q_i\tilde{q}_i\,, \tag{2.13}$$

with $\phi_0 \equiv \phi_{r+1}$. In addition, the D-term potential imposes the relations

$$|q_i|^2+|\tilde{q}_{i-1}|^2-|\tilde{q}_i|^2-|q_{i-1}|^2=0 \qquad i=1,\dots,r+1\,. \tag{2.14}$$

Besides its dynamical deformations, the theory admits background deformations by mass parameters and FI terms. In the A_r case, there is a single complex mass parameter that cannot be reabsorbed by shifts of the fields ϕ_i; it can be interpreted as the scalar in a background vector multiplet for a $U(1)$ flavor symmetry [93]. Since the theory is three-dimensional, one may also turn on the corresponding real mass parameter. In addition, the theory possesses r triplets of FI parameters. Each triplet splits into a complex FI parameter, entering the superpotential, and a real FI parameter, modifying the D-term relations (6.37). These FI terms can be regarded as background vector multiplets for an additional rank-r flavor symmetry characteristic of three-dimensional gauge theories. Geometrically, the FI correspond to the sizes of the $\mathbb{P}^1$ cycles blown up in the resolution or deformation of the surface.

This extra symmetry is the *topological symmetry*. For each $U(1)$ factor in the gauge group, there is a conserved one-form current

$$J_T=*F=d\gamma\,,$$

which generates a $U(1)_T$ symmetry. γ is a compact scalar known as the dual photon. It represents the states charged under the topological symmetry, under which it shifts by multiples of $2\pi/g^2$. In many examples, this abelian symmetry is enhanced in the infrared to a non-abelian one [28, 94, 95]. In quiver gauge theories, this enhancement occurs when the nodes are balanced, namely when the number of flavors attached to a gauge node is twice its rank. For the quiver gauge theories living on a D2-brane probing an ADE singularity, the topological symmetry enhances precisely to the Lie group associated with the corresponding ADE algebra [33, 94, 95].

The operators charged under the topological symmetry are the *monopole operators*. These are local disorder operators[3] that are most naturally defined in the infrared conformal field theory [30]. In 3d Maxwell theory, they can be perturbatively defined in terms of an exponential of the scalar σ and of the dual photon:

$$V_{\pm} \sim e^{\frac{\pm}{g^2}(\sigma+i\gamma)} \tag{2.15}$$

Here, ± 1 is the charge under the topological $U(1)$.

For an abelian gauge group $U(1)^n$, the corresponding topological symmetry is $U(1)_T^n$, and monopole operators are labeled by their magnetic charges,

$$V_{m_1,\dots,m_n} \, .$$

For a non-abelian gauge group G of rank r, abelian monopole operators are similarly associated with the Cartan subalgebra $\mathfrak{h} \subset \mathfrak{g}$, and are labeled by magnetic charges $V_{m_1,\dots,m_{\mathsf{r}}}$. Gauge-invariant operators are obtained by taking Weyl-invariant combinations of these monopoles together with the complex scalars in the vector multiplets.

2.2.1 Moduli space of vacua

The moduli space of vacua splits into two branches, the Higgs branch (HB) and the Coulomb branch (CB). As opposed to the 4d case, in which the HB is HyperKhäler while the CB has a special Khäler structure, the two branches are both HyperKhäler. Aside from their perturbative definition, in terms of vevs of hypermultiplet and vector multiplet scalars, they can be distinguished non-perturbatively by their group of isometries. This is a $SU(2)$ subgroup of the R-symmetry $SU(2)_C \times SU(2)_H$. $SU(2)_H$ is the component acting on hypermultiplets in the doublet represen-

[3] When inserted in the path integral, a monopole operator imposes monopole-like boundary conditions for the gauge field, producing a magnetic flux through a sphere surrounding the insertion point.

tation, also present in 4d. $SU(2)_C$ is the non-abelian enhancement of the $U(1)$ that in 4d acts on the complex scalar in the vector multiplet. The scalars (σ, φ) form a triplet of $SU(2)_C$.

- The Higgs branch is classically exact. It is parametrized by vacuum expectation values of gauge-invariant combinations of hypermultiplet scalars, modulo the classical F-term relations. In quiver language, these operators correspond to closed paths in the quiver. For ADE quivers, the resulting Higgs branch is always a complex surface of dimension two, and in fact reproduces the ADE surface probed by the D2-brane.

  When the hypermultiplets acquire non-zero vevs, the gauge group is completely broken, up to the diagonal $U(1)$ which always decouples. From the brane point of view, this corresponds to recombining the fractional branes into a single D2-brane moved away from the singular point. The decoupled diagonal $U(1)$ describes the free center-of-mass multiplet, whose scalars parametrize the motion of the brane in the three directions transverse to the ADE surface.

- The Coulomb branch, by contrast, receives quantum corrections. At a generic point on this branch, the three real scalars in the $\mathcal{N} = 4$ vector multiplets acquire vacuum expectation values, breaking the gauge group to its maximal abelian subgroup. The remaining massless abelian gauge fields can then be dualized to scalars, and the Coulomb branch becomes a hyperkähler manifold whose metric is corrected quantum mechanically.

  In the $\mathcal{N} = 2$ language, an $\mathcal{N} = 4$ vector multiplet decomposes into an $\mathcal{N} = 2$ vector multiplet and an adjoint chiral multiplet. Quantum mechanically, the appropriate coordinates on the Coulomb branch are not just the classical vector multiplet scalars, but monopole operators [31]. Their vevs satisfy non-trivial relations. For example, in a 3d $\mathcal{N} = 4$ $U(1)$ gauge theory with N_f flavors, there are two basic monopole operators $V_\pm$ obeying

$$V_+ V_- = \prod_{i=1}^{N_f} M_i(\varphi, \mathrm{m}_j)\,, \tag{2.16}$$

  where $M_i(\varphi, \mathrm{m}_j)$ is the mass of the i-th hypermultiplet, expressed in terms of the complex scalar φ in the vector multiplet and the mass parameters m_j. When all m_j vanish, this reduces to

$$V_+ V_- = \varphi^{N_f}\,,$$

  showing that the Coulomb branch develops an A_{N_f-1} singularity. For higher-rank theo-

ries, the Coulomb branch geometry is more intricate, but monopole operators continue to provide its natural quantum coordinates.

Masses and FI parameters deform the two branches in complementary ways. In the $U(1)$ theory with N_f flavors, turning on complex masses deforms the Coulomb branch to a smooth space, while simultaneously lifting the Higgs branch by giving mass to the hypermultiplets. In ADE quiver gauge theories, FI parameters instead act naturally on the Higgs branch: turning on the FI parameter associated with a node corresponds to blowing up the corresponding cycle in the singular surface. Real FI parameters resolve the surface, while complex FI parameters deform it. From the string-theory perspective, these FI parameters arise from background vector multiplets associated with the topological symmetry. These vector multiplets are the 7d vectors that descend from the supergravity C_3 field and from wrapped $M2$-branes in the geometric engineering setup introduced at the beginning.

2.2.2 3d mirror symmetry

Both the Higgs and Coulomb branches are hyperkähler manifolds. This suggests the existence of pairs of theories in which the two branches are exchanged. More precisely, given a theory A with

$$\mathcal{M}_A = HB_A \times CB_A \,,$$

there may exist a theory B with

$$\mathcal{M}_B = HB_B \times CB_B,$$

such that

$$HB_A = CB_B \,, \qquad CB_A = HB_B \,.$$

This infrared duality is known as mirror symmetry [28]. In addition to exchanging Higgs and Coulomb branches, mirror symmetry maps FI parameters to masses, and masses to FI parameters.

One of its main advantages is that it translates the quantum problem of determining the Coulomb branch into the classical problem of studying the Higgs branch of the mirror theory. For ADE quivers, the mirror can be reconstructed directly from the brane setup by uplifting the type IIA configuration to M-theory and performing the 9–11 flip discussed in the previous section.

For instance, in the A_r case, a D2-brane probing the singular surface S_{sing} is mapped to a D2-

brane probing a stack of $r+1$ D6-branes in flat space. The quiver theory is then mirrored by a 3d $U(1)$ gauge theory with $r+1$ flavors. The mass parameter of the A_r quiver is mapped to the single FI parameter of the $U(1)$ theory, while the hypermultiplet masses m_j of the latter are mapped to the geometric moduli of the surface, encoded in background vector multiplets for the topological symmetry.

2.2.3 D2-branes probing an A_1 singularity and its mirror

We now turn to the simplest example, namely the A_1 singularity. This case illustrates explicitly the general discussion above and will serve as the basic building block for more complicated singularities.

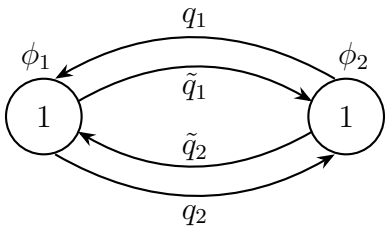

Figure 2.3: A_1 quiver.

The worldvolume theory of a D2-brane probing the A_1 singularity is a 3d $\mathcal{N}=4$ quiver gauge theory with the quiver shown in Figure 2.3 and superpotential

$$W_B = (\phi_1 - \phi_2)(q_1\tilde{q}_1 - q_2\tilde{q}_2)\,. \tag{2.17}$$

We refer to this theory as Theory B. One linear combination of the two $U(1)$ gauge factors decouples, so the interacting part is simply a $U(1)$ gauge theory with two hypermultiplets; the scalar in the coupled vector multiplet is

$$\phi_- \equiv \phi_1 - \phi_2\,.$$

This theory is self-mirror. Its mirror, which we call Theory A, is again a $U(1)$ gauge theory with two hypermultiplets, together with a decoupled hypermultiplet, and superpotential

$$W_A = \varphi(Q_1\tilde{Q}_1 + Q_2\tilde{Q}_2)\,. \tag{2.18}$$

In the type IIA picture, Theory A describes a D2-brane probing a stack of two D6-branes in flat space, which is related to the singular geometry of Theory B by the 9–11 flip.

Mirror symmetry exchanges gauge-invariant operators of Theory A and Theory B, and in particular swaps Higgs and Coulomb branch coordinates. In this simple example, the map is completely explicit [31]. The map between CB_B and HB_A is

$$\begin{pmatrix} \phi_- & w_+ \\ w_- & -\phi_- \end{pmatrix} \leftrightarrow \begin{pmatrix} Q_1\tilde{Q}_1 & Q_1\tilde{Q}_2 \\ Q_2\tilde{Q}_1 & Q_2\tilde{Q}_2 \end{pmatrix}, \tag{2.19}$$

where $w_\pm$ are the monopole operators of the relative $U(1)$ in Theory B, and the matrix on the right is the meson matrix of Theory A.

Similarly, the map exchanging HB_B and CB_A is

$$\begin{pmatrix} q_1\tilde{q}_1 & -q_1q_2 \\ \tilde{q}_2\tilde{q}_1 & -\tilde{q}_2q_2 \end{pmatrix} \leftrightarrow \begin{pmatrix} \varphi & -v_+ \\ v_- & -\varphi \end{pmatrix}, \tag{2.20}$$

where the left-hand side gives Higgs-branch coordinates of Theory B, while the right-hand side gives Coulomb-branch coordinates of Theory A.

This example makes manifest that mirror symmetry exchanges mesonic operators with monopole operators, and, more generally, that it maps the quantum description of one branch into the classical description of the other. This will be the basic mechanism repeatedly exploited in the following chapters.

2.2.4 The A_1 T-brane and $\mathcal{N} = 2$ mirror symmetry

In this section, we briefly show with a simple example how the T-brane backgrounds that were introduced in Section 6, are detected by the $D2$ probe[37]. For $SU(2)$, a T-brane is defined by the Higgs background

$$\Phi = \begin{pmatrix} 0 & 1 \\ 0 & 0 \end{pmatrix}. \tag{2.21}$$

Theory A

Let us first analyse its effect in the $D6$-brane vacuum picture. Here, the worldvolume theory on the $D2$ is $U(1)$ with 2 flavours, theory A, as we called it above. A vev for the Higgs field appears as a background mass deformation on the $D2$, which appears in the superpotential:

$$\Phi \neq 0 \quad \Longrightarrow \quad \delta_\Phi W \sim \mathrm{Tr}(\Phi Q \tilde{Q}). \tag{2.22}$$

For the profile in 2.21, the deformation is:

$$\delta_\Phi W_A = m Q_2 \tilde{Q}_1. \tag{2.23}$$

Note that the mass term breaks supersymmetry down to $\mathcal{N} = 2$ because Φ is non-diagonalizable (then, $[\Phi, \Phi^\dagger] \neq 0$). If we integrate out the massive fields, the effective superpotential yields:

$$W_{A,\,eff} = -\frac{1}{m}\varphi^2 Q_1 \tilde{Q}_2. \tag{2.24}$$

The effective theory has no flavour symmetry. The meson $Q_1\tilde{Q}_2$ is the only remnant of the originary HB, namely the $SU(2)$ instanton moduli space. It is reasonable to expect that the CB becomes

$$CB_A: \quad V_+ V_- = -\frac{1}{m}\varphi^2. \tag{2.25}$$

Indeed, we expect a singularity to appear in the CB when the charged chirals become massless. We can see that the deformation has left the singularity structure of the CB unchanged. Now let us exploit the $3d$ $\mathcal{N} = 4$ mirror symmetry to see what happens to the $D2$-brane probing the A_1 singularity with Φ turned on.

Theory B

Applying the mirror map 2.19, we get

$$\delta_\Phi W_A = m Q_2 \tilde{Q}_1 \quad \underset{mirror}{\longleftrightarrow} \quad \delta_\Phi W_B = m w_-. \tag{2.26}$$

The first observation to make is that the T-brane generates a monopole deformation in theory A. The authors in [37] showed that this is a good way to define what a T-brane is, which is

independent of the Type IIA construction. A way to reconstruct the RG flow triggered by 2.26 is to follow the effects on the mirror side and eventually apply mirror symmetry to the effective theory. However, mirror symmetry is no longer as well-defined as before, since monopole deformations break supersymmetry to $\mathcal{N} = 2$. Then, we lose the non-perturbative distinction between CB and HB. Nevertheless, when the $\mathcal{N} = 2$ 3d theory is obtained from a susy breaking deformation of a $\mathcal{N} = 4$ UV theory, it is still possible to identify a mirror map in the IR.[4] Let us illustrate the mechanism in this simple case. To derive the effective IR description of theory B, we need to understand what the dual of theory A is in the IR. Integrating out the massive fields has produced a $\mathcal{N} = 2$ supersymmetric theory with two electrons, a $U(1)$ gauge group, and the superpotential in equation 2.24. To derive its mirror, we first discuss the case of $U(1)$ with one flavor and vanishing superpotential.

$\mathcal{N} = 2$ $U(1)$ with 1 flavour and $W = 0$

We start from the $\mathcal{N} = 4$ parent theory, that is, $U(1)$ with one hypermultiplet. We deform the superpotential with a mass term for the chiral $\hat{\varphi}$:

$$W_{def} = \hat{\varphi} Q \tilde{Q} + X \hat{\varphi}. \tag{2.27}$$

Here, X is a singlet field acting as a Lagrange multiplier [31]. Upon integrating out $\hat{\varphi}$ we get

$$W_{eff} = 0. \tag{2.28}$$

$\mathcal{N} = 2$ mirror

The mirror of $U(1)$ with one hypermultiplet is a free hyper (Y, Z)[5]. So originally, there is no superpotential. The superpotential is generated by the deformation, which appears as:

$$W'_{eff} = XYZ. \tag{2.29}$$

[4] Usually there are consistency checks that can be made: list the symmetries on both sides, compare the superconformal indeces of the two theories, match the monopoles of one theory with the mesons of the other, and vice versa. We stress that mirror symmetry is a bit of a misnomer in $\mathcal{N} = 2$ susy theories. The duality is not related to the geometry of the branches in the moduli space. It should be conceived as a 3d Seiberg-like duality that acts by exchanging mesons and monopoles.

[5] This can be seen from the moduli space. The existence of a HB is excluded by the superpotential. The CB is $V_+ V_- = \hat{\varphi}$, which is isomorphic to $\mathbb{C}^2$.

This is the so-called XYZ model, whose moduli space is the union of the three cones spanned by X, Y, Z. Now we can treat the effective A theory as a deformation of 2.2.4 by the superpotential term 2.24. Then, the mirror is a XYZ model with a deformed superpotential:

$$W^B_{eff} = \frac{X}{m}(YZ - \varphi^2) = -\frac{X}{m}\det\mathfrak{M}. \tag{2.30}$$

The theory has a manifest $SU(2)$ global symmetry, under which fields (φ, Y, Z) transform as a triplet. The vevs of the matrix $\mathfrak{M}$ parametrize the nilpotent cone of A_1, that is, the $\mathbb{C}^2/\mathbb{Z}_2$ singularity probed by the $D2$-brane. The $SU(2)$ triplet is indeed the effective description of the 2 hypers of the original A theory. X is a neutral field that originally corresponded to the monopole w_+. It parametrizes what is left of the CB of theory A, that is, a $\mathbb{C}$-plane.

Therefore, we can draw the following conclusions:

- The monopole deformation breaks the topological symmetry completely and induces the condensation of the charged matter fields into gauge invariant operators, namely mesons (φ) and baryons (Y, Z).
- The monopole term can be interpreted as the signal of an obstruction to resolving the singularity. The signal is the absence of the real FI term that controls the volume of the exceptional $\mathbb{P}^1$, which only couples to the $U(1)$ gauge field.
- For monopole operators identified by a charge vector that corresponds to a simple root α of the ADE Lie algebra, the deformation has a local effect on the quiver gauge theory. It affects only the part of the spectrum that is charged under the $U(1)$ gauge factor corresponding to the dual Cartan element α^*. The effect of the deformation can be qualitatively described by removing the node associated with the $U(1)$ and composing the arrows across the node to form invariants.

Another confirmation of the identification between the monopole operator deformation and the T-brane configuration arises from the interpretation of three-dimensional monopole operators as wrapped $M2$-branes in the geometric engineering framework of M-theory. Upon reduction to Type IIA string theory, the $M2$-brane is mapped to a $D2$-brane wrapping the corresponding two-cycle. In this picture, the fractional $D2$-brane can equivalently be described as a $D4$-brane wrapped on the same two-cycle. From the perspective of the $D4$-brane worldvolume theory,

the wrapped $D2$-brane appears as a solitonic state that sources a non-trivial flux for the five-dimensional field strength.

From $D3$ to $D2$-probes As a final comment, let us highlight the connection between the $D3$-brane case discussed in Section 2 and that involving the $D2$. First, consider a $D3$ probing an ADE singularity in Type IIB string theory. Then, compactify to $S^1_{R'}$ one of the directions wrapped by the $D3$-brane. Let it be x_4 as in the case illustrated above. With a T-duality along S^1_R, we land on Type IIA. The circle is mapped to a new circle of radius $R = \sqrt{\alpha'}/R'$, and the $D3$ has become a $D2$-brane. This is precisely the configuration we have just described. The real scalar σ, parametrizing the position of the $D2$ along S^1_R, is mapped to the Wilson line of the 4d vector wrapping $S^1_{R'}$. The non-compact limit $R' \to \infty$ corresponds to $R \to 0$, a limit in which σ is forced to zero. In this limit, the Coulomb branch of the $D2$ collapses on its origin, but the Higgs branch survives untouched. This means that the moduli spaces of $D3$ and $D2$-probe reproduce the ALE geometry in the same way.

Before closing this section, we want to reinforce some key takeaways:

- Geometric singularities give rise to new localized brane states, known as fractional branes.
- A probe $D3$- or $D2$-brane can be understood as a bound state of a distinguished set of fractional branes, whose low-energy effective dynamics are described by a quiver gauge theory.
- The moduli space of the gauge theory reproduces the probed geometry across its various phases. In particular, the fully resolved phase corresponds to the regime in which all Fayet–Iliopoulos (FI) parameters are turned on. In this picture, the moduli space describes the motion of the $D3$- or $D2$-brane along the transverse directions, so that the probe is identified with a point on the ALE space.

  By contrast, fractional branes are not associated with points, but rather with 2-cycles: a fractional $D2$- (respectively $D3$-) brane can be understood as a $D4$- (respectively $D5$-) brane wrapped on an effective 2-cycle inside the Calabi–Yau geometry. Considering the worldvolume theory of a single wrapped brane, one finds that its moduli space is a complex line. This reflects the fact that the moduli space of deformations of the corresponding curve inside the

total space $ADE \times \mathbb{C}$ is isomorphic to the complex plane, over which the ADE singularity is trivially fibered.

Schematically, this correspondence can be summarized as

Gauge Theory Description	**Geometric Description**
fractional branes (wrapped branes)	stable sheaves on curves
probe brane	stable sheaves at points
fractional brane moduli space	moduli space of stable sheaves on curves
probe moduli space	moduli space of stable sheaves at points

As discussed previously, branes wrapped on effective curves within the geometry are identified with stable BPS states in the corresponding geometrically engineered theory—seven-dimensional in the case of trivially fibered ADE geometries, and five-dimensional for a generic Calabi–Yau threefold.

We conclude this review by relating the quiver gauge theory description to that of geometric engineering on the same Calabi–Yau threefold. In this framework, the quiver provides a natural language to describe and analyze the stability of coherent sheaves—or equivalently wrapped branes—on the threefold, thereby encoding the BPS spectrum of the corresponding five-dimensional theory. This perspective will serve as the starting point for the discussion of geometric engineering of five-dimensional SCFTs and BPS quivers in the next section.

Chapter 3

5d SCFTs, BPS quivers and geometric engineering

One of the most remarkable insights provided by string theory is the existence of interacting quantum field theories in spacetime dimensions greater than four. From the perspective of conventional quantum field theory, such theories are highly unexpected: perturbative arguments indicate that gauge theories in dimensions higher than four are non-renormalizable and therefore ill-defined in the ultraviolet. Nevertheless, string theory furnishes a geometric framework in which strongly coupled superconformal fixed points arise naturally, often without admitting any Lagrangian description.

Five-dimensional superconformal field theories provide a particularly subtle realization of this phenomenon. Their peculiarity can be understood from a simple scaling argument. In five dimensions, the Yang–Mills coupling has positive mass dimension, $[g^2_{YM}] = \text{mass}^{-1}$. As a consequence, the dimensionless effective coupling at an energy scale E behaves as

$$g^2_{\text{eff}}(E) \sim g^2_{YM}\, E\,.$$

It follows that the theory is infrared-free, becoming weakly coupled at low energies, whereas the effective coupling grows at high energies, signaling the breakdown of the perturbative description.

This behavior has an important conceptual implication. In contrast to four-dimensional theories, where non-trivial fixed points can often be identified by following the renormalization group

flow of a weakly coupled theory, in five dimensions, this strategy fails. The RG flow of a weakly coupled gauge theory always moves away from the ultraviolet regime where an interacting fixed point could exist. In this sense, the search for non-trivial 5d fixed points requires reversing the usual logic of quantum field theory: rather than flowing from weak to strong coupling, one must instead postulate the existence of a strongly coupled ultraviolet fixed point and understand weakly coupled gauge theories as deformations away from it.

Because of this intrinsic limitation of field-theoretic methods, geometric and string-theoretic constructions play a central role in the study of 5d SCFTs. Their existence was first uncovered through M-theory geometric engineering on singular Calabi-Yau threefolds [20, 38–41, 58, 64, 90, 96–100] and independently through Type IIB (p, q) five-brane webs [7–9, 11, 14, 15, 44, 87, 101–105], which provide a complementary description of the same fixed points. In these frameworks, the data of the quantum field theory—such as couplings, mass deformations, global symmetries, and BPS spectra—are encoded in the geometry of the threefold and its singular limits. In the following, we generalise the discussion on M-theory geometric engineering to generic Calabi-Yau threefolds and present a powerful tool to characterize the spectrum of stable particles of the SCFT: the BPS quiver. This review section is intended to guide the reader through chapter 7.

3.1 Geometric engineering on local CY3: generalities

In close analogy with the two-dimensional case discussed in Section 1.1, gauge and flavor symmetries in M-theory compactified on a local Calabi-Yau threefold X are encoded by harmonic two-forms. Let $\{\omega_I\}$ be a basis of $H^{1,1}(X)$. Expanding the three-form potential as

$$C_3 = A^I \wedge \omega_I + \cdots , \tag{3.1}$$

one obtains five-dimensional vector fields A^I. Normalizable two-forms, Poincaré dual to compact divisors $S_I \subset X$, give rise to dynamical vector multiplets, while non-normalizable two-forms, dual to non-compact divisors, correspond to background vector multiplets associated with flavor symmetries.

The charged BPS spectrum arises from wrapped branes. M2-branes wrapped on compact holomorphic curves $C \subset X$ give rise to electrically charged particles with charges

$$q_I = \int_C \omega_I = S_I \cdot C , \tag{3.2}$$

and masses

$$M_{M2}(C) = \int_C J\,, \tag{3.3}$$

where J is the Kähler form. M5-branes wrapped on compact divisors S_I instead give rise to magnetically charged strings, with tensions scaling as

$$T_{M5}(S_I) \sim \int_{S_I} J \wedge J\,. \tag{3.4}$$

This reflects the fact that M2-branes couple electrically to C_3, while M5-branes are magnetic sources.

The Kähler form admits an expansion

$$J = \phi^I \omega_I\,, \tag{3.5}$$

where the real scalars ϕ^I parameterize the Coulomb branch of the five-dimensional theory. The low-energy effective action is determined by a cubic prepotential

$$\mathcal{F}(\phi) = \frac{1}{6} C_{IJK}\, \phi^I \phi^J \phi^K\,, \tag{3.6}$$

where the coefficients are given by the triple intersection numbers of divisors,

$$C_{IJK} = S_I \cdot S_J \cdot S_K\,. \tag{3.7}$$

Non-abelian gauge symmetry arises when the compact divisors are ruled surfaces. Concretely, a ruled surface S is a fibration

$$\pi : S \to \Sigma \tag{3.8}$$

whose generic fiber is a rational curve $f \simeq \mathbb{P}^1$. M2-branes wrapped on the fiber class give rise to the W-bosons of the enhanced gauge symmetry, with masses

$$m_W \sim \int_f J\,, \tag{3.9}$$

which vanish when the fiber collapses. The volume of the base curve Σ instead controls the gauge

coupling,

$$\frac{1}{g_{\rm YM}^2} \sim \mathrm{vol}(\Sigma)\,. \tag{3.10}$$

The Dirac pairing between electric particles and magnetic strings in five dimensions is geometrically realized by the intersection pairing

$$H_4(X) \times H_2(X) \to \mathbb{Z}\,. \tag{3.11}$$

Indeed, an M2-brane wrapped on a compact curve C defines an electrically charged particle, while an M5-brane wrapped on a compact divisor S defines a magnetically charged string, and their pairing is given by the intersection number

$$\langle S, C\rangle = S \cdot C\,. \tag{3.12}$$

When the compact divisors are ruled surfaces and the shrinking fiber curves $f_i \simeq \mathbb{P}^1$ form an ADE configuration, these intersection numbers reproduce the Cartan matrix of the enhanced gauge algebra,

$$S_j \cdot f_i = -\,C_{ji}\,, \tag{3.13}$$

up to conventions. Thus the wrapped M2-branes on the fiber classes give the W-bosons associated with the simple roots, while the wrapped M5-branes on the compact divisors give the magnetic strings associated with the dual coroot lattice.

The Kähler moduli thus parameterize the extended Coulomb branch, including mass deformations associated with non-compact divisors, which correspond to non-dynamical background fields. In contrast, complex structure deformations are parameterized by $H^{2,1}(X)$ and are encoded in the periods of the holomorphic three-form Ω over a symplectic basis of three-cycles $(A^I, B_I) \subset H_3(X, \mathbb{Z})$,

$$X^I = \int_{A^I} \Omega\,, \qquad \mathcal{F}_I = \int_{B_I} \Omega\,, \tag{3.14}$$

with intersection pairing

$$A^I \cap B_J = \delta^I{}_J\,, \qquad A^I \cap A^J = 0\,, \qquad B_I \cap B_J = 0\,. \tag{3.15}$$

In the local, non-compact setting, only normalizable complex structure deformations correspond to dynamical fields in the five-dimensional theory. These are associated with compact

three-cycles and arise in symplectic pairs, ensuring a well-defined period structure. Normalizability guarantees finite kinetic terms and thus identifies genuine moduli. From the field theory perspective, these modes correspond to Higgs branch directions, as they describe finite-energy deformations smoothing the singular geometry. Non-normalizable deformations, on the other hand, modify the asymptotic structure of the Calabi-Yau and are interpreted as background parameters rather than vacuum expectation values of dynamical fields.

Remark. For non-compact Calabi-Yau threefolds, the structure of three-cycles differs from the compact case. In particular, compact three-cycles need not organize into symplectic pairs among themselves. While for compact Calabi–Yau threefolds the intersection pairing defines a non-degenerate symplectic form on $H_3(X, \mathbb{Z})$, in the non-compact case, the natural non-degenerate pairing involves compact and relative homology, schematically

$$H_3^{\mathrm{cpt}}(X) \times H_3(X, \partial X) \to \mathbb{Z}\,. \tag{3.16}$$

As a consequence, the intersection form restricted to compact three-cycles may be degenerate. The number of compact three-cycles that do not admit a compact dual—that is, the number of "unpaired" cycles—is given by the dimension of the kernel of this restricted intersection form. A simple example is provided by the deformed conifold, where a single compact S^3 appears without a compact dual cycle, the latter being non-compact. From the physical viewpoint, these unpaired compact three-cycles correspond to normalizable complex structure deformations that are not paired within the compact sector, but still give rise to genuine Higgs branch moduli in the five-dimensional theory.

3.2 5d SCFTs and BPS quivers

The BPS spectrum of M-theory on a Calabi-Yau threefold X is generated by wrapped M2- and M5-branes. These configurations preserve supersymmetry because the relevant wrapped cycles are calibrated: M2-branes wrap holomorphic curves, calibrated by the Kähler form J, while M5-branes wrap holomorphic divisors, calibrated by $\frac{1}{2}J \wedge J$. Since the volumes of the wrapped cycles are the masses of the branes, and calibrated cycles minimize volume in their homology class, the wrapped branes saturate the BPS bound

$$|Z(\gamma)| \leq M(\gamma). \tag{3.17}$$

Where γ is the charge vector of the $M2$ or $M5$ brane state, and Z is the central charge of the supersymmetry algebra, evaluated on the state. In order to study the BPS spectrum on the Coulomb branch while avoiding a direct treatment of tensionless strings, it is convenient to compactify the five-dimensional theory on the M-theory circle and consider the resulting four-dimensional $\mathcal{N} = 2$ Kaluza–Klein theory. Under the M-theory/type IIA duality, an M2-brane wrapped on a compact curve C descends to a D2-brane wrapped on C, while Kaluza–Klein momentum along the circle becomes D0-brane charge. Similarly, an M5-brane wrapped on a compact divisor S and on the external circle gives a D4-brane wrapped on S, which appears as a particle in four dimensions. Therefore, the charge lattice of BPS particles in the KK theory is naturally identified with the even compact homology

$$\Gamma_{\rm BPS} \;\cong\; H^{\rm cpt}_{\rm even}(X,\mathbb{Z}) \;=\; H^{\rm cpt}_0(X,\mathbb{Z}) \oplus H^{\rm cpt}_2(X,\mathbb{Z}) \oplus H^{\rm cpt}_4(X,\mathbb{Z}) \cong \mathbb{Z}^{2r+f}\,, \tag{3.18}$$

corresponding respectively to D0-, D2- and D4-brane charges. The integers r and f are respectively the rank of the Coulomb branch and the number of conserved flavour charges, including the KK momentum

Actually, this correspondence can be reformulated as an equivalence between the BPS category of the 5d theory compactified on a circle and the bounded derived category of coherent sheaves with compact support on a crepant resolution $\widetilde{X}$ of the singular Calabi-Yau [106]:

$$\mathcal{T}_{\rm BPS}\big(D_{S^1}T^{5d}_X\big) \;\simeq\; D^b\big(\mathrm{Coh}_{\rm cpt}(\widetilde{X})\big)\,. \tag{3.19}$$

From the type IIA viewpoint, the relevant BPS particles are thus D0/D2/D4 bound states, and in the B-model description, they are represented by B-branes, namely objects of the derived category. This provides a categorical framework in which questions about the BPS spectrum are translated into questions about stable objects in $D^b(\mathrm{Coh}_{\rm cpt}(\widetilde{X}))$.

The interpretation of wrapped branes in terms of objects in the derived category of sheaves allows us to shed new light on the mysterious connection between branes at singularities and quivers. In the review section 2.1, we have discussed the generation of fractional brane states at orbifold singularities, and we have seen how fractional branes give rise to gauge theories that are naturally described by a quiver. In this description, a configuration of fractional branes is a representation of the quiver path algebra, and the stable representations correspond to the supersymmetric vacua of the gauge theory associated with the fractional brane configuration. Finally, we have argued that fractional branes are nothing but bound states of higher-dimensional branes

wrapped on the vanishing cycles of the singular geometry.

Indeed, the mathematical reason for the appearance of the quiver is the existence, in many relevant non-compact Calabi-Yau examples, of a derived equivalence between coherent sheaves on the resolution and modules over a noncommutative crepant resolution, often realized concretely as the Jacobian algebra of the quiver with potential[1]. In CY orbifold examples, a non-commutative crepant resolution of the space always exists and is represented by a quiver of Dynkin shape. The representation theory of the quiver is the derived category of coherent sheaves on the resolved space and its equivariant structure under the orbifold group is dictated by the derived McKay correspondence [107].
In general, when a suitable tilting object exists, one has an equivalence of triangulated categories of the schematic form

$$D^b\big(\mathrm{Coh}(\widetilde{X})\big) \;\simeq\; D^b\big(\text{mod-}A\big)\,, \tag{3.20}$$

where A is the relevant quiver algebra.

Now, from equivalences 3.19 and 3.20 we argue that the physically stable BPS particles correspond to stable objects in the derived category, which in the quiver description become stable representations in the sense of King [108]. In this way, the notions of stable BPS state, stable quiver representation, and stable coherent sheaf are different incarnations of the same underlying concept. It follows that the spectrum of stable particles in the five-dimensional theory, after compactification on a circle, can be studied through the representation theory of the associated BPS quiver.

A BPS quiver provides an effective description of the spectrum of stable states in a given chamber of the moduli space. It encodes a choice of basis of elementary BPS states, whose charges $\{\gamma_i\}$ generate the charge lattice in that chamber. Each node of the quiver corresponds to one such elementary state, while the arrows are determined by the Dirac pairing

$$\langle \gamma_i, \gamma_j \rangle \in \mathbb{Z}\,, \tag{3.21}$$

so that the antisymmetric adjacency matrix of the quiver coincides with the Dirac pairing matrix:

$$B_{ij} = (\#\text{ arrows } i \to j) - (\#\text{ arrows } j \to i), \tag{3.22}$$

Flavour charges have by definition zero Dirac pairing with everything, so that having the matrix

[1]Look at Appendix D for the definition of quiver path algebras and algebras with potential

B, we can immediately identify the flavour and Coulomb charges respectively as

$$\Gamma_f = \ker B, \qquad \Gamma_c = \Gamma_c = \mathrm{coker} B, \tag{3.23}$$

i.e.

$$f = \dim \ker B, \qquad 2r = \mathrm{rk}\, B. \tag{3.24}$$

In this way, the quiver captures both the charge lattice and the structure of electromagnetic interactions among BPS particles. In the geometric engineering framework, the charge vectors are identified with elements of $H^{\mathrm{cpt}}_{\mathrm{even}}(X, \mathbb{Z})$, so that the Dirac pairing is inherited from the intersection pairing of the Calabi–Yau threefold.

From a physical perspective, quiver representations describe BPS bound states and admit an interpretation in terms of supersymmetric quantum mechanics on the worldline of the corresponding particle. Given a charge $\gamma = \sum_i d_i \gamma_i$, one associates a representation of the quiver with dimension vector $\mathbf{d} = (d_i)$, whose dynamics is governed by a one-dimensional $\mathcal{N} = 4$ supersymmetric quantum mechanics determined by the quiver and its superpotential. The classical moduli space of vacua of this quantum mechanics coincides with the moduli space of stable quiver representations, and upon quantization, its cohomology encodes the protected quantum numbers of the BPS state. In particular, BPS indices can be computed in terms of topological invariants of these moduli spaces.

To sum up, we can rephrase the chain of equivalences in this way

$$\left\{ \begin{array}{c} \text{BPS state with} \\ \text{charge } \underline{\gamma} \end{array} \right\} \leftrightarrow \left\{ \begin{array}{c} \text{Coherent sheaf with} \\ \text{Chern vector} \\ \underline{\gamma} \in K_0 D_c(X) \end{array} \right\} \leftrightarrow \left\{ \begin{array}{c} \text{Representation of A with} \\ \text{dimension vector} \\ \underline{\gamma} \end{array} \right\} \tag{3.25}$$

The BPS quiver, therefore, constitutes a fundamental datum in the analysis of the spectrum of BPS states. For cDV geometries, the associated quivers are unoriented and endowed with a comparatively simple algebra of relations, rendering their representation theory amenable to direct analysis; this is developed in detail in Appendix D. In contrast, for higher-rank theories, the structure of the quiver becomes considerably more intricate, and for generic Calabi-Yau threefolds, a corresponding BPS quiver is, in general, not known.

In 7, we will demonstrate that the Reid Pagoda, one of the simplest examples of simple flops,

admits orbifold quotients that possess crepant resolutions. These resolutions are naturally encoded by quivers, which we construct via the generalised McKay correspondence [107]. This framework constitutes a substantial refinement of the classical McKay correspondence and, crucially, enables one to deduce information about the BPS spectrum of quotient geometries from the analysis of the spectrum of the parent geometry[109–111].

Chapter 4

The geometric toolkit: Algebraic Spaces and Singularities

By definition, a Calabi–Yau manifold is a compact Kähler manifold with vanishing first Chern class. By Yau's solution of the Calabi conjecture, such a manifold admits a unique Ricci-flat Kähler metric in each Kähler class, thereby providing the geometric input required by the low-energy effective theory (Ricci-flatness is necessary to have at most $SU(n)$ holonomy). The Kähler condition equips the manifold with a symplectic form compatible with an integrable complex structure, implying that deformations of the metric split into complex structure and Kähler moduli governed by Dolbeault cohomology. As a consequence, many physically relevant quantities—such as superpotentials, BPS observables, and protected couplings—depend holomorphically on the moduli and are therefore stable under perturbative quantum corrections. These holomorphic and cohomological structures are naturally and efficiently encoded within algebraic geometry. Moreover, by Kodaira's embedding theorem, any compact Kähler manifold with integral Kähler class admits a projective embedding; in particular, smooth complex projective varieties are automatically Kähler, placing a large and physically relevant class of supersymmetric compactification spaces within the category of algebraic varieties. Beginning in the 1990s, further impetus for this algebraic–geometric perspective arose from the study of string theory dynamics near singular limits of Calabi–Yau moduli spaces, particularly in the neighborhood of orbifold points. In such limits, smooth Calabi–Yau manifolds degenerate to singular spaces that nonetheless remain physically meaningful within string theory. It was observed that, in type IIA and type IIB compactifications, the effective physics localized near codimension-four singularities is governed by ADE Lie alge-

bras, appearing through gauge symmetry enhancement and the emergence of additional massless degrees of freedom. This phenomenon generated a strong interest in the classification of singular degenerations of K3 surfaces—where the ADE correspondence plays a fundamental role—and later of Calabi–Yau varieties in higher dimensions. As emphasized in the analysis of Witten [Witten, 2002, singularities in string theory], such singular spaces should not be regarded as pathological but rather as essential loci encoding genuinely non-perturbative physics.

From a mathematical standpoint, singular geometries are most precisely described as algebraic varieties, which we are now going to introduce.

The goal of this chapter is to introduce the geometric tools that will be used throughout the thesis to analyze singular spaces and extract their physical content. We begin with the local definition of algebraic singularities and the criteria that distinguish smooth and singular points. We then introduce the two fundamental operations that control their behavior—resolutions and deformations—and explain their geometric and physical interpretation.

A central theme of this chapter is that, for a distinguished class of singularities, these structures are governed by Lie-theoretic data. This is exemplified by ADE surface singularities, whose resolutions, deformations, and intersection theory are controlled by root systems and Weyl groups. Building on this correspondence, we introduce families of deformed ADE spaces and show how they naturally lead to higher-dimensional singular geometries, in particular compound Du Val (cDV) threefolds.

Finally, we place these constructions within the broader framework of the classification of threefold singularities and their crepant resolutions, emphasizing the role of flops and their algebraic description via quivers and noncommutative resolutions. These tools will provide the mathematical backbone for the physical constructions developed in the subsequent chapters.

4.1 What is an algebraic singularity?

We begin with the simplest possible setting: algebraic curves in the complex plane.

A first example: a singular plane curve

Consider the plane curve $C \subset \mathbb{C}^2$ defined by the equation

$$f(x, y) = y^2 - x^3 = 0. \tag{4.1}$$

Geometrically, this curve has a cusp at the origin. While the curve is well defined as a set, the point $(0, 0)$ is distinguished from all other points by the fact that the curve fails to be locally smooth there.

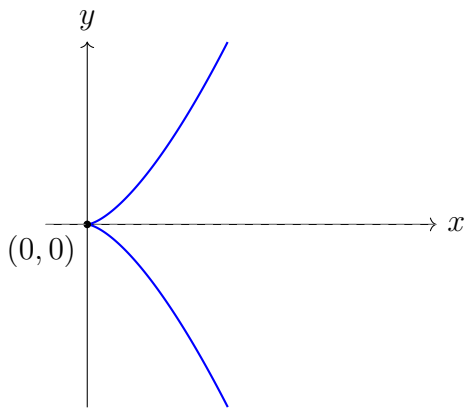

Figure 4.1: Projection on the real plane of the hypersurface: $y^2 - x^3 = 0$

To make this precise, note that the gradient of f is given by

$$\nabla f = \left(\frac{\partial f}{\partial x}, \frac{\partial f}{\partial y} \right) = (-3x^2,\ 2y). \tag{4.2}$$

At the origin, both partial derivatives vanish:

$$\nabla f(0, 0) = (0, 0).$$

This failure of the gradient to be nonzero signals the presence of a singularity.

By contrast, at any other point on the curve, ∇f does not vanish, and the curve is locally a smooth one-dimensional complex manifold.

Smooth points and the Jacobian criterion

This example illustrates the general principle underlying the definition of algebraic singularities. Let

$$X = \{f_1 = \cdots = f_k = 0\} \subset \mathbb{C}^n,$$

be an affine algebraic variety defined by holomorphic polynomials f_i.

The *Jacobian matrix* of the defining equations is

$$J(p) = \left(\frac{\partial f_i}{\partial x_j}(p) \right). \tag{4.3}$$

Definition 4.1.1 (Smooth and singular points)**.** A point $p \in X$ is called *smooth* if the Jacobian matrix has maximal rank at p, i.e.

$$\operatorname{rank} J(p) = n - k.$$

If this condition fails, the point p is called a *singular point* of X.

Equivalently, a point is smooth if X is locally biholomorphic to $\mathbb{C}^{n-k}$ in a neighborhood of that point.

The set of all singular points is called the *singular locus* of X and is denoted by $\operatorname{Sing}(X)$.

An intrinsic definition

The Jacobian criterion provides a concrete computational tool, but the notion of singularity admits an intrinsic formulation independent of any embedding.

Let $\mathcal{O}_{X,p}$ denote the local ring of regular functions on X at a point p, with maximal ideal $\mathfrak{m}_p$.

Definition 4.1.2 (Intrinsic definition)**.** A point $p \in X$ is *smooth* if the local ring $\mathcal{O}_{X,p}$ is a regular local ring, i.e.

$$\dim_{\mathbb{C}} \mathfrak{m}_p/\mathfrak{m}_p^2 = \dim X.$$

If this condition is not satisfied, p is a singular point.

This definition reflects the fact that, at a smooth point, the tangent space has the expected dimension, while at a singular point the Zariski tangent space is larger than the dimension of the

variety, signaling a local failure of smoothness.

In the following sections, we show how different types of singularities admit controlled modifications, such as resolutions and smoothings, and how these operations acquire a natural physical interpretation.

4.1.1 Resolving singularities: the blow-up

One of the fundamental ways to study and modify a singular space is through a *resolution of singularities*. Intuitively, a resolution replaces a singular point by a smooth geometric object that encodes the local structure of the singularity.

Blow-up of a point: a basic example

We illustrate the idea with the simplest nontrivial example. Consider the affine plane $\mathbb{C}^2$ with coordinates (x, y) and its origin $(0, 0)$. The *blow-up of* $\mathbb{C}^2$ *at the origin* replaces the point $(0, 0)$ by the space of complex lines passing through it.

Concretely, the blow-up $\widetilde{\mathbb{C}^2}$ can be defined as

$$\widetilde{\mathbb{C}^2} = \left\{(x, y, [u : v]) \in \mathbb{C}^2 \times \mathbb{P}^1 \;\middle|\; xv = yu\right\}, \tag{4.4}$$

with the projection map

$$\pi : \widetilde{\mathbb{C}^2} \to \mathbb{C}^2$$

given by forgetting the $\mathbb{P}^1$ coordinate.

Away from the origin, π is an isomorphism. The inverse image of the origin,

$$E = \pi^{-1}(0, 0) \simeq \mathbb{P}^1,$$

is called the *exceptional divisor*. It replaces the singular point with a smooth curve that records the possible tangent directions at the origin.

4.1.2 Resolution of surface singularities

Blow-ups can be used to resolve singularities of algebraic varieties. For instance, consider the A_1 surface singularity

$$X : uv = z^2 \subset \mathbb{C}^3. \tag{4.5}$$

This space has an isolated singular point at the origin. A suitable sequence of blow-ups replaces the singular point by a smooth rational curve $\mathbb{P}^1$, yielding a smooth surface $\widetilde{X}$ together with a map

$$\pi : \widetilde{X} \to X,$$

That is an isomorphism away from the singular point. A simple realization of the resolved geometry is given by the following embedding in $\mathbb{C}^3 \times \mathbb{P}^1$:

$$\tilde{X} = \left\{ (u, v, z, [\lambda_4 : \lambda_1]) \in \mathbb{C}^3 \times \mathbb{P}^1 | \quad uv = z^2, \quad \begin{pmatrix} z & u \\ -v & -z \end{pmatrix} \cdot \begin{pmatrix} \lambda_4 \\ \lambda_1 \end{pmatrix} = 0 \right\}.$$

It is easy to see that $\tilde{X}$ is isomorphic to the original space away from the singularity. Indeed, the linear system has a unique solution when the rank of the matrix is 1, which is a point on $\mathbb{P}^1$. Consequently, the inverse map π^{-1} associates to any point $(u, v, z) \neq (0, 0, 0)$ on the surface a point on $\mathbb{P}^1$. Only when $(u, v, z) = (0, 0, 0)$, the kernel of the matrix is the full $\mathbb{P}^1$, which means that $\pi^{-1}(0, 0, 0) \simeq \mathbb{P}^1$. It is important to stress that the resolution map is not uniquely defined. Indeed, there are various equivalent ways to resolve a singularity. For a comprehensive introduction, we suggest [112–114]

More generally, the minimal resolution of an ADE surface singularity replaces the singular point by a collection of $\mathbb{P}^1$ curves whose intersection pattern reproduces the Dynkin diagram of the corresponding ADE Lie algebra. This structure plays a central role in both algebraic geometry and string theory, as we will see shortly.

Definition of resolution

Definition 4.1.3 (Resolution of singularities)**.** Let X be an algebraic variety. A *resolution of singularities* of X is a smooth variety $\widetilde{X}$ together with a proper birational morphism

$$\pi : \widetilde{X} \to X,$$

such that π restricts to an isomorphism over the smooth locus of X.

In this thesis, we will always consider resolutions that are crepant, namely, such that they preserve the canonical bundle of the singular geometry. From the physical perspective, resolutions are typically associated Kähler deformation parameters and correspond to Coulomb-branch or tensor-branch directions in the geometrically engineered quantum field theory.

4.1.3 Smoothing singularities

An alternative way to eliminate a singularity is through a *smoothing*, which deforms the complex structure rather than modifying the space birationally.

A simple smoothing example

Returning to the A_1 singularity,

$$f : uv - z^2 = 0, \tag{4.6}$$

a smoothing is obtained by deforming the defining equation to

$$f_{def} : uv - z^2 = \epsilon, \tag{4.7}$$

where $\epsilon \in \mathbb{C}$ is a deformation parameter. For $\epsilon \neq 0$, the space is smooth (the origin of the ambient space is excised from the surface), and the singular point is replaced by a non-holomorphic $\mathbb{P}^1$ cycle.

Definition of versal deformation

Definition 4.1.4 (Versal deformation)**.** Consider a hypersurface singularity X defined as the zero locus of a polynomial $F(x_1, .., x_n)$ in $\mathbb{C}^n$. The versal deformation of X is a family of varieties

$$\begin{array}{c} \mathcal{X} \\ \downarrow \\ Def(X) \end{array}$$

over the space $Def(X)$ such that the central fiber is X, while all nearby fibers are smooth.

$\mathcal{X}$ is defined as the zero locus of the equation:

$$F_{def} = F(x_1, .., x_n) + \sum_i^r \delta_i(x_1, ..x_n)\epsilon_i, \quad \delta_i \in \mathcal{R}_{def}, \quad \epsilon_i \in \mathbb{C}^r. \tag{4.8}$$

The complex coefficients ϵ_i are the moduli of the deformation, spanning $Def(X)$. Monomials $\delta_i(x_1, ..x_n)$ are the generators of the ring:

$$\mathcal{R}_{def} = \frac{\mathbb{C}[x_1, ..., x_n]}{\langle \nabla F \rangle},$$

where $\langle \nabla F \rangle$ denotes the ideal generated by the Jacobian of the function F. Intuitively, $\mathcal{R}_{def}$ encodes the normal directions to the hypersurface in the ambient space $\mathbb{C}^n$

In geometric engineering setups, smoothings are typically associated with Higgs-branch deformations, corresponding to turning on expectation values for matter fields. Unlike resolutions, which preserve the complex structure, smoothings alter it, leading to qualitatively different physical phases.

Resolution and smoothing are inequivalent operations that reflect distinct geometric and physical mechanisms: Resolutions modify the geometry by introducing exceptional cycles, while preserving the complex structure. Smoothings deform the complex structure and eliminate the singularity without introducing exceptional divisors.

In higher-dimensional Calabi-Yau varieties, a singularity may admit a resolution, a smoothing, both, or neither. The distinction between these possibilities plays a central role in string theory and will be particularly important in the study of compound Du Val singularities discussed later in this thesis.

A crucial and far-reaching observation in the study of algebraic singularities is that their local geometry is invariant under analytic changes of coordinates. More precisely, two hypersurface singularities defined by equations

$$f(x_1, \ldots, x_n) = 0 \qquad \text{and} \qquad g(x_1, \ldots, x_n) = 0,$$

are considered *analytically equivalent* if there exists a local biholomorphic change of coordinates transforming one equation into the other. From a geometric point of view, analytically equivalent equations describe the same singularity, even though their explicit algebraic expressions may

differ substantially.

This principle led, beginning in the 1960s, to the systematic classification of isolated hypersurface singularities up to analytic equivalence. One of the most prominent and influential outcomes of this program is the classification of the so-called *simple* singularities, also known as *rational double points* or *du Val singularities*.

4.2 ADE classification and McKay correspondence

The Du Val (or ADE) surface singularities form a distinguished class of isolated hypersurface singularities in complex dimension two. All of them are terminal, in the sense that they admit a minimal resolution in which the exceptional locus contains only a collection of rational curves (or $\mathbb{P}^1$). The resolution is also crepant, for the canonical bundle of the smooth geometry is simply pulled back from the canonical bundle of the singular space.

The Du Val are examples of quotient singularities, namely orbifolds of the form $\mathbb{C}^2/\Gamma$, with Γ a discrete subgroup of $SU(2)$[1] They admit a complete classification up to analytic equivalence and exhibit properties that relate them to the root systems of the simply-laced Lie algebras:

$$\mathfrak{g} = \Big\{ A_n, \quad D_n, \quad E_6, \quad E_7, \quad E_8 \Big\}.$$

This connection is due to a correspondence between the list of $\Gamma \subset SU(2)$ (namely, the binary polyhedral groups) and the ADE Dynkin diagrams, first detected and proven by McKay [115].

In the next paragraph, we describe both resolutions and deformations of Du Val singularities without any intention of being exhaustive, but to highlight the connection with simply laced Lie algebras.

It is known that all these singularities emerge from singular limits of local $K3$ surfaces or ALE spaces. The term 'local' indicates that we are examining only the space in proximity to the singularity, which is equivalent to considering the space as a non-compact limit of a $K3$.

$K3$ surfaces have a very special feature, the so-called hyperkäler structure. Let us briefly explain what it means.

[1] Why not a subgroup of SO(4)? The restriction is due to the crepancy requirement.

Definition 4.2.1 (Hyperkäler Structure)**.** A complex manifold $\mathcal{M}$ of dimension n is hyperkähler if:

- $\mathcal{M}$ admits a complete kähler metric g[2]
- There exist three independent choices of complex structures (I_1, I_2, I_3) with respect to which g is kähler
- The complex structures I_i form a quaternion algebra

In other words, the real dimension of $\mathcal{M}$ must be $4k, \quad k \in \mathbb{N}$, and the holonomy group must be in Sp(k). This is required to represent the tangent space as a quaternionic space, because it guarantees that the holonomy acts linearly with respect to the three complex structures I_i[3]. In our case, which is $k = 1$, the group of rotations in $\mathbb{R}^4$ is:

$$SO(4) \simeq \frac{SU(2)_+ \times SU(2)_-}{\mathbb{Z}_2}.$$

Now consider the adjoint representation of $SO(4)$. As occurs for any $SO(2n)$ group, the adjoint coincides with the antisymmetric 2-tensor representation. In this space, the antisymmetric Levi-Civita tensor acts as an involution, implying that the representation splits into a direct sum of two eigenspaces: the self-dual and the antiself-dual tensors. Self-dual tensors transform in the adjoint of the $SU(2)_+$ subgroup and are invariant under $SU(2)_-$. Vice versa holds for antiself-dual tensors. In a hyperkähler surface, the Ricci tensor is antiself-dual, or equivalently, the holonomy is in the factor $SU(2)_-$, and the three Kähler forms ω_i (remind that $\omega_i = g(\cdot, I_i \cdot)$ associated to the metric g and the complex structures I_i are self-dual. In other words, the ω_i form an invariant subspace under the holonomy group. We shall see that the existence of an $SO(3)$ symmetry acting on the ω_i renders deformations and resolutions of ADE singularities essentially equivalent. By contrast, in the case of Calabi–au threefolds, these two procedures constitute fundamentally distinct geometric operations.

[2]The fact that $\mathcal{M}$ is complex implies that the Riemannian metric g is preserved by an integrable almost complex structure I:

$$g(u, v) = g(Iu, Iv), \forall u, v \in T\mathcal{M}$$

. The metric being kähler means that the associated two-form ω is compatible with I, in the sense that $g(\cdot, \cdot) = \omega(\cdot, I\cdot)$, and ω is symplectic and closed.

[3]The corresponding Kahler forms define a subspace of the adjoint rep of $SO(4k)$ that is left invariant by Sp(k)

4.2.1 Resolutions and exceptional spheres

Let $\tilde{X}$ denote the minimal resolution of an ADE singularity:

$$\begin{array}{c} \tilde{X} \\ \downarrow \quad \pi \\ X \end{array}$$

The exceptional locus $\pi^{-1}(0) \in \tilde{X}$ consists of a union of smooth rational curves (namely, curves isomorphic to the projective line):

$$E = \bigcup_{i=1}^{r} S_i, \qquad S_i \simeq \mathbb{P}^1,$$

where r is the rank of the associated ADE Lie algebra. These curves generate the compact homology

$$H_2(X, \mathbb{Z}) \cong \mathbb{Z}^r.$$

The smooth geometry admits r independent harmonic normalizable (or compactly supported) two forms, and a non-normalizable one η_{r+1}. [4] One can check that it is always possible to identify a basis η_i such that:

$$\int_{S_j} \eta_i = S_j \cdot S_i = -\alpha_i \cdot \alpha_j, \tag{4.9}$$

where $\alpha_i \cdot \alpha_j$ is the Cartan matrix of the corresponding ADE Lie algebra. Explicitly,

- $S_i \cdot S_i = -2$,
- $S_i \cdot S_j = 1$ if nodes i, j are adjacent in the Dynkin diagram,
- $S_i \cdot S_j = 0$ otherwise.

This identifies the configuration of exceptional curves with the Dynkin diagram of the ADE algebra. Each S_i can be identified with the simple root α_i. The η_i are naturally associated with the generators of the Cartan algebra in the Chevalley basis. The only non-normalizable form is

[4] In this case, each normalizable form is Poincaré dual to a compact divisor, which is one of the S_i.

Poincaré dual to a non-compact divisor D_{r+1} such that:

$$\alpha_k \cdot \alpha_{r+1} = \int_{S_k} \eta_{r+1} = S_k \cdot D_{r+1} = d_k, \tag{4.10}$$

where α_{r+1} corresponds to the opposite of the highest root, and d_k are the Dynkin labels (weights of the highest root in the coroot basis). [5]

4.2.2 Root lattice and hyperkähler structure

As anticipated, from the Kähler metric, one can construct three possible Kähler forms:

$$\omega_i = g(v, I_i w), \quad v, w \in T\mathcal{M}.$$

For each exceptional sphere S_k, one defines the hyperkähler period vector

$$\vec{\xi}_k = \left(\int_{S_k} \omega_1, \int_{S_k} \omega_2, \int_{S_k} \omega_3 \right) \in \mathbb{R}^3. \tag{4.11}$$

which rotates under the symmetry $SU(2)_+$.

In the complex structure I_1, the holomorphic symplectic form is

$$\Omega_1 = \omega_2 + i\,\omega_3,$$

In terms of which one constructs the complex periods:

$$T_k = \int_{S_k} \Omega_1 = \xi_k^{(2)} + i\xi_k^{(3)} = \alpha_k(h) \in \mathbb{C}, \quad h \in \mathfrak{h}. \tag{4.12}$$

Then, $\xi_k^{(1)}$ is said to be the Kahler volume of the curve S_k, whereas T_k is the complex structure modulus or holomorphic volume. The last equality implies that the complex variable T_k is in one-to-one correspondence with the simple root α_k, being the eigenvalue or the corresponding operator e_{α_k} under a generic element $h = \sum_i t_i e_{ii} = \sum_k T_k \alpha_k^*$ of the Cartan algebra $\mathfrak{h}$.[6] Kahler and holomorphic volumes represent resolution and deformation parameters. The former spans

[5] With Chevalley basis we mean the set $h_{\alpha_i} = [e_{\alpha_i}, e_{-\alpha_i}]$.

[6] $h \in \mathfrak{h}$ here is written in the basis of the α_j^*, defined by the condition: $\alpha_i \cdot \alpha_j^* = \delta_{ij}$.

the Kahler cone or Kahler moduli space of the surface. The latter spans the complex structure moduli space. However, the distinction is essentially an artifact of the choice of complex structure that we made. In fact, turning on a $\xi_k^{(1)}$ or a T_k has in both cases the effect of replacing the singularity with a 2-cycle. In the next section, we will see where the T_k appear in the context of deformations.

4.2.3 Semiuniversal Deformations

Another possible presentation of ADE surfaces is in terms of polynomials in $\mathbb{C}^3$:

$$A_n: \quad x^2+y^2-z^{n+1}=0, \tag{4.13}$$
$$D_n: \quad x^2+y^2z+z^{n-1}=0, \tag{4.14}$$
$$E_6: \quad x^2+y^3+z^4=0, \tag{4.15}$$
$$E_7: \quad x^2+y^3+yz^3=0, \tag{4.16}$$
$$E_8: \quad x^2+y^3+z^5=0. \tag{4.17}$$

Following the definition in 4.8, deformations are performed by adding to the defining equation monomials in the Jacobi algebra:

$$\mathcal{R}_f=\frac{\mathbb{C}[x,y,z]}{(\partial_x f,\partial_y f,\partial_z f)}.$$

A general versal deformation is defined as the zero locus of

$$X_{def}: \quad f(x,y,z)+\sum_{a=1}^{r} u_a\, g_a(x,y,z)=0,$$

where $\{g_a\}$ is a basis of $\mathcal{R}_f$ and u_a are complex deformation parameters. For ADE singularities, the dimension of the deformation space equals the rank of the corresponding ADE Lie algebra. For each ADE X, there is indeed an isomorphism between the deformation space $Def(X)$ and (the Weyl invariant coordinates on) the Cartan algebra $\mathfrak{h}$:

$$Def(X)\leftrightarrow \mathfrak{h}/\mathcal{W}, \tag{4.18}$$

$\mathcal{W}$ being the Weyl group.

There is indeed a choice of generators of R_{def} for which the deformed ADE can be written as:

$$A_{n-1}: \qquad x^2+y^2 \;=\; z^n + u_2 z^{n-2} + u_3 z^{n-3} + \cdots + u_{n-1} z + u_n, \tag{4.19}$$

$$D_n: \qquad x^2 + y^2 z + z^{n-1} \;+\; \sum_{k=1}^{n-1} u_{2k}\, z^{n-1-k} \;+\; U_n\, y \;=\; 0, \tag{4.20}$$

$$E_6: \qquad x^2 + y^3 + z^4 + u_2\, yz^2 + u_5\, yz + u_6\, z^2 + u_8\, y + u_9\, z + u_{12} = 0, \tag{4.21}$$

$$E_7: \qquad x^2 + y^3 + yz^3 + u_2\, z^4 + u_6\, y^2 + u_8\, yz + u_{10}\, z^2 + u_{12}\, y + u_{14}\, z + u_{18} = 0, \tag{4.22}$$

$$E_8: \qquad x^2 + y^3 + z^5 + u_2\, yz^3 + u_8\, yz^2 + u_{12}\, z^3 + u_{14}\, yz + u_{18}\, z^2 + u_{20}\, y + u_{24}\, z + u_{30} = 0, \tag{4.23}$$

where the complex parameters u_l are the Casimir invariants of the ADE algebra, of degree $\deg(u_l) = l$ with respect to the Weyl group. This identification manifests naturally in the framework of Grotendieck-Springer resolutions. Before going into it, let us make some important observations:

- The deformation blows up $r = \text{rank}(\mathfrak{g})$ (non-holomorphic) 2-spheres that intersect with a pattern given by the Dynkin diagram of the corresponding ADE algebra, where the spheres are identified with the *simple roots* of the Lie algebra.[7]
- By treating the u_i's as coordinates, the equation 4.19 defines a space X_{r+2} as an hypersurface in $\mathbb{C}^{r+3}$. It has the structure of a fibration, where the fiber is the (deformed) ADE surface X_{def} and the base is the space spanned by u_i. At the origin $u_i = 0$, the fiber has the full ADE singularity, i.e., all the r simple roots have zero size.
- Even though the central fiber is singular, the space X_{r+2} is smooth.[8] This can be seen by simply computing the Jacobian of f_{def}. However, by performing a *base change*, one can create a singular space whose resolution blows up a subset of the roots of the central ADE fiber.

To explain this last point, let us go back to the A_1 example. The defining equation for the A_1

[7] With an abuse of terminology, we will refer to the shrinking 2-spheres as 'simple roots'.

[8] To be precise, not solely the fiber at the origin is singular. There are loci along the base along which some of the roots have vanishing holomorphic volume. There, the fiber is singular, and the type of singularity is determined by the subalgebra generated by the roots with vanishing holomorphic volume. Like the singularity of the central fiber, these are not singularities of the total space.

singularity is[9]

$$uv = z^2 \,. \tag{4.24}$$

The equation for the family X_3 is

$$uv = z^2 + \epsilon \qquad \subset \qquad \mathbb{C}^4_{u,v,z,\epsilon} \,, \tag{4.25}$$

That is a smooth three-dimensional space. If we make the base change $\epsilon = -t^2$, i.e., we pull-back the ALE fibration w.r.t. the map

$$\begin{aligned} \mathfrak{h} &\longrightarrow \mathfrak{h}/\mathbb{Z}_2 \\ t &\mapsto \epsilon = -t^2 \,, \end{aligned} \tag{4.26}$$

where $\mathfrak{h} \cong \mathbb{C}$ for $\mathfrak{g} = A_1$, we obtain a three-dimensional space with an isolated singularity:

$$uv = z^2 - t^2 \,. \tag{4.27}$$

This is the well-known Conifold geometry [68, 88, 116–120]. The origin of the family is at $t = 0$, where the surface develops an A_1 singularity $uv = z^2$. At $t \neq 0$ the singularity of the surface is deformed and replaced by a sphere of holomorphic volume $\alpha = 2t = T$. Notice that the holomorphic volume of the root is linear in the t coordinate. The holomorphicity of α as a function over the base of the fibration is crucial to guarantee the blowup of the corresponding curve in the resolution. If we invert the base change, we see that the holomorphic volume has a branch cut $\alpha(\epsilon) \sim \sqrt{\epsilon}$. In other words, the root is a monodromic function. Every time we go around the origin of the ϵ plane, the monodromy acts as: $\alpha(\epsilon) \mapsto -\alpha(\epsilon)$[10]. When we consider the total space X_3, all the geometric data must be holomorphic (equivalently, Weyl-invariant) in the coordinates of the base. Then, the curve that corresponds to α must be zero in $H_2(X_3, \mathbb{Z})$. From this point of view, X_3 is the simplest example of monodromic ADE fibration [12]. The conifold is instead a non-monodromic fibration as its (small) resolution blows up the simple root of A_1 in the central fiber; this is known as a *total simultaneous resolution*. The family is now fibered over the base $\mathfrak{h}$.

Consider a generic ADE algebra of rank r. Analogously to the A_1 case, we can make a base

[9] Derived from 4.13 by a change of variables.

[10] The monodromy group is the Weyl group that defines the quotient $\mathfrak{h}/\mathcal{W}$

change by pulling back the ADE family with respect to the map (see [121])

$$\begin{aligned} \mathfrak{h} &\longrightarrow B_u \equiv \mathfrak{h}/\mathcal{W} \\ t_i &\mapsto u_j = u_j(t) \end{aligned} \tag{4.28}$$

by taking u_j's as $\mathcal{W}$-invariant functions of coordinates t_i on $\mathfrak{h}$. This resolves all the simple roots of the ADE algebra in the central fiber. In the new variables, the families can be presented in the following form:

$$\begin{aligned} A_n: &\quad x^2+y^2+\prod_{i=1}^{n+1}(z+t_i)=0, \qquad \sum_{i=1}^{n+1} t_i = 0, \\ D_n: &\quad x^2+y^2z+\frac{\prod_{i=1}^{n}(z+t_i^2)-\prod_{i=1}^{n} t_i^2}{z}+2y\prod_{i=1}^{n} t_i = 0, \\ E_6: &\quad x^2+y^3+z^4+\epsilon_2 yz^2+\epsilon_5 yz+\epsilon_6 z^2+\epsilon_8 y+\epsilon_9 z+\epsilon_{12}=0, \\ E_7: &\quad x^2+y^3+yz^3+\epsilon_2 y^2 z+\epsilon_6 y^2+\epsilon_8 yz+\epsilon_{10} z^2+\epsilon_{12} y+\epsilon_{14} z+\epsilon_{18}=0, \\ E_8: &\quad x^2+y^3+z^5+\epsilon_2 yz^3+\epsilon_8 yz^2+\epsilon_{12} z^3+\epsilon_{14} yz+\epsilon_{18} z^2+\epsilon_{20} y+\epsilon_{24} z+\epsilon_{30}=0. \end{aligned} \tag{4.29}$$

The ϵ_i are homogeneous polynomials in the t_i with $\deg(\epsilon_i)=i$, invariant under permutations of the t_i [121]. The holomorphic volumes of the roots are all linear in the t_i:

$$\begin{aligned} A_n: &\quad \alpha_i(h) = t_i - t_{i+1}, && i=1,\dots,n, \\ D_n: &\quad \alpha_i(h) = t_i - t_{i+1}, && i=1,\dots,n-1, \\ &\quad \alpha_n(h) = t_{n-1}+t_n, \\ E_n: &\quad \alpha_i(h) = t_i - t_{i+1}, && i=1,\dots,n-1, \\ &\quad \alpha_n(h) = -t_1-t_2-t_3. \end{aligned} \tag{4.30}$$

Clearly, when all the t_i's are zero, all volumes are vanishing, and the ALE fiber develops the full singularity that defines the family. However, there are also loci where only part of the roots have

zero volume. The fibers on such loci are therefore singular. The singularity type depends on the subalgebra preserved by the subspace of deformations defined by each locus. As opposed to the previous case, where all the singularities in the fibers were not singularities of the total space, the resolution of the total space of the fibration will replace all of these singularities with the corresponding patterns of $\mathbb{P}^1$ cycles. Let us consider a slightly more complicated example than the conifold to appreciate this phenomenon.

Total simultaneous resolution of A_3

$$X_5(t): \quad x^2+y^2+(z+t_1)(z+t_2)(z+t_3)(z+t_4)=0, \quad \sum_i t_i = 0 \tag{4.31}$$

We can identify singular loci of different codimension d:

- $d=3$: $t_i=0 \quad \forall\, i$. Full A_3 singularity $x^2+y^2+z^4=0$.
- $d=2$: $t_i=t_j=t_k=t$ for $i,j,k=0,1,2,3$. There are four distinct loci where the singularity is A_2. With a simple change of variables, X_5 can be written as:

$$x^2+y^2+z^3(z-4t) \underset{z\to 0}{\sim} x^2+y^2+az^3. \tag{4.32}$$

- $d=2$: $(t_1=t_2=t, t_3=t_4=-t)$ + permutations. Three loci where the singularity is $A_1\times A_1$:

$$x^2+y^2+(z+t)^2(z-t)^2 \tag{4.33}$$

- $d=1$: $t_i=t_j=t$ for $i,j=0,1,2,3$. There are six loci, one for each positive root, where the singularity is A_1:

$$k\neq i,j \quad , \quad x^2+y^2+z^2(z+t_k-t)(z-3t-t_k) \underset{z\to 0}{\sim} x^2+y^2+\tilde{a}z^2. \tag{4.34}$$

All in all, there are six hyperplanes where the fiber develops a singularity with small irreducible resolution (i.e., the blow-up is just a single rational curve or $\mathbb{P}^1$). The intersections between the hyperplanes form seven distinct lines. Two roots are blown up on each of them. All these lines intersect only at the origin, where the A_3 is fully resolved.

Now we want to consider different choices for the base change, which will make the family X_{r+2} singular, but will lead to different resolution patterns.

One can define a base change, where

$$\begin{aligned} \mathfrak{h} &\longrightarrow B_\varrho \equiv \mathfrak{h}/\mathcal{W}' \\ t_i &\mapsto \varrho_k = \varrho_k(t), \end{aligned} \tag{4.35}$$

with $\mathcal{W}' \subset \mathcal{W}$. A choice of simple roots determines this subset of the Weyl group, call them

$$\alpha_1, ..., \alpha_\kappa \qquad \text{with} \qquad \kappa \leq r \ ; \tag{4.36}$$

$\mathcal{W}'$ is generated by the reflections under $\alpha_{\kappa+1}, ..., \alpha_r$. One can visualize it by coloring the roots in (4.36). The resolution of the family now blows up only these simple roots in the central fiber. This is called a *partial simultaneous resolution*. The base of the fibration, that we call B_ϱ, is now parametrized by the r $\mathcal{W}'$ invariants ϱ_i ($i = 1, ..., r$). We call these partial casimirs, and they are symmetric polynomials in the t_i that are permuted by $\mathcal{W}'$. Note that $\mathcal{W}'$ is always of the form: $S_{l_1} \times \cdots \times S_{l_m}$, with S_l denoting the group of permutations of l elements, and $l_1, ..., l_m$ the lengths of the Dynkin subdiagrams delimited by colored nodes.

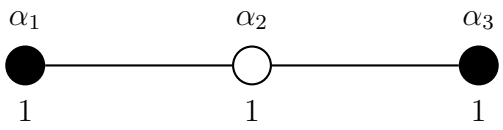

Figure 4.2: A_3 Dynkin diagram. The colored nodes correspond to the obstructed spheres in the partial simultaneous resolution of the A_3 family.

Partial simultaneous resolution of A_3 Let us consider a partial simultaneous resolution that blows up only the central root α_2 (see Figure 5.1). In this case:

$$\mathcal{W}' = \langle s_1, s_3 \rangle \simeq S_2 \times S_2, \tag{4.37}$$

where s_1 and s_3 are the reflections associated to the simple roots α_1 and α_3, acting on $\mathfrak{h}$ as:

$$\begin{aligned} s_1 : &\quad t_1 \leftrightarrow t_2, \quad t_3 \leftrightarrow t_3, \quad t_4 \leftrightarrow t_4 \\ s_3 : &\quad t_1 \leftrightarrow t_1, \quad t_2 \leftrightarrow t_2, \quad t_3 \leftrightarrow t_4 \end{aligned} \tag{4.38}$$

The ring of polynomial invariants is generated by the symmetric polynomials:

$$\sigma_1(t_1, t_2) = t_1 t_2, \quad \sigma_3(t_3, t_4) = t_3 t_4, \quad \sigma_2(t_1, t_2) = t_1 + t_2 = -t_3 - t_4 \tag{4.39}$$

Then, we can pull back $X_5(u)$ with respect to the change:

$$\begin{array}{ccc} \mathfrak{h}/\mathcal{W}' & \mapsto & \mathfrak{h}/\mathcal{W} \\ (\sigma_1, \sigma_3, \sigma_2) & \mapsto & (u_2(\sigma), u_3(\sigma), u_4(\sigma)) \end{array} . \tag{4.40}$$

Which yields:

$$X_5'(\sigma): \quad x^2 + y^2 = (z^2 + \sigma_2 z + \sigma_1)(z^2 - \sigma_2 z + \sigma_3). \tag{4.41}$$

In order to make the dependence on the holomorphic volumes $T_i = t_i - t_{i+1}$ manifest, we introduce a further change of variables:

$$\sigma_1 = -\varrho_1 + \varrho_2^2, \quad \sigma_2 = 2\varrho_2, \quad \sigma_3 = -\varrho_3 + \varrho_2^2. \tag{4.42}$$

Rewriting 4.41 in terms of the ϱ, we get:[11]

$$X_5'(\varrho): \quad x^2 + y^2 = ((z + \varrho_2)^2 - \varrho_1)((z - \varrho_2)^2 - \varrho_3). \tag{4.44}$$

Let us focus on the right-hand side of the equation. As opposed to the previous case (see equation (4.31)), the polynomial in z is not fully factorizable. The holomorphic volumes of the roots are monodromic functions:

$$\begin{aligned} \alpha_1 &= \mp 2\sqrt{\varrho_1} = t_1 - t_2, \\ \alpha_2 &= 2\varrho_2 \pm \sqrt{\varrho_1} \mp \sqrt{\varrho_3} = t_2 - t_3, \\ \alpha_3 &= \pm 2\sqrt{\varrho_3} = t_3 - t_4, \end{aligned} \tag{4.45}$$

On the quotient B_ϱ, different branches that are mapped to each other by elements of $\mathcal{W}'$ are identified. We can rewrite the equations for the vanishing loci of the volumes in a holomorphic way by considering the following $\mathcal{W}'$-invariant expressions:

$$\begin{aligned} \alpha_1 = 0 \quad &\leftrightarrow \quad \alpha_1^2 = 4\varrho_1 = 0, \\ \alpha_2 = 0 \quad &\leftrightarrow \quad (\varrho_1 - \varrho_3)^2 - 8\varrho_2^2(\varrho_3 + \varrho_1) + 16\varrho_2^4 = 0, \\ \alpha_3 = 0 \quad &\leftrightarrow \quad \alpha_3^2 = 4\varrho_3 = 0, \end{aligned} \tag{4.46}$$

[11] In terms of the T_i we have:

$$\varrho_1 = T_1^2/4, \quad \varrho_2 = \frac{T_2 - T_4}{4}, \quad \varrho_3 = T_3^2/4 \tag{4.43}$$

The second expression comes from setting α_2 to zero:

$$2\varrho_2 \pm \sqrt{\varrho_1} \mp \sqrt{\varrho_3} = 0, \tag{4.47}$$

and taking the following squares:

$$\begin{aligned} \left(2\varrho_2 \pm \sqrt{\varrho_1}\right)^2 &= \varrho_3, \\ 16\varrho_2^2\varrho_1 &= \left(\varrho_3 - \varrho_1 - 4\varrho_2^2\right)^2. \end{aligned}$$

By performing the same manipulations on the expressions for $\alpha_2+\alpha_1,\ \alpha_2+\alpha_3,\ \alpha_2+\alpha_1+\alpha_3$, one can check that the final equation is the same. As we are going to explain, this happens because these roots are all identified in the quotient over $\mathcal{W}'$.

We now compare this situation with the previous one, namely, the total simultaneous resolution of the A_3 family. First of all, we notice that the hyperplanes which are connected by Weyl transformations in $\mathcal{W}'$ are identified in the quotient. Each hyperplane is associated with a positive root (or a negative root):

$$\begin{aligned} &\mathcal{H}_1 : t_1 = t_2 \quad &&\leftrightarrow \alpha_1 = 0, \\ &\mathcal{H}_2 : t_2 = t_3 \quad &&\leftrightarrow \alpha_2 = 0, \\ &\mathcal{H}_3 : t_3 = t_4 \quad &&\leftrightarrow \alpha_3 = 0, \\ &\mathcal{H}_{12} : t_1 = t_3 \quad &&\leftrightarrow \alpha_1 + \alpha_2 = 0, \\ &\mathcal{H}_{23} : t_2 = t_4 \quad &&\leftrightarrow \alpha_2 + \alpha_3 = 0, \\ &\mathcal{H}_{123} : t_4 = t_1 \quad &&\leftrightarrow \alpha_1 + \alpha_2 + \alpha_3 = 0, \end{aligned} \tag{4.48}$$

The subgroup $\mathcal{W}'$ fixes hyperplanes $\mathcal{H}_1$ and $\mathcal{H}_3$, while permuting $\mathcal{H}_2, \mathcal{H}_{12}, \mathcal{H}_{23}, \mathcal{H}_{123}$.[12] In the quotient, the distinct A_1 loci are precisely the expressions in (4.46):

$$\begin{aligned} &\mathcal{H}_1^{\mathcal{W}'} : \varrho_1 = 0, \\ &\mathcal{H}_2^{\mathcal{W}'} : (\varrho_1 - \varrho_3)^2 - 8\varrho_2^2(\varrho_3 + \varrho_1) + 16\varrho_2^4 = 0, \\ &\mathcal{H}_3^{\mathcal{W}'} : \varrho_3 = 0, \end{aligned} \tag{4.49}$$

[12] This implies that $\mathcal{H}_2 \sim \mathcal{H}_{12} \sim \mathcal{H}_{23} \sim \mathcal{H}_{123}$ (equivalently, $\alpha_2 \sim \alpha_2 + \alpha_1 \sim \alpha_2 + \alpha_3 \sim \alpha_1 + \alpha_2 + \alpha_3$) in the quotient B_ϱ.

The fiber over $\mathcal{H}_1^{\mathcal{W}'}$ is:

$$x^2+y^2=\left((z+\varrho_2)^2-\varrho_1\right)\left((z-\varrho_2)^2-\varrho_3\right)\cap\ \varrho_1=0\quad\longrightarrow$$

$$x^2+y^2=(z+\varrho_2)^2\left((z-\varrho_2)^2-\varrho_3\right).$$

One would expect to find an A_1 singularity at $z=-\varrho_2$. However, the family is smooth unless where $\mathcal{H}_1^{\mathcal{W}'}$ intersects $\mathcal{H}_2^{\mathcal{W}'}$. The same thing occurs when we look at the locus $\mathcal{H}_3^{\mathcal{W}'}$. In fact, the only truly singular locus is $\mathcal{H}_2^{\mathcal{W}'}$, which is where the volume of α_2 (and all its $\mathcal{W}'$- images) vanishes.

Let us analyse what happens on the locus $\mathcal{H}_2^{\mathcal{W}'}$. For simplicity, we focus on the branch $\varrho_2=0$ (which automatically implies $\varrho_1=\varrho_3\equiv\varrho$), so that we can rewrite the equation for the fiber as[13]:

$$x^2+y^2=\left(z^2-\varrho\right)^2. \tag{4.51}$$

The singularity is manifestly of type A_1 and occurs on the irreducible locus:

$$x=0,\quad y=0,\quad z^2=\varrho \tag{4.52}$$

Let us conclude with an observation. The volumes of the roots were all monodromic; however, it is always possible to consider a linear combination that is well defined on B_ϱ ($\alpha_2-\alpha_4=\varrho_2$). This is the signal that only one of the 2-cycles generating $H_2(X)$ is preserved in $H_2(X_5)$.

To sum up, the total space of an ADE-family X_{r+2} has the fibration structure

$$\begin{array}{ccccc} X'_{def} & \hookrightarrow & X'_{r+2} & \to & X_{r+2} \\ & & \downarrow & & \downarrow \\ & & B_\varrho & \to & B_u, \end{array} \tag{4.53}$$

where X'_{def} is the deformed ADE surface, expressed in terms of the ϱ coordinates.

This fundamental correspondence between deformations and resolutions provides a frame-

[13] It is easy to see that the singular locus of the family is given by:

$$\varrho_1-(z+\varrho_2)^2=0,\quad \varrho_3-(z-\varrho_2)^2=0. \tag{4.50}$$

The equation for $\mathcal{H}_2^{\mathcal{W}'}$ is automatically satisfied if we impose these two, meaning that the singular locus is contained in $\mathcal{H}_2^{\mathcal{W}'}$.

work for the explicit construction of threefolds with terminal singularities—namely, those whose exceptional loci consist exclusively of curves—and, moreover, yields their crepant resolutions in a canonical and automatic manner. Starting from the equation for the family of deformed ADE X_{r+2}(with total or partial simultaneous resolution), one can obtain a threefold by imposing $r-1$ extra conditions on the coordinates.In particular, threefolds with isolated terminal singularities can be obtained by considering the fibration of deformed surfaces along a curve. The curve is embedded in the deformation space. Singularities appear where the curve intersects the singular locus of the family of deformed surfaces. Threefolds that admit this description are known as *compound Du Val* points.

4.2.4 Compound Du Val singularities

As we said, compound Du Val threefolds (cDV) come about naturally from the families of deformed surfaces we have just described. If we express the coordinates on the B_t base as holomorphic functions of a single complex parameter w, and require all of them to vanish when $w=0$, we can rewrite the generic deformed ADE as:

$$P_{\mathfrak{g}}(x,y,z)+wg(x,y,z,w)=0 \quad (x,y,z,w)\in\mathbb{C}^4. \tag{4.54}$$

Where $P_{\mathfrak{g}}(x,y,z)$ is the ADE singularity associated with the Lie algebra $\mathfrak{g}$ (in the form of equation 4.13). The vanishing of the second summand at $w=0$ ensures that the base-curve intersects the origin of B_t (or B_ϱ, depending on the fibration we are considering), where the full singularity is developed.

The resolution patterns of these singularities are automatically determined by the way they are embedded in the family X_{r+2} (i.e., by the explicit dependence of the deformation parameters on the extra coordinate) and by the simultaneous resolutions of the associated ADE surface. Not only does this direct link to ADE algebras make this class of geometries particularly easy to access, but it also provides a way of classifying all terminal singularities in three dimensions. In the following paragraph, we will get an intuition of why this happens.

Having constructed explicit classes of singular geometries, we now place them within the more general classification program of canonical threefold singularities, which will be relevant for the physics of geometric engineering setups.

4.3 Classification of threefold singularities

When dealing with complex two-dimensional varieties, a theorem by Reid [53] proves that all singularities[14] with crepant minimal resolution [15] are of Du Val type (ADE singularities). However, in higher dimensions, it is much more difficult, if not impossible, to provide a full list of the singularities that admit a crepant resolution. Most often, even when such a resolution exists, it is not at all clear how to construct it in practice. The most relevant attempts to provide such a classification fall in the so-called Minimal Model Program (MMP). Even though it did not provide a full classification, the program, proposed by Reid in the eighties [53] and generalised by Mori [122], captured a series of important properties of singularities in 3 dimensions. Here, we only mention the main results.

In [53], Reid introduces the concept of canonical singularity to distinguish between singularities which are too severe to be resolved crepantly and those which are mild enough.

Definition 4.3.1 (Canonical singularity)**.** A singularity X of dimension ≥ 2 is canonical if:

- X is $\mathbb{Q}$-Gorenstein (K_X is $\mathbb{Q}$-Cartier)[16]
- For any *partial resolution* $f : Y \to X$, we have: $K_Y = f^* K_X + \sum_i a_i(X, E_i) E_i, \quad a_i \geq 0$

In particular, f is crepant if:

$$a_i = 0 \quad \forall\ i \tag{4.56}$$

. Here, K_X and K_Y are the canonical divisors of X and Y. The a_i are rational coefficients and are known as *discrepancies*. Each E_i is an exceptional divisor extracted in Y. Intuitively, we can see that negative a_i are bad because whenever a divisor introduces a relative discrepancy with respect to X that is negative, the uplift to Y of the holomorphic volume form develops a singularity on that divisor. As anticipated, all surface singularities with a full crepant resolution are Du Val. Indeed, they are canonical and Gorenstein (or index one singularities). For a canonical threefold,

[14] We will always tacitly assume normality for any variety we will be considering.

[15] A minimal resolution of a surface singularity X is a resolution map:

$$\pi : Y \to X \tag{4.55}$$

, such that Y is smooth and does not contain (-1)-curves (namely, curves which can be contracted to a smooth point).

[16] A Weyl divisor D is $\mathbb{Q}$-Cartier if mD is Cartier for some $m \in \mathbb{N}$.

the existence of a full crepant resolution is not always granted. What is ensured, though, and this is the scope of MMP, is that a partial crepant resolution exists. Partial here means that the resolved space may still have singularities somewhere, but of a milder nature. These are called terminal singularities:

Definition 4.3.2 (Terminal singularity)**.** A singularity X of dimension ≥ 2 is terminal if: X is canonical with $a_i(X, E_i) \geq 0 \quad \forall\ i$.

This automatically implies that either the resolution is totally discrepant (there are no crepant divisors), or Y (the resolved variety) and X are isomorphic in codimension 1. In the latter case, the two varieties are isomorphic up to subsets of codimension ≥ 2. In other words, the exceptional locus of the resolution contains at most rational curves. These are the so-called small resolutions. By definition, for a terminal singularity, the only crepant (partial and total) resolutions are small. As it turns out, the condition defining terminal singularities is strong enough to allow for a classification. Indeed, it is a Theorem by Reid that terminal Gorenstein threefold singularities are all compound Du Val points (terminal $\mathbb{Q}$-Gorenstein singularities are some specific cyclic quotients of cDV classified by Mori [123].

To sum up, for a variety X of complex dimension 3, we have:

$$\begin{aligned} &X \quad \text{canonical} \quad \Rightarrow \quad \text{Partial crepant resolution exists, and it's called minimal model over X (MM)}^{17} \\ &X \quad \text{terminal and Gorenstein} \quad \Rightarrow \quad X \quad \text{isolated cDV with small simultaneous resolution} \end{aligned} \tag{4.57}$$

A couple of comments are in order. First, in both cases, the resolution is not unique. Reid suggests that all the possible minimal models over a canonical variety X should be connected by elementary transformations. These transformations are called *flops* (see Appendix A.2.5). A flop is a modification of the geometry that only acts on a specific curve. Consider two varieties Y and Y^+ that map to a singular variety X through the contraction of a curve C and C^+. Then, a flop is the birational map between Y and Y^+, obtained by contracting C in Y and blowing up C^+ in X (the inverse operation is also a flop). The map is constructed in such a way that $Y \backslash C \simeq Y^+ \backslash C^+$ (namely, it is an isomorphism in codimension 1).

Second, even though an MM over X exists for any X canonical, it is often very hard to produce the explicit map to it. From the physics perspective, canonical isolated singularities play a particularly important role in the context of geometric engineering, where they provide the geometric input used to define five-dimensional superconformal field theories (5d SCFTs). In this frame-

work, M-theory compactified on a Calabi–Yau threefold with a canonical singularity can give rise to an interacting superconformal fixed point in five dimensions. It is widely believed that every canonical singularity defines a well-behaved 5d SCFT fixed point [44]. We will present an overview of this connection in the second part of the thesis. For the present discussion, we simply emphasize that the classification of canonical singularities closely parallels the physics program of classifying 5d superconformal fixed points, which so far have only been realized through such geometric constructions.

The examples of (CY3) isolated canonical singularities that have been analyzed in this context are mostly of the following kind:

- Hypersurface singularities in $\mathbb{C}^4$ [14, 91]
- Quotients of $\mathbb{C}^3$, $\mathbb{C}^3/G$ with G discrete and $G \subset SL(3,\mathbb{C})$ [124]
- cDV and $\mathbb{Q}$-Gorenstein quotients of cDV [19, 26, 97]
- Toric canonical threefolds [101, 102]

In this thesis, we focus exclusively on the cDV family, which provides an ideal framework for uncovering new correspondences between geometry and gauge theories. This setting allows us to capture physical phenomena that are not reproduced in toric constructions and, to our knowledge, have not been observed in other non-toric frameworks. A key technical advantage of cDV singularities is their particularly transparent connection with Lie algebra theory, which allows many of their properties to be derived constructively and interpreted naturally from a physical perspective. The examples we analyze in detail mainly belong to the subclass of Simple Flops. These may be regarded as the simplest families within the cDV class—the conifold providing the only toric example—and therefore constitute the most natural and controlled starting point for our analysis. We now turn to their definition.

4.3.1 Simple flop classification

The term simple threefold flop indicates a geometry whose crepant resolution is small and contains a single irreducible rational curve. Such a curve can be flopped, in the sense that there exists a sequence of birational morphisms (flop) that contracts the curve and blows up a different curve in such a way that the canonical bundle of the variety remains invariant. A remarkable fact is

that any geometry of this kind can be explicitly realized as a fibration of deformed ADE surfaces over a curve [19].

A first coarse classification was proposed by Reid by examining the normal bundle of the exceptional curve. Let

$$\pi : Y \to X,$$

be a small crepant contraction of a smooth threefold Y contracting a curve

$$C \simeq \mathbb{P}^1.$$

Since Y is Calabi-Yau in a neighbourhood of the contraction, the adjunction formula implies that

$$\deg N_{C/Y} = -2.$$

Consequently, the possible splitting types of the normal bundle are

$$N_{C/Y} \simeq \mathcal{O}(-1) \oplus \mathcal{O}(-1), \qquad \mathcal{O}(0) \oplus \mathcal{O}(-2), \qquad \mathcal{O}(1) \oplus \mathcal{O}(-3).$$

These three possibilities provide a first rough classification of simple threefold flops according to the geometry of the exceptional curve.

This classification was later refined by the introduction of the *length* invariant, defined by Kollár [125] and used in the systematic study of threefold flops by Katz [121]. The length ℓ measures roughly the multiplicity of the exceptional curve in the resolution and takes six possible values[18]

$$\ell = 1, \dots, 6.$$

Remarkably, this invariant admits a natural group-theoretical interpretation within the framework of ADE Lie algebras, where it is identified with one of the Dynkin labels of the ADE diagram.

Such a classification was given in [121]. The length classification is accompanied by a construction producing what is known as the *universal flop of length* ℓ [17]. This is the total space of

[18] More rigorously it is defined by

$$\pi^{-1}(O_p) = \mathcal{O}_{S_p}^{\oplus \ell} \tag{4.58}$$

where π denotes the contraction map, O_p the skyscraper sheaf at the singularity p and $\mathcal{O}_{S_p}$ the structure sheaf of the exceptional cycle S_p.

a family of deformed ADE surface singularities of types

$$A_1,\ D_4,\ E_6,\ E_7,\ E_8,$$

and has complex dimension $r+2$, where r is the rank of the associated ADE Lie algebra.

These are nothing but subcases of the general framework of ADE families with partial simultaneous resolution that we introduced in 4. As we showed, these spaces can be described as fibrations whose base is the space of deformation parameters (collectively denoted by $\boldsymbol{\varrho}$), while the fiber is the corresponding deformed ADE surface. At the origin of the parameter space, the surface displays the full ADE singularity, while at a generic point of the base, the surface becomes smooth. At certain loci in the parameter space, the fiber still develops a singularity governed by a subalgebra of the initial ADE algebra.

In 4 we also observed that the singularity of the fiber does not necessarily imply a singularity of the total space X_{r+2} of the family. However, the latter often harbors singularities of its own, which can sometimes be resolved. In particular, at the origin, the resolution of X_{r+2} may not fully resolve the fiber surface but instead blows up only a subset of the two-spheres that shrink at the ADE singularity. This procedure is the *partial simultaneous resolution*.

Any threefold flop of length ℓ can be constructed via a map to the universal flop of length ℓ. In this work we focus on the cases $\ell = 1, 2$. The known examples of threefold flops of length $\ell = 1$ include the conifold and Reid's pagoda [126]. Prominent examples of $\ell = 2$ threefold flops are the Laufer [127] and Morrison–Pinkham [128] geometries, as well as the more recent Brown–Wemyss threefold [129].

Let us now describe the specific class of ADE fibrations that corresponds to universal flops.

4.3.2 Universal Flops

As we said, universal flops are classified by the possible lengths $\ell \in \{1, \dots, 6\}$. Namely, for each length ℓ, there exists a universal flop

$$\pi_\ell : Y_\ell \to X_\ell,$$

which parametrises all simple flops of that length.

The geometry of the universal flop is governed by the Cartan data of a Dynkin diagram. In fact, each universal flop is naturally associated with a Du Val surface. A generic hyperplane section of X_ℓ is a deformed ADE. Which ADE this is depends on the length. Length 1 is A_n, length 2 D_n, length $3, 4, 5, 6$ can have E_6, E_7, E_8. Now, let Γ denote the affine Dynkin diagram of type A, D, or E and let $\mathfrak{h}_\Gamma$ be the corresponding Cartan subalgebra. The universal flop X_ℓ is a fibration over a base space

$$H_\ell = \mathfrak{h}_\Gamma / \mathcal{W}_C.$$

Where $\mathcal{W}_C$ is a subgroup of the ADE Weyl group $\mathcal{W}_\Gamma$. $\mathcal{W}_C$ is generated by the simple reflections associated with the Levi subdiagram Γ_C obtained by deleting a distinguished vertex from Γ. This vertex is represented by the coloured node in the Dynkin diagram. Geometrically, it corresponds to the root whose dual element $\alpha^* \in \mathfrak{h}_\Gamma$ determines the curve that is contracted in the simultaneous resolution of the surface singularity. The Dynkin label of the colored node is the length of the flop. The coordinates along H_ℓ are the Casimir invariants of the Levi subalgebra associated with Γ_C. In the following section, we introduce a method to reconstruct the crepant resolutions associated with universal flops starting from the total simultaneous resolution of the ADE families. Recall that the total Simultaneous resolution corresponds to the deformation of the ADE surface singularity in which all exceptional curves in the singular fibres are blown up.

The construction we review is formulated in the language of quiver path algebras. This perspective provides an explicit description of the resolution in terms of noncommutative algebras, known as NCCR (noncommutative crepant resolution). In this framework, the geometry of the resolution is naturally encoded in the representation theory of a quiver with relations.

Reviewing this construction will allow us to connect in a precise way the quiver structures that appear in the physics description of D3-branes probing ALE spaces (discussed in Section 2) with the geometric framework of crepant resolutions of singularities.

4.3.3 Quivers and Universal Flopping Algebras

A quiver Q is essentially a collection of nodes and oriented links (arrows) between them. The composition of the arrows, which has to follow their orientation, defines a product. The product allows us to define paths of varying length along the graph of the quiver. The set of paths defines an algebra, the *quiver path algebra*, $\mathcal{A}_Q$. For a more complete definition of quivers, see Appendix

D.

This object naturally arises in the context of minimal resolutions of ADE surface singularities. We have seen how McKay correspondence relates the affine ADE Dynkin diagrams and the geometry of the resolution. Moreover, we have seen how fractional $D3$-branes (equivalently, wrapped $D5$-branes) generate a gauge theory, graphically encoded in a doubled Dynkin quiver Q_Γ (see Figure 4.3)

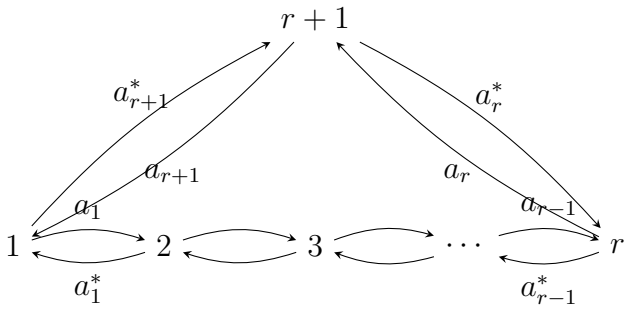

Figure 4.3: Doubled affine Dynkin quiver of A_r

The associated algebra is the preprojective algebra

$$\mathcal{A}_\Gamma = \mathbb{H}_\Gamma Q_\Gamma / \langle \sum_{a \in Q_\Gamma} [a, a^*] - \sum_{i=1}^{r+1} T_i e_i \rangle, \quad \mathbb{H}_\Gamma = \mathbb{C}[T_1, ..., T_{r+1}] / \langle \sum_i d_i T_i \rangle. \tag{4.59}$$

Here the coordinate ring $\mathbb{H}_\Gamma$ describes the space of complex deformations of the ADE surface. The T_i are coordinates along $\mathfrak{h}_\Gamma$. The e_i factors are idempotents associated with each node of the quiver, namely loops satisfying:

$$e_i e_j = 0 \quad \text{for} \quad i \neq j, \qquad e_i^2 = e_i, \qquad \sum_{i=1}^{r+1} e_i = \mathbb{1}. \tag{4.60}$$

Finally, r is the rank of the ADE Lie algebra, and the d_i are the Dynkin labels.

The universal flopping algebras are then obtained by suitable contractions and base changes of these preprojective algebras, reflecting the passage from the total simultaneous resolution to the partial resolutions [18, 130].

Universal flopping algebras $\mathcal{A}_\ell$ provide noncommutative crepant resolutions for universal flops. For an introduction to NCCR and its relation with quiver path algebras, we refer to [54].

The two small resolutions of the universal flop can be recovered as moduli spaces of representations of $\mathcal{A}_\ell$ with opposite stability conditions. The universal flopping algebra is constructed from $\mathcal{A}_\Gamma$ through the following operations.

1. **Idempotent contraction.** Let C denote the set consisting of the affine vertex and the coloured vertex of the Dynkin diagram, and define the idempotent

$$e_C = \sum_{i \in C} e_i.$$

   The corner algebra

$$e_C \mathcal{A}_\Gamma e_C,$$

   contract the remaining vertices of the diagram. Algebraically, paths that pass through the removed vertices, and become composite arrows between the two retained vertices.

2. **Invariant base.** The Weyl subgroup W_C acts naturally on the Cartan parameter ring H_Γ. The base of the universal flop is obtained by passing to the invariant ring

$$H_\ell = H_\Gamma^{W_C}.$$

3. **Base change.** The universal flopping algebra is obtained by replacing the Cartan parameters with their invariant combinations:

$$\mathcal{A}_\ell \cong e_C \mathcal{A}_\Gamma e_C \otimes_{H_\Gamma} H_\ell.$$

The resulting algebra will be a quiver with relations. The quiver typically has two vertices, while its arrows arise from paths in the Dynkin quiver that travel through the contracted vertices. The relations are inherited from the preprojective relations after contraction and invariant-theoretic reduction.

This construction also provides a uniform procedure for obtaining the path algebras associated with all simple threefold flops of Dynkin types A_n, D_n, and E_6, E_7, E_8. Given a universal flopping algebra of length ℓ, the path algebra for a threefold flop of the same length is given by a change of base in the ring of Casimir invariants $H_\Gamma^{W_C}$.

example: $\mathcal{A}_{A_3} \to \mathcal{A}_1$ To be more explicit, we show here an example of the technique employed in [130] to derive universal flopping algebras from the preprojective algebras describing the resolutions of the deformed ADE families. We want to derive the noncommutative resolution of a family of deformed A_3 surfaces that admits only simple flops. We already discussed this case, although from a different perspective in 4.2.3. This is not the universal family of length 1 flops as was defined in [130], but it will be an instructive example for the physical derivation of simple flops of Chapter 6.

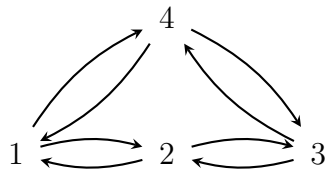

Figure 4.4: Doubled affine Dynkin diagram for A_3.

Let $Q = \widetilde{A}_3$ be the affine A_3 quiver with vertices $1, 2, 3, 4$ (see Figure 4.4) and arrows

$$a_4 : 4 \to 1, \qquad a_1 : 1 \to 2, \qquad a_2 : 2 \to 3, \qquad a_3 : 3 \to 4,$$

together with reverse arrows

$$a_4^* : 1 \to 4, \qquad a_1^* : 2 \to 1, \qquad a_2^* : 3 \to 2, \qquad a_3^* : 4 \to 3.$$

The preprojective algebra associated with the deformed A_3 family is

$$\mathcal{A}_{\widetilde{A}_3} = \mathbb{H}Q \Big/ \left(\sum_{a \in Q} [a, a^*] - \sum_{i=1}^{4} T_i e_i \right), \qquad \mathbb{H} = \mathbb{C}[T_1, ..., T_4]/(\sum_i T_i)$$

equivalently with vertex relations

$$\begin{aligned} a_4^* a_4 - a_3 a_3^* &= T_4 e_4, \\ a_1^* a_1 - a_4 a_4^* &= T_1 e_1, \\ a_2^* a_2 - a_1 a_1^* &= T_2 e_2, \\ a_3^* a_3 - a_2 a_2^* &= T_3 e_3. \end{aligned}$$

This path algebra describes the total simultaneous resolution of the family of deformed A_3 surfaces

4.31. Our goal is to obtain a partial simultaneous resolution that blows up a single 2-cycle. Assume that we want to obstruct the blow-up of all the simple roots but α_2. Then, the subset of nodes in Q that we need to preserve is $C = \{4, 2\}$.

Let us consider the idempotent

$$e_C = e_4 + e_2.$$

Now, we proceed in steps

Step 1: Contracting to opposite vertices.

We contract to the corner algebra

$$\mathcal{A}_C = e_C \mathcal{A}_{\widetilde{A}_3} e_C.$$

Keeping the opposite vertices 4 and 2, there are exactly two length-two paths from 4 to 2:

$$\alpha_1 := a_1 a_4, \qquad \alpha_2 := a_2^* a_3^*,$$

and two length-two paths from 2 to 4:

$$\beta_2 := a_4^* a_1^*, \qquad \beta_1 := a_3 a_2.$$

Then, we have two length-one loops at node 4:

$$\gamma_4 := a_4^* a_4, \qquad \gamma_3 := a_3 a_3^*,$$

And two at node 2:

$$\gamma_2 := a_2^* a_2, \qquad \gamma_1 := a_1 a_1^*,$$

These are not independent, due to the vertex relations at nodes 4 and 2, which we can rewrite as:

$$\gamma_1 = \gamma_2 - T_2 e_2, \qquad \gamma_3 = \gamma_4 - T_4 e_4,$$

Now, we contract the vertex relation at node 1 with a_4^* and a_1^* from the left and a_4, a_1 from the right:

$$-\alpha_1\beta_2 + \gamma_1^2 = T_1\gamma_1, \qquad \beta_2\alpha_1 - \gamma_4^2 = T_4\gamma_4. \tag{4.61}$$

Similarly, we contract the relation at node 3 with a_2 and a_3 from the left and $\{a_2^*, a_3^*\}$ from the right:

$$\alpha_2\beta_1 - \gamma_2^2 = T_3\gamma_2, \qquad -\beta_1\alpha_2 + \gamma_3^2 = T_3\gamma_3. \tag{4.62}$$

Finally, contracting the same relations with $\{a_4, a_1^*\}$ and $\{a_2, a_3^*\}$ from the right and $\{a_1, a_4^*\}$, $\{a_2^*, a_3\}$ from the left, we obtain relations between the paths from 4 to 2 and from 2 to 4:

$$\begin{aligned}
\gamma_1\alpha_1 - \alpha_1\gamma_4 &= T_1\alpha_1,\\
\gamma_3\beta_1 - \beta_1\gamma_2 &= T_3\beta_2,\\
\alpha_2\gamma_3 - \gamma_2\alpha_2 &= T_3\alpha_2,\\
\beta_2\gamma_1 - \gamma_4\beta_2 &= T_1\beta_1,
\end{aligned}$$

Eliminating γ_1 and γ_3 we have:

$$\begin{aligned}
\gamma_2\alpha_i - \alpha_i\gamma_4 &= (T_1 + T_2)\alpha_i,\\
\beta_i\gamma_2 - \gamma_4\beta_i &= (T_1 + T_2)\beta_i,
\end{aligned} \tag{4.63}$$

In Figure 4.6 we can see the quiver resulting from the contraction.

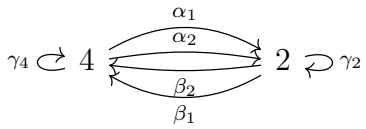

Figure 4.5: Quiver of the contracted algebra $e_C\mathcal{A}_{\widetilde{A}_3}e_C$.

Step 2: $\mathcal{W}_C$-Invariant coordinates. In order to produce a simple flop fibration we have to make a change of coordinates along the base:

$$\mathfrak{h} \mapsto \mathfrak{h}/\mathcal{W}_C \tag{4.64}$$

Where $\mathcal{W}_C$ is the Weyl subgroup generated by the simple reflections: s_1, s_3. The action of s_1, s_3 on the T_i coordinates is:

$$\begin{aligned}
&s_1 : T_1 \leftrightarrow -T_1, \quad T_2 \leftrightarrow T_2 + T_1, \quad T_3 \leftrightarrow T_3, \quad T_4 \leftrightarrow T_4 + T_1,\\
&s_3 : T_1 \leftrightarrow T_1, \quad T_2 \leftrightarrow T_2 + T_3, \quad T_3 \leftrightarrow -T_3, \quad T_4 \leftrightarrow T_4 + T_3,
\end{aligned} \tag{4.65}$$

A convenient choice of invariants is the one we did in 4.42:

$$\varrho_1 = \frac{T_1^2}{4}, \quad \varrho_3 = \frac{T_3^2}{4}, \quad \varrho_2 = \frac{T_2 - T_4}{4}. \tag{4.66}$$

In order to express all relations in terms of these invariants we make a shift:

$$\gamma_4 \longrightarrow \gamma_4 - T_1/2, \qquad \gamma_2 \longrightarrow \gamma_2 - T_3/2. \tag{4.67}$$

Then, the paths in 4.68 become:

$$\begin{aligned} \gamma_2\alpha_i - \alpha_i\gamma_4 &= 2\varrho_2\alpha_i, \\ \beta_i\gamma_2 - \gamma_4\beta_i &= 2\varrho_2\beta_i, \end{aligned} \tag{4.68}$$

While 4.61 and 4.62 yield:

$$\begin{aligned} \alpha_1\beta_2 &= (\gamma_2 - 2\varrho_2)^2 - \varrho_1 e_2, \\ \beta_2\alpha_1 &= \gamma_4^2 - \varrho_1 e_4 \qquad , \\ \alpha_2\beta_1 &= \gamma_2^2 - \varrho_3 e_2 \qquad , \\ \beta_1\alpha_2 &= (\gamma_4 + 2\varrho_2)^2 - \varrho_3 e_4, \end{aligned} \tag{4.69}$$

Step 3: Comparison with the universal flopping algebra of length 1. So far, the path algebra describes the family of deformed A_3 surfaces with simple flop, which is a fibration over a three-dimensional base. According to the definition given by [130], the universal flopping algebra of length 1 is instead a fibration of deformed A_1 surfaces over its space of versal deformations. Such a family corresponds to the total simultaneous resolution of A_1, which blows up the single $\mathbb{P}^1$ of the singular fiber. The path algebra is defined in the following way

$$\mathcal{A}_1 \cong \mathbb{H}_{A_1}\langle e_2, e_1, a_2, a_1, a_2^*, a_1^*\rangle \Big/ \begin{pmatrix} a_2a_2^* - a_1^*a_1 = g_1e_1, \\ a_1a_1^* - a_2^*a_2 = g_2e_2 \end{pmatrix}. \tag{4.70}$$

With $a_2, a_1^* \in e_1Ae_2, \quad a_2^*, a_1 \in e_2Ae_1$, and $\mathbb{H}_{A_1} = \mathbb{C}[g_1, g_2]/(g_1 + g_2)$.

Clearly, the two path algebras are not isomorphic. However, there is a class of simple threefold flops which maps to both. This is the Reid Pagoda, a geometry that will be a protagonist in the construction of the next chapters.

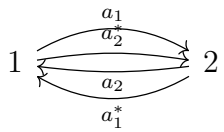

Figure 4.6: Quiver for the universal flop of length 1.

4.3.4 NCCR for Simple flops: The Reid Pagoda

The singular geometry is defined by the equation:

$$f_k: \quad x^2+y^2+z^2-w^{2k}=0, \quad (x,y,z,w)\in\mathbb{C}^4. \tag{4.71}$$

In this example $k=2$. From the equation we can see that the geometry has the structure of a fibration of deformed A_1 singularities over the w plane, and of a deformed A_{2k-1} along z. Adopting the first interpretation the total space appears as the collision of k conifold points:

$$x^2+y^2=(z+(w-a_1)(w-a_2)\cdots(w-a_k))(z-(w-a_1)(w-a_2)\cdots(w-a_k)), \quad a_i\to 0 \ \ \forall i. \tag{4.72}$$

With the second, this is a monodromic fibration of A_{2k-1} over the z-plane, in the sense that the volumes of the exceptional $\mathbb{P}^1$'s are monodromic functions of the variable z. In this specific case, monodromies obstruct the blow up of all the 2-cycles but one.

Let us see how to derive the resolution from $\mathcal{A}_C$ and $\mathcal{A}_1$.

NCCR of the Reid Pagoda from $\mathcal{A}_C$.

Going back to the discussion we did in 4.2.3, we can see that the locus: $\varrho_1+\varrho_3=0,\ \varrho_2=0$ intersects the singular locus of the A_3 family in 4.46 only at the origin: $\varrho_1=\varrho_2=\varrho_3=0$.

So, projecting on this subspace:

$$\mathcal{H}_C\to\tilde{\mathcal{H}}_C=\mathbb{C}[\varrho_1,\varrho_2,\varrho_3,t]/(\varrho_1+t,\ \varrho_3-t,\ \varrho_2), \tag{4.73}$$

$$\mathcal{A}_C\to\tilde{\mathcal{A}}_C=\mathcal{A}_C\otimes_{\mathcal{H}_C}\tilde{\mathcal{H}}_C. \tag{4.74}$$

Relations in 4.69 reduce to:

$$\begin{aligned}
\alpha_1\beta_2 - \alpha_2\beta_1 &= 2te_2,\\
\beta_1\alpha_2 - \beta_2\alpha_1 &= -2te_4,\\
\alpha_2\beta_1 + \alpha_1\beta_2 &= \gamma_2^2,\\
\beta_1\alpha_2 + \beta_2\alpha_1 &= \gamma_4^2,\\
\gamma_2\alpha_i - \alpha_i\gamma_4 &= 0,\\
\beta_i\gamma_2 - \gamma_4\beta_i &= 0.
\end{aligned} \tag{4.75}$$

The last two relations imply that the element $\gamma = \gamma_2 \oplus \gamma_4$ is central. Moreover, we interpret t as a central element. Since it depends linearly on other length 2 loops, we can remove it.[19] We can thus, rewrite the ideal of relations as:

$$\begin{aligned}
\alpha_2\beta_1 + \alpha_1\beta_2 &= \gamma^2 e_2,\\
\beta_1\alpha_2 + \beta_2\alpha_1 &= \gamma^2 e_4,\\
[z, \alpha_i] &= 0,\\
[z, \beta_i] &= 0.
\end{aligned} \tag{4.77}$$

The coordinate ring of the singular threefold $R = \mathbb{C}[x, y, z, w]/(f_2)$ is (ismorphic to) the center of the path algebra $\mathcal{Z}(\tilde{\mathcal{A}}_C) \simeq e_4\tilde{\mathcal{A}}_C e_4$ [130]. So, we have:

$$U \equiv \beta_1\alpha_1, \quad V \equiv \beta_2\alpha_2, \quad \frac{W^2 + Z}{2} \equiv \beta_1\alpha_2, \quad W = \gamma, \tag{4.78}$$

$$UV = \beta_1\alpha_1\beta_2\alpha_2 = (\gamma^2 - \beta_1\alpha_2)\beta_1\alpha_2 = \frac{(W^2 + Z)}{2}\frac{(W^2 - Z)}{2}. \tag{4.79}$$

Setting

$$U = \frac{X + iY}{2}, \quad V = \frac{X - iY}{2} \tag{4.80}$$

we recover 4.71. The quiver of this path algebra is still the one in Figure 4.5.

NCCR of the Reid Pagoda from $\mathcal{A}_1$.

[19] Promoting a deformation parameter to an element of the center of the path algebra requires adding relations that impose the vanishing of commutators with all the independent paths in the algebra. In this case, we should add relations of the form:

$$[te_2 + te_4, \alpha_i] = 0, \quad [te_2 + te_4, \beta_i] = 0 \tag{4.76}$$

However, all these turn out to be redundant.

Let us go back to the definition in 4.70. In particular, the relations read:

$$\begin{aligned} a_2 a_2^* - a_1^* a_1 &= g e_1, \\ a_1 a_1^* - a_2^* a_2 &= -g e_2. \end{aligned} \tag{4.81}$$

Where we set $g_1 = -g_2 = g$. First, we perform a change of coordinates:

$$w \mapsto g(w) = w^2 \tag{4.82}$$

Now, we want to promote the deformation parameter w to a central element of the path algebra:

$$w \mapsto w_1 e_1 + w_2 e_2, \quad [w, a] = 0, \ \forall a \in Q \tag{4.83}$$

Then, for convenience, we rename our paths:

$$a_1 \to \alpha_1, \quad a_2^* \to \alpha_2, \quad a_2 \to \beta_1, \quad a_1^* \to \beta_2. \tag{4.84}$$

Thus, our relations become:

$$\begin{aligned} \beta_1 \alpha_2 - \beta_2 \alpha_1 &= w_1^2 e_1, \\ \alpha_1 \beta_2 - \alpha_2 \beta_1 &= w_2^2 e_2, \\ \alpha_i w_1 &= w_2 \alpha_i, \\ \beta_i w_2 &= w_1 \beta_i. \end{aligned} \tag{4.85}$$

The variables w_i are now loops in the quiver, which turns into the one of Figure 4.5. The algebra is isomorphic to the one we found in 4.3.4.

example: $\mathcal{A}_{A_{2k+1}} \to \mathcal{A}_1$ The generalization is straightforward and leads to the path algebra defined by the quiver in Figure 4.7

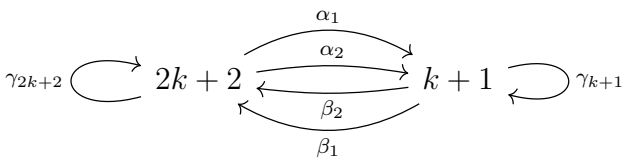

Figure 4.7: Quiver of the contracted algebra $e_C \mathcal{A}_{\tilde{A}_{2k+1}} e_C$, with $e_C = e_{k+1} + e_{2k+2}$.

With the relations:

$$\begin{aligned}
\alpha_1\beta_2 - \alpha_2\beta_1 &= 2te_{k+1}, \\
\beta_1\alpha_2 - \beta_2\alpha_1 &= -2te_{2k+2}, \\
\alpha_2\beta_1 + \alpha_1\beta_2 &= (\gamma_{k+1})^{k+1}, \\
\beta_1\alpha_2 + \beta_2\alpha_1 &= (\gamma_{2k+2})^{k+1}, \\
\gamma_{k+1}\alpha_i - \alpha_i\gamma_{2k+2} &= \quad 0, \\
\beta_i\gamma_{k+1} - \gamma_{2k+2}\beta_i &= \quad 0.
\end{aligned} \tag{4.86}$$

Following the reasoning of the previous paragraph, one can obtain the path algebra for the Pagoda with k generic.

Part II

3d Quiver Gauge Theories, 5d SCFTs and Canonical Singularities: towards a systematic extension of the toric paradigm

Chapter 5

A $D2$-brane view on Universal Flops

In the previous part of this thesis we reviewed how configurations of D6-branes in Type IIA string theory, described by a background Higgs field profile, provide a powerful framework for engineering families of ADE singularities in M-theory. This Higgs vev construction offers a particularly explicit and physically grounded realization of geometric backgrounds that are not easily accessible through the standard techniques of toric geometry. In this sense, it provides a complementary perspective on geometric engineering, allowing one to explore classes of Calabi–Yau singularities that lie beyond the toric regime.

At the same time, this point of view reveals subtleties in the relation between geometry and field theory that are not yet fully understood. In particular, the Higgs field description contains information that is not completely captured by the holomorphic structure of the associated geometry. As discussed in the introduction, configurations such as T-branes provide a striking illustration of this phenomenon. In these backgrounds, the holomorphic equation describing the singularity remains unchanged, while the physical vacuum of the theory is nevertheless modified in a substantial way. From the geometric perspective, this manifests itself as an obstruction to resolving the singularity: certain Kähler moduli are frozen to zero despite the absence of any apparent obstruction in the complex structure description. T-brane backgrounds have also been analyzed in the context of brane webs and incorporated in the framework of Generalized Toric Polygons [14].[1]

[1] GTPs are the only example of non-toric brane webs that have been realized so far. Therefore, an interesting question is whether cDV could be described by brane webs with white dots.

In the introductory sections, we have seen how this obstruction to resolving the singularity manifests itself in the context of non-trivial ADE fibrations. In particular, when one turns on a non-constant Higgs vev that is not holomorphically diagonalizable along the base of the fibration and reduces to a T-brane profile at the origin, the resulting geometry develops a characteristic obstruction to blowing up certain cycles in the singular fibers. Physically, this obstruction is tied to a monodromy of the associated holomorphic volumes when regarded as functions of the base coordinate. As one moves around the origin in the base, the periods of the vanishing cycles undergo a non-trivial monodromy, preventing a global choice of resolution compatible with the fibration. As discussed in the previous sections, such monodromic ADE fibrations are examples of compound Du Val singularities, which arise naturally as three-dimensional complex subspaces of the families of deformed ADE surfaces with partial simultaneous resolution 4.3.1. In 1.3 we reviewed how $D2$-brane probes offer a way to detect the presence of a T-brane background. The T-brane produces a magnetic monopole deformation on the worldvolume of the $D2$, and its effect can be reconstructed from the 3d mirror theory. It is then natural to ask whether the monodromic structure of the Higgs background can be similarly captured by deformations induced on the probe.

In this work, we exploit this probe perspective by analyzing the three-dimensional theory living on a D2-brane probing an ADE surface in the presence of a background Higgs field Φ. In this chapter, we will focus on constant Higgs field backgrounds, to prepare the ground for the non-constant monodromic cases discussed in 6. The introduction of Φ induces a deformation of the superpotential of the D2-brane worldvolume theory that, in many interesting cases, includes monopole operators. These monopole deformations play a crucial role in determining the infrared dynamics of the theory but are notoriously difficult to treat because of their non-perturbative nature. The techniques that we have introduced in Section 2.2 to analyze their effects in the IR were mostly developed by [35, 37, 77]. Applying these methods, we are able to determine the quiver and the superpotential of an effective three-dimensional theory that is valid for every value of the deformation parameters $\boldsymbol{\varrho}$.[2] As the parameters $\boldsymbol{\varrho}$ are varied, the three-dimensional theory and its moduli space change accordingly. In this way one obtains a family of three-dimensional gauge theories whose moduli spaces contain a geometric branch isomorphic to the corresponding deformed ADE surface. By fibering this branch over the deformation parameter space $\boldsymbol{\varrho}$, the full family of deformed ADE surfaces is reconstructed. This perspective provides a powerful tool for studying families of deformed ADE singularities, particularly in the context of universal flops.

[2]For a given value of $\boldsymbol{\varrho}$ there may still exist additional massive states that can be integrated out. The relevance of our IR theory is that we have already integrated out the fields that are massive for all values of $\boldsymbol{\varrho}$.

The quiver describing the three-dimensional theories in the family is related to the original quiver associated with the Dynkin diagram through operations such as node removal and arrow condensation, governed by the monopole deformation. Restricting to the maps that reproduce the deformed Higgs branches and consistently setting the others to zero, one obtains a quiver and a set of relations whose representation space reproduces the ADE family. These data match those obtained in [131] and reviewed in 4.3.3, where universal flops were constructed by determining the contraction algebra [132] through operations on the quiver closely related to those appearing in the present analysis. In particular, for the flop of length 2 we reproduce the universal flopping algebra of length 2 derived in [131].[3]

The three-dimensional gauge theory framework not only reconstructs the total space X_{r+2} but also faithfully reproduces its singularities. These singularities arise in specific regions of the deformation parameter space and appear in the probe description as additional branches of the moduli space. For generic values of $\boldsymbol{\varrho}$ the moduli space contains a single branch corresponding to the deformed Higgs branch inherited from the undeformed theory. At special loci in parameter space, however, new branches emerge, signaling that the fiber of the family becomes singular at those points. These fiber singularities coincide with singularities in the total space X_{r+2} when the simultaneous resolution of X_{r+2} blows up spheres that are shrunk in the singular surface. In the probe description, the sizes of the blown-up spheres correspond to Fayet–Iliopoulos parameters of the effective three-dimensional theory. At the points $\boldsymbol{\varrho}$ where additional branches appear, the $U(1)$ gauge factor associated with the FI term may or may not be broken; if it remains unbroken, the simultaneous resolution occurs, meaning that X_{r+2} is actually singular at those points.

Finally, the ADE families can be used to construct Calabi-Yau threefolds relevant for M-theory and Type IIA compactifications. In particular, starting from the universal flop X_6 of length $\ell = 2$ and allowing the parameters $\boldsymbol{\varrho}$ to depend on a single complex coordinate, one obtains the Morrison–Park threefold [133]. Compactifying M-theory or Type IIA string theory on this space gives rise to M2/D2 states with both charge 1 and 2 under a given $U(1)$ gauge symmetry, a feature that has been extensively exploited in the F-theory literature. Finally, we show how the monopole operators of the effective three-dimensional theory associated with X_6 can be used to extract information about the charges of M2/D2 states in compactifications on Calabi-Yau threefolds constructed from this geometry.

[3]The algorithm used in [131] to obtain the contraction of the quiver and the relations for the ADE families was already introduced in [12] from a more physical perspective. In that approach the parameters $\boldsymbol{\varrho}$ are allowed to depend on an additional field, making it possible to encode the relations of the family into a four-dimensional superpotential describing D3-branes probing Calabi–Yau threefold singularities in Type IIB string theory.

In this chapter, we provide a detailed analysis of the effective three-dimensional theories describing the universal flops of length 1 and 2, successfully reproducing their known geometric structures. The more intricate cases with $\ell > 2$ are left for future investigation.

The chapter is organized as follows. in Section 5.1 we analyze the effect of turning on a background for Φ and construct the universal flop of length 1 from a family of deformed A_1 singularities with simultaneous resolution; we also study the effective theory associated with a specific A_3 family in preparation for the more intricate $\ell = 2$ case. Section 5.2 presents our main result, where the universal flop of length 2 and its geometric properties are derived from the family of three-dimensional theories obtained through monopole deformation of the D2-brane probe of a D_4 singularity.

5.1 D2-branes and families of ADE surfaces

We now switch on a vev for Φ. This will deform the worldvolume theory of the D2-brane as it is now probing a different background (deformed by non-zero Φ).

5.1.1 A_1-family from D2-branes and universal flop of length 1

We start again considering the A_1 case studied in Section 2.2.3.

On the Theory A side, the effect of a non-zero vev for Φ is straightforward to understand, as Φ is the complex adjoint scalar living on the worldvolume of a stack of two D6-branes. This induces the following superpotential deformation on the worldvolume of the probing D2-brane:

$$\delta W_A = \mathrm{Tr}\Phi M \qquad \text{with} \qquad M_{ij} = Q_i \tilde{Q}_j \,, \tag{5.1}$$

that is a mass term for some flavors.

Applying the mirror maps to (5.1), one obtains the superpotential deformation induced by Φ in Theory B. We notice that when the matrix Φ has off-diagonal elements, the trace in (5.1) involves operators $Q_i\tilde{Q}_j$ with $i \neq j$ that are mapped by mirror symmetry to monopole operators (see (2.19)). Hence, in this case δW_B includes these non-elementary operators. In order to deal with monopole superpotentials, we follow the procedure in [35, 37, 77]: one maps the 3d theory with monopole superpotential to a dual 3d theory with a superpotential that depends only on

elementary fields. We now work in Theory B. In the A_1 example, a non-zero vev for Φ generates the deformation

$$\delta W_B = \text{Tr}\left[\Phi(\varrho)\begin{pmatrix}\phi_1-\phi_2 & w_+\\ w_- & \phi_2-\phi_1\end{pmatrix}\right]. \tag{5.2}$$

We two choices of Φ:

$$\Phi(t)=\begin{pmatrix}t & 0\\ 0 & -t\end{pmatrix}, \qquad \Phi(\mu)=\begin{pmatrix}0 & 1\\ \mu & 0\end{pmatrix} \tag{5.3}$$

The diagonal one is the Φ corresponding to the universal flop of length one; the other will be important for addressing the more complicated cases discussed in the upcoming sections.

- Case 1:

  $$\delta W_B = 2t(\phi_1-\phi_2).$$

  This is a complex FI term. The Higgs branch of the moduli space is simply deformed to

  $$uv = z^2 - t^2$$

  in terms of the gauge invariant variables $u = q_1q_2$, $v = \tilde{q}_1\tilde{q}_2$ and $z = q_1\tilde{q}_1 + t$. This is the expression for the A_1 family with simultaneous resolution, i.e. *the universal flop of length one.*

  Let us check the presence of other branches allowed by the F-terms: When $t \neq 0$ the $U(1)$ gauge group of the 3d theory is broken and the HB is the only branch of the theory. At $t = 0$, a new branch arises, i.e. the CB with geometry $\mathbb{C}^2/\mathbb{Z}_2$; moreover, along this branch the $U(1)$ gauge group is unbroken.

- Case 2:

  $$\delta W_B = w_- + \mu\, w_+. \tag{5.4}$$

  This superpotential depends on monopole operators. We go to the mirror theory, where the deformed superpotential is

  $$W_A^{\text{def}} = \varphi(Q_1\tilde{Q}_1 + Q_2\tilde{Q}_2) + Q_2\tilde{Q}_1 + \mu Q_1\tilde{Q}_2 \tag{5.5}$$

  The deformations are now simple mass terms. Since we want to obtain the moduli space for each value of the parameter μ, we integrate only the fields that are massive $\forall\mu$, i.e. in

this case Q_2 and $\tilde{Q}_1$. After doing this, one obtains an $\mathcal{N} = 2$ 3d[4] U(1) gauge theory with one flavor, one singlet φ and the superpotential

$$W_{A,\text{eff}} = (\mu - \varphi^2) Q_1 \tilde{Q}_2 \,. \tag{5.6}$$

We now apply mirror symmetry on this effective theory [37, 77]. The mirror symmetric of a U(1) gauge theory with one flavor and zero superpotential is the XYZ model, with mirror map given by $X \leftrightarrow Q_1\tilde{Q}_2$, $Y \leftrightarrow v_+$, $Z \leftrightarrow v_-$. When the U(1) model is deformed by the superpotential (5.6), the XYZ model has the superpotential

$$W_{B,\text{eff}} = XYZ + X(\mu - \varphi^2) = X \, \det \mathfrak{M} + \mu \, X \,, \qquad \text{with } \mathfrak{M} \equiv \begin{pmatrix} \varphi & -Y \\ Z & -\varphi \end{pmatrix} . \tag{5.7}$$

The matrix $\mathfrak{M}$ is in the adjoint representation[5] of the original flavor group $SU(2)$ (that was acting on the HB) that is not broken by the deformation δW_B. The F-terms are

$$\frac{\partial W}{\partial X} = 0 \quad : \qquad Y\,Z = \varphi^2 - \mu \,; \tag{5.8}$$

$$\frac{\partial W}{\partial \varphi} = 0 \quad : \qquad X\,\varphi = 0 \,; \tag{5.9}$$

$$\frac{\partial W}{\partial Y} = 0 \quad : \qquad X\,Z = 0 \,; \tag{5.10}$$

$$\frac{\partial W}{\partial Z} = 0 \quad : \qquad X\,Y = 0 \,. \tag{5.11}$$

The last two equations give two branches: $X = 0$ or $Y = Z = \varphi = 0$. The second one is excluded when $\mu \neq 0$, because of (5.8). The first one is the space parametrized by Y, Z, φ subject to the relation $YZ = \varphi^2 - \mu$, that is the defining equation of the A_1 family with no simultaneous resolution. For $\mu = 0$, the branch $Y = Z = \varphi = 0$ is allowed. It is a complex one-dimensional space parametrized by X. There is still no $U(1)$ gauge group when $\mu = 0$.

From the point of view of the probe D2-brane, the two Φ's in 5.3 deform the worldvolume theory in the same manner away from the origin ($t \neq 0$ or $\mu \neq 0$); at this point however the worldvolume theory of the probe D2-brane is different even though the geometry is the singular A_1 surface. What distinguishes the two Φ's at the origin is that in Case 2, the geometry is sup-

[4] When $\mu \neq 0$, the 3d $\mathcal{N} = 4$ supersymmetry is recovered as emergent in the IR [74, 134, 135]. In fact, [74] considered deformation like the one in this example, with μ a dynamical field.

[5] One can interpret the fields φ, Y, Z as condensates of $q_i, \tilde{q}_j$ (see (2.20)).

plemented by a T-brane background. The theory on a D2-brane probing a T-brane background was studied first in [37] and is exactly the one discussed in 2.2.4. In particular, we notice that the original CB is partially lifted to the $\mathbb{C}$ parametrized by X.

5.1.2 ADE family from the D2- probe for generic ADE algebra

We now extend the lesson we learned in the simple A_1 example to a generic ADE singularity. One probes such a singularity by a D2-brane. The singular background can be deformed by switching on the adjoint complex scalar Φ. From the point of view of the probe theory, it is an object in the adjoint representation of the flavor group G_F acting on one branch of the moduli space (the CB on the B-side) of the probe 3d theory. The flavor algebra is the ADE algebra associated with the singularity.

The deformation of the superpotential takes an elementary form:

$$\delta W = \mathrm{Tr}\left[\Phi \boldsymbol{\mu}\right] \ , \tag{5.12}$$

where $\boldsymbol{\mu}$ is the moment map of the flavor symmetry G_F. In Theory B (D2-branes at ADE singularities) $\boldsymbol{\mu}$ is the moment map on the CB, that involves several monopole operators. Hence, to deal with this deformation one needs to be able to treat monopole superpotentials. We will illustrate how to do this in the following section, in preparation for the more complicated universal flop of length 2.

The form (5.12) of the deformation can be generalized to any ADE algebra. It can be checked explicitly by string duality for the A and D algebras (as done for the A_1 case). Adding (5.12) to the superpotential deforms the Higgs branch of the probe 3d theory. The family of such deformed HB moduli spaces over the parameter space B_{ϱ} *is* the ADE-family, with the simultaneous resolution determined by the form of Φ or, equivalently, by the Levi subalgebra in which $\Phi(\varrho)$ resides.

The effective 3d theory provides more information than the defining equation of the ADE family. When the parameters $\boldsymbol{\varrho}$ are such that the ADE surface becomes singular, the HB of the D2-brane probe theory develops singularities, and new branches of the moduli space emerge from those singularities. However, this does not imply that the entire $(r+2)$-fold family X_{r+2} becomes singular at that value of $\boldsymbol{\varrho}$. A singularity arises in the family when, upon resolving it, certain roots

of the singular fiber blow up.[6] In the effective 3d theory, the sizes of these roots are determined by the FI parameters, as explained in Section 2.2. Activating one of these parameters forces the corresponding root to blow up at the singularity of the HB. These FI parameters correspond one-to-one with the $U(1)$ factors in the gauge group of the 3d theory. When the effective theory lacks any $U(1)$ factors, even in the presence of a singular HB, it indicates a T-brane background, which obstructs the resolution [37]. This means that no roots can be resolved at that point in B_{ϱ}, and consequently, the family is not singular there. This is the mechanism by which partial simultaneous resolutions are implemented in the effective theory.

In other words, the deformation (5.12) leads to an effective 3d theory with its own quiver (i.e. gauge group and matter) and superpotential W_{eff}; varying $\boldsymbol{\varrho}$ the superpotential changes and the moduli space of the 3d theory is modified. At generic points in B_{ϱ} the moduli space has only one branch, the deformed HB, where the gauge group is broken completely. At points of B_{ϱ} where a new branch arises, the effective theory may have points in the moduli space (in particular the common origin of the branches) where (part of) the gauge group of the quiver is unbroken. If this (sub)group contains $U(1)$ factors, there is the possibility to activate real FI-parameters, that lead to the resolution of the singularity of the HB.

We therefore present the following statement, which will be supported by the examples that follow:

Consider the set of effective 3d theories over the space B_{ϱ}. The family of HB moduli spaces is the family of ADE-surfaces. Singular surfaces arise at values of $\boldsymbol{\varrho}$ where the 3d theory develops an additional branch beyond the HB. Furthermore, at such points in B_{ϱ}, the gauge group of the effective theory at the intersection of the new branch with the HB may or may not have some $U(1)$ factors; the number of the corresponding FI-parameters indicates how many roots of the singular fiber are blown up in the (partial) simultaneous resolution.

This statement is, in particular, verified in the A_1 case studied above. There, the gauge group has only one $U(1)$ factor, hence there is at most one FI-parameter. This is related to the fact that A_1 has one simple root, that may or may not be resolved in the family, corresponding to the fact

[6] This means that actual curves have shrunk to zero size in the singular limit.

that the in the effective theory the $U(1)$ survives or not. Let us see the two possible cases:

- Case 1. At $t = 0$, a new branch arises, corresponding to the fiber developing an A_1 singularity, and a $U(1)$ factor survives, with its real FI-term that would blow up the simple root of the A_1 singularity. This is in agreement with our statement, as Case 1 is the family *with* simultaneous resolution, i.e., the *universal flop of length* $\ell = 1$.

- Case 2. When $\mu \neq 0$ the deformed A_1 surface is the only branch of the moduli space. At $\mu = 0$, we have a new branch that tells us the corresponding ADE surface is singular as it can be checked from the defining equation of the family. However, now there is no $U(1)$ factor in the gauge group, hence the effective theory cannot be deformed by a non-zero real FI-term, which means that the shrunk A_1 root cannot be blown up. This is compatible with the fact that this family has no simultaneous resolution of the simple root in the central fiber (as this family is a smooth space).

Another simple example to test our statement is an A_2 family with complete simultaneous resolution. The corresponding Higgs field is a diagonal matrix, $\Phi =$Diag$(t_1, t_2, -t_1 - t_2)$, where t_1, t_2 are the parameters parametrizing the base B_ϱ. The defining equation takes the form

$$u\, v = (z - t_1)(z - t_2)(z + t_1 + t_2)\,. \tag{5.13}$$

The superpotential deformation is just a sum of complex FI-term:

$$\delta W = (2t_1 + t_2)\phi_1 - (t_1 - t_2)\phi_2 - (2t_2 + t_1)\phi_3\,. \tag{5.14}$$

At a generic point in B_ϱ, the $U(1) \times U(1)$ gauge symmetry is fully broken, and the HB is deformed into a smooth surface, which remains the only branch of the moduli space. When the coefficient of one of the ϕ_i in (5.14) vanishes, the corresponding $U(1)$ factor is preserved in the effective theory, and its CB emanates from the HB. The effective theory possesses a real FI parameter, consistent with the fact that at these points, the equation (5.13) develops an A_1 singularity, which is blown up in the simultaneous resolution of the family. Finally, when $t_1 = t_2 = 0$, the gauge group retains both $U(1)$ factors with corresponding FI parameters and CB. This is the origin of the family, where the surface has an A_2 singularity, and both roots are blown up in the simultaneous resolution.

5.1.3 Example: A_3-family from D2-branes

As a preliminary step toward tackling the universal flop of length $\ell = 2$, we first consider a simpler A_n case, which we introduced in 4.2.3.

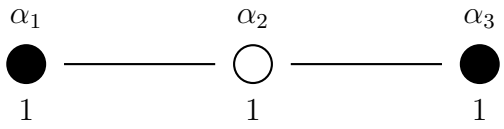

Figure 5.1: A_3 Dynkin diagram. The colored nodes corresponds to the obstructed spheres in the partial simultaneous resolution of the A_3 family.

We want to realize a family of A_3 surfaces with the simultaneous resolution only of the central node of the corresponding Dynkin diagram (see Figure 5.1). This means that the Levi subalgebra $\Phi(\varrho)$ should belong to is

$$\mathcal{L} = A_1^{\alpha_1} \oplus A_1^{\alpha_3} \oplus \langle \alpha_2^* \rangle \tag{5.15}$$

where $A_1^{\alpha_i}$ is the A_1 subalgebra $\langle e_{\alpha_i}, e_{-\alpha_i}, [e_{\alpha_i}, e_{-\alpha_i}] \rangle$.

Following the rules given in Section 1.4.3, the corresponding Higgs field takes the form

$$\Phi = \begin{pmatrix} \varrho_2 & 1 & & \\ \varrho_1 & \varrho_2 & & \\ & & -\varrho_2 & 1 \\ & & \varrho_3 & -\varrho_2 \end{pmatrix} \tag{5.16}$$

and the equation for the family is, according to (1.29),

$$uv = \left((z-\varrho_2)^2 - \varrho_1\right)\left((z+\varrho_2)^2 - \varrho_3\right) \ . \tag{5.17}$$

We now consider a D2-brane probing the A_3 surface deformed by (5.16) and we will show that the family of its HB moduli spaces over B_ϱ is exactly the family (5.17).

The worldvolume theory of a D2-brane probing the A_3 singularity is a 3d $\mathcal{N} = 4$ supersym-

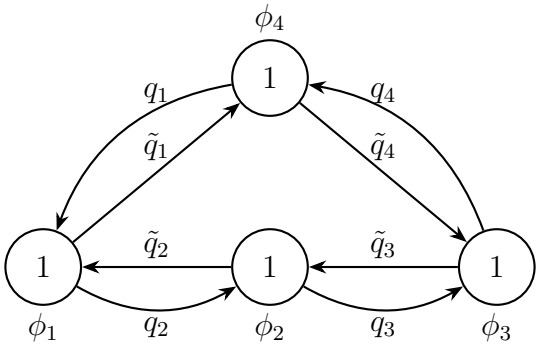

Figure 5.2: A_3 quiver.

metric quiver gauge theory, with the quiver in Figure 5.2 and the superpotential

$$W_{A_3} = \sum_{i=1}^{4} (\phi_i - \phi_{i-1}) q_i \tilde{q}_i \ , \tag{5.18}$$

with the convention $\phi_0 = \phi_4$.

To write down the deformation (5.12) that Φ induces, we need to say what is the moment map on the CB of this theory. The flavor symmetry on the CB is $SU(4)$ and the moment map is (according to mirror symmetry [28, 31])

$$\boldsymbol{\mu} = \begin{pmatrix} \phi_4 - \phi_1 & w_{1,0,0} & w_{1,1,0} & w_{1,1,1} \\ w_{-1,0,0} & \phi_1 - \phi_2 & w_{0,1,0} & w_{0,1,1} \\ w_{-1,-1,0} & w_{0,-1,0} & \phi_2 - \phi_3 & w_{0,0,1} \\ w_{-1,-1,-1} & w_{0,-1,-1} & w_{0,0,-1} & \phi_3 - \phi_4 \end{pmatrix} . \tag{5.19}$$

Plugging (5.16) and (5.19) into $\delta W = \mathrm{Tr}\,[\Phi\, \boldsymbol{\mu}]$, we obtain

$$\delta W = 2\varrho_2(\phi_4 - \phi_2) + w_{-1,0,0} + \varrho_1 w_{1,0,0} + w_{0,0,-1} + \varrho_3 w_{0,0,1} \ . \tag{5.20}$$

The monopole operators that appear in this deformation are those related to the white nodes (2 and 4), i.e. the roots that are not blown up in the partial simultaneous resolution of the family.

We now write the deformed superpotential $W^{\rm def} = W_{A_3} + \delta W$ in the following form

$$\begin{aligned} W^{\rm def} &= \phi_1 {\rm Tr}\mathcal{M}_1 + w_{-1,0,0} + \varrho_1 w_{1,0,0} + {\rm Tr}\left[\begin{pmatrix}\phi_4 & 0\\ 0 & \phi_2\end{pmatrix}\mathcal{M}_2\right] \\ &+ 2\varrho_2(\phi_4 - \phi_2) \\ &+ \phi_3 {\rm Tr}\mathcal{M}_3 + w_{0,0,-1} + \varrho_3 w_{0,0,1} + {\rm Tr}\left[\begin{pmatrix}\phi_2 & 0\\ 0 & \phi_4\end{pmatrix}\mathcal{M}_4\right] , \end{aligned} \tag{5.21}$$

where $\mathcal{M}_i$, $i = 1, 3$, are the meson matrices of nodes 1 and 3, i.e.

$$\mathcal{M}_1 = \begin{pmatrix} q_1\tilde{q}_1 & -q_1 q_2 \\ \tilde{q}_2\tilde{q}_1 & -\tilde{q}_2 q_2 \end{pmatrix} \qquad \text{and} \qquad \mathcal{M}_3 = \begin{pmatrix} q_3\tilde{q}_3 & -q_3 q_4 \\ \tilde{q}_4\tilde{q}_3 & -\tilde{q}_4 q_4 \end{pmatrix} . \tag{5.22}$$

The superpotential operators in (5.21) are relative to the U(1) gauge group of nodes 1 and 3 respectively. In order to deal with such situations, with monopole operators in the superpotential, [37] proposed the following procedure:

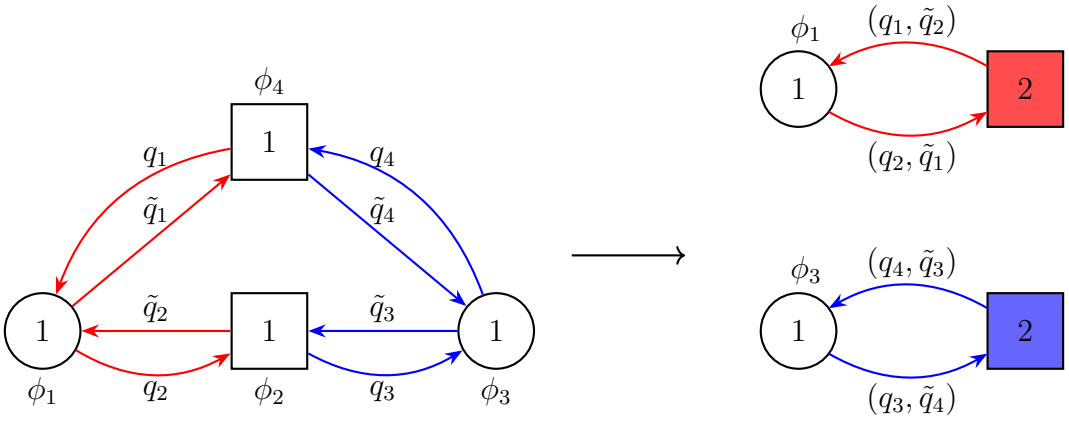

Figure 5.3: A_3 theory: ungauging nodes 2 and 4, we end up with two copies of a $U(1)$ gauge theory with 2 flavors.

1. The monopole operator is charged under the topological $U(1)_T$ relative to one node. Consider that abelian node, and ungauge the nearby U(1) gauge factors; in our example, one ungauges node 2 and 4, isolating nodes 1 and 3 as depicted in Figure 5.3. The isolated theory is coupled back to the nearby nodes (to obtain the full quiver gauge theory) by gauging a subgroup of its flavor symmetry; this is implemented by the last terms in row 1 and 3 in (5.21).

For each isolated (balanced) node one has a 3d $\mathcal{N}=4$ supersymmetric $U(1)$ gauge theory with two flavors and a monopole superpotential deformation. Let us consider node 1 in our example: The isolated theory is $U(1)$ with two flavors and superpotential

$$W_1 = \phi_1 \mathrm{Tr}\mathcal{M}_1 + w_{-1,0,0} + \varrho_1 w_{1,0,0} \,. \tag{5.23}$$

This is clearly of the form (5.2) encountered in the A_1 case, with $\mu = \varrho_1$. We have the same for node 3, with $\mu = \varrho_3$.

2. Now, we apply ('local') mirror symmetry to the isolated 3d theory to go to a $U(1)$ gauge theory with two flavors and mass term deformations like in the A_1 case. We then compute the effective theory after integrating out the massive field (massive for all values of $\boldsymbol{\varrho}$). Finally, we apply mirror symmetry back obtaining an effective theory. This theory has the same flavor symmetry as the original isolated theory on its HB.

   Basically we need to follow the same steps as in the A_1 case of Section 5.1.1. We obtain a modified XYZ theory with superpotential

$$W_1^{\text{eff}} = X_1 \det \mathfrak{M}_1 + \varrho_1 X_1 \qquad \text{with} \qquad \mathfrak{M}_1 \equiv \begin{pmatrix} \varphi_1 & -Y_1 \\ Z_1 & -\varphi_1 \end{pmatrix} \tag{5.24}$$

   and flavor symmetry $SU(2)$. For node 3 we have the same theory with analogous superpotential.

3. We now have to couple this effective theory back to the quiver. The superpotential terms realizing it are traces of the product of the moment map of the $SU(2)$ flavor symmetry with the ϕ-dependent matrix appearing at the end of rows 1 and 3 in (5.21).

   For node 1, we need to add

$$\mathrm{Tr}\left[\begin{pmatrix} \phi_4 & 0 \\ 0 & \phi_2 \end{pmatrix} \mathfrak{M}_1\right] = \mathrm{Tr}\left[\begin{pmatrix} \frac{\phi_4-\phi_2}{2} & 0 \\ 0 & \frac{\phi_2-\phi_4}{2} \end{pmatrix} \mathfrak{M}_1\right] = \varphi_2(\phi_4-\phi_2) \,. \tag{5.25}$$

   We do analogously for node 3.

We can now write down the effective superpotential for the effective theory, by adding also

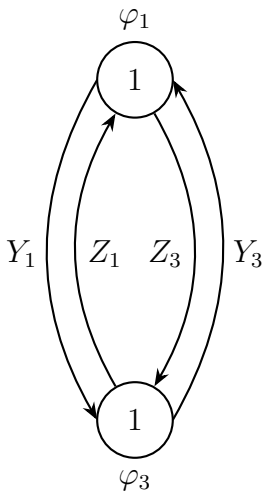

Figure 5.4: Quiver for the universal flop of length 1.

the term in the second line of (5.21):

$$W^{\text{eff}} = X_1 \left(\det \mathfrak{M}_1 + \varrho_1\right) + X_3 \left(\det \mathfrak{M}_3 + \varrho_3\right) + (\varphi_1 - \varphi_3 + 2\varrho_2)(\phi_4 - \phi_2) \,. \tag{5.26}$$

Note that the final quiver, depicted in Figure 5.4, has now two nodes less, as the U(1) of nodes 1 and 3 now disappeared from the effective theory (see [37]).

Let us check that the family of moduli spaces over the variety parametrized by $(\varrho_1, \varrho_2, \varrho_3)$ is the A_3 family we are probing. Before computing the F-terms, we integrate out the massive fields $(\phi_4 - \phi_2)$ and $(\varphi_1 - \varphi_3)$, obtaining:

$$W^{\text{eff}} = X_1 \left(Y_1 Z_1 - (\varphi - \varrho_2)^2 + \varrho_1\right) + X_3 \left(Y_3 Z_3 - (\varphi + \varrho_2)^2 + \varrho_3\right) \,, \tag{5.27}$$

with $\varphi \equiv \frac{\varphi_1+\varphi_3}{2}$. The F-terms are the following

$$\frac{\partial W}{\partial X_2} = 0 \quad : \qquad Y_1 Z_1 = (\varphi - \varrho_2)^2 - \varrho_1 \, ; \tag{5.28}$$

$$\frac{\partial W}{\partial X_4} = 0 \quad : \qquad Y_3 Z_3 = (\varphi + \varrho_2)^2 - \varrho_3 \, ; \tag{5.29}$$

$$\frac{\partial W}{\partial \varphi} = 0 \quad : \qquad \varrho_2(X_1 - X_3) - \varphi(X_1 + X_3) = 0 \, ; \tag{5.30}$$

$$\frac{\partial W}{\partial Y_i} = 0 \quad : \qquad X_i Z_i = 0 \qquad i = 1, 3 \, ; \tag{5.31}$$

$$\frac{\partial W}{\partial Z_i} = 0 \quad : \qquad X_i Y_i = 0 \qquad i = 1, 3 \, . \tag{5.32}$$

The last equations select four branches: $\{X_1 = X_3 = 0\}$, $\{X_1 = Y_3 = Z_3 = 0\}$, $\{X_3 = Y_1 = Z_1 = 0\}$ and $\{Y_1 = Z_1 = Y_3 = Z_3 = 0\}$. The last three branches are incompatible with the first set of equations for generic $\varrho_1, \varrho_2, \varrho_3$. As we will see shortly, these branches are allowed on some special loci in the space B_ϱ, where the deformed HB develops singularities.

The A_3 family from the deformed HB

Let us concentrate on the space given by $X_1 = X_3 = 0$ with the relations (5.28) and (5.29) and modded out by the $U(1) \times U(1)$ gauge transformations. The gauge invariant coordinates on this moduli space are:

$$U \equiv Y_1 Y_3 \, , \qquad V \equiv Z_1 Z_3 \, , \qquad P_1 \equiv Y_1 Z_1 \, , \qquad P_3 \equiv Y_3 Z_3 \, , \tag{5.33}$$

together with φ. These are related by $UV = P_1 P_3$. The relations (5.28) and (5.29) become

$$P_1 = (\varphi - \varrho_2)^2 - \varrho_1 \qquad \text{and} \qquad P_3 = (\varphi + \varrho_2)^2 - \varrho_3 \, . \tag{5.34}$$

Hence, the moduli space is the set parametrized by U, V, φ modulo the relation

$$U\,V = \left((\varphi - \varrho_2)^2 - \varrho_1\right)\left((\varphi + \varrho_2)^2 - \varrho_3\right) \, . \tag{5.35}$$

This is exactly the A_3 family with defining equation (5.17).

Singularities of the family from the effective 3d theory

For generic values of $\varrho_1, \varrho_2, \varrho_3$, the surface singularity is completely deformed, i.e. the HB is smooth and it is the only component of the moduli space. We expect new branches of the moduli space emerging at singularities of the HB. To understand which loci of B_ϱ support singular surfaces, it is then enough to see when the moduli space of the probe D2-brane theory develops new branches. In this way, the effective 3d theory detects the loci where new singularities arise.

Let us see what happens over some specific loci of B_ϱ:

- When $16\varrho_2^4 - 8\varrho_2^2(\varrho_1+\varrho_3)^2 + (\varrho_1-\varrho_3)^2 = 0$, the relations above allow the new branch

$$Y_1 = Z_1 = Y_3 = Z_3 = 0\,, \quad \varphi = \frac{\varrho_3 - \varrho_1}{4\varrho_2}\,, \quad X_3 = \left(\frac{4\varrho_2^2 + \varrho_1 - \varrho_3}{4\varrho_2^2 - \varrho_1 + \varrho_3}\right) X_1\,. \tag{5.36}$$

  Along this branch, the relative $U(1)$ is unbroken and X_1 takes any value. The monopole operators of the relative $U(1)$ can take vev subject to the relation $V_+V_- = \left(\frac{4\varrho_2^2+\varrho_1-\varrho_3}{4\varrho_2^2-\varrho_1+\varrho_3}\right) X_1^2$. I.e. we find a branch with the geometry of $\mathbb{C}^2/\mathbb{Z}_2$, that is what one expects for the CB of a D2-brane probing an A_1 singularity. In fact, it can be checked that on the locus under consideration, the A_3 surface develops an A_1 singularity. We have detected it by looking at the effective theory. Moreover, the $U(1)$ is untouched and one can switch on a real FI-parameter, which corresponds to a resolution of the A_1 singularity. This signals that this is also a singularity of the full family and that we can do a simultaneous resolution.

- When $\varrho_1 = 0$, the following new branch arises:

$$Y_1 = Z_1 = X_3 = 0 \quad \varphi = \varrho_2\,, \quad Y_3 Z_3 = 4\varrho_2^2 - \varrho_3\,, \tag{5.37}$$

  with X_1 unconstrained. We then see a complex 1-dimensional branch. This may look strange for a D2-brane probing a singularity. In fact, when $\varrho_1 = 0$ the equation of the surface manifestly develops an A_1 singularity at $U = V = \varphi - \varrho_2 = 0$. However, the background still has a T-brane deformation, that is not visible at the level of the geometry. Our effective theory is however able to detect such background, as the effective theory we obtain is the same as the one of a D2-brane probing an A_1 singularity with a T-brane background (see [37, 77]). In particular, along this branch there is no unbroken $U(1)$ (as the charged fields Y_3, Z_3 must take non-zero vev). Correspondingly, one loses the possibility to deform the theory by an FI-term and there is no simultaneous resolution.

- When $\varrho_3 = 0$, the following new branch arises:

$$Y_3 = Z_3 = X_1 = 0 \quad \varphi = -\varrho_2 \,, \quad Y_1 Z_1 = 4\varrho_2^2 - \varrho_1 \,, \tag{5.38}$$

  with X_3 unconstrained. All considerations done for the previous case hold here.

- At the intersection of the first and one of the other two loci, the effective theory is the same one would obtain by probing an A_2 singularity with a given T-brane background. In particular there is only one $U(1)$ gauge group, with the possibility of turning on one non-zero FI-parameter: only one 2-sphere is blown up in the simultaneous resolution.

- At the intersection $\varrho_1 = \varrho_3 = 0$, there are new branches, but the T-brane is so severe that no $U(1)$ is left. In fact, the fiber develops an $A_1 \oplus A_1$ singularity, but the sixfold is smooth.

- At $\varrho_1 = \varrho_2 = \varrho_3 = 0$, the A_3 surface has the full A_3 singularity. Together with the HB displaying the A_3 singularity, there is another branch. This is what is left from the A_3 CB after switching on the T-brane background. There is only one $U(1)$ in the effective 3d theory with the possibility of turning on an FI-term. Again this means that the simultaneous resolution blows up just the central node.

The effective theory tells us that the A_3 family has singularities only along the first locus, as it can be checked directly from its defining equation. As expected, the analysis of the singularities along the HB and the F-term relations that are non-trivial in the geometric sector (that is, when $X_1 = X_3 = 0$) reproduce the results derived in 4.2.3 and 4.3.3 from the Springer theory of resolutions of the families of deformed ADE and the non-commutative resolutions constructed à la Karmazyn.

5.2 Universal flop of length 2 from D2-branes

In this section, we want to realize the universal flop of length 2 as the family of HB moduli spaces of D2-branes probing a D_4 singularity deformed by a specific form of $\Phi(\boldsymbol{\varrho})$.

5.2.1 Universal flop of length 2 and the Higgs field Φ

The Higgs field that realizes the universal flop of length $\ell = 2$ should allow the simultaneous resolution only of the simple root corresponding to the central node of the D_4 Dynkin diagram.

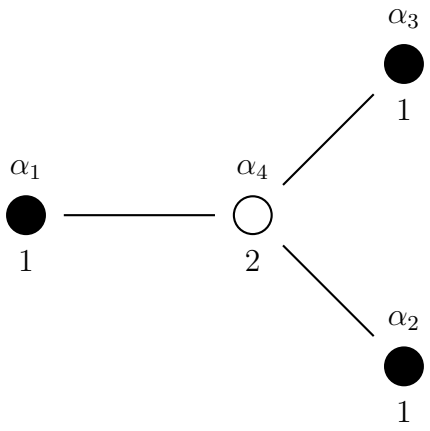

Figure 5.5: D_4 Dynkin diagram. The colored nodes correspond to the obstructed spheres in the partial simultaneous resolution of the D_4 family realizing the universal flop of $\ell = 2$.

We call this root α_4 (see Figure 5.5). This requirement implies that Φ must live in the following Levi subalgebra:

$$\mathcal{L} = A_1^{(\alpha_1)} \oplus A_1^{(\alpha_2)} \oplus A_1^{(\alpha_3)} \oplus \langle \alpha_4^* \rangle \subset D_4 \,. \tag{5.39}$$

Following the prescription (6.72) for each A_1 summand we have

$$\Phi|_{A_1^{(i)}} = \begin{pmatrix} 0 & 1 \\ \varrho_i & 0 \end{pmatrix} = e_{\alpha_i} + \varrho_i e_{-\alpha_i} \qquad i = 1, 2, 3 \,, \tag{5.40}$$

where ϱ_i ($i = 1, 2, 3$) is the Casimir of the $s\ell_2$ algebra $A_1^{(i)}$. Moreover Φ can have a component along α_4^* with coefficient ϱ_4.

Employing the standard basis of [136][7] we can write Φ as the matrix

$$\Phi = \left(\begin{array}{cccc|cccc} \varrho_4 & 1 & 0 & 0 & 0 & 0 & 0 & 0 \\ \varrho_1 & \varrho_4 & 0 & 0 & 0 & 0 & 0 & 0 \\ 0 & 0 & 0 & 1 & 0 & 0 & 0 & 1 \\ 0 & 0 & \varrho_3 & 0 & 0 & 0 & -1 & 0 \\ \hline 0 & 0 & 0 & 0 & -\varrho_4 & -\varrho_1 & 0 & 0 \\ 0 & 0 & 0 & 0 & -1 & -\varrho_4 & 0 & 0 \\ 0 & 0 & 0 & -\varrho_2 & 0 & 0 & 0 & -\varrho_3 \\ 0 & 0 & \varrho_2 & 0 & 0 & 0 & -1 & 0 \end{array}\right) . \tag{5.41}$$

The equation for the universal flop of $\ell = 2$ can be derived by plugging (6.86) into (1.46):

$$\begin{aligned} &x^2 + y^2 z - 2(\varrho_1 - \varrho_4^2)(\varrho_3 - \varrho_2) y \\ &\quad - \frac{((z + \varrho_1 - \varrho_4^2)^2 + 4\varrho_4^2 z)((z + \varrho_3 - \varrho_2)^2 + 4\varrho_2 z) - (\varrho_1 - \varrho_4^2)^2(\varrho_3 - \varrho_2)^2}{z} = 0 \end{aligned} \tag{5.42}$$

For later convenience, we introduce a change of variables to realize the versal deformation of the D_4 singularity written as $X^2 = Y\,Z\,(Y + Z)$. The coordinate transformation is

$$\begin{pmatrix} x \\ y \\ z \end{pmatrix} = \begin{pmatrix} 2X \\ Y - Z \\ Y + Z - (\varrho_1 + \varrho_2 + \varrho_3 + \varrho_4^2) \end{pmatrix} . \tag{5.43}$$

In terms of the variables X, Y, Z, the equation for the family is

$$\begin{aligned} X^2 =& YZ(Y + Z) - (\varrho_1 + \varrho_2 + \varrho_3 + \varrho_4^2) YZ + (\varrho_1 - \varrho_2)(\varrho_3 - \varrho_4^2) Y \\ &+ (\varrho_1 - \varrho_3)(\varrho_2 - \varrho_4^2) Z + (\varrho_1 - \varrho_2 - \varrho_3 + \varrho_4^2)(\varrho_1 \varrho_4^2 - \varrho_2 \varrho_3) . \end{aligned} \tag{5.44}$$

[7] I.e. we choose a basis such that an element M of D_4 is not an antisymmetric matrix but instead satisfies $MI + IM^T = 0$ with $I = \left(\begin{array}{c|c} & \mathbb{1}_4 \\ \hline \mathbb{1}_4 & \end{array}\right)$.

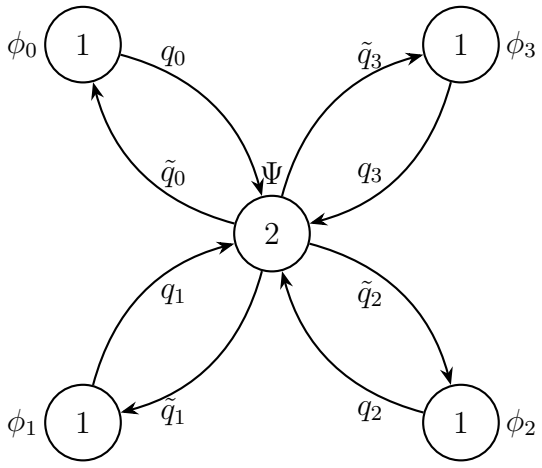

Figure 5.6: D_4 quiver.

5.2.2 D2-branes and universal flop of length $\ell = 2$

We now describe the universal flop of length $\ell = 2$ through the effective theory of a D2-brane probing a family of D_4 surfaces. We begin by discussing the theory at the D_4 singularity, followed by an analysis of how the superpotential deformation induced by Φ modifies the effective theory.

D2-brane probing a D_4 singularity

The worldvolume theory of a D2-brane probing a D_4 singularity is a 3d $\mathcal{N} = 4$ supersymmetric quiver gauge theory, with the quiver in Figure 5.6 and the superpotential

$$W = \sum_{i=0}^{3} \mathrm{Tr}\left[\Psi q_i \tilde{q}_i\right] - \sum_{i=0}^{3} \phi_i \tilde{q}_i q_i, \tag{5.45}$$

where $q_i, \tilde{q}_i$ $(i = 0, 1, 2, 3)$ are the bifundamental hypermultiplets, ϕ_i $(i = 0, 1, 2, 3)$ are the scalars in the $U(1)$ vector multiplets at the external nodes and Ψ is the scalar in the adjoint of $U(2)$ at the central node. In (5.45) q_i must be understood as a two-component column vector, while $\tilde{q}_i$ is a row vector.

The topological symmetry is $SO(8)$. The Cartan torus is the product of the $U(1)_T$'s of each node, whose generators can be identified with α_i^*. The monopole operators are labeled by the charges relative to these $U(1)_T$'s, i.e. $(\mathrm{q}_0, \mathrm{q}_1, \mathrm{q}_2, \mathrm{q}_3, \mathrm{q}_4)$. Due to the decoupling of a $U(1)$ gauge

multiplet, the charges of the monopoles are defined up to the shift $(\mathfrak{q}_0, \mathfrak{q}_1, \mathfrak{q}_2, \mathfrak{q}_3, \mathfrak{q}_4) \mapsto (\mathfrak{q}_0 + 1, \mathfrak{q}_1 + 1, \mathfrak{q}_2 + 1, \mathfrak{q}_3 + 1, \mathfrak{q}_4 + 2)$. To deal with this redundancy one sets $\mathfrak{q}_0 = 0$ [95]. The monopole operators are then written as $w_{\mathfrak{q}_1,\mathfrak{q}_2,\mathfrak{q}_3,\mathfrak{q}_4}$. The topological $U(1)_T$ associated with the central node deserves further elaboration. At this node, the gauge group is $U(2)$. To define the monopole operators, the theory is first abelianized into $U(1) \times U(1)$ [32]. For each $U(1)$ factor, a topological $U(1)_T$ is defined: Thus, in the abelianized theory the monopole operators are labeled by two charges, that can be denoted $(\mathfrak{q}_4^1, \mathfrak{q}_4^2)$. However, one must quotient by the Weyl group of the original $U(2)$, which identifies the two topological $U(1)_T$. The resulting charge after the quotient is $\mathfrak{q}_4 \equiv \mathfrak{q}_4^1 + \mathfrak{q}_4^2$ and the invariant monopole operator with charge $\mathfrak{q}_4 = 1$ is given by $w_1 \equiv w_{1,0} + w_{0,1}$ (where, for clarity, we have omitted the charges under nodes 1,2,3).

The moment map on the CB is given by [37]:[8]

$$\boldsymbol{\mu} = \left(\begin{array}{cccc|cccc} P_1 & w_{1,0,0,0} & w_{1,0,0,1} & w_{1,0,1,1} & 0 & w_{1,1,1,2} & w_{1,1,1,1} & w_{1,1,0,1} \\ -w_{-1,0,0,0} & P_2 & w_{0,0,0,1} & w_{0,0,1,1} & -w_{1,1,1,2} & 0 & w_{0,1,1,1} & w_{0,1,0,1} \\ -w_{-1,0,0,-1} & -w_{0,0,0,-1} & P_3 & w_{0,0,1,0} & -w_{1,1,1,1} & -w_{0,1,1,1} & 0 & w_{0,1,0,0} \\ -w_{-1,0,-1,-1} & -w_{0,0,-1,-1} & -w_{0,0,-1,0} & P_4 & -w_{1,1,0,1} & -w_{0,1,0,1} & -w_{0,1,0,0} & 0 \\ \hline 0 & w_{-1,-1,-1,-2} & w_{-1,-1,-1,-1} & w_{-1,-1,0,-1} & -P_1 & w_{-1,0,0,0} & w_{-1,0,0,-1} & w_{-1,0,-1,-1} \\ -w_{-1,-1,-1,-2} & 0 & w_{0,-1,-1,-1} & w_{0,-1,0,-1} & -w_{1,0,0,0} & -P_2 & w_{0,0,0,-1} & w_{0,0,-1,-1} \\ -w_{-1,-1,-1,-1} & -w_{0,-1,-1,-1} & 0 & w_{0,-1,0,0} & -w_{1,0,0,1} & -w_{0,0,0,1} & -P_3 & w_{0,0,-1,0} \\ -w_{-1,-1,0,-1} & -w_{0,-1,0-1} & -w_{0,-1,0,0} & 0 & -w_{1,0,1,1} & -w_{0,0,1,1} & -w_{0,0,1,0} & -P_4 \end{array}\right)$$

with

$$(P_1, P_2, P_3, P_4) = (\phi_0 - \phi_1, -2\psi + \phi_0 + \phi_1, 2\psi - \phi_2 - \phi_3, \phi_3 - \phi_2)\,. \tag{5.46}$$

Monopole deformations and the effective theory

The field Φ in (6.86) generates the following superpotential deformation[9] $\delta W = \frac{1}{2}\mathrm{Tr}[\Phi\boldsymbol{\mu}]$ on the D2-brane probe worldvolume:

$$\delta W = -w_{-1,0,0,0} - w_{0,-1,0,0} - w_{0,0,-1,0} + \varrho_1 w_{1,0,0,0} + \varrho_2 w_{0,1,0,0} + \varrho_3 w_{0,0,1,0} + 2\varrho_4(\phi_0 - \psi)\,. \tag{5.47}$$

We note that the expression is symmetric in the exchange of the three external simple roots $\alpha_1, \alpha_2, \alpha_3$.

We now apply the algorithm explained in Section 5.1.3:

[8] We use a slightly different notation, that we justify in Appendix B.2.

[9] The $1/2$ normalization factor is due to the matrix representation we are using for Φ and μ.

1. Let us consider node 1. Nodes 2 and 3 behave in the same way due to the symmetry between the three external nodes. The isolated theory is $U(1)$ with two flavors and superpotential

$$W_1 = -\phi_1 \mathrm{Tr}\mathcal{M}_1 - w_{-1,0,0,0} + \varrho_1 w_{1,0,0,0} \,. \tag{5.48}$$

This is of the form (5.2) encountered in the A_1 case.

2. Following the same steps as in the previous examples, we obtain for each node a modified XYZ theory with superpotential

$$W_i^{\text{eff}} = X_i \det \mathfrak{M}_i + \varrho_i X_i \qquad \text{with} \qquad \mathfrak{M}_i \equiv \begin{pmatrix} \varphi_i & -Y_i \\ Z_i & -\varphi_i \end{pmatrix} \qquad i = 1,2,3 \tag{5.49}$$

and flavor symmetry $SU(2)$.

3. We now couple these isolated theories to the nearby nodes. For each node, we need to add

$$\mathrm{Tr}\left[\Psi \mathfrak{M}_i\right] = \mathrm{Tr}\left[\tilde{\Psi}\mathfrak{M}_i\right] \qquad \text{with} \quad \tilde{\Psi} \equiv \Psi - \psi \mathbf{1} \;\text{ and }\; \psi \equiv \frac{1}{2}\mathrm{Tr}(\Psi)\,, \tag{5.50}$$

and where on the right-hand side only the traceless part of Ψ survives, as $\mathfrak{M}_i$ is traceless.

Adding all the terms together, we obtain the effective superpotential

$$W_{\text{eff}} = \sum_{i=1}^{3} X_i \left(\det \mathfrak{M}_i + \varrho_i\right) + \mathrm{Tr}\left[\tilde{\Psi}\left(q_0\tilde{q}_0 + \sum_{i=1}^{3}\mathfrak{M}_i\right)\right] + \hat{\psi}\left(\tilde{q}_0 q_0 - 2\varrho_4\right)\,, \tag{5.51}$$

with $\hat{\psi} \equiv \psi - \phi_0$. The quiver of this effective theory is given in Figure 5.7.

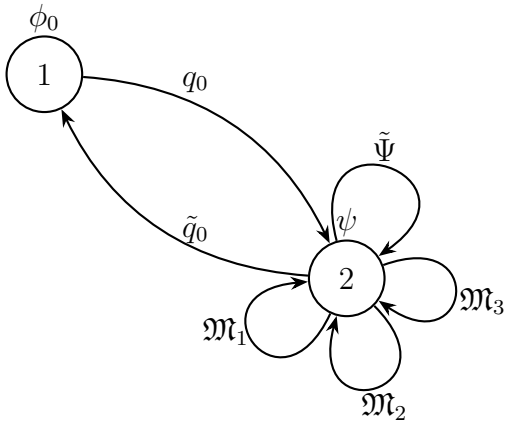

Figure 5.7: Quiver for the effective theory.

The F-terms are the following:

$$\frac{\partial W}{\partial X_i} = 0 \quad : \qquad \det \mathfrak{M}_i = -\varrho_i \qquad i = 1,2,3 \tag{5.52}$$

$$\frac{\partial W}{\partial \hat{\psi}} = 0 \quad : \qquad \tilde{q}_0 q_0 = 2\varrho_4 \tag{5.53}$$

$$\frac{\partial W}{\partial \tilde{\Psi}} = 0 \quad : \qquad \sum_{i=1}^{3} \mathfrak{M}_i + \left(q_0 \tilde{q}_0 - \frac{1}{2}(\tilde{q}_0 q_0)\mathbb{1} \right) = 0 \tag{5.54}$$

$$\frac{\partial W}{\partial \mathfrak{M}_i} = 0 \quad : \qquad \tilde{\Psi} - X_i \mathfrak{M}_i = 0 \qquad i = 1,2,3 \tag{5.55}$$

$$\frac{\partial W}{\partial q_0} = 0 \quad : \qquad \tilde{q}_0 \left(\tilde{\Psi} + \hat{\psi}\mathbb{1} \right) = 0 \tag{5.56}$$

$$\frac{\partial W}{\partial \tilde{q}_0} = 0 \quad : \qquad \left(\tilde{\Psi} + \hat{\psi}\mathbb{1} \right) q_0 = 0 \, . \tag{5.57}$$

The 3d gauge theory with quiver in Figure 5.7 has also a D-term potential. The gauge group is $U(1) \times U(2)$. The D-term relations are:

$$\begin{aligned} & q_0^\dagger q_0 - \tilde{q}_0 \tilde{q}_0^\dagger = 2\xi \, , \\ & q_0 q_0^\dagger - \tilde{q}_0^\dagger \tilde{q}_0 + [\tilde{\Psi}, \tilde{\Psi}^\dagger] + \sum_{i=1}^{3} [\mathfrak{M}_i, \mathfrak{M}_i^\dagger] = \xi \mathbb{1}_2 \, . \end{aligned} \tag{5.58}$$

where ξ is the real FI-parameter associated with the $U(1)$ generator $T_1 - T_2$, where T_i generates

the diagonal $U(1)$ factor of the gauge group at the i-th node in Figure 5.7 (the diagonal $U(1)$ generated by $T_1 + T_2$ decouples as no field is charged under it).

As we will see shortly, these relations can potentially give rise to distinct branches of the moduli space. For generic values of $\boldsymbol{\varrho} = (\varrho_1, \ldots, \varrho_4)$, the moduli space of the effective 3d theory has a single branch, corresponding to the deformed HB. The family of these spaces is the universal flop of length $\ell = 2$. At special points in the space B_ϱ, parametrized by $\varrho_1, \ldots, \varrho_4$, the fiber surface develops singularities, leading to new branches in the moduli space. By analyzing the $U(1)$ factors in the gauge group of the effective theory, one can determine whether the universal flop sixfold is singular at these points in B_ϱ. We will examine this in detail in the following.

The universal flop of length 2 as a family of deformed HB's

Let us consider the case in which $\varrho_1, ..., \varrho_4$ take generic non-zero values. As we will prove next, in this case the relations (5.52)-(5.57) imply that $X_1 = X_2 = X_3 = 0$, $\tilde{\Psi} = 0$ and $\hat{\psi} = 0$. We are therefore left with a moduli space parametrized by the traceless matrices $\mathfrak{M}_i$ ($i = 1, 2, 3$) and the bifundamentals q_0 and $\tilde{q}_0$ organized in an effective quiver, that we show in Figure 5.8. The maps in the quiver are subject to the relations

$$\sum_{i=1}^{3} \mathfrak{M}_i + q_0 \tilde{q}_0 = \varrho_4 \mathbb{1} \qquad \text{and} \qquad \det \mathfrak{M}_i = -\varrho_i \qquad i = 1, 2, 3 \,. \tag{5.59}$$

These relations, together with the quiver in Figure 5.8, reproduce the 'universal flopping algebra of length $\ell = 2$' derived by [131], from which the universal flop of $\ell = 2$ can be recovered by a moduli construction.[10]

The invariants that parametrize this branch of the moduli space consist of single trace chiral operators, which correspond to closed loops in the quiver. A convenient choice for a basis is

$$A_i \equiv \mathrm{Tr}\,[\mathfrak{M}_0 \mathfrak{M}_i] \,, \qquad B \equiv \mathrm{Tr}\,[\mathfrak{M}_0 \mathfrak{M}_2 \mathfrak{M}_3] \,, \tag{5.60}$$

where we defined $\mathfrak{M}_0 \equiv q_0 \tilde{q}_0$.

[10] The precise match with Example 4.23 in [131] works in the following way: 1) the quiver is the same; 2) the relations in [131] imply that the self-arrows of the rank-2 node are traceless; 3) one uses that for traceless 2×2 matrices $\tilde{M}$, the relation $\tilde{M}^2 = -\det(\tilde{M})\, \mathbb{1}_2$ holds.

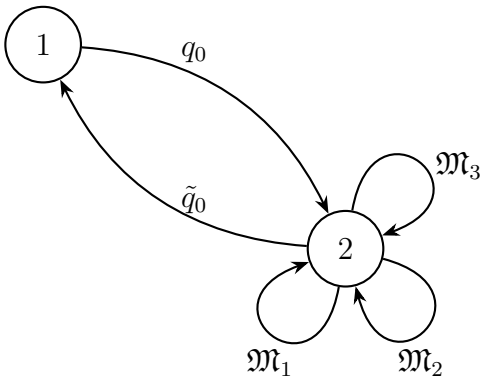

Figure 5.8: Quiver for the universal flop of length 2.

Crucially $A_1,\ A_2,\ A_3$ and B are not independent. In particular, (5.54) implies that:

$$\sum_i A_i = -2\varrho_4^2\,. \tag{5.61}$$

Moreover, there is an additional relation involving B, which we derive in Appendix B.1:

$$\begin{aligned} A_1A_2A_3 =& -B^2 + 2B\varrho_4(A_3+\rho_4^2+\rho_1-\rho_2-\rho_3) \\ & -(\rho_2A_3+\rho_3A_2)(A_1+2\rho_4^2) - A_2A_3(\rho_4^2+\rho_1) - 4\rho_4^2\rho_2\rho_3\,. \end{aligned} \tag{5.62}$$

We write A_1 in terms of A_2 and A_3 by using the first relation, and make the following redefinition of the gauge invariant coordinates:

$$A_2 = Y - \varrho_2 - \varrho_4^2\,, \tag{5.63}$$

$$A_3 = Z - \varrho_3 - \varrho_4^2\,, \tag{5.64}$$

$$B = X - (Y+Z-\varrho_1)\varrho_4 + \varrho_4^3\,. \tag{5.65}$$

with $A_1 = -Y - Z + \varrho_2 + \varrho_3$. Plugging these redefinitions into (6.103), we obtain a space parametrized by X, Y, Z subject to the relation

$$\begin{aligned} X^2 =& YZ(Y+Z) - (\varrho_1+\varrho_2+\varrho_3+\varrho_4^2)YZ + (\varrho_1-\varrho_2)(\varrho_3-\varrho_4^2)Y \\ & + (\varrho_1-\varrho_3)(\varrho_2-\varrho_4^2)Z + (\varrho_1-\varrho_2-\varrho_3+\varrho_4^2)(\varrho_1\varrho_4^2-\varrho_2\varrho_3)\,. \end{aligned} \tag{5.66}$$

This is exactly the equation (5.44), that defines the *universal flop of length* $\ell = 2$ as a hypersurface in the seven dimensional ambient space $\mathbb{C}^3_{XYZ} \times B_\varrho$.

Singularities of the sixfold from the effective 3d theory

We now search for loci in B_ϱ where the moduli space of the effective 3d theory develops new branches. As explained in Section 5.1.2, at these loci, the ADE surface develops a singularity. From the quiver in Figure 5.7, we observe that there is only one relevant $U(1)$ subgroup, which is the relative $U(1)$ between the $U(1)$ factors at each node (the diagonal $U(1)$ is decoupled). Hence the theory has only one real FI-parameter that can be activated (leading to the simultaneous resolution of the family). To determine whether the loci in B_ϱ that support new branches of the moduli space correspond to singularities in the sixfold family, it is crucial to verify if a $U(1)$ gauge group is preserved at the intersection of these branches.

There are two loci of B_ϱ where we detect a singularity of the fiber that is blown up in the simultaneous resolution of the family:

- When $\varrho_4 = 0$, the relations (5.52)-(5.57) allow to set $q_0 = \tilde{q}_0 = 0$; the corresponding new branch is determined by the following relations:

$$\sum_{i=1}^{3} \mathfrak{M}_i = 0\,, \qquad \det \mathfrak{M}_i = -\varrho_i \;\text{ and }\; \tilde{\Psi} - X_i \mathfrak{M}_i = 0 \quad (i = 1,2,3)\,. \tag{5.67}$$

  For generic $\varrho_1, \varrho_2, \varrho_3$, (5.67) imply $X_i = 0$ and $\tilde{\Psi} = 0$.[11] The first two relations in (5.67) imply that $\mathfrak{M}_i$ are fixed (up to gauge transformations) to a specific value determined by the parameters $\varrho_1, \varrho_2, \varrho_3$.[12] The only field that can vary along the new branch is $\hat{\psi}$. Along this branch the relative $U(1)$ of the two nodes is unbroken. Its monopole operators $V_\pm$ can get non zero vev as well, subject to the relation $V_+ V_- = \hat{\psi}^2$. The new branch has then the geometry of a $\mathbb{C}^2/\mathbb{Z}_2$, like the CB of a $U(1)$ theory with two flavors.

  In fact, at the intersection of the new branch with the HB, the effective theory *is* a 3d $\mathcal{N} = 4$ supersymmetric $U(1)$ gauge theory with two flavors: integrating out the massive fields $\tilde{\Psi}, \mathfrak{M}_i, X_i$ one obtains the superpotential $W'_{\text{eff}} = \hat{\psi}\, \tilde{q}_0 q_0$. This is compatible with the fact that the D2-brane is probing an A_1 singularity. In fact, when $\varrho_4 = 0$ the equation (5.66)

[11] The matrices $\mathfrak{M}_i$ are invertible. $\tilde{\Psi} = X_i \mathfrak{M}_i$ says that the X_i are either all zero or all non-zero. In the second case, the $\mathfrak{M}_i$ should be proportional to each other. But this is in conflict with $\sum_{i=1}^{3} \mathfrak{M}_i = 0$ for generic $\varrho_1, \varrho_2, \varrho_3$.

[12] The first relation implies $\mathfrak{M}_1 = -\mathfrak{M}_2 - \mathfrak{M}_3$; the other three relations determine all the gauge invariants of two traceless 2×2 matrices. In particular, $\det \mathfrak{M}_2 = -\varrho_2$, $\det \mathfrak{M}_3 = -\varrho_3$ and $\mathrm{Tr}\mathfrak{M}_2\mathfrak{M}_3 = -\det(\mathfrak{M}_2 + \mathfrak{M}_3) + \det \mathfrak{M}_2 + \det \mathfrak{M}_3 = \varrho_1 - \varrho_2 - \varrho_3$, where we used the fact that for traceless matrices $\mathfrak{M}_i$ the following relation holds: $\det \mathfrak{M}_i = -\frac{1}{2}\mathrm{Tr}(\mathfrak{M}_i^2)$.

takes the form

$$X^2 = \varrho_3(Y-\varrho_2)^2 + \varrho_2(Z-\varrho_3)^2 + (Y-\varrho_2)(Z-\varrho_3)(Y+Z-\varrho_1)\ , \tag{5.68}$$

that has a manifest A_1 singularity at $X = Y - \varrho_2 = Z - \varrho_3 = 0$.

The D-term condition of the effective theory can be derived by looking at (5.58) and setting the massive fields as above, i.e. $\tilde{\Psi} = 0$ and $\mathfrak{M}_i$ traceless invertible matrices, that are then diagonalizable by gauge transformations. This leaves the following D-term:

$$q_0^\dagger q_0 - \tilde{q}_0 \tilde{q}_0^\dagger = 2\xi\ . \tag{5.69}$$

Switching on a non-zero real FI-parameter ξ blows up the A_1 singularity of the HB. This is the FI-parameter of the theory with quiver in Figure 5.7, hence the simultaneous resolution of the family sixfold blows up the A_1 simple root.

The effective theory has detected a singular locus in the sixfold, where a $\mathbb{CP}^1$ is blown up in the simultaneous resolution of the family.

- When

$$\begin{aligned} 64\varrho_4^2\varrho_1\varrho_2\varrho_3 = \big[&\varrho_1^2+\varrho_2^2+\varrho_2^2-2\varrho_1\varrho_2-2\varrho_1\varrho_3-2\varrho_2\varrho_3 \\ &-2\varrho_4^2(\varrho_1+\varrho_2+\varrho_3)+\varrho_4^4\big]^2\ , \end{aligned} \tag{5.70}$$

a new branch emerges, as we now show. To present in a cleaner shape what happens at one point along this locus in B_ϱ, let us write

$$\varrho_1 = r_1^2\,, \qquad \varrho_2 = r_2^2\,, \qquad \varrho_3 = r_3^2\,, \qquad \varrho_4 = r_4\,. \tag{5.71}$$

We stress that the holomorphic coordinates on B_ϱ are still $\varrho_1, ..., \varrho_4$. The locus (5.70) can then be written as points where

$$\pm\, r_1 \pm r_2 \pm r_3 + r_4 = 0\,. \tag{5.72}$$

The different choices of signs select distinct regions of the locus (5.70)(that is connected).

At the locus (5.70), the relations (5.52)-(5.57) allow the X_i to be non-zero and consequently among the other fields $\hat{\psi} \neq 0$ is permitted. When the X_i are non-zero (they either all vanish or none do), $\mathfrak{M}_i$ ($i = 1, 2, 3$) and $\tilde{\Psi}$ are all proportional to each other. Hence, we can

partially fix the gauge by diagonalizing them simultaneously.[13] The matrices $\mathfrak{M}_i$ are then determined up to a sign by (5.52), and $\tilde{\Psi}$ depends on one complex scalar ψ_3:

$$\mathfrak{M}_i = \sigma_i \begin{pmatrix} r_i & 0 \\ 0 & -r_i \end{pmatrix} \quad \text{with} \quad \sigma_i = \pm\,, \qquad \text{and} \qquad \tilde{\Psi} = \begin{pmatrix} \psi_3 & 0 \\ 0 & -\psi_3 \end{pmatrix}\,. \tag{5.73}$$

Due to (5.55), we immediately see that $X_i = \frac{\sigma_i}{r_i}\psi_3$. Moreover, (5.57) says that q_0 is an eigenvector of $\tilde{\Psi}$ with eigenvalue $\hat{\psi}$. After the gauge fixing (5.73), this implies two possibilities for q_0 and $\hat{\psi}$:

$$q_0 = \begin{pmatrix} q_0^1 \\ 0 \end{pmatrix} \text{ and } \hat{\psi} = -\psi_3 \qquad \text{or} \qquad q_0 = \begin{pmatrix} 0 \\ q_0^2 \end{pmatrix} \text{ and } \hat{\psi} = \psi_3\,. \tag{5.74}$$

Analogous considerations can be taken from the relation (5.56):

$$\tilde{q}_0 = \begin{pmatrix} \tilde{q}_0^1 & 0 \end{pmatrix} \text{ and } \hat{\psi} = -\psi_3 \qquad \text{or} \qquad \tilde{q}_0 = \begin{pmatrix} 0 & \tilde{q}_0^2 \end{pmatrix} \text{ and } \hat{\psi} = \psi_3\,. \tag{5.75}$$

Let us consider the case $\hat{\psi} = -\psi_3$ (the second case is obtained from the first one by applying the Weyl group of the $SU(2)$ of the second node). The relation (5.53) says $\tilde{q}_0^1 q_0^1 = 2r_4$.

We can now plug everything into (5.54), obtaining $\sum_{i=1}^3 \sigma_i r_i + r_4 = 0$, i.e. all the relations are compatible with each other only over the locus (5.70). Moreover, the choice of signs σ_i determines which region of the locus we are on.

Summing up, over the locus (5.70) in B_ϱ, the effective 3d theory moduli space has a new branch parametrized by ψ_3. The vev of the fields break the $U(1) \times U(2)$ gauge group to $U(1) \times U(1)$, with one combination of them that decouples.

After performing a series of involved steps, which we omit here for brevity, one can verify that, by integrating out the fields that become massive for each value of the moduli, the resulting effective theory at the intersection of the new branch with the HB is a $U(1)$ gauge theory with two flavors (one from $q_0, \tilde{q}_0$ and the other from the off-diagonal elements of a combination of $\mathfrak{M}_i$). This is compatible with the fact that over the locus (5.70) the surface fiber develops an A_1 singularity. For example, plugging (5.71) with $r_4 = r_1 + r_2 + r_3$ into (5.66) and shifting the coordinates as $Y = \mathrm{y} + (r_1 + r_3)^2$ and $Z = \mathrm{z} + (r_1 + r_2)^2$, one obtains

$$X^2 = (r_1 + r_2)^2 \mathrm{y}^2 + (r_1 + r_3)^2 \mathrm{z}^2 + 2(y + z + r_1^2 + r_1(r_2 + r_3) - 2r_2 r_3)\mathrm{y}\,\mathrm{z}\,, \tag{5.76}$$

[13] They are invertible and traceless, meaning they have distinct non-zero eigenvalues.

that manifestly has an A_1 singularity at $X = \mathrm{y} = \mathrm{z} = 0$.

Also in this case, switching on the FI-term in the original theory with quiver in Figure 5.7 will produce a real FI-term in the effective theory just described, that will blow up the A_1 singularity of the HB.

The effective theory has detected in this way a singularity of the sixfold along the locus (5.70).

When $\varrho_i = 0$ for one of $i \in 1, 2, 3$, the effective theory develops a new branch beyond the HB. Let us take $i = 1$ as a reference (the same arguments apply for $i = 2, 3$). In this case, $\mathfrak{M}_1$ can acquire a zero vev, allowing X_1 to take any value. The new branch is parametrized by this field. The non-zero vevs for the fields $\mathfrak{M}_{2,3}$ and $q_0, \tilde{q}_0$, that are forced by the relations (5.52)-(5.57), break the gauge group completely at any point in the moduli space, leaving no $U(1)$ factor. This indicates that, along this locus, the sixfold family develops no singularities (even though the fiber surface exhibits an A_1 singularity, as can be confirmed from the equation).

There are also relevant subloci:

- The two singular loci described above intersect at

$$\varrho_4 = 0 \qquad \text{and} \qquad \varrho_1^2 + \varrho_2^2 + \varrho_2^2 - 2\varrho_1\varrho_2 - 2\varrho_1\varrho_3 - 2\varrho_2\varrho_3 = 0\,. \tag{5.77}$$

  Studying the moduli space of the effective theory over this locus in parameter space, one discovers that the ADE surface has an A_2 singularity. In fact, switching on the only possible real FI-parameter one blows up two $\mathbb{CP}^1$'s [21].

- The origin of the parameter space is at $\varrho_1 = \varrho_2 = \varrho_3 = \varrho_4 = 0$. At this point, the effective theory corresponds to a D2-brane probing a D_4 singularity with a T-brane background. The blown-up $\mathbb{CP}^1$ corresponds to the central node of the D_4 diagram and has length 2.

This reveals the structure of the simultaneous resolution of the universal flop of length 2 (here derived by analyzing the moduli space of an effective 3d theory of a D2-brane probing deformed D_4 surfaces). There are two codimension-1 loci in B_ϱ where a single $\mathbb{CP}^1$ is blown up. At the intersection of these loci, the exceptional locus consists of two $\mathbb{CP}^1$'s that intersect at a single point. At the origin of B_ϱ, the two spheres coincide, forming a degree-two $\mathbb{CP}^1$ (see e.g. [21]).

5.2.3 Monopole operators as D2 states

The D2-branes wrapped on vanishing spheres give rise to particles propagating in six dimensions. The D2-branes are charged under the Ramond-Ramond C_3 3-form potential. In an ADE surface there are r 2-forms ω_i $i = 1, ..., r$ such that their integral over a basis of simple roots is

$$\int_{\alpha_j} \omega_i = \delta_i^j \, . \tag{5.78}$$

C_3 can be expanded as $C_3 \sim \sum_{i=1}^r A^i \wedge \omega_i$, with A_i a gauge field propagating in six dimensions. These are background fields from the D2-brane 3d theory point of view. Given a D2-brane wrapping a root α, its charge under the $U(1)$ gauge group generated by ω_i is

$$\mathrm{q}_i(D2_\alpha) = \int_\alpha \omega_i \, . \tag{5.79}$$

The simple roots are seen as linear functional acting on the space of two-forms, that is then identified with the Cartan subalgebra of the corresponding ADE Lie algebra. The relations (5.78) then mean that $\omega_i = \alpha_i^*$, i.e. the dual basis of the simple roots.

In [37], the authors studied the 3d theory living on the worldvolume of D2-branes probing the ADE singularity and extending in the non-compact $\mathbb{R}^{1,2}$ spacetime. As explained before, the symmetry associated with the A^i's is the topological symmetry in the 3d theory. In this context [37] showed that monopole operators map to states of D2-branes wrapping vanishing spheres: the existence of a monopole operator with charge q with respect to one α_j^* means that the string theory produces a D2-state with charge q under the $U(1)$ symmetry with gauge field A^j. In the 3d theory supported on the probe D2-brane (that should be distinguished from the D2-branes generating charged states), the A^i's are background gauge fields for the topological symmetry and the D2-brane wrapping vanishing spheres are mapped to monopole operators with the proper charges under the Cartan torus of the topological ADE symmetry.

Now, let us come to the universal flop of length two. This has been obtained by switching on a particular monopole deformation on the worldvolume theory of a D2-brane probing a D_4 singularity. Before turning on the deformation, the topological symmetry was $SO(8)$. The new terms in the superpotential break explicitly this symmetry to a $U(1)_T$ symmetry generated by α_4^*. This is the topological symmetry that can be read off from the quiver of the effective theory in

Figure 5.7. The abelianization of the gauge group has gauge group $U(1)\times U(1)^2$, with one combination of them that decouples. The topological charges of the abelianized theories are $(\mathrm{q}_0, \mathrm{q}_4^1, \mathrm{q}_4^2)$, that are defined up to a shift, due to the decoupled $U(1)$. To fix the ambiguity, we set $\mathrm{q}_0 = 0$. The charge under the topological $U(1)$ is $\mathrm{q}_4 \equiv \mathrm{q}_4^1 + \mathrm{q}_4^2$.

At a generic point of B_ϱ, the effective 3d theory lacks a $U(1)$ gauge group, resulting in the absence of monopole operators. Consequently, we conclude that there are no charged states coming from D2-branes wrapping vanishing cycles (the surface is smooth here). On the locus $\varrho_4 = 0$ there is a preserved $U(1)$; in the abelianized theory its associated monopole operators have charges $(\mathrm{q}_0, \mathrm{q}_4^2, \mathrm{q}_4^2) = (\pm 1, 0, 0) \cong \pm(0, 1, 1)$, i.e. they are the monopole operators $w_{\pm 2}$. On the second locus (5.70), the monopole operators associated with the surviving $U(1)$ generator have charges $(\mathrm{q}_0, \mathrm{q}_4^2, \mathrm{q}_4^2) = (0, \pm 1, 0)$ (one needs to consider the Weyl transformed as well); they are the monopole operators $w_{\pm 1}$. We conclude that on the first locus we have a D2-state of charge 2, while on the second locus we have a D2-state of charge 1. At the origin of B_ϱ, we have both types of states.

Following [21], when we let all ϱ_i depend on a complex coordinate, this generates a threefold known as the Morrison-Park threefold [133]. Our analysis above reproduces the structure of charge one and charge two states coming from reducing type IIA/M-theory on such a threefold (see [21] for a review). The same can be done for fourfolds, constructed by making ϱ_i depend on two complex variables. We leave for future work the analysis of the fourfolds.

This analysis can also be applied to CY threefold flops of $\ell = 2$. The structure of charged states is more intricate than for the Morrison-Park threefold and it has been preliminarily analyzed for the Laufer threefold in [97], whose results match with the types of monopole operators at the origin of the D_4-family that realize the universal flop of $\ell = 2$.

Chapter 6

D2 branes at non-toric threefold singularities

In the previous chapter, we analyzed families of deformed ADE singularities and their associated universal flops from the perspective of probe branes. By studying the three-dimensional gauge theory living on a D2-brane probing these geometries, we showed how the structure of the ADE families can be reconstructed from the moduli space of the probe theory. In particular, monopole operator deformations induced by the Higgs field background encode the necessary information about the geometry for the probe gauge theory to reproduce both the smooth fibers and the singular loci of the family. This analysis demonstrated that three-dimensional probe theories provide a powerful diagnostic tool for understanding geometric transitions and obstructions to resolution in non-toric Calabi-Yau backgrounds.

A natural question is whether this probe-based framework can be extended to the threefold singularities that originate from the ADE families. In this chapter, we address this question by considering $D2$-branes probing compound Du Val (cDV) threefold singularities. As we have seen in Sections 4.2.4 and 1.4, these geometries can be viewed as fibrations of ADE surface singularities over a complex base, and therefore provide a natural generalization of the structures studied in the previous chapter. Developing a systematic method to construct the corresponding probe gauge theories would significantly broaden the applicability of the brane–geometry correspondence beyond the toric regime.

We have already seen how D-branes probing singular Calabi-Yau geometries provide a pow-

erful bridge between gauge theory dynamics and complex geometry. When a stack of D-branes is placed at a Calabi-Yau singularity, the worldvolume theory is a supersymmetric quiver gauge theory whose vacuum moduli space reproduces the local geometry of the singularity.

For toric Calabi-Yau threefolds, this geometry-gauge theory correspondence is particularly well developed. A rich arsenal of techniques—including brane tilings, dimer models, and toric polygons [8, 9, 137, 138]—provides explicit, algorithmic constructions of the probe brane theories. In particular, a correspondence between toric data and brane webs gives direct access to the quiver associated to the CY3. The key to the success of these methods is the combinatorial structure of toric geometry, which allows one to systematically derive quiver gauge theories, compute their moduli spaces, and verify that these spaces match the target geometry.

Progress has also been made for certain classes of non-toric singularities. Notably, Aspinwall and Morrison [18] employed matrix factorization techniques to derive quiver gauge theories for specific compound Du Val (cDV) threefolds, including Reid's pagodas and Laufer's example. Their approach exploits the hypersurface presentation of these geometries within weighted projective spaces, providing explicit constructions for these important examples.

However, a general systematic method applicable to arbitrary cDV threefolds has remained elusive. Compound Du Val singularities, the threefold analogs of classical ADE surface singularities, form a rich class of non-toric geometries that arise naturally in M-theory and F-theory compactifications [18, 91, 97], where they engineer superconformal field theories in various dimensions. While the geometric structure of cDV singularities has been extensively studied [126, 128, 131, 132], a unified approach to constructing their probe brane theories that goes beyond specific examples has been lacking.

In this chapter we want to present a new method for extracting the quiver gauge theory of a brane probe, which applies to all simple threefold flops of length 1 and 2. The method stems from what we understood probing constants backrounds, which can be summarised in the following points:

- Non-trivial Higgs backgrounds in Type IIA string theory on ADE surfaces realize complex structure deformations. A $D2$-brane probing the ADE space reproduces in the Higgs branch of its worldvolume effective theory. This correspondence must also hold in the presence of a non-trivial Higgs vev, which should couple to the worldvolume of the $D2$ as a background field deformation.

- In the mirror configuration, where the $D2$-brane probes a $D6$-brane stack, the effect is naturally identified as a mass deformation. Φ is in the background vector multiplet of the gauge symmetry $\mathcal{G}_F$ generated by the stack of $D6$, seen as flavor from the $D2$, and couples with the moment map for $\mathcal{G}_F$, that is the meson matrix of the $D2$.

- The mirror of the mass deformation is the coupling between the same Φ and the moment map for $\mathcal{G}_F$, now representing the topological symmetry of the theory on the probe. The mirror moment map is explicitly given in the cases that we are going to present. The components along the Cartan of $\mathcal{G}_F$ are vector multiplet chirals, whereas simple factors are magnetic monopole operators.

- A Higgs vev with non-trivial components along the simple factors of $\mathfrak{g}_F$ produces monopole superpotential deformations that lift the Coulomb branch, except for a Levi subalgebra (the commutant of Φ).

- In the presence of diagonalizable Higgs vevs the HB geometry reproduces the deformed ADE surface. For some special values of the deformation parameters, the surface may still be singular. When this is the case, a CB opens up at the origin of the HB. However, the global symmetry on the CB is determined by the profile of the Higgs for the chosen values of deformation parameters. If the Higgs acquires components along some roots $\alpha \in \mathfrak{g}_F$, that is, nilpotent components, then all the shrinking 2-cycles that correspond to those roots are obstructed, meaning that the singularity is not resolvable or only partially so. In other words, the topological symmetry is broken to the commutant of Φ. If the commutant contains residual Cartan factors $\alpha_i^* \in \mathfrak{h}_F$[1], then these will generate abelian background vector multiplets. These vector multiplets contain a real scalar ξ_i, whose vev produces a Fayet-Iliopulos deformation on the $D2$-probe. Geometrically, the FI ξ_i controls the Kahler volume of the shrinking cycle $\alpha_i \in \mathfrak{g}_F$. So, the existence of the FI in the effective theory at the origin of the HB implies that the corresponding 2-cycle can be blown up. Each FI ξ_i couples to a massless $U(1)$ vector multiplet V_i on the worldvolume through:

$$(\xi_i \alpha_i^*, h_{\alpha_j} V_j) = \xi_i V_j \alpha_j(\alpha_i^*) = \xi_i \delta_{ij} V_j \tag{6.2}$$

[1]The Cartan factors are expanded in the base of the fundamental coweigths $\{\alpha_i^*\}$:

$$\alpha_i \cdot \alpha_j^* = \delta_{ij} \tag{6.1}$$

Finally, we can conclude that each $U(1)$ massless vector appearing at the origin of the HB signals the presence of a 2-cycle that can be blown up by turning on the corresponding FI. When the origin is singular but the CB has no global flavor symmetry, the Higgs field develops a maximal T-brane, which obstructs all the shrinking 2-cycles.

in Section 1.4 we have observed how the obstructive effect of a T-brane on the resolution is translated into the monodromy properties of non-trivially fibered ADE, once we promote the Higgs vev to a non-constant holomorphic function of a subset of spacetime coordinates. As we are going to show, non-constant Higgs vevs produce two distinct classes of deformations on the probe: *non-monodromic* and *monodromic* deformations[2]. The first case corresponds to diagonal Higgs vevs $\Phi = f_i(w)\alpha_i^*$, whose eigenvalues depend holomorphically on a complex direction transverse to the ADE. In particular, the case $f_i(w) = a_i w$ with a_i constant, is well understood also from the point of view of the mirror $D6$ brane configuration, where it corresponds to rotating each brane at a different relative angle $\theta_i = \arctan(|a_i|)$, so that the stack produces a 5-dimensional intersection. This lifts the HB of the probe, as now, it can only move along one $D6$ brane at a time outside the intersection locus. In the mirror, the CB is lifted since the diagonal Higgs deforms all the ADE fibers outside the origin of the $\mathbb{C}$-plane base. Fractional branes are now trapped at the origin, on which the singular ADE develops. This effect is produced by individual mass terms for the CB chirals ϕ_i of the probe theory. In our framework, they originate from field-dependent complex FI terms:

$$(a_i\phi_i\alpha_i^*, \phi_j h_{\alpha_j}) = \phi_j\alpha_j(a_i\phi_i\alpha_i^*) = \phi_j\delta_{ji}a_i\phi_i \tag{6.3}$$

Recalling that $\alpha_j(h)$, for $h \in \mathfrak{h}$, is the holomorphic volume of the 2-cycle S_j in the ADE, we can see that for each fractional brane $\mathcal{E}_i$ there is an individual superpotential deformation. This deformation is proportional to the holomorphic volume of the cycle S_i wrapped by the brane. It is easy to see that this generates a potential that vanishes only when such volume is zero, which forces the positions of the fractional branes along the $\mathbb{C}$ base (i.e., the ϕ_i vevs) to zero. This effect mirrors the localization of the ADE singularity at the origin of the transverse $\mathbb{C}$-plane, induced by the Higgs vev. It must be noted that non-constant Higgs backgrounds break half of the supersymmetry on the probe brane, and it is not restored in the IR (as opposed to what we saw in the previous chapter). This fact will have important consequences on the structure of the moduli space of the probe.

This case is called non-monodromic because the volumes $\alpha_j(a_i\phi_i\alpha_i^*) = \phi_i a_i$ are holomor-

[2]It must be mentioned that monodromic and non-monodromic ADE fibrations have been studied, though with a substantially different approach in the work of [12]

phic along the CB directions ϕ_i. Indeed, a diagonal Higgs produces only fibrations with total simultaneous resolution. The most interesting phenomena occur when we consider Higgs vevs that engineer cDV threefolds with partial simultaneous resolution. We have seen that the corresponding Higgs background takes values in a Levi subalgebra $\mathcal{L}_\Phi$ of the ADE Lie algebra, and the Casimirs of $\mathcal{L}_\Phi$ are holomorphic functions of the coordinate along the base of the ADE fibration. In this work, we formulate and test a proposal for the coupling of these generalised Higgs vevs to the $D2$-brane. A first important observation is that $\mathcal{L}_\Phi$ always decomposes into a sum of independent subalgebras $\mathcal{L}_\Phi = \bigoplus_m \mathfrak{g}_m$, obviously preserved by the Weyl group of the full Levi. Each independent factor has its own Casimirs, holomorphically varying along the base and vanishing at its origin. Then, in analogy with the non-monodromic deformation, we assume that each $\mathfrak{g}_m$ factor in Φ will couple to a $\mathfrak{g}_m$ moment map on the CB of the probe. The latter will involve the CB degrees of freedom of the subsystem of fractional $D2$-branes wrapping the roots of $\mathfrak{g}_m$. Moreover, we know that the Weyl group of each $\mathfrak{g}_m$ acts non-trivially on the roots of the subalgebra, whereas the base of the ADE fibration is parametrized by the Casimir invariants. We interpret this as the generation of a bound state among the fractional branes associated with $\mathfrak{g}_m$. Consequently, on the probe, the non-constant Casimirs of the subalgebra $\mathfrak{g}_m$ are identified with the center of mass position of the corresponding brane subsystem along the base of the ADE fibration. We confirm these claims in a series of examples of simple threefold flops (with and without monodromies) of length 1 and 2, where we show that the moduli space of the $D2$-probe correctly reproduces the background. Higher length cases are left for future investigations as they require a generalization of the monopole deformation techniques employed here to non-abelian gauge theories.

This chapter is organised as follows. In Section 6.1 we comment on the connection between the effective theory derived on the $D2$-probe and the worldvolume theory of a $D3$-brane probing the same background in Type IIB string theory. We argue that the moduli spaces of both theories coincide in the limit in which the $D3$ becomes fully non-compact and the CB of the $D2$ collapses on its origin. in Sections 6.2 we introduce toy models of 3d $\mathcal{N} = 2$ mirror symmetry, that we extensively use in the subsequent derivations. In 6.3 we recall the main geometric data associated with Higgs backgrounds and their relation with Lie algebra theory. In 6.4.2, we introduce non-monodromic ADE fibrations in general and with examples (Conifold, Generalised Conifold, Reid Pagoda). In 6.4.3 we treat monodromic cases. In particular, we rederive the Pagoda of order k, treating it as a monodromically fibered A_{2k-1} singularity. We finally test our method on two interesting cases in the family of D-type fibrations. One is a simple flop of length 2. The other is a non-resolvable D_4 singularity, a situation in which the T-brane background is so severe that the threefold singularity does not admit crepant resolutions.

6.1 D3-branes vs D2-branes probing CY3

Let us consider a single D3-brane probing an isolated Calabi-Yau (CY) threefold singularity. This configuration geometrically engineers a four-dimensional $\mathcal{N} = 1$ supersymmetric quiver gauge theory. Its moduli space of vacua, parametrized by the vacuum expectation values (VEVs) of the bifundamental scalar fields, is isomorphic to the CY threefold itself, representing the transverse motion of the D3-brane away from the singularity.

To explore the three-dimensional counterpart, we compactify one spatial dimension of the D3-brane worldvolume on a circle of radius R and perform a T-duality transformation along this direction. This procedure yields a D2-brane probing the same singularity, where the transverse geometry is now effectively $CY \times S^1$, with the dual circle radius $r \propto \alpha'/R$. This T-dual setup results in a 3d $\mathcal{N} = 2$ supersymmetric gauge theory.

The vacuum moduli space of 3d $\mathcal{N} = 2$ theories is notoriously more complex than the 3d $\mathcal{N} = 4$ case. In theories with only four supercharges, the distinction between the Coulomb Branch (CB) and the Higgs Branch (HB) is less rigid: such branches can be lifted by quantum corrections, or they may intersect in a way that prevents a clear-cut separation. Furthermore, the $U(1)_R$ symmetry, which typically helps define these branches, can mix with flavor symmetries along the RG flow.

However, for theories possessing a well-defined UV Lagrangian, we can employ a standard working definition: the CB is parametrized by the scalar field σ in the vector multiplet together with the dual photon γ, while the HB is parametrized by the VEVs of the matter fields.

The physical interpretation of the 3d Coulomb branch scalar differs on the two sides of the T-duality. In Type IIB, before T-duality, the scalar σ descends from the 4d photon compactified on the circle: it is the Wilson line $\oint A_4$ around the compact direction, and hence exhibits periodicity with period set by the radius R. After T-duality to Type IIA, the same scalar σ parametrizes the position of the D2-brane along the dual circle of radius $r \propto \alpha'/R$.

In the limit $r \to 0$ (corresponding to the 4d decompactification limit $R \to \infty$), these two descriptions converge to the same conclusion: the Coulomb branch is forced to collapse. On the IIB side, as $R \to \infty$, the Wilson line becomes non-dynamical and is frozen at zero. On the IIA side, as $r \to 0$, the dual circle shrinks and the D2-brane position loses its physical meaning, forcing $\langle\sigma\rangle = 0$. Thus, in both descriptions, the decompactification limit naturally restricts the

3d dynamics to the origin of the Coulomb branch.

Consequently, to recover the 4d D3-brane theory from the 3d D2-brane perspective, one must work at the origin of the Coulomb branch. This restriction isolates the Higgs branch, which remains robust under the compactification. Notably, the tree-level superpotential W, being a holomorphic function of the chiral matter fields, remains unaltered in this transition. While 3d theories often develop non-perturbative superpotential contributions from monopole-instantons, these effects vanish in the 4d limit where the Coulomb branch decouples.

In summary, the geometric information of the CY_3 is fully encoded in the 3d theory of the D2-brane. To systematically retrieve the 4d CY_3 moduli space from the 3d perspective, one proceeds by first identifying the 3d theory that shares the same quiver and field content as the 4d model. By then taking the 4d limit ($r \to 0$) and restricting the dynamics to the origin of the Coulomb branch, the vacuum selection is governed purely by the Higgs branch equations. Algebraically, this corresponds to the space of solutions to the F-term equations derived from the superpotential,

$$\mathcal{M}_{HB} = \{\langle \Phi_{ij} \rangle \,|\, \partial_{\Phi_{ij}} W = 0\} // G \,, \tag{6.4}$$

where G is the gauge group of the quiver. This quotient recovers the Calabi-Yau threefold as the vacuum moduli space of the D3-brane, effectively completing the bridge between the 3d gauge dynamics and the 4d transverse geometry.

6.2 $\mathcal{N} = 2$ 3d mirror symmetry: linear quivers

To set the notation and guide the reader through the computations that will follow, we introduce a simple case of $\mathcal{N} = 2$ mirror symmetry, which generalizes what was discussed in 2.2.4.

Theory A: Let us consider a 3d $\mathcal{N} = 2$ $U(1)$ gauge theory with $N+1$ flavors of positron/electron pairs $(Q_i, \tilde{Q}_i)$ and no superpotential. There is an $SU(N+1) \times SU(N+1)$ flavor symmetry that rotates the Q_i and $\tilde{Q}_i$, respectively. The diagonal $SU(N+1)_\Delta$ has the moment map defined by mesons, transforming in the adjoint of $SU(N+1)_\Delta$:

$$M_i^j = Q_i \, \tilde{Q}^j \,. \tag{6.5}$$

We can add mass deformations that break the full flavor group to its diagonal as follows:

$$\delta_m W = Q \cdot \Phi \cdot \tilde{Q} \,, \tag{6.6}$$

where Φ is a background, non-dynamical $SU(N+1)$-valued Higgs field.

Theory B: Its mirror dual, which we name Theory B, is a linear quiver gauge theory (see Figure 6.1) with $U(1)^N$ gauge group, $N+1$ bifundamentals $q_i, \tilde{q}_i$, $N+1$ singlets s_i and superpotential

$$W_B = \sum_{i=1}^{N+1} s_i q_i \tilde{q}_i \,. \tag{6.7}$$

On this side, we can consider adding Polonyi terms, of the form

$$\delta W_{\text{diag}} = \tilde{\Phi}_i^i \, s_i \,. \tag{6.8}$$

where $\tilde{\Phi}$ is a background diagonal matrix. Equally importantly, as we will explain later, we can add monopole terms of the form

$$\delta W_{\text{mon}} = \tilde{\Phi}_{\alpha^\star} \, w_{-\alpha} \,, \tag{6.9}$$

where the notation will be explained shortly.

Figure 6.1: Theory B. For each node i, $i = 1, ..., N$, there is a $\mathcal{N} = 2$ $U(1)$ vector multiplet V_i. Square nodes denote flavor symmetries. Oriented lines between adjacent nodes represent bifundamental chiral multiplets.

Theory B has an $SU(N+1)$ acting on the Coulomb Branch coordinates. In particular, Theory B has a manifest topological $U(1)_T^N$ symmetry, which is expected to enhance to a $SU(N+1)$ global symmetry in the IR[3]. The moment map for Theory B is given by μ in the adjoint of $SU(N+1)$, with $\mu_{ii} = s_i$, and the off-diagonal components are the monopole operators with charges in one-to-one correspondence with the roots of the A_N Lie algebra associated with the topological symmetry.

[3]The arguments for this are solid for $\mathcal{N} = 4$. However, the $\mathcal{N} = 2$ case requires more indirect checks, such as identifying $SU(N+1)$ characters in the superconformal index. [139, 140]

Let us now fix our conventions for monopole operators. A monopole operator is specified by an N-tuplet of magnetic charges

$$\vec{m} = (m_1, \ldots, m_N) \in \mathbb{Z}^N \,.$$

Now, we recall the results of [36, 95], that conclude that the IR R-charge of a monopole operator $w_{\vec{m}}$ with magnetic charges $\vec{m}$ will be given by[4]

$$\Delta(w_{\vec{m}}) = \frac{1}{2} \sum_{i=1}^{N} |m_i - m_{i+1}| \,. \tag{6.10}$$

The monopole operators of interest, meaning those that lead to an enhanced global symmetry, are those with $\Delta = 1$. The only possible solutions are monopoles with a single cluster of consecutive ones, regadless of the length. So, the simple 'length-1' solutions are following:

$$\vec{m}_1^{(1)} = (1, 0, 0, \ldots, 0) \tag{6.11}$$
$$\vec{m}_2^{(1)} = (0, 1, 0, \ldots, 0) \tag{6.12}$$
$$\ldots \tag{6.13}$$
$$\vec{m}_N^{(1)} = (0, \ldots, 0, 1) \,, \tag{6.14}$$

These monopoles correspond to the simple roots of the enhanced flavor algebra. For 'length-2' we have

$$\vec{m}_1^{(2)} = (1, 1, 0, \ldots, 0) \tag{6.15}$$
$$\vec{m}_2^{(2)} = (0, 1, 1, \ldots, 0) \tag{6.16}$$
$$\ldots \tag{6.17}$$
$$\vec{m}_N^{(2)} = (0, \ldots, 1, 1) \,, \tag{6.18}$$

and so on up to length-$(N-2)$, filling out the rest of the root system of the enhanced $SU(N+1)$.

To clarify the link between this basis of $U(1)$-charges, and the usual Dynkin labels for the adjoint representation of Lie(G), we define the following basis $\mathfrak{h}_G = \langle \alpha_i^* \rangle$ for the Cartan subalgebra[5]

[4] This applies to a balanced Abelian quiver.

[5] These $\alpha^\star$ are often referred to as *fundamental coweights*, not to be confused with the coroots.

$\mathfrak{h}_G$ such that

$$\alpha_i(\alpha_j^*) = \delta_{ij} \,. \tag{6.19}$$

This is the appropriate language to describe monopole operators charged w.r.t. a single gauge node. Given this, we will refer to a monopole ω_α as the one charged under α^* only.

Mirror map The mirror map works as follows:

$$M_i^j = Q_i \tilde{Q}_j \longleftrightarrow \mu_{ij} \,, \qquad V_+ \longleftrightarrow B \,, \qquad V_- \longleftrightarrow \tilde{B} \,, \tag{6.20}$$

where $V_\pm$ are the monopole operators of the $U(1)$ theory, while $B = q_1 q_2 ... q_{N+1}$ and $\tilde{B} = \tilde{q}_1 \tilde{q}_2 ... \tilde{q}_{N+1}$ are the baryons of the second theory. The diagonal $\mu_{ii} = s_i$, and the off-diagonal μ_{ij} are monopole operators pointing in the root space directions matching the meson of the A-side.

The deformations (6.6) and (6.9) are also mapped into each other via the following identifications:

$$\Phi \leftrightarrow \tilde{\Phi} \tag{6.21}$$

$$M_\alpha \leftrightarrow w_\alpha \,, \tag{6.22}$$

where M_α is the A-side meson that points along the α-root of $SU(N+1)$.

Let us now add to Theory B $N+1$ singlets T_i and deform the superpotential (6.7) to the following one

$$W_{B'} = \sum_{i=1}^{N+1} s_i q_i \tilde{q}_i - \sum_{i=1}^{N+1} s_i T_i \,. \tag{6.23}$$

It is a mass term for T_i and s_i. Integrating them out, one obtains a zero superpotential. The new theory will be called Theory B'.

We can obtain the mirror dual of Theory B', that we call Theory A', by adding the dual of the superpotential deformation to Theory A; on this side we then get the superpotential

$$W = -\sum_{i=1}^{N+1} T_i Q_i \tilde{Q}_i \,. \tag{6.24}$$

Note, that $W_{B'}$ implies the chiral ring identification

$$\langle q_i \tilde{q}_i \rangle = \langle T_i \rangle \,. \tag{6.25}$$

6.2.1 Monopole superpotentials

The examples below will serve as building blocks for deriving the effective superpotentials of the theories arising on D2-branes probing cDV singularities.

Building block I

Let us consider a 3d $\mathcal{N} = 2$ supersymmetric $U(1)$ gauge theory with two flavors and with the following superpotential that includes monopole operators:

$$W = \phi(q_1\tilde{q}_1 - q_2\tilde{q}_2) + w_- + P(\phi)w_+ \,, \tag{6.26}$$

where $P(\phi)$ is a polynomial in ϕ. This theory can be seen as a deformation of a 3d $\mathcal{N} = 2$ abelian linear quiver gauge theory with one node and without superpotential. Let us think of it as taking the B' theory in the language of (6.23) plus deformation.

Its mirror can be found by taking the corresponding Theory A' and adding to its superpotential the dual of (6.26). One obtains a $U(1)$ gauge theory with 2 flavors and superpotential

$$W = -T_1Q_1\tilde{Q}_1 - T_2Q_2\tilde{Q}_2 + \phi(T_1 - T_2) + P(\phi)Q_1\tilde{Q}_2 + Q_2\tilde{Q}_1 \,, \tag{6.27}$$

where we have also used (6.25). The fields Q_2 and $\tilde{Q}_1$ are massive and can be integrated out: their equations of motion give

$$Q_2 = T_1Q_1 \qquad \text{and} \qquad \tilde{Q}_1 = T_2\tilde{Q}_2 \,. \tag{6.28}$$

Plugging this into (6.27), one obtains the effective superpotential[6]

$$W_{\text{eff}} = (P(\phi) - T_1T_2)Q_1\tilde{Q}_2 + \phi(T_1 - T_2) \,. \tag{6.29}$$

[6]We do not integrate out the massive fields $T_1 - T_2$ and ϕ. The reason will become clear in the following sections.

One obtains a $U(1)$ gauge theory with one flavor. Its mirror dual is an XYZ model, with modified superpotential[7]

$$W_{\text{eff}} = X(Y\,Z + P(\phi) - T_1 T_2) + \phi(T_1 - T_2)\,. \tag{6.30}$$

Building block II

Let us now consider the more generic case, i.e. a 3d abelian linear quiver with N nodes and with the following superpotential that includes monopole operators:

$$W = \sum_{i=1}^{N} \phi_i (q_i \tilde{q}_i - q_{i+1}\tilde{q}_{i+1}) + \sum_{i=1}^{N} w_{-\alpha_i} + \left(\frac{1}{N}\sum_{i=1}^{N}\phi_i\right) w_{+\alpha_{\text{high}}}\,. \tag{6.31}$$

where, as explained previously, $\omega_{-\alpha_i}$ refers to the monopole operator with charge -1 w.r.t. to the α_i node, and zero for the others. This theory can be seen as a deformation of a 3d $\mathcal{N}=2$ abelian linear quiver gauge theory with N nodes and without superpotential.

Its mirror can be found by taking the corresponding Theory A' and adding to its superpotential the dual of (6.31). One obtains a $U(1)$ gauge theory with $N+1$ flavors and superpotential

$$W = -\sum_{i=1}^{N+1} T_i Q_i \tilde{Q}_i + \sum_{i=1}^{N} \phi_i (T_i - T_{i+1}) + \sum_{i=1}^{N} Q_{i+1}\tilde{Q}_i + \left(\frac{1}{N}\sum_{i=1}^{N}\phi_i\right) Q_1 \tilde{Q}_{N+1}\,. \tag{6.32}$$

Integrating out the massive fields $Q_{i+1}, \tilde{Q}_i$ with $i = 1, ..., N$ one obtains the effective superpotential

$$W_{\text{eff}} = \left(\frac{1}{N}\sum_{i=1}^{N}\phi_i - T_1 T_2 ... T_{N+1}\right) Q_1 \tilde{Q}_{N+1} + \sum_{i=1}^{N}\phi_i (T_i - T_{i+1})\,. \tag{6.33}$$

Hence, we have a $U(1)$ gauge theory with one flavor and superpotential (6.33). Its mirror dual is an XYZ model, with modified superpotential

$$W_{\text{eff}} = X\left(Y\,Z + \frac{1}{N}\sum_{i=1}^{N}\phi_i - T_1 T_2 ... T_{N+1}\right) + \sum_{i=1}^{N}\phi_i (T_i - T_{i+1})\,. \tag{6.34}$$

[7] In some of the cases analyzed in the following sections, the sign in front of $q_2, \tilde{q}_2$ in (6.26) will be $+$ instead of $-$. In such instances, it is sufficient to replace T_2 with $-T_2$.

6.3 cDV singularities and the Higgs field

Let us recall the most important facts about Higgs field fibrations that we will use for the construction of the theory on the probe.
For the A- and D-type cDV threefold that we consider in this work, the hypersurface equations induced by $\Phi(w)$ are

$$\begin{aligned} A_n: &\qquad x^2+y^2=\det(z\mathbb{1}_{n+1}-\Phi) \\ D_n: &\qquad x^2+zy^2-\frac{\sqrt{\det(z\mathbb{1}_{2n}+\Phi^2)}-\text{Pfaff}^2(\Phi)}{z}+2y\text{Pfaff}(\Phi)=0 \end{aligned} \tag{6.35}$$

where Φ is written as a matrix in the fundamental representation of A_n or D_n respectively. As w varies, the Higgs field $\Phi(w)$ takes values in a subalgebra $\mathcal{L}$ of the ADE Lie algebra [19]. The commutant $\mathcal{H}$ of $\mathcal{L}$ — that is, the set of elements commuting with all of $\mathcal{L}$ — is an abelian subalgebra contained in the Cartan subalgebra $\mathcal{C}$.[8] By evaluating the roots α on elements $h \in \mathcal{H}$, one can determine which simple roots are resolved: if $\alpha(h) \neq 0$ for some $h \in \mathcal{H} \subset \mathcal{C}$, then the root α is a vanishing two-cycle that can be resolved in the (partial) simultaneous resolution. The subalgebra $\mathcal{L}$ is known as a *Levi subalgebra*, since it commutes with an abelian subalgebra. This implies that the resolution of the threefold induced by Φ can be understood by identifying the Levi subalgebra to which it belongs.

One can define invariant coordinates on the Levi subalgebra as follows: for each simple summand, choose the Casimir invariants of that algebra;[9] the remaining coordinates are given by the coefficients in the expansion of Φ along the basis $(\alpha_1^*,\dots,\alpha_k^*)$ of $\mathcal{H}$. For example, consider $\mathcal{L} = A_1^{(1)} \oplus A_1^{(2)} \oplus \langle\alpha_3^*\rangle$. For a generic element $\Phi \in \mathcal{L}$, we have: (i) invariant coordinate $\varrho_1 = \frac{1}{2}\text{Tr}(\Phi_1^2)$ for the first A_1 summand, (ii) invariant coordinate $\varrho_2 = \frac{1}{2}\text{Tr}(\Phi_2^2)$ for the second A_1 summand, and (iii) invariant coordinate ϱ_3 (coefficient along α_3^*) for the $U(1)$ part. A generic $\Phi \in \mathcal{L}$ can then be written as $\Phi(\varrho_1,\varrho_2,\varrho_3)$, and specifying a base change $\varrho_i = f_i(w)$ gives a specific cDV threefold. The sphere associated with α_i may return to itself after traversing the loop. In this case, it extends globally as a holomorphic cycle in the threefold and can be resolved. Alternatively, the sphere may undergo monodromy, mixing non-trivially with other spheres as we encircle $w = 0$. In this case, it does not lift to a globally well-defined holomorphic curve in the threefold. Geometries in which some spheres exhibit the latter behavior are

[8] The reason for this is traced back to the M-theory origin of the field Φ and it is explained in [19, 25].
[9] For an A_n summand, an element $g \in A_n$ has invariant coordinates $\varrho_{\lambda_q} = \text{Tr}\, g^q$.

referred to as *monodromic* cDV threefolds, while those in which all spheres behave as in the former case are called *non-monodromic* [12, 89]. The resolution pattern is thus encoded in a colored Dynkin diagram: white nodes correspond to resolvable roots (globally defined spheres), while colored nodes correspond to non-resolvable roots (spheres undergoing monodromy). Connected subdiagrams of colored nodes correspond to simple summands of the Levi subalgebra $\mathcal{L}$. Algebraically, this structure is encoded in the Higgs field $\Phi(w)$: a root α is colored if and only if Φ contains off-diagonal components—the step operators $e_{\pm\alpha}$—beyond just Cartan elements. For example, $\Phi(w) = e_\alpha + \varrho(w)e_{-\alpha}$ contains step operators, indicating that α is colored and undergoes monodromy. In contrast, $\Phi(w) = \varrho(w)\alpha^*$ lies purely in the Cartan, indicating that α is white (resolvable).

6.4 D2-brane probing a cDV threefold singularity

The main point of this work can be summarized as follows. The (undeformed) ADE surfaces appear as the Higgs branch moduli space of the three-dimensional $\mathcal{N} = 4$ worldvolume theory on a D2-brane probing an ADE singularity. By deforming the ADE surface along an additional complex direction in spacetime, one obtains a cDV threefold. We show that this cDV threefold can be reproduced as the Higgs branch moduli space[10] of a 3d $\mathcal{N} = 2$ theory obtained by a suitable superpotential deformation of the D2-brane worldvolume theory.

The technical core of our construction is the systematic treatment of these superpotential deformations through mirror symmetry and ungauging, ultimately yielding an effective theory with polynomial superpotential whose Higgs branch reproduces the cDV geometry. As discussed in the introduction, upon decompactification this 3d theory flows to the 4d $\mathcal{N} = 1$ gauge theory engineered by D3-branes probing the same cDV singularity.

In order to derive the 3d $\mathcal{N} = 2$ worldvolume theory on D2-branes probing cDV threefold singularities from the geometric data encoded in the Higgs field $\Phi(w)$, we adopt the following three-step strategy:

1. Start with the 3d $\mathcal{N} = 4$ quiver for a D2-brane probing the ADE surface singularity.

[10] Throughout the paper, when referring to the Higgs branch of the 3d $\mathcal{N} = 2$ theory, we implicitly mean the branch that matches the moduli space of the corresponding 4d worldvolume theory on a D3-brane. As discussed in Section 6.1, the D2-brane description arises from compactifying the D3-brane on a circle; the additional 3d Coulomb-branch directions associated with the circle are frozen when identifying the geometric moduli space.

2. Deform the superpotential using $\Phi(w)$.

3. Integrate out massive fields to obtain the effective IR theory. The Higgs branch moduli space of this 3d theory reproduces the probed cDV threefold. Upon decompactification to 4d, this theory flows to the worldvolume theory of a D3-brane probing the same singularity.

For non-monodromic fibrations (all roots resolved), Φ belongs to the Cartan subalgebra and induces a simple deformation. For monodromic cases (colored nodes), Φ contains nilpotent elements that induce monopole operators in the superpotential.

6.4.1 D2-brane probing an ADE singularity

Our starting point is the worldvolume theory on a D2-brane probing an ADE singularity, reviewed in greater detail in Section 2.2.

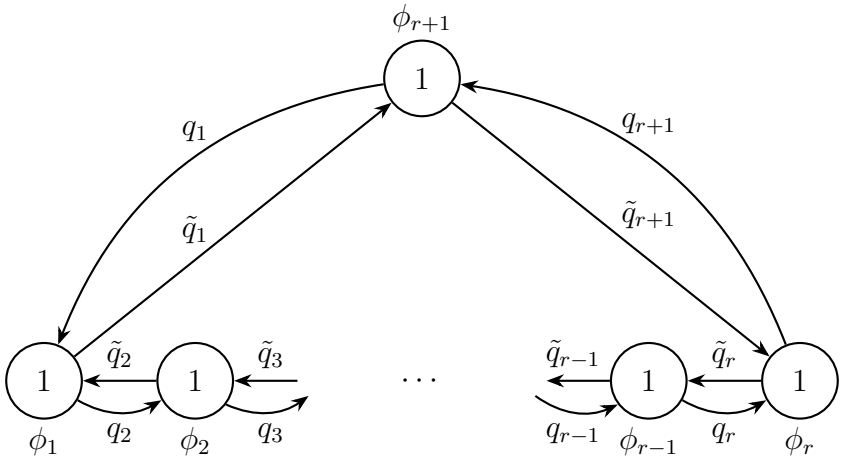

Figure 6.2: A_r theory. For each node i, $i = 1, ..., r+1$, there is a $\mathcal{N} = 4$ $U(1)$ vector multiplet V_i containing a $\mathcal{N} = 2$ vector multiplet and an adjoint chiral ϕ_i. Pairs of oriented lines between adjacent nodes represent bifundamental hypermultiplets $(q_i, \tilde{q}_i)$.

The quiver has the shape of the affine Dynkin diagram of the corresponding ADE Lie algebra [2]. The nodes of the quiver correspond to fractional D2-branes; the gauge group at each node is $U(n_i)$, where n_i is the dual Coxeter label of the i-th node in the associated Dynkin diagram. Each pair of arrows connecting the nodes in the quiver is a bifundamental hypermultiplet. As an example, Figure 6.2 illustrates the A_r quiver. In this case, the gauge group is $\left(\prod_{i=0}^{r} U(1)\right)/U(1)$.

The vector multiplet chiral fields ϕ_i are coupled to the hypermultiplets $(q_i, \tilde{q}_i)$ via the $\mathcal{N} = 4$ superpotential

$$W = \sum_{i=1}^{r+1} (\phi_i - \phi_{i-1}) q_i \tilde{q}_i, \ , \tag{6.36}$$

with $\phi_0 \equiv \phi_{r+1}$. There is also a D-term potential that produces the D-term relations

$$|q_i|^2 + |\tilde{q}_{i-1}|^2 - |\tilde{q}_i|^2 - |q_{i-1}|^2 = 0 \qquad\qquad i = 1, ..., r \ . \tag{6.37}$$

The A_r theory features r triplets of FI-parameters: the triplet can be separated in a complex FI-parameter that appears in the superpotential, and a real one that modifies the relations (6.37); these can be regarded as mass parameters (i.e., background vector multiplets) for the $U(1)^r_T$ topological symmetry.

As we said above, for $\mathcal{N} = 4$ quiver gauge theories, monopole operators and the scalar fields ϕ_i can be assembled into the moment map μ for the topological symmetry. μ is object transforming in the adjoint representation of the Lie algebra $\mathcal{G}$. Under mirror symmetry, the A_r quiver is mapped to a $U(1)$ gauge theory with $r+1$ flavors that has a manifest $SU(r+1)$ symmetry, with moment map $\mu_{ij}^{\text{mirror}} = Q_i \tilde{Q}_j$. As we discussed above, mirror symmetry maps the moment map μ of the original theory to the moment map μ^{mirror} in the dual theory.

6.4.2 Non-monodromic ADE fibrations

The theory of a D2-brane probing the threefold singularity X can be viewed as a deformation of the theory describing a D2-brane probing the corresponding ADE surface singularity. This deformation is governed by the *background* Higgs field $\Phi(w)$, which is non-dynamical from our 3d point of view and should not be confused with the dynamical adjoint scalars ϕ_i in the quiver gauge theory.

Fractional branes and holomorphic volumes

To understand the superpotential deformation, we first recall the classic result of [12] (building on earlier work [141–143]). Consider D5-branes wrapping 2-cycles in a fibered ADE geometry over a base $\mathbb{C}_w$. In the absence of background fields, the D5-branes give rise to an $\mathcal{N} = 2$ gauge

theory with FI parameters α_i equal to the holomorphic volumes of the wrapped 2-cycles. When a non-trivial fibration is introduced a superpotential is generated in the worldvolume theory.

The key observation of [12] is that the BPS tension of domain walls, computed by integrating the holomorphic three-form $\Omega = \omega \wedge dw$ over a three-chain, determines the superpotential:

$$W(\phi) = \int_{w=\Phi} \alpha(w)\, dw \,, \tag{6.38}$$

where ϕ is the scalar field parametrizing the position of the fractional brane along the base, and $\alpha(w) = \int_{S^2(w)} \omega$ is the holomorphic volume of the wrapped cycle at position w. Here ω denotes the holomorphic $(2,0)$-form of the ADE fiber. This formula implies that

$$\frac{\partial W}{\partial \phi} = \alpha(\phi) \,, \tag{6.39}$$

i.e., the derivative of the superpotential reproduces the holomorphic volume of the wrapped cycle at the brane's position.

Conversely, if one wishes to engineer a gauge theory with a specified superpotential $W(\phi) = P(\phi)$, the fibration must be chosen such that $\alpha(w) = P'(w)$. This establishes a direct dictionary between the geometric deformation of the ADE fiber and the superpotential of the gauge theory.

In our setup, fractional D4-branes (arising from the D2-brane probe splitting into components) wrap the vanishing spheres associated with each simple root α_i of the ADE Dynkin diagram. The Cachazo-Vafa formula (6.38) will guide our construction of the superpotential deformation induced by the background Higgs field $\Phi(w)$.

Deriving the deformation from $\Phi(w)$

We now show how the geometric data encoded in the Higgs field $\Phi(w)$ reproduces the Cachazo-Vafa superpotential deformation (6.38).

For balanced quivers (where each node has rank N_i and $2N_i$ flavors), consider isolating a single fractional brane at node i together with its $2N_i$ hypermultiplets. This subsystem supports a $U(N_i)$ gauge group with $\mathcal{N} = 4$ supersymmetry. The Coulomb branch of this subsystem possesses an $SU(2)$ flavor symmetry—distinct from the $SU(2N_i)$ flavor symmetry acting on the

Higgs branch—which corresponds to the $\mathfrak{su}(2)_{\alpha_i}$ subalgebra of $\mathcal{G}$ generated by

$$\langle e_{\alpha_i}, e_{-\alpha_i}, h_{\alpha_i} \equiv [e_{\alpha_i}, e_{-\alpha_i}] \rangle.$$

The background Higgs field Φ, which transforms in the adjoint representation of $\mathcal{G}$, couples to the fractional brane worldvolume theory through the moment map μ_{α_i} associated to this Coulomb branch flavor symmetry $\mathfrak{su}(2)_{\alpha_i}$. In the non-monodromic case, where Φ lies entirely in the Cartan subalgebra, this coupling involves only the Cartan part of μ_{α_i}, namely $\phi_{\alpha_i} h_{\alpha_i}$, where ϕ_{α_i} is the scalar field parametrizing the position of the fractional brane along the base.

The Higgs field admits a polynomial expansion

$$\Phi(w) = \sum_{\ell=0}^{k} \Phi_\ell \, w^\ell \,, \tag{6.40}$$

where the brane's position in the base is $w = \phi_i$. The coupling between $\Phi(\phi_i)$ and the moment map generates an induced superpotential in the worldvolume theory:

$$\delta W_i = \sum_{\ell=0}^{k} \frac{\phi_i^\ell}{\ell+1} \, \kappa\left(\Phi_\ell \,,\, \mu_{\alpha_i}\right) = \sum_{\ell=0}^{k} \frac{\phi_i^{\ell+1}}{\ell+1} \, \kappa\left(\Phi_\ell \,,\, h_{\alpha_i}\right) \,, \tag{6.41}$$

where κ denotes the Killing form. The factor $(\ell+1)^{-1}$ is chosen precisely to satisfy the Cachazo-Vafa condition (6.38):

$$\frac{\partial \delta W_i}{\partial \phi_i} = \sum_{\ell=0}^{k} \phi_i^\ell \, \kappa(\Phi_\ell, h_{\alpha_i}) = \kappa\left(\Phi(\phi_i), h_{\alpha_i}\right) = \alpha_i\left(\Phi(\phi_i)\right) \,, \tag{6.42}$$

where in the last step we have used the normalization of the Killing form for ADE algebras, $\kappa(h_\alpha, h_\beta) = \alpha \cdot \beta$.

This has a clear geometric interpretation: at a given value w in the base, the holomorphic volume of the sphere α_i in the deformed fiber is $\alpha_i(\Phi(w))$. Since the fractional brane wrapping α_i sits at position $w = \phi_i$, equation (6.42) correctly reproduces the holomorphic volume, in agreement with [12].

In the following, we examine some well-known examples and verify that the proposed deformation indeed reproduces the expected geometry in the moduli space.

Example 1: Conifold

We start with the easiest and famous example, the conifold given by the hypersurface

$$uv = z^2 - w^2 \,. \tag{6.43}$$

This threefold can be regarded as a family of deformed A_1 singularities, where w is the deformation parameter. The corresponding $\Phi(w)$ is the following 2×2 matrix [25]

$$\Phi(w) = \begin{pmatrix} w & 0 \\ 0 & -w \end{pmatrix} = 2w\alpha^* \,. \tag{6.44}$$

Plugging this into (6.35) one reproduces correctly (6.43).

Let us probe the conifold singularity by a D2-brane. According to what we have said in this section and due to the formula (6.41) (with $\ell = 1$), the resulting theory is the A_1 quiver gauge theory deformed by

$$\delta W_1 = \frac{\phi_1}{2}\alpha(\Phi(\phi_1)) = \phi_1^2 \tag{6.45}$$

$$\delta W_2 = -\frac{\phi_2}{2}\alpha(\Phi(\phi_2)) = -\phi_2^2 \,. \tag{6.46}$$

Here we have used that the fractional brane corresponding to the extended node in the affine Dynkin diagram is wrapping $\alpha_2 = -\alpha$.

Now, let us consider the complete deformed superpotential:

$$W = (\phi_1 - \phi_2)(q_1\tilde{q}_1 - q_2\tilde{q}_2) + \phi_1^2 - \phi_2^2 = \phi_-(q_1\tilde{q}_1 - q_2\tilde{q}_2 + \phi_+) \tag{6.47}$$

where we have redefined $\phi_- = \phi_1 - \phi_2$ and $\phi_+ = \phi_1 + \phi_2$. Notice that this deformed superpotential for the conifold was already introduced by Klebanov-Witten [88], as noticed in [12].

The fields $\phi_\pm$ are massive. Integrating them out, we get a quiver gauge theory, with the A_1 quiver and zero superpotential, i.e., we obtain exactly the theory of a D-brane probing the conifold.

We have verified that the moduli space reproduces the conifold geometry. This confirms our prescription (6.40) in the simplest case where Φ contains only linear terms. The next examples will test the method for higher-degree base changes.

Example 2: Reid's Pagodas as a family of deformed A_1 surfaces

Let us now consider the following three-fold, known as Reid's pagoda:

$$uv = z^2 - w^{2k} \,. \tag{6.48}$$

This is again a non-monodromic A_1-fibration (that reduces to the conifold for $k = 1$), whose corresponding Higgs field is

$$\Phi(w) = \begin{pmatrix} w^k & 0 \\ 0 & -w^k \end{pmatrix} = 2w^k \alpha^* \,. \tag{6.49}$$

This induces the superpotential deformations

$$\delta W_1 = \frac{\phi_1}{k+1}\alpha(\Phi(\phi_1)) = \frac{2}{k+1}\phi_1^{k+1} \tag{6.50}$$

$$\delta W_2 = -\frac{\phi_2}{k+1}\alpha(\Phi(\phi_2)) = -\frac{2}{k+1}\phi_2^{k+1} \,. \tag{6.51}$$

We obtain, then an A_1 quiver with the superpotential

$$W = (\phi_1 - \phi_2)(q_1\tilde{q}_1 - q_2\tilde{q}_2) + \frac{2}{k+1}\phi_1^{k+1} - \frac{2}{k+1}\phi_2^{k+1} \,. \tag{6.52}$$

This superpotential appeared in [12, 89], and we will rederive it in the following in a different way, by considering Reid's Pagoda as a family of deformed A_{2k-1} singularities (by exchanging the roles of z and w in (6.48)).

Let us check that the F-term moduli space is the CY threefold (6.48). The F-terms are

$$\begin{aligned} \partial_{\phi_1} W = 0 : &\qquad q_1\tilde{q}_1 - q_2\tilde{q}_2 + 2\phi_1^k = 0 \\ \partial_{\phi_2} W = 0 : &\qquad q_1\tilde{q}_1 - q_2\tilde{q}_2 + 2\phi_2^k = 0 \\ \partial_{q_i} W = 0 : &\qquad (\phi_1 - \phi_2)\,\tilde{q}_i = 0 \qquad i = 1,2 \\ \partial_{\tilde{q}_i} W = 0 : &\qquad (\phi_1 - \phi_2)\,q_i = 0 \qquad i = 1,2 \end{aligned} \tag{6.53}$$

The solutions are given by $\phi_2 = \phi_1 \equiv \phi$ and $q_2\tilde{q}_2 = q_1\tilde{q}_1 + 2\phi^k$. The moduli space is then given by defining gauge-invariant combinations and finding the relations they need to satisfy. Here we have the following four gauge invariants (plus the field ϕ):

$$U \equiv q_1 q_2, \qquad V \equiv \tilde{q}_1\tilde{q}_2, \qquad X_1 \equiv q_1\tilde{q}_1, \qquad X_2 \equiv q_2\tilde{q}_2 \tag{6.54}$$

They satisfy the obvious relation $U\,V = X_1\,X_2$. Imposing the relation coming from the F-term, i.e. $X_2 = X_1 + 2\phi^k$, we have

$$U\,V = X_1\,(X_1 + 2\phi^k)\,, \tag{6.55}$$

that can be brought in the form (6.48) by redefining the coordinates as $X_1 = Z - \phi^k$.

Notice that ϕ plays the role of w. At a generic point of the moduli space $\phi_1 = \phi_2 = \phi$, i.e., the fractional branes move (as a bound state) away from the origin at $w = \phi$, that is consistent with the interpretation of the theory of D-branes probing an ADE surface singularity fibered over the complex plane $\mathbb{C}_w$.

This example demonstrates that our method correctly handles polynomial base changes $\varrho(w) = w^k$. Notice that the effective superpotential now contains terms ϕ^{k+1}, reflecting the degree of the base change. We will revisit this geometry in the next section from a different perspective (as a monodromic A_{2k-1} fibration).

Examples 3: Generalized conifold

The final example of non-monodromic fibration that we consider is the following hypersurface equation

$$uv = z(z-w)(z+w)\,. \tag{6.56}$$

This is a family of A_2 deformed singularities.

The corresponding Higgs field is

$$\Phi(w) = \begin{pmatrix} w & & \\ & -w & \\ & & 0 \end{pmatrix} = w(2\alpha_1^* - \alpha_2^*)\,. \tag{6.57}$$

The induced superpotential deformations are

$$\delta W_1 = \frac{\phi_1}{2}\alpha_1(\Phi(\phi_1)) = \phi_1^2\,, \tag{6.58}$$

$$\delta W_2 = \frac{\phi_2}{2}\alpha_2(\Phi(\phi_2)) = -\frac{1}{2}\phi_2^2\,, \tag{6.59}$$

$$\delta W_3 = -\frac{\phi_3}{2}(\alpha_1(\Phi(\phi_3)) + \alpha_2(\Phi(\phi_3))) = -\frac{1}{2}\phi_3^2\,. \tag{6.60}$$

We then obtain the A_2 quiver with the following superpotential

$$W = \sum_{i=1}^{3}(\phi_i - \phi_{i-1})q_i\tilde{q}_i + \phi_1^2 - \frac{1}{2}\phi_2^2 - \frac{1}{2}\phi_3^2\,. \tag{6.61}$$

This is the same superpotential found in [12]. By simple computations, one shows that the resulting moduli space reproduces the geometry (6.56), with $\phi_1 = \phi_2 = \phi_3 \equiv \phi$ that correctly plays the role of w.

Unlike the previous A_1 cases, this example involves multiple roots, showing how different fractional branes couple independently to different components of Φ. The next section addresses the more challenging monodromic cases where Φ contains off-diagonal terms.

6.4.3 Monodromic ADE fibrations

In monodromic fibrations, some curves of the fiber do not give rise to holomorphic curves in the total space of the threefold. This data is encoded in a *colored Dynkin diagram*. We color the nodes of such curves, and leave blank those that will be small-resolvable curves in the threefold.

In terms of our Higgs field language, the way we will achieve this is by selecting a *Levi subalgebra* of the semi-simple Lie algebra (see appendix C for two brief definitions). The Higgs field will take non-zero entries along this Levi. Graphically, this is encoded as follows: Connected subdiagrams of colored nodes are the Dynkin diagrams of the simple summands of the Levi (see Figure 6.3).[11][12]

[11] These diagrams involve the exceptional node of the original Dynkin diagram only when the corresponding Levi subalgebra is maximal within the original Lie algebra (or within one of its maximal subalgebras).

[12] In this paper, we primarily focus on cases where the coloring does not involve the extended node of the affine Dynkin diagram. This node corresponds to a bound state of the (anti)-fractional branes wrapping the simple roots plus an integral D2-brane. There also exist cDV Calabi–Yau threefolds in which the coloring involves the extended

These connected subdiagrams are related to subquivers of the original ADE quiver, whose symmetry in their CB is given by the Levi summand.

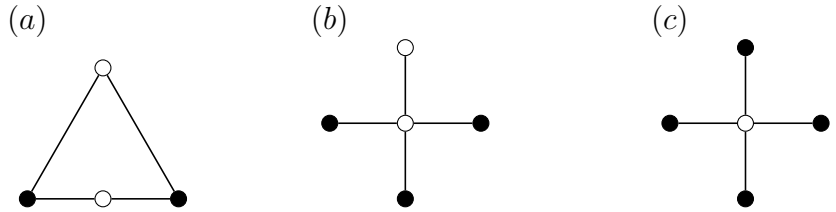

Figure 6.3: Graphic representation of partial simultaneous resolutions. Colored nodes correspond to obstructed 2-cycles. Colored subdiagrams are identified with the subalgebras that compose the Levi subalgebra associated with $\mathbf{\Phi}$. Here we show examples of simple flops of length 1, 2, and a non-resolvable D_4 singularity. (a) The colouring of the $\tilde{A}_3$ diagram corresponds to the choice of Levi $\mathcal{L}_\Phi = A_1^{(1)} \oplus A_1^{(3)} \oplus \langle \alpha_2^* \rangle$. (b) $\tilde{D}_4$ diagram. Coloring corresponds to $\mathcal{L}_\Phi = A_1^{(1)} \oplus A_1^{(2)} \oplus A_1^{(3)} \oplus \langle \alpha_4^* \rangle$. (c) Non-resolvable singularity. Here $\mathcal{L}_\Phi = A_1^{(0)} \oplus A_1^{(1)} \oplus A_1^{(2)} \oplus A_1^{(3)}$

In physical terms, given a choice of a Φ-background that generates a monodromic fibration, a probe D2-brane will see this as a superpotential deformation in the following way: For each summand of the Levi subalgebra, we introduce a superpotential term given by

$$\delta W = \kappa \left(\Phi(\phi_{cm}), \mu \right) \tag{6.62}$$

Here, μ is the moment map of the symmetry generated by the Levi summand in the CB of the corresponding subquiver. In the superpotential deformation (6.62), Φ depends on $\phi_{cm} = \frac{1}{m} \sum_{i=1}^{m} \phi_i$ that is the scalar controlling the motion of the center of mass of the fractional branes. Our claim is that the colored connected nodes must be treated together, as if the fractional branes were bound together by the non-zero Φ-background.

The extreme case is when all simple roots are colored, i.e., the Levi subalgebra coincides with the full ADE algebra. When this happens, the resolution of the threefold contains no holomorphic spheres. As a consequence, type IIA on this threefold does not admit fractional branes. The ordinary D2-brane, however, remains, and its $U(1)$ gauge group must be preserved. This $U(1)$ is naturally associated with the extended node of the quiver.

Let us consider the simplest example in order to illustrate the mechanism explicitly. First, we

nodes. In this case, the corresponding linear combination of exceptional cycles ceases to define an independent curve in the threefold. Equivalently, this introduces a relation among the simple roots, thereby eliminating one exceptional cycle from the resolution of the threefold.

put the D2-brane on $A_1 \times \mathbb{C}$. The worldvolume theory is the quiver gauge theory in 6.4.

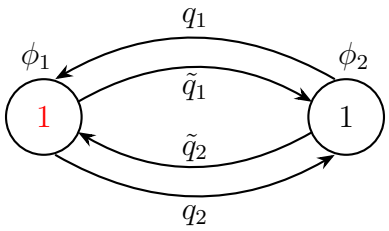

Figure 6.4: A_1 theory. The $\mathcal{N} = 4$ superpotential is given by 6.36 with $r = 1$.

Then, we consider the following Higgs field:

$$\Phi = \begin{pmatrix} 0 & 1 \\ w & 0 \end{pmatrix} = e_\alpha + w\, e_{-\alpha} \tag{6.63}$$

The corresponding Levi subalgebra is the A_1 algebra itself. The threefold equation is $uv = z^2 - w$, i.e. it is $\mathbb{C}^3$.

According to what we have written above, this Φ generates the following superpotential deformation

$$\delta W = \kappa(\Phi(\phi_1)\mu_\alpha) = w_{-\alpha} + \phi_1 w_\alpha \qquad \text{where} \qquad \mu_\alpha = \begin{pmatrix} \phi_1 & w_\alpha \\ w_{-\alpha} & -\phi_1 \end{pmatrix} \tag{6.64}$$

To deal with quivers with monopole superpotentials, one follows the prescription in [37]: one isolates the abelian node relative to $w_{\pm\alpha}$ by ungauging the adjacent $U(1)$; in our example, this amounts to ungauging the extended node. The isolated theory can then be coupled back to the rest of the quiver by gauging a subgroup of its flavor symmetry.

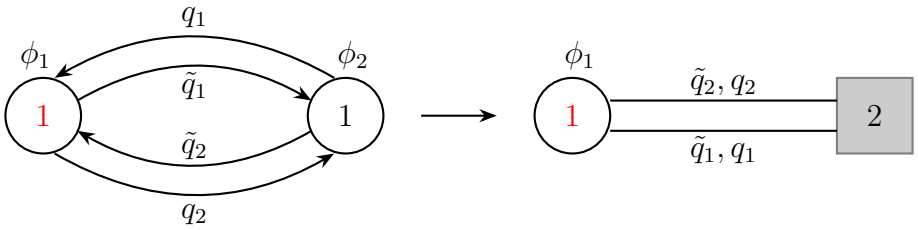

Figure 6.5: A_1 theory. Ungauging of the affine node.

For the isolated (balanced) node, the theory is a 3d $\mathcal{N}=4$ supersymmetric $U(1)$ gauge theory with two flavors, and deformed superpotential

$$W^{(1)} = \phi_1(q_1\tilde{q}_1 - q_2\tilde{q}_2) + w_{-\alpha} + \phi_1 w_\alpha \,, \tag{6.65}$$

i.e. we obtain the Building Block I in Section 6.2.1. The effective theory has no $U(1)$ and a superpotential

$$W^{(1)}_{\text{eff}} = X_1(Y_1Z_1 + \phi_1 - T_1T_2) + \phi_1(T_1 - T_2) \,. \tag{6.66}$$

We now gauge the $U(1)$ of the node 2 back and obtain a $U(1)$ gauge theory with a given number of singlets and superpotential

$$W_{\text{eff}} = X_1(Y_1Z_1 + \phi_1 - T_1T_2) + (\phi_1 - \phi_2)(T_1 - T_2) \,. \tag{6.67}$$

One can make a field redefinition $(\phi_1, \phi_2, T_1, T_2) \longleftrightarrow (A, B, T_+, T_-)$ in the following way: $A = \phi_1 + Y_1Z_1 - T_1T_2$, $B = \phi_1 - \phi_2$, $T_\pm = T_1 \pm T_2$. The superpotential can then be written as

$$W_{\text{eff}} = X_1 A + B\, T_- \,. \tag{6.68}$$

Hence, X_1, A, B, T_- are massive, and we can integrate them out.

The final theory has a quiver with one node and three loops, namely the quiver whose moduli space is $\mathbb{C}^3$, in agreement with the Φ in (6.63). The node corresponds to the D2-brane that probe $\mathbb{C}^3$ (originally it was the extended node of the A_1 affine Dynkin diagram).

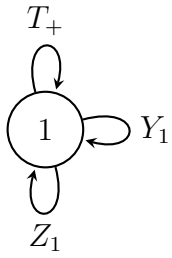

Figure 6.6: $\mathbb{C}^3$ theory.

In the next sections, we study interesting monodromic cases.

6.5 Reid's pagodas

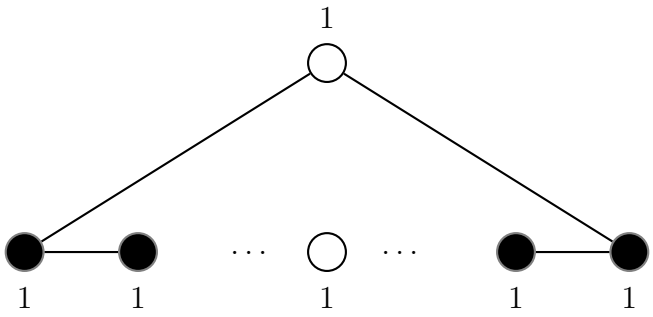

Figure 6.7: A_{2k-1} partial simultaneous resolution

We now return to Reid's Pagoda, studied earlier in Section 6.4.2 as a non-monodromic A_1 fibration. Here we re-analyze the same geometry from a different perspective: as a monodromic A_{2k-1} fibration where most nodes are colored. This provides a highly non-trivial check of our method.

The defining equation of the Reid's Pagoda is

$$uv = z^{2k} - w^2 \,. \tag{6.69}$$

This is the same equation as (6.48), but with the roles of z and w exchanged. The equation (6.69) can be seen as a A_{2k-1} singularity deformed at $w \neq 0$. It is already known that the resolution of this manifold contains a single exceptional sphere. This immediately implies that most of the nodes in the A_{2k-1} Dynkin diagram must be colored. Indeed, the corresponding colored Dynkin diagram is shown in Fig. 6.7. The associated Levi subalgebra is

$$\mathcal{L} = \langle \alpha_k^* \rangle \oplus A_{k-1}^L \oplus A_{k-1}^R \tag{6.70}$$

and the Higgs field takes the following block diagonal form

$$\Phi = \begin{pmatrix} \Phi_+ & \\ & \Phi_- \end{pmatrix} \tag{6.71}$$

with the two blocks given by

$$\Phi_{\pm} = \begin{pmatrix} 0 & 1 & 0 & \cdots & 0 \\ 0 & 0 & 1 & \ddots & \vdots \\ \vdots & \ddots & \ddots & \ddots & 0 \\ 0 & \cdots & 0 & 0 & 1 \\ \pm w & 0 & \cdots & 0 & 0 \end{pmatrix} , \tag{6.72}$$

i.e.

$$\Phi(w) = \sum_{m=1}^{k-1} e_{\alpha_m} + w\, e_{-\alpha_1 - \ldots - \alpha_{k-1}} + \sum_{m=k+1}^{2k-1} e_{\alpha_m} - w\, e_{-\alpha_{k+1} - \ldots - \alpha_{2k-1}} . \tag{6.73}$$

We notice that Φ has no component along α_k^*.

Following the algorithm outlined in Section 6.4, the superpotential deformation splits into two distinct contributions, each associated with a simple summand of the Levi subalgebra:

$$\begin{aligned} \delta W =& \kappa \left(\Phi \left(\tfrac{1}{k-1} \sum_{m=1}^{k-1} \phi_m \right) , \mu_L \right) + \kappa \left(\Phi \left(\tfrac{1}{k-1} \sum_{m=k+1}^{2k-1} \phi_m \right) , \mu_R \right) \\ =& \sum_{m=1}^{k-1} w_{-\alpha_m} + \left(\tfrac{1}{k-1} \sum_{m=1}^{k-1} \phi_m \right) w_{+\alpha_1 + \ldots + \alpha_{k-1}} + \\ &+ \sum_{m=k+1}^{2k-1} w_{-\alpha_m} - \left(\tfrac{1}{k-1} \sum_{m=k+1}^{2k-1} \phi_m \right) w_{+\alpha_{k+1} + \ldots + \alpha_{2k-1}} \end{aligned} \tag{6.74}$$

We see that each block of Φ produces a deformation like in Building Block II, see (6.31). It is then easy to obtain the effective potential by applying the ungauging/gauging procedure of [37] and using Building Block II in Section 6.2.1. We obtain a quiver with two nodes (that originally

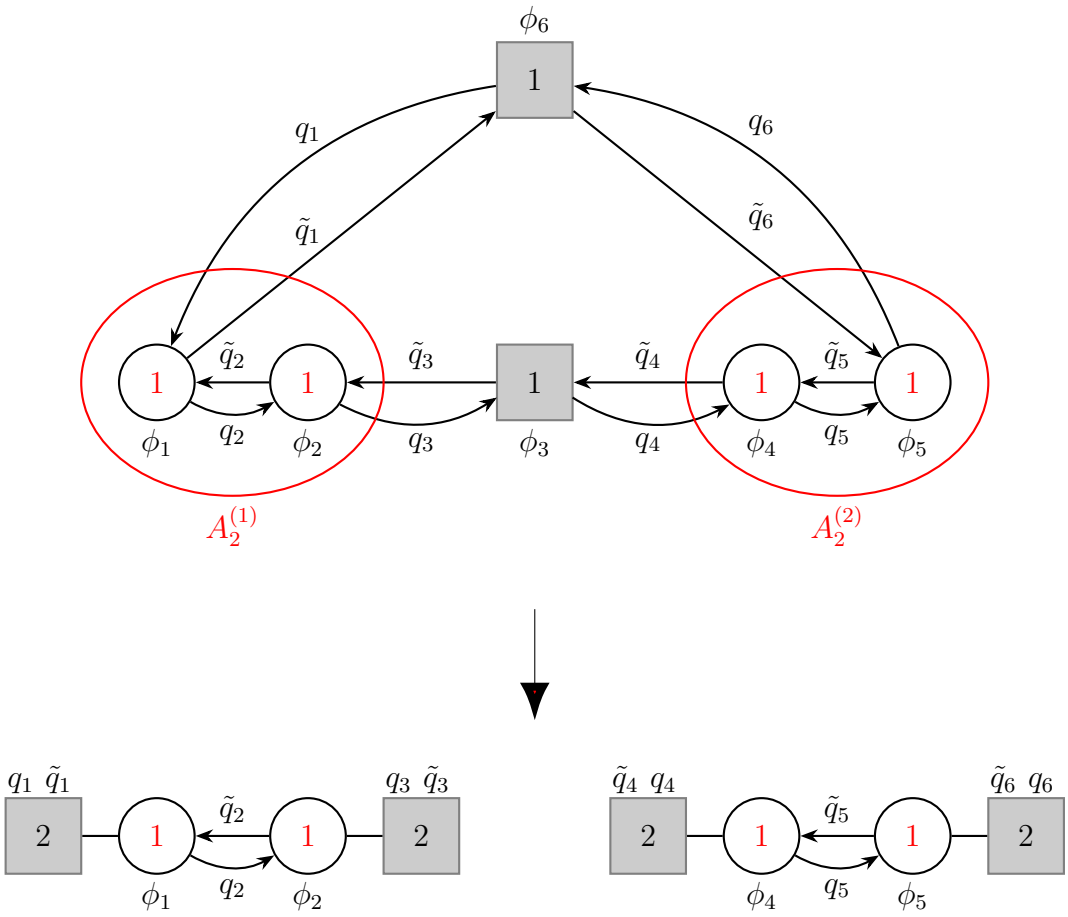

Figure 6.8: Example with k=3. Ungauging of the two Levi blocks.

corresponded to the root α_k and the extended node) depicted in Fig. 6.9 and superpotential

$$\begin{aligned} W_{\text{eff}} =& X_L \left(Y_L Z_L + \tfrac{1}{k-1} \sum_{m=1}^{k-1} \phi_m - T_1 T_2 ... T_k \right) \\ &+ X_R \left(Y_R Z_R - \tfrac{1}{k-1} \sum_{m=k+1}^{2k-1} \phi_m - T_{k+1} T_{k+2} ... T_{2k} \right) \\ &+ \sum_{m=1}^{2k} \phi_m (T_m - T_{m+1}) \,, \end{aligned} \tag{6.75}$$

where we have also recoupled the fields ϕ_k and ϕ_{2k} ($T_{2k+1} \equiv T_1$).

Looking at the superpotential (6.75), we notice several mass terms. In particular the F-terms

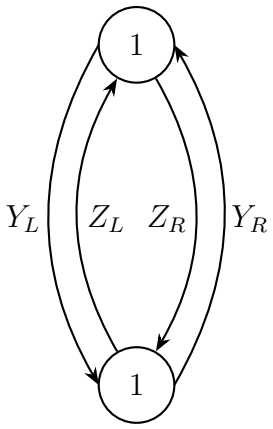

Figure 6.9: Quiver for effective .

for ϕ_i's imply the following relations

$$\begin{cases} T_m = T_{m+1} - \frac{1}{k-1} X_L \\ T_{k+m} = T_{k+m+1} + \frac{1}{k-1} X_R \\ T_{k+1} = T_k \\ T_1 = T_{2k} \end{cases} \rightarrow \begin{cases} T_m = T_k - \frac{k-m}{k-1} X_L & m = 1, ..., k-1 \\ T_{k+m} = T_{2k} + \frac{k-m}{k-1} X_R & m = 1, ..., k-1 \\ T_{2k} + X_R = T_k \\ T_k - X_L = T_{2k} \end{cases} \tag{6.76}$$

that can be solved as

$$\begin{aligned} T_{k-j} &= \tfrac{k-j-1}{k-1} T_k + \tfrac{j}{k-1} T_{2k} \qquad j = 1, ..., k-1 \\ T_{k+j+1} &= \tfrac{k-j-1}{k-1} T_k + \tfrac{j}{k-1} T_{2k} \qquad j = 0, ..., k-2 \\ X_L &= X_R = T_k - T_{2k} \end{aligned} \tag{6.77}$$

Integrating out the $4k$ massive fields $X_L, X_R, T_1, ..., T_{k-1}, T_{k+1}, ..., T_{2k-1}, \phi_1, ..., \phi_{2k}$, we obtain

$$\begin{aligned} W_{\text{eff}} &= (T_k - T_{2k}) \left(Y_L Z_L + Y_R Z_R - 2 \left(\frac{1}{k-1} \right)^k \prod_{j=0}^{k-1} [j\, T_k + (k-j-1) T_{2k}] \right) \\ &= (T_k - T_{2k}) \left(Y_L Z_L + Y_R Z_R - Q_k(T_k, T_{2k}) \right) \end{aligned} \tag{6.78}$$

where $Q_k(T, T) = 2T^k$.

We are now ready to compute the classical moduli space. The F-term equations are

$$\begin{array}{lll} \partial_{T_k} W_{\text{eff}} & : & Y_L Z_L + Y_R Z_R - Q_k(T_k, T_{2k}) - (T_k - T_{2k})\partial_{T_k} Q_k(T_k, T_{2k}) = 0 \\ \partial_{T_{2k}} W_{\text{eff}} & : & Y_L Z_L + Y_R Z_R - Q_k(T_k, T_{2k}) + (T_k - T_{2k})\partial_{T_{2k}} Q_k(T_k, T_{2k}) = 0 \\ \partial_{Y_i} W_{\text{eff}} & : & Z_i\,(T_k - T_{2k}) = 0 \\ \partial_{Z_i} W_{\text{eff}} & : & Y_i\,(T_k - T_{2k}) = 0 \end{array} \tag{6.79}$$

These equations imply $T_k = T_{2k} \equiv T$ and [13]

$$Y_L Z_L + Y_R Z_R - 2T^k = 0\,. \tag{6.80}$$

Let us write down the hypersurface equation. The gauge invariants are

$$A_1 \equiv Y_L Z_L\,, \qquad A_2 \equiv Y_R Z_R\,, \qquad B_1 \equiv Y_L Z_R\,, \qquad B_2 \equiv Y_R Z_L\,, \tag{6.81}$$

with relation $B_1 B_2 = A_1 A_2$. Using (6.80), one obtains

$$B_1 B_2 = A_1(-A_1 + 2T^k) \tag{6.82}$$

By redefining the variables as $B_1 = u$, $B_2 = v$, $T = z$, $A_1 = -w + z^k$ one obtains the defining equation (6.69) of the kth Reid's Pagoda

If we consider the F-term equations for the fields T_i's and X_L, X_R implied by (6.75), we see that on the vacuum the fields ϕ_i's satisfy

$$\phi_k = \phi_{2k} = \tfrac{1}{k-1}\sum_{m=1}^{k-1}\phi_m = \tfrac{1}{k-1}\sum_{m=k+1}^{2k-1}\phi_m = w\,. \tag{6.83}$$

We can then correctly conclude that in a generic point of the moduli space, the branes recombine into a normal brane; moreover, their location in the w-plane is given by the vev for the corresponding fields ϕ_i.

We have derived the quiver and superpotential for a D-brane probing a Reid's Pagoda threefold singularity by interpreting the threefold equation either as a non-monodromic family of deformed

[13] The last two equations seems to allow a branch with $Z_i = Y_i = 0$; however, the first two homogeneous independent equations in T_k, T_{2k} would give $T_k = T_{2k} = 0$.

A_1 singularities or as a monodromic family of deformed A_{2k-1} singularities. In both cases, the resulting quiver is the same. Although the corresponding superpotentials take different forms, they generate the same ideal of F-term equations.

6.6 Simple flops of length 2

In this section we consider the effective theory on the worldvolume of a D2-brane probing threefolds which admit a simple flop of length 2. The singularity has an exceptional locus given by a single $\mathbb{CP}^1$, analogous to the conifold, but—unlike the conifold—it does *not* admit a toric description. A key distinction with the conifold is the so-called length invariant ℓ, which (for simple threefold flops) measures the multiplicity of the exceptional $\mathbb{CP}^1$ in the contraction.[14] For the conifold $\ell = 1$, while in the present example we have $\ell = 2$.

6.6.1 The geometry and the Higgs field

The threefold flops of length 2 are one-parameter D_4 families, and hence belong to the class of threefolds we are considering in this paper. They are described by the colored Dynkin diagram in Figure 6.10. The associated Levi subalgebra is

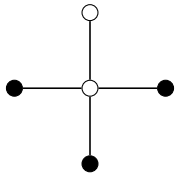

Figure 6.10: Length 2 flop from the family of deformed D_4 singularities. In this construction length 2 flops are three-dimensional cuts in the family of deformed D_4 surfaces with small irreducible resolution.

$$\mathcal{L} = A_1^{(\alpha_1)} \oplus A_1^{(\alpha_2)} \oplus A_1^{(\alpha_3)} \oplus \langle \alpha_4^* \rangle \tag{6.84}$$

The Higgs field is [19, 56]

$$\Phi = e_{\alpha_1} + \varrho_1 e_{-\alpha_1} + e_{\alpha_2} + \varrho_2 e_{-\alpha_2} + e_{\alpha_3} + \varrho_3 e_{-\alpha_3} + \varrho_4 \alpha_4^* \,, \tag{6.85}$$

[14] More precisely, if the local blowdown $\pi : X \to Y$ contracts the $\mathbb{CP}^1$, then $\pi_*(\mathcal{O}_{\rm pt}) \cong \mathcal{O}_{\mathbb{CP}^1}^{\oplus \ell}$.

where ϱ_i are the invariant coordinates of the Levi subalgebra. The threefold with a flop of length 2 is obtained by the choice of a base change $\varrho_i = \varrho_i(w)$, that makes the partial invariant ϱ_i depend on the coordinate w.

Written in matrix form, the Higgs field is [19, 25]

$$\Phi(w) = \left(\begin{array}{cccc|cccc} \varrho_4 & 1 & 0 & 0 & 0 & 0 & 0 & 0 \\ \varrho_1 & \varrho_4 & 0 & 0 & 0 & 0 & 0 & 0 \\ 0 & 0 & 0 & 1 & 0 & 0 & 0 & 1 \\ 0 & 0 & \varrho_3 & 0 & 0 & 0 & -1 & 0 \\ \hline 0 & 0 & 0 & 0 & -\varrho_4 & -\varrho_1 & 0 & 0 \\ 0 & 0 & 0 & 0 & -1 & -\varrho_4 & 0 & 0 \\ 0 & 0 & 0 & -\varrho_2 & 0 & 0 & 0 & -\varrho_3 \\ 0 & 0 & \varrho_2 & 0 & 0 & 0 & -1 & 0 \end{array}\right) . \tag{6.86}$$

We now specialize to a class of threefold flops of length two that were studied in [19]. and that is obtained by the following base change [19]:

$$\varrho_1(w) = c_1 w, \quad \varrho_2(w) = c_2 w, \quad \varrho_3(w) = c_3 w, \quad \varrho_4(w) = c_4 w \, . \tag{6.87}$$

The defining equation can be obtained by plugging (6.85) and (6.87) into (6.35). When we will need a reference example in the family, we will take $c_1 = 4$, $c_2 = c_3 = 1$ and $c_4 = 2$; in this case, the defining equation takes the following form:

$$x^2 + z\, y^2 - (z + 4w)\left(16 z\, w^2 + (z + 4w - 4w^2)^2\right) = 0 \, . \tag{6.88}$$

By construction it is a one-parameter family of deformed D_4 singularities. There are four point-like singularities: at the origin, where the fiber has a full D_4 singularity, and other three points, where the fiber has an A_1 singularity.

6.6.2 Probing the threefold by a D2-brane

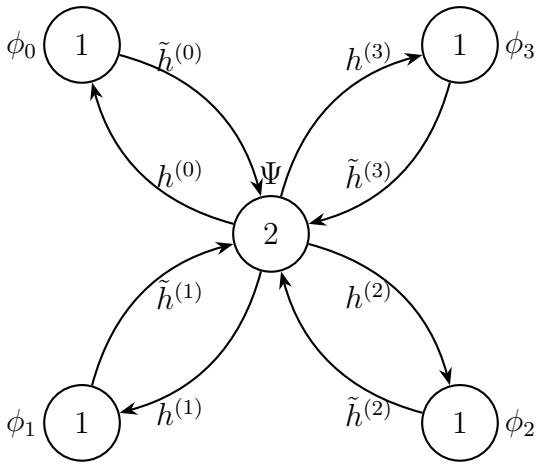

Figure 6.11: D_4 quiver gauge theory.

Let us begin from the superpotential of the D_4 quiver:

$$W = \sum_{i=0}^{3} \mathrm{Tr}\left[\Psi h^{(i)} \tilde{h}^{(i)}\right] - \sum_{i=0}^{3} \phi_i \tilde{h}^{(i)} h^{(i)}, \tag{6.89}$$

where $(h^{(i)}, \tilde{h}^{(i)})$ are bifundamental hypers coupled to the vector multiplets associated to the nodes in 6.11. Ψ and the ϕ_i's are the adjoint chirals of the vector multiplets.

Following the algorithm outlined in Section 6.4, the superpotential deformation generated by the $\Phi(w)$ in (6.85) splits into five distinct contributions: three are associated with the three simple summands of the Levi subalgebra, the other two are due to the diagonal Φ-component:

$$\delta W = \delta W_1 + \delta W_2 + \delta W_3 + \delta W_4 + \delta W_0 \,, \tag{6.90}$$

with

$$\begin{aligned}
\delta W_1 =& \kappa\left(\Phi\left(\phi_1\right)\ ,\ \mu_1\right) = w_{-\alpha_1} + \varrho_1(\phi_1) w_{\alpha_1}\ ,\\
\delta W_2 =& \kappa\left(\Phi\left(\phi_2\right)\ ,\ \mu_2\right) = w_{-\alpha_2} + \varrho_2(\phi_2) w_{\alpha_2}\ ,\\
\delta W_3 =& \kappa\left(\Phi\left(\phi_3\right)\ ,\ \mu_3\right) = w_{-\alpha_3} + \varrho_3(\phi_3) w_{\alpha_3}\ ,\\
\delta W_4 =& \tfrac{1}{2}\mathrm{Tr}\left[\Psi\kappa\left(h_{\alpha_4}, \Phi(\Psi)\right)\right] = \tfrac{1}{2}\mathrm{Tr}\left[\Psi\varrho_4(\Psi)\right]\ ,\\
\delta W_0 =& \frac{\phi_0}{2}\kappa\left(h_{\alpha_0}, \Phi(\phi_0)\right) = -\phi_0\varrho_4(\phi_0)\ .
\end{aligned} \tag{6.91}$$

We now derive the effective superpotential. We ungauge the central node of the quiver. After doing this, each colored node supports an abelian theory with monopole superpotential

$$W_i = -\phi_i(h_1^{(i)}\tilde{h}_1^{(i)} + h_2^{(i)}\tilde{h}_2^{(i)}) + w_{-\alpha_i} + \varrho_i(\phi_i) w_{\alpha_i} \tag{6.92}$$

Following the computation done in Section 6.2.1 (Building Block I), the $U(1)$ disappears in the effective theory and we obtain an effective local superpotential

$$\begin{aligned}
W_{\text{eff},i} =&\ X_i(Y_i\, Z_i + \varrho_i(\phi_i) - T_1^{(i)}T_2^{(i)}) - \phi_i(T_1^{(i)} + T_2^{(i)})\\
=&\ -X_i\left(\det\mathfrak{M}_i - \varrho_i(\phi_i)\right) - \phi_i\mathrm{Tr}\mathfrak{M}_i
\end{aligned} \tag{6.93}$$

with $\mathfrak{M}_i \equiv \begin{pmatrix} T_1^{(i)} & Y_i \\ Z_i & T_2^{(i)} \end{pmatrix}$.

We now re-gauge the central node symmetry and we obtain the quiver in Figure 6.12 with superpotential

$$\begin{aligned}
W_{\text{eff}} =& \sum_{i=1}^{3}\mathrm{Tr}\left[\Psi\left(\mathfrak{M}_i + h^{(0)}\tilde{h}^{(0)}\right)\right] - \phi_0\,\tilde{h}^{(0)}h^{(0)}\\
&- \sum_{i=1}^{3}\left[X_i\left(\det\mathfrak{M}_i - \varrho_i(\phi_i)\right) + \phi_i\mathrm{Tr}\mathfrak{M}_i\right] + \tfrac{1}{2}\mathrm{Tr}\left[\Psi\varrho_4(\Psi)\right] - \phi_0\varrho_4(\phi_0)
\end{aligned} \tag{6.94}$$

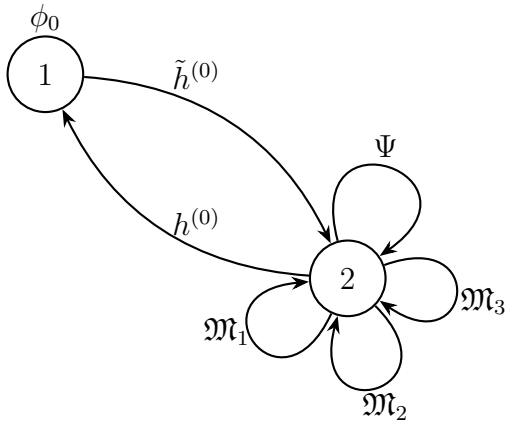

Figure 6.12: Quiver of the effective $\mathcal{N}=2$ theory that emerges in the IR, when monopole deformations of 6.91 are turned on. Singlet chirals (ϕ_i, X_i) are not represented in the quiver but they couple to the theory through the superpotential.

In the specific example (6.87), this superpotential becomes

$$\begin{aligned} W_{\text{eff}} = &\sum_{i=1}^{3} \text{Tr}\left[\Psi\left(\mathfrak{M}_i + h^{(0)}\tilde{h}^{(0)}\right)\right] - \phi_0\,\tilde{h}^{(0)}h^{(0)} \\ &- \sum_{i=1}^{3}\left[X_i\left(\det\mathfrak{M}_i - c_i\phi_i\right) + \phi_i \text{Tr}\mathfrak{M}_i\right] + \tfrac{c_4}{2}\text{Tr}\Psi^2 - c_4\phi_0^2\,. \end{aligned} \tag{6.95}$$

We can integrate out the massive fields ϕ_i and X_i $(i=1,2,3)$, by using their F-term equations:

$$\begin{aligned} \partial_{X_j} W_{\text{eff}} = 0: &\qquad \phi_j = -\tfrac{1}{c_j}\,\det\mathfrak{M}_j \\ \partial_{\phi_j} W_{\text{eff}} = 0: &\qquad X_j = \tfrac{1}{c_j}\,\text{Tr}\mathfrak{M}_j \end{aligned} \tag{6.96}$$

We obtain the effective superpotential:

$$\begin{aligned} W_{\text{eff}} = &\sum_{i=1}^{3} \text{Tr}\left[\Psi\left(\mathfrak{M}_i + h^{(0)}\tilde{h}^{(0)}\right)\right] - \phi_0\,\tilde{h}^{(0)}h^{(0)} \\ &+ \sum_{i=1}^{3}\left[\tfrac{1}{c_i}\text{Tr}\mathfrak{M}_i\,\det\mathfrak{M}_i\right] + \tfrac{c_4}{2}\text{Tr}\Psi^2 - c_4\phi_0^2\,, \end{aligned} \tag{6.97}$$

whose fields are represented in the effective quiver in Figure 6.12. We claim that these are the

quiver and the superpotential of a D2(D3)-brane probing the threefold we are analysing in this section.

We are now ready to work out the moduli space. For convenience, let us first write

$$\mathfrak{M}_i = t_i \mathbb{1} + \tilde{\mathfrak{M}}_i \text{ and } \Psi = \phi_4 \mathbb{1} + \tilde{\Psi} \qquad \text{with} \quad \mathrm{Tr}\tilde{\mathfrak{M}}_i = \mathrm{Tr}\tilde{\Psi} = 0\,. \tag{6.98}$$

The relations that one obtains from the superpotential (6.97) are:

$$\begin{aligned}
&\partial_\Psi W_{\text{eff}} = 0 \quad : \quad \sum_{i=1}^{3} \mathfrak{M}_i + h^{(0)}\tilde{h}^{(0)} + c_4 \Psi = 0 \\
&\partial_{\tilde{\mathfrak{M}}_j} W_{\text{eff}} = 0 \quad : \quad \tilde{\Psi} - \tfrac{2t_j}{c_j}\tilde{\mathfrak{M}}_j = 0 \\
&\partial_{t_j} W_{\text{eff}} = 0 \quad : \quad \phi_4 + \tfrac{1}{c_j}\left(3t_i^2 - \tfrac{1}{2}\mathrm{Tr}\tilde{\mathfrak{M}}_j^2\right) = 0 \\
&\partial_{\phi_0} W_{\text{eff}} = 0 \quad : \quad \tilde{h}^{(0)} h^{(0)} + 2c_4\phi_0 \\
&\partial_{\tilde{h}^{(0)}} W_{\text{eff}} = 0 \quad : \quad (\Psi - \phi_0 \mathbb{1})\, h^{(0)} \\
&\partial_{h^{(0)}} W_{\text{eff}} = 0 \quad : \quad \tilde{h}^{(0)}\,(\Psi - \phi_0 \mathbb{1})
\end{aligned} \tag{6.99}$$

Here we have also used the fact that $\det \tilde{\mathfrak{M}}_i = -\frac{1}{2}\mathrm{Tr}\tilde{\mathfrak{M}}_i^2$.

There are no solutions to these equations, unless[15] $\tilde{\Psi} = 0$ and $t_i = 0$ $(i = 1, 2, 3)$. We are then left with

$$\sum_{i=1}^{3} \tilde{\mathfrak{M}}_i + h^{(0)}\tilde{h}^{(0)} + c_4\phi_4 \mathbb{1} = 0\,, \qquad \phi_0 = \phi_4 = -\frac{\det \tilde{\mathfrak{M}}_j}{c_j}\,. \tag{6.100}$$

In [56] (in Section 5.2.3), the authors considered a set of relations formally identical to these. Following their steps, one readily finds that the moduli space of the effective theory coincides with the threefold given by equation (6.88). Let us briefly sketch the derivation below.

The moduli space si parametrized by ϕ_4 and the gauge invariants build up from $h^{(0)}, \tilde{h}^{(0)}$ and

[15] If all t_i's are non-zero, the $\tilde{\mathfrak{M}}_i$'s are all proportional to $\tilde{\Psi}$ with proportionality factor depending on t_i and c_i; hence also $\mathrm{Tr}\tilde{\mathfrak{M}}_i^2$ depends on t_i and c_i. For generic c_i's one cannot solve both the third and the first relations. The same is true if some t_i is non-zero. Hence, all of them must vanish, and then also $\tilde{\Psi}$ must be equal to zero.

the traceless matrices $\tilde{\mathfrak{M}}_i$. One chooses as a basis of gauge invariants

$$A_i \equiv \text{Tr}\left[\mathfrak{M}_0\tilde{\mathfrak{M}}_i\right], \qquad B \equiv \text{Tr}\left[\mathfrak{M}_0\tilde{\mathfrak{M}}_2\tilde{\mathfrak{M}}_3\right], \tag{6.101}$$

where we have defined $\mathfrak{M}_0 \equiv h^{(0)}\tilde{h}^{(0)}$.

The invariants $A_1,\ A_2,\ A_3$ and B are not independent, but $A_1,\ A_2,\ A_3$ satisfy the linear reation

$$\sum_i A_i = -2c_4^2\phi_4^2 \tag{6.102}$$

and they are also related to B by (see Appendix A in [56])

$$\begin{aligned} A_1A_2A_3 = &- B^2 + 2Bc_4\phi_4(A_1 + \phi_4(c_4^2\phi_4 + c_1 - c_2 - c_3)) \\ &- \phi_4(c_2A_3 + c_3A_2)(A_1 + 2c_4^2\phi_4^2) - \phi_4A_2A_3(c_4^2\phi_4 + c_1) - 4c_4^2c_2c_3\phi_4^4 \,. \end{aligned} \tag{6.103}$$

From now on, we set $c_1 = 4$, $c_2 = c_3 = 1$ and $c_4 = 2$ as above. We write A_1 in terms of A_2 and A_3 by using the first relation, and make the following redefinition of the gauge invariant coordinates:

$$A_2 = \tfrac{1}{2}\left(y + z - 4w(w-1)\right), \tag{6.104}$$

$$A_3 = \tfrac{1}{2}\left(-y + z - 4w(w-1)\right), \tag{6.105}$$

$$B = -\tfrac{1}{2}x + 2w(z + 2w), \tag{6.106}$$

$$\phi_4 = w \,. \tag{6.107}$$

Plugging these redefinitions into equation (6.103), with the chosen values of the c_i, we obtain the defining equation (6.88) of the threefold under consideration.

6.7 D2-brane probing a non resolvable cDV singularity: the (A_2, D_4) three-fold

In this section we will apply our techniques to determine the effective theory of a D2-brane probing threefolds with an isolated singularity that do not admit a crepant resolutions.

6.7.1 Geometry and Higgs field Φ

Let us consider the one parameter D_4 family, also known as[16] (A_2, D_4), given by the equation

$$x^2 + z\,y^2 + z^3 + w^3 = 0 \tag{6.108}$$

This threefold was studied in [26, 27] with the techniques of [19, 24, 25], so we have the corresponding Higgs field Φ. As explained in [26], Φ belongs to a maximal subalgebra of the Levi subalgebra. In this case the Levi subalgebra is the whole D_4 Lie algebra, consistently with the fact that one cannot blow up any two-sphere. If Φ were a generic element in $\mathcal{L} = D_4$, the threefold would be smooth. Instead in this case,

$$\Phi \in \mathcal{M} = A_1^{(\alpha_1)} \oplus A_1^{(\alpha_2)} \oplus A_1^{(\alpha_3)} \oplus A_1^{(\alpha_0)} \subset \mathcal{L} = D_4\,, \tag{6.109}$$

where α_0 corresponds to the extra node in the extended Dynkin diagram (see Figure 6.13).

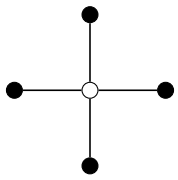

Figure 6.13: Non-resolvable singularity. The coloring of the diagram signals the obstruction to the resolution of all the linearly independent 2-cycles.

This choice of $\mathcal{M}$ ensures that at $w = 0$, the singularity is isolated but *non-resolvable*.

The Higgs field in (6.109) can be written as

$$\Phi = e_{\alpha_1} + \varrho_1 e_{-\alpha_1} + e_{\alpha_2} + \varrho_2 e_{-\alpha_2} + e_{\alpha_3} + \varrho_3 e_{-\alpha_3} + e_{\alpha_0} + \varrho_0 e_{-\alpha_0}\,, \tag{6.110}$$

where ϱ_i are the invariant coordinates of the Levi subalgebra and α_0 is minus the highest root.

[16] Type IIB on this singularity engineers Argyres-Douglas theory of type (A_2, D_4).

Written in matrix form, the Higgs field is [27]

$$\Phi(w) = \left(\begin{array}{cccc|cccc} 0 & 1 & 0 & 0 & 0 & \varrho_0 & 0 & 0 \\ \varrho_1 & 0 & 0 & 0 & -\varrho_0 & 0 & 0 & 0 \\ 0 & 0 & 0 & 1 & 0 & 0 & 0 & 1 \\ 0 & 0 & \varrho_3 & 0 & 0 & 0 & -1 & 0 \\ \hline 0 & -1 & 0 & 0 & 0 & -\varrho_1 & 0 & 0 \\ 1 & 0 & 0 & 0 & -1 & 0 & 0 & 0 \\ 0 & 0 & 0 & -\varrho_2 & 0 & 0 & 0 & -\varrho_3 \\ 0 & 0 & \varrho_2 & 0 & 0 & 0 & -1 & 0 \end{array}\right) . \tag{6.111}$$

The particular threefold (6.108) is obtained by the base change

$$\varrho_i = c_i w \quad (i = 0, 1, 2, 3) \qquad \text{with} \qquad c_1 = c_2 = c_3 = \tfrac{1}{4} , \;\; c_0 = -\tfrac{3}{4} . \tag{6.112}$$

6.7.2 D2-brane probe theory

The Higgs field $\Phi(w)$ in (6.111), which encodes the background geometry, induces a superpotential deformation on the worldvolume theory of the probe D2-brane. This deformation decomposes into four distinct contributions, each associated with a simple summand of the maximal subalgebra $\mathcal{M} \subset D_4$:

$$\delta W = \delta W_1 + \delta W_2 + \delta W_3 + \delta W_4 \tag{6.113}$$

with

$$\begin{aligned} \delta W_1 &= \kappa\left(\Phi\left(\phi_1\right) , \mu_1\right) = w_{-\alpha_1} + \varrho_1(\phi_1) w_{\alpha_1} , \\ \delta W_2 &= \kappa\left(\Phi\left(\phi_2\right) , \mu_2\right) = w_{-\alpha_2} + \varrho_2(\phi_2) w_{\alpha_2} , \\ \delta W_3 &= \kappa\left(\Phi\left(\phi_3\right) , \mu_3\right) = w_{-\alpha_3} + \varrho_3(\phi_3) w_{\alpha_3} , \\ \delta W_0 &= \kappa\left(\Phi\left(\phi_0\right) , \mu_0\right) = w_{-\alpha_0} + \varrho_0(\phi_0) w_{\alpha_0} . \end{aligned} \tag{6.114}$$

with $\varrho_i(w)$ given in (6.112).

We now derive the effective superpotential. We ungauge the central node of the quiver: afterwards, each colored node supports an abelian theory with monopole superpotential

$$W_i = -\phi_i(h_1^{(i)}\tilde{h}_1^{(i)} + h_2^{(i)}\tilde{h}_2^{(i)}) + w_{-\alpha_i} + c_i\phi_i w_{\alpha_i} \qquad i = 0, 1, 2, 3 . \tag{6.115}$$

Following the computation done in Section 6.2.1 (Building Block I), the $U(1)$ disappears and we obtain an effective local superpotential

$$\begin{aligned} W_{\text{eff},i} = &\quad X_i(Y_i\, Z_i + c_i\phi_i - T_1^{(i)}T_2^{(i)}) - \phi_i(T_1^{(i)} + T_2^{(i)}) \\ = &\quad -X_i\left(\det \mathfrak{M}_i - \varrho_i(\phi_i)\right) - \phi_i \text{Tr}\mathfrak{M}_i \end{aligned} \tag{6.116}$$

with $\mathfrak{M}_i \equiv \begin{pmatrix} T_1^{(i)} & Y_i \\ Z_i & T_2^{(i)} \end{pmatrix}$.

We now re-gauge the central node symmetry and we obtain the quiver in Figure 6.14 with superpotential

$$W_{\text{eff}} = \text{Tr}\left[\Psi \sum_{i=0}^{3} \mathfrak{M}_i\right] + \sum_{i=0}^{3} \left(-X_i\left(\det \mathfrak{M}_i - c_i\phi_i\right) + (\phi_4 - \phi_i)\text{Tr}\mathfrak{M}_i\right) \ . \tag{6.117}$$

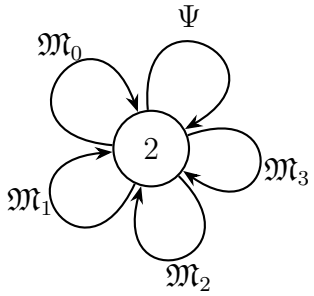

Figure 6.14: Effective D_4 quiver describing the fields coupling to the residual gauge symmetry.

Analogously to the flop of length two case, we can integrate out ϕ_i and X_i, by using (6.96), with now $i = 0, 1, 2, 3$. They are determined as We obtain

$$\begin{aligned} W_{\text{eff}} = &\text{Tr}\left[\Psi \sum_{i=0}^{3} \mathfrak{M}_i\right] + \sum_{i=0}^{3} \left[\tfrac{1}{c_i}\text{Tr}\mathfrak{M}_i \ \det \mathfrak{M}_i\right] \\ = &\text{Tr}\left[\tilde{\Psi} \sum_{i=0}^{3} \tilde{\mathfrak{M}}_i\right] + 2\phi_4 \sum_{i=0}^{3} t_i + \sum_{i=0}^{3} \tfrac{t_i}{c_i}\left(t_i^2 - \tfrac{1}{2}\text{Tr}\tilde{\mathfrak{M}}_i^2\right) \ , \end{aligned} \tag{6.118}$$

where in the second line we have used (6.98).

The relations that one obtains from the superpotential (6.118) are very similar to the simple

flop of legth two cases studied above:

$$\begin{aligned}
\partial_{\tilde{\Psi}} W_{\text{eff}} = 0 \quad &: \quad \sum_{i=0}^{3} \tilde{\mathfrak{M}}_i = 0 \\
\partial_{\phi_4} W_{\text{eff}} = 0 \quad &: \quad \sum_{i=0}^{3} t_i = 0 \\
\partial_{\tilde{\mathfrak{M}}_j} W_{\text{eff}} = 0 \quad &: \quad \tilde{\Psi} - \tfrac{2t_j}{c_j} \tilde{\mathfrak{M}}_j = 0 \\
\partial_{t_j} W_{\text{eff}} = 0 \quad &: \quad \phi_4 + \tfrac{3t_i^2}{c_j} - \tfrac{1}{2c_j} \text{Tr} \tilde{\mathfrak{M}}_j^2 = 0
\end{aligned} \tag{6.119}$$

Let us explore the moduli space. The relations (6.119) imply $\tilde{\Psi} = 0$ and $t_i = 0$ $(i = 0, ..., 3)$.[17] We are then left with the space parametrized by the four traceless matrices $\mathfrak{M}_i$ and the singlet ϕ_4, subject to the relations

$$\sum_{i=0}^{3} \tilde{\mathfrak{M}}_i = 0 \qquad \text{and} \qquad \text{Tr} \tilde{\mathfrak{M}}_j^2 = 2c_i \phi_4 \, . \tag{6.120}$$

Out of four traceless 2×2 matrices we can construct the quadratic and the cubic invariants

$$q_{ij} = \text{Tr} \left[\tilde{\mathfrak{M}}_i \tilde{\mathfrak{M}}_j \right] \qquad \text{and} \qquad c_{ijk} = \text{Tr} \left[\tilde{\mathfrak{M}}_i \tilde{\mathfrak{M}}_j \tilde{\mathfrak{M}}_k \right] \, , \tag{6.121}$$

that are related by[18]

$$c_{ijk}^2 = -\frac{1}{2} \det \begin{pmatrix} q_{ii} & q_{ij} & q_{ik} \\ q_{ij} & q_{jj} & q_{jk} \\ q_{ik} & q_{jk} & q_{kk} \end{pmatrix} \tag{6.122}$$

The quadratic invariants satisfy $q_{ii} = 2c_i \phi_4$ and $\sum_{j=0}^{3} q_{ij} = 0 \; \forall i$. This reduces the number of independent quadratic invariants to two. Let us take q_{12} and q_{13} as the independent ones. The cubic invariants are all proportional to each others.[19] Let us take c_{123} as the independent one.

[17] If $\tilde{\Psi}$ and/or some of the t_i's are non-zero, it easy to check that the equations (6.119) have no solutions (except for non generic values of c_i, that do not include (6.112)).

[18] By expanding the traceless matrices $\tilde{\mathfrak{M}}_i$'s in terms of the Pauli matrices, we can associate three-dimensional vectors v_i to them. We then have $q_{ij} = 2v_i \cdot v_j$ and $c_{ijk} = 2iv_i \cdot (v_j \times v_k)$.

[19] Let us see it in terms of the vectors v_i's. Since $\sum_i v_i = 0$, we have $v_{i_1} \cdot (v_{i_2} \times v_{i_4}) = v_{i_1} \cdot (v_{i_2} \times (-v_{i_1} - v_{i_2} - v_{i_3})) = v_{i_1} \cdot (v_{i_2} \times (-v_{i_3}))$. Hence $c_{i_1 i_2 i_4} = -c_{i_1 i_2 i_3} =$ for any choice of the ordered quadruple (i_1, i_2, i_3, i_4).

We can then are parametrize the moduli space by $\phi_4, q_{12}, q_{13}, c_{123}$ that satisfy the relation

$$c_{123}^2 = -\frac{1}{2}\det\begin{pmatrix} \frac{\phi_4}{2} & q_{12} & q_{13} \\ q_{12} & \frac{\phi_4}{2} & -q_{12}-q_{13}-\frac{3}{2}\phi_4 \\ q_{13} & -q_{12}-q_{13}-\frac{3}{2}\phi_4 & \frac{\phi_4}{2} \end{pmatrix} \tag{6.123}$$

where we have used that (with the choice (6.112)) $q_{11} = q_{22} = q_{33} = \frac{\phi_4}{2}$ and $q_{23} = -q_{12} - q_{13} - \frac{3}{2}\phi_4$.[20]

If we now redefine the coordinates, according to

$$c_{123} = \tfrac{1}{2}x\,, \qquad q_{12} = \tfrac{i}{2}y + \tfrac{1}{2}z - \tfrac{1}{2}w\,, \qquad q_{13} = -\tfrac{i}{2}y + \tfrac{1}{2}z - \tfrac{1}{2}w\,, \qquad \phi_4 = w\,, \tag{6.124}$$

then the equation (6.123) becomes (6.108), confirming once again that the moduli space coincides with the probed threefold.[21]

Summary We have developed a systematic method to derive the 3d $\mathcal{N} = 2$ worldvolume theories of D2-branes probing compound Du Val (cDV) threefold singularities. Our approach extends beyond toric geometries, where conventional techniques fail, by using the geometric data encoded in the Higgs field $\Phi(w)$ as the primary input. Our main results are:

- We established a general prescription relating the superpotential deformation to the Higgs field components, applicable to any cDV threefold with known $\Phi(w)$.
- For non-monodromic fibrations, where Φ lies in the Cartan subalgebra, the prescription reduces to simple polynomial deformations, which we verified against known examples (conifold, Reid's pagodas, generalized conifold).
- For monodromic fibrations, where Φ contains step operators, we developed an ungauging/mirror symmetry procedure that systematically reduces the problem to previously solved building blocks.
- We successfully derived the quiver theories for several non-toric examples, including simple flops of length 2 and the non-resolvable (A_2, D_4) threefold, in each case verifying that the

[20] This is obtained by taking the proper linear combination of the four relations $\sum_{j=0}^{3} q_{ij} = 0$.

[21] We finally observe that using (6.120), together with (6.96), one obtains along the moduli space that $\phi_i = \phi_4$, for $i = 0, 1, 2, 3$. This is consistent with the fact that at generic point in the moduli space, the fractional branes have recombined into a single D2-brane probing smooth points.

moduli space reproduces the target geometry.

Systematic treatment of E-type examples presents additional technical challenges. Unlike the ADE cases considered here, E-type colored Dynkin diagrams involve non-abelian colored nodes, which complicates both the identification of the appropriate monopole superpotential deformations and the procedure for integrating out monopole operators through mirror symmetry. Our results provide a concrete dictionary between geometric data (Higgs field, Levi subalgebra, base change, colored nodes) and field theory data (superpotential, quiver structure, coupling constants, monopole terms). This bridges algebraic geometry and supersymmetric gauge theory for an important class of singularities not accessible by other methods.

Chapter 7

5D GEOMETRIC ENGINEERING: SIMPLE FLOPS AND THEIR ORBIFOLDS

Over the past decades, considerable effort has been devoted to the classification of 5d SCFTs, mostly within the paradigm of geometric engineering. The guiding idea has been to identify a minimal set of geometric conditions on Calabi-Yau threefold singularities that ensure the existence of a well-defined interacting fixed point [39–44, 48–51, 91, 144, 145]. For rank-one theories, a remarkably successful picture emerges from Seiberg's analysis [38], in which the classification is closely related to that of del Pezzo surfaces. This correspondence has undergone several refinements and is by now understood to provide a robust description of rank-one 5d SCFTs.

Building on these insights, it was later conjectured that all 5d SCFTs should be classified by Calabi-Yau threefold singularities of canonical type [44]. While this perspective provides a natural extension of the rank-one story, explicit constructions realizing this proposal remain relatively sparse. In practice, most of the well-understood examples arise in toric geometry, where powerful combinatorial tools—most notably the technology of (p, q) five-brane webs—allow for a systematic analysis. Beyond the toric setting, the best understood non-toric examples are given by constructions such as blow-ups of $\mathbb{P}^2$ or Hirzebruch surfaces at multiple points, which still admit a relatively controlled geometric description[41].[1]

[1] The authors of [41] introduce the concept of shrinkable threefold as a necessary and sufficient condition for the geometry to produce a non-trivial SCFT fixed point. Shrinkable threefolds display canonical singularities. However, a clear connection between the notion of shrinkability and the conditions stated in the Yau-Xie conjecture [44] remains unclear.

A key underlying assumption in these classification programs is that the local structure of the singularity is sufficient to determine the physics of the corresponding 5d theory. In other words, it is typically assumed that global features of the geometry do not play an essential role in defining the fixed point. While this assumption is natural in many of the known constructions, it is not a priori guaranteed in more general, non-toric settings.

In this work, we focus again on compound Du Val (cDV) singularities. In the previous chapters, we have shown that these harbour a special class of K3 fibered threefolds (namely, threefold flops) with a non-trivial monodromy structure. On the one hand, we have related this structure to the group-theoretic derivation of the small resolution of the threefold 4.2.3. On the other hand, we have managed to connect it to an interesting non-perturbative phenomenon occurring on a $D2$-brane probe, that is, the generation of monopole superpotentials that lift the CB of the probe 5.1.2. Now, we want to leverage what we have learnt from the probe to gain a deeper understanding of what happens in five dimensions. So far, we have just briefly commented on the nature of the 5d SCFTs arising from geometric engineering of M-theory on such threefolds (See section 1.4). At first sight, these appear rather mild, as they do not give rise to non-Abelian gauge interactions in five dimensions. However, they exhibit features that are intrinsically non-toric and lead to some physical puzzles. These features call for a clearer understanding within the existing framework: they must either be accommodated within the current classification picture or signal the need for a natural generalization of it.

The simplest and most instructive example is provided by Reid's Pagoda, a geometry that closely resembles the conifold but differs in a crucial global aspect, namely in the way the local patches of the normal bundle to the exceptional $\mathbb{P}^1$ are glued together. As we will see, this seemingly minor modification has significant physical consequences. It provides a concrete setting in which global features of the geometry play a non-trivial role, and offers a window into a class of 5d theories that would seem only partially captured by existing classification schemes.

This work aims to analyze these geometries in detail and to propose a physical interpretation. In particular, we will construct rank N families of 5d theories from orbifolds of Pagoda singularities, extract their BPS quiver, and the main physical data associated with the singularity. We will provide a detailed description of the rank 1 family. Although exhibiting strong similarities with the toric $Loc\mathbb{F}_2$, this case harbours a peculiar matter sector, inherited from its parent, the Pagoda. This matter sector is responsible for a mechanism that is not observed in the toric case. A mechanism that constrains the behavior of the gauge coupling, illustrating how these constructions call for a refinement of the current picture of 5d SCFTs. We provide a physical interpretation

of this phenomenon by viewing these 5d SCFTs as deformations of toric orbifolds (such as local $\mathbb{F}_2$) by a *non-constant flavor background*. By promoting the global flavor symmetry parameters to position-dependent Higgs fields $\Phi(w)$, we show that the geometry now has only an isolated point-like singularity supporting a localized sector of fluctuations. We explain how the exotic Pagoda matter is "trapped" by the geometry and elucidate the observed obstruction of the Kähler moduli. We bolster our claim by supplying a 3d mirror symmetry analysis of D2-brane probes of our geometries, based on the work presented in Chapter 6 (Soon to appear on the archive [37]).

These results open up several new directions for future investigation. Among the most interesting are the analysis of wall-crossing and the stability of BPS states, aimed at determining the BPS spectrum of the theories presented here, and the extension of the procedure developed in this paper to higher-length flops [19], i.e., isolated threefold singularities generalizing Reid's Pagoda. In the latter case, preliminary results suggest that infinite families of higher-rank 5d SCFTs emerge from abelian orbifolds of the Laufer length-two flop.

This chapter is based on original contributions, already submitted for publication to JHEP and accessible at [58]. **Outline.** Section 7.1 reviews the Reid Pagoda, its quiver description, and semistable representations. Section 7.2 Extracts the BPS quiver for a $\mathbb{Z}_2$ orbifold of the Pagoda, that engineers a family of rank one 5d SCFTs. Section 7.3 analyses the resulting moduli spaces and their compact 4-cycles. Section 7.4 derives the central physical result: the freezing of the gauge coupling at infinity. Section 7.5 offers a physical interpretation of the construction in terms of a non-constant flavour background, first from the viewpoint of D2-branes and then directly in 5d. Finally, Section 7.6 extends the construction to more general abelian orbifolds, giving explicit BPS quivers with superpotentials for new 5d theories with rank anywhere from zero to an arbitrary high number. In Appendix D, we expand the discussion on quiver representation theory, resolutions, and stability conditions, connecting GLSM constructions, GIT quotients, and NCCR theory. We discuss in detail the classification of stable representations of the 2-Kronecker quiver, which is instrumental to the derivation of the stable spectrum of the conifold and the pagoda. Finally, we describe the spectrum of semistable representations of Pagoda geometries.

7.1 The Parent Theory: Pagoda Flops

The first ingredient we need is a construction of threefolds that behave very similarly to the conifold, usually described as the equation in $\mathbb{C}^4$

$$X_{\text{conifold}}: \quad uv = z^2 + w^2\,, \tag{7.1}$$

which admits a small resolution $\tilde{X}_{\text{conifold}}$, such that the smooth threefold is the total space of the normal bundle to the flopping curve, i.e.:

$$\tilde{X}_{\text{conifold}} \cong \mathcal{O}(-1) \oplus \mathcal{O}(-1)_{\mathbb{P}^1}\,. \tag{7.2}$$

This resolved space admits a description as the moduli space of the Abelian Klebanov-Witten quiver [88] (see Figure 7.1).

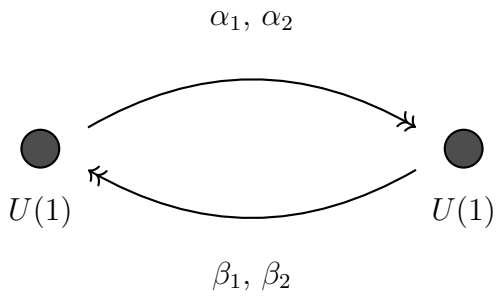

Figure 7.1: Abelian Klebanov-Witten quiver.

For this Abelian case, the superpotential is trivial, and the moduli space is toric. The quiver (with superpotential) can be physically interpreted either as the $d = 4, \mathcal{N} = 1$ theory on a probe D3-brane, or as the supersymmetric quantum mechanics of a probe D0-brane. In this work, we will always choose the D0-brane interpretation, which will be later generalized beyond the abelian case through the notion of *BPS quivers* [87, 146, 147]. Therefore, all arrows appearing in our quivers are to be interpreted as chiral multiplets for $d = 1, \mathcal{N} = 4$ *quiver quantum mechanics*. M-theory on the conifold is believed to give rise to a 5d (trivial) SCFT with a free hypermultiplet, realized by an M2-brane wrapping the exceptional $\mathbb{P}^1$. The only non-vanishing Gopakumar-Vafa invariant is $n_{d=1}^{g=0} = 1$, which matches this expectation.

Our main object of interest is the class of local Calabi-Yau threefolds known as Reid's *Pagodas*

[148], given by

$$X_{\text{k-Pagoda}}: \quad uv = z^2 - w^{2k}\,. \tag{7.3}$$

They are an infinite family indexed by an integer k, with the $k = 1$ case being the conifold. They, too, admit a small resolution that gives rise to a single floppable $\mathbb{P}^1$. Much like the conifold, we can perform a small resolution of this via the following standard procedure: We enhance the ambient space from $\mathbb{C}^4$ to a product space $\mathbb{C}^4 \times \mathbb{P}^1$, and we impose the following system of constraints:

$$\mathcal{R} \cdot \begin{pmatrix} s_1 \\ s_2 \end{pmatrix} = 0 \qquad \subset \mathbb{C}^4_{u,v,z,w} \times \mathbb{P}^1_{[s_1:s_2]}\,, \tag{7.4}$$

whereby

$$\mathcal{R} := \begin{pmatrix} u & z + w^k \\ z - w^k & v \end{pmatrix} \tag{7.5}$$

is a two-by-two matrix whose determinant is the defining equation for the Pagoda hypersurface. Hence, along the hypersurface $\text{rk}(\mathcal{R}) \leq 1$, and the matrix-valued constraint (7.4) fixes a point in $\mathbb{P}^1$. Whenever $\mathcal{R} = 0$ strictly, then (7.4) is trivially satisfied, and a whole $\mathbb{P}^1$ is 'freed up'. A substantial difference with the conifold, though, is the multiplicity of the $\mathbb{P}^1$. Here, the locus where the 2-cycle sits is:

$$u = v = z = 0,\ w^k = 0 \tag{7.6}$$

The last equation is the typical manifestation of a fat point structure. The $\mathbb{P}^1$ should be seen as a superposition of k copies of the same curve, localised at the origin of $\mathbb{C}^4$. Indeed, we will see that any sheaf supported on this curve has a non-reduced moduli space. A way to characterize the nature of the resolved geometry in full glory is to analyze the moduli space of representations of its quiver path algebra. In Figure D.4, we have displayed the representation with $U(1) \times U(1)$ gauge group. This particular representation corresponds to the integral $D0$-brane state, whose moduli space spans the full resolved geometry. As we show in Appendix D.4, this is not the only stable BPS state of the 5d theory. There are other (semi)stable representations which correspond to the fractional $D0$ branes or equivalently $D2$ and anti-$D2$-branes wrapped on the $\mathbb{P}^1$. These representations are rigid in the sense that the moduli space is a point, since fractional branes cannot leave the singularity. However, the moduli space is not a variety, but a scheme, more precisely, a fat point. This fact renders the physical interpretation of the BPS states less clear. When the moduli space is a variety, there is a well-established criterion, proposed by Witten [106], to determine the R-symmetry and the spin of the corresponding particle from the compact Dolbeault cohomology

of the moduli space. This option is not applicable in the present case. Moreover, a naive interpretation of the spectrum as k 5d hypers is in tension with the flavor symmetry determined by the geometry. The fact that this geometry has only a single $\mathbb{P}^1$ has the striking consequence that only one real mass parameter is available. The corresponding Kähler modulus gives an equal mass to all k matter fields, without possibility of tuning them independently. In other words, the $USp(2k)$ global symmetry that one would expect is broken down to $USp(2)$. The QFT explanation for such a phenomenon is not known to us. One possible mechanism for this might be a discrete S_k gauge symmetry acting on the matter fields. This peculiar matter sector is central to our construction of non-toric 5d SCFTs.

The theory exhibits a manifest $SU(2)$ flavor symmetry acting on the bifundamental fields. The pairs (α_1, α_2) and (β_1, β_2) each transform as doublets under this symmetry. To write the superpotential compactly and manifestly invariant, we introduce the $SU(2)$-invariant symplectic contraction:

$$\boldsymbol{\alpha} \cdot \boldsymbol{\beta} := \epsilon^{ij}\alpha_i\beta_j = \alpha_1\beta_2 - \alpha_2\beta_1 \,. \tag{7.7}$$

With this notation, the superpotential takes the form:

$$\mathcal{W} = \mathrm{Tr}\left[w_1\left(\boldsymbol{\alpha}\cdot\boldsymbol{\beta} + \frac{1}{k+1}w_1^k\right) + w_2\left(\boldsymbol{\beta}\cdot\boldsymbol{\alpha} - \frac{1}{k+1}w_2^k\right)\right] \,. \tag{7.8}$$

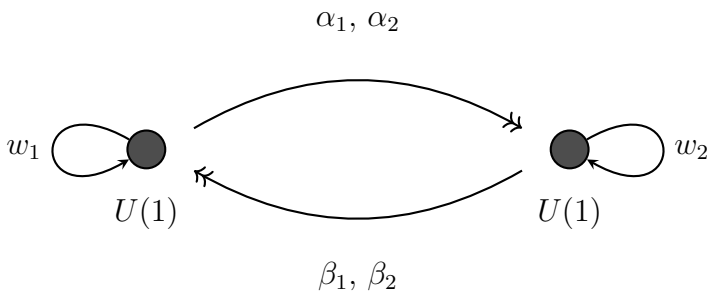

Figure 7.2: The D0-brane quiver of the Reid Pagoda.

The sum of the two terms linear in the w_i's give the usual superpotential that would have led to $\mathbb{C}^2/\mathbb{Z}_2 \times \mathbb{C}$. For $k = 1$, the higher-order terms correspond to the mass terms used by Klebanov and Witten.

One easily recovers the singular geometry by defining the bilinear invariants. The F-term

equations with respect to w_1 and w_2 impose:

$$\boldsymbol{\alpha} \cdot \boldsymbol{\beta} + w_1^k = 0 \quad \text{and} \quad -(\boldsymbol{\beta} \cdot \boldsymbol{\alpha}) + w_2^k = 0\,. \tag{7.9}$$

Using the property that $\boldsymbol{\beta} \cdot \boldsymbol{\alpha} = -\boldsymbol{\alpha} \cdot \boldsymbol{\beta}$ in the abelian case, this implies:

$$w_1^k = -(\boldsymbol{\alpha} \cdot \boldsymbol{\beta}) \quad \text{and} \quad w_2^k = \boldsymbol{\beta} \cdot \boldsymbol{\alpha} = -(\boldsymbol{\alpha} \cdot \boldsymbol{\beta})\,. \tag{7.10}$$

The F-terms of $\boldsymbol{\alpha}$ and $\boldsymbol{\beta}$ imply that $w_1 = w_2 \equiv w$, so we simply write:

$$\alpha_1\beta_2 - \alpha_2\beta_1 = -w^k\,. \tag{7.11}$$

We define the remaining affine coordinates as the symmetric combinations of the fields (with a factor of 2 for convenience):

$$u \equiv 2\alpha_1\beta_1\,, \quad v \equiv 2\alpha_2\beta_2\,, \quad z \equiv \alpha_1\beta_2 + \alpha_2\beta_1\,. \tag{7.12}$$

To find the relation between them, we square the z coordinate and use the F-term constraint:

$$z^2 - w^{2k} = (\alpha_1\beta_2 + \alpha_2\beta_1)^2 - (\alpha_1\beta_2 - \alpha_2\beta_1)^2 = 4(\alpha_1\beta_2)(\alpha_2\beta_1)\,. \tag{7.13}$$

Comparing this to the product uv, we see:

$$uv = (2\alpha_1\beta_1)(2\alpha_2\beta_2) = 4\alpha_1\beta_2\alpha_2\beta_1\,. \tag{7.14}$$

Thus, we recover the Reid Pagoda equation exactly:

$$uv - z^2 + w^{2k} = 0\,. \tag{7.15}$$

7.2 The Orbifold Construction

In the previous subsections, we constructed rank-zero theories. By orbifolding these geometries, however, four-cycles will inevitably be generated, taking us to rank-one theories. As before, the geometry will emerge from a quiver that will be obtained through a powerful mathematical construction known as the McKay correspondence. These (not necessarily abelian) quivers are known

as BPS quivers and describe the supersymmetric quantum mechanics on the worldline of BPS states formed by D0-D2-D4 bound states on the orbifold.

The bridge between the geometry and the quiver is the Derived McKay Correspondence [107]. For an orbifold Y/H, there is an equivalence of derived categories $D_c(X) \cong D_c^H(Y)$, where X is the crepant resolution and $D_c^H(Y)$ is the derived category of H-equivariant coherent sheaves. Practically, this implies that the fractional branes of the theory correspond to the irreducible representations of the orbifold group H, and the quiver can be derived via group theory. We have already seen an important instance of this in Section 2, when we reviewed the work of Douglas and Moore [2] describing D-branes probing orbifolds $\mathbb{C}^2/\mathbb{Z}_n$. We recall that the path algebra underlying quiver gauge theories coincides with the NCCR of the probed threefold and fractional branes can be mapped to objects in $D_c^H(Y)$.

7.2.1 Orbifolding the Pagoda

We now apply the Mckay construction to Reid's Pagoda. A priori we can choose from several inequivalent $\mathbb{Z}_2$-actions; however, we have to impose that the superpotential be *invariant* under it. If it were simply homogeneous, this would imply that the superspace θ-variables would have to transform under it, which means that H wouldn't commute with the supercharges. Hence, gauging such an H-action would break SUSY. Among the remaining choices, we will focus on the action defined by the following weights (see however Section 7.6 for a quiver of more general abelian orbifolds):

	α_1	α_2	β_1	β_2	w_1	w_2
$U(1)_{\text{gauge}}$	1	1	-1	-1	0	0
$H = \mathbb{Z}_2$	0	0	1	1	1	1

(7.16)

This is only compatible with Pagodas of *odd* k. Using the matrix presentation of section 2, we immediately write down the orbifold-invariant field content of the theory:

1. **Neutral Fields ($\boldsymbol{\alpha}$):** Being in the trivial representation of group H, $r_\alpha = \rho_0$, $\boldsymbol{\alpha}$ becomes a diagonal matrix representing arrows within each sector:

$$\boldsymbol{\alpha} \longrightarrow \hat{\boldsymbol{\alpha}} = \begin{pmatrix} \boldsymbol{\alpha}^{(00)} & 0 \\ 0 & \boldsymbol{\alpha}^{(11)} \end{pmatrix} . \tag{7.17}$$

2. **Charged Fields ($\boldsymbol{\beta}$):** Since $r_\beta = \rho_1$, $\boldsymbol{\beta}$ becomes an off-diagonal matrix connecting the two sectors:

$$\boldsymbol{\beta} \longrightarrow \hat{\boldsymbol{\beta}} = \begin{pmatrix} 0 & \boldsymbol{\beta}^{(01)} \\ \boldsymbol{\beta}^{(10)} & 0 \end{pmatrix} . \tag{7.18}$$

3. **Charged Adjoints (w_i):** Similarly, the adjoints w_i ($i = 1, 2$) are charged and become off-diagonal:

$$w_i \longrightarrow \hat{w}_i = \begin{pmatrix} 0 & w_i^{(01)} \\ w_i^{(10)} & 0 \end{pmatrix} . \tag{7.19}$$

The resulting quiver is shown in Figure 7.3.

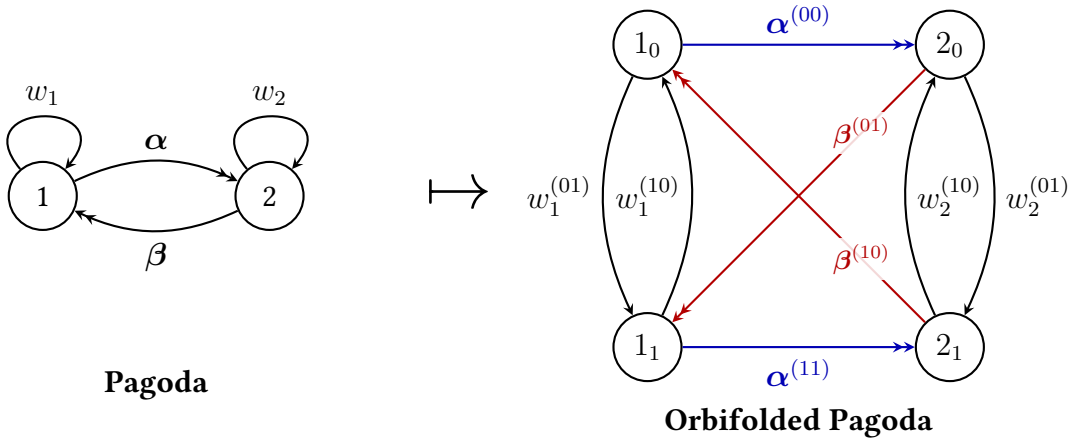

Figure 7.3: The Quiver diagram transition. Bold symbols denote flavor doublets. Notation: $\boldsymbol{\phi} \equiv (\phi_1, \phi_2)$ represents an $SU(2)$ flavor doublet.

Superpotential

The superpotential is determined by the gauge-invariant closed loops. We start with the parent superpotential:

$$W_{\text{Pagoda}} = \text{Tr}\Big(\boldsymbol{\alpha} \cdot \boldsymbol{\beta}\, w_1\Big) + \text{Tr}\Big(\boldsymbol{\beta} \cdot \boldsymbol{\alpha}\, w_2\Big) + \frac{1}{k+1}\text{Tr}\left(w_1^{k+1} - w_2^{k+1}\right) . \tag{7.20}$$

The orbifolded superpotential is obtained by substituting the block matrices into Eq. (7.20) and taking the trace. For the polynomial term w^{k+1}, since $\hat{w}_i$ are off-diagonal, a non-zero trace

requires an even number of insertions forming an alternating path $0 \to 1 \to 0 \ldots$. The surviving terms are:

$$W_{Orb} = \mathrm{Tr}\left(\hat{\boldsymbol{\alpha}} \cdot \hat{\boldsymbol{\beta}}\, \hat{w}_1\right) + \mathrm{Tr}\left(\hat{\boldsymbol{\beta}} \cdot \hat{\boldsymbol{\alpha}}\, \hat{w}_2\right) + \frac{1}{k+1}\mathrm{Tr}\left(\hat{w}_1^{k+1}\right) - \frac{1}{k+1}\mathrm{Tr}\left(\hat{w}_2^{k+1}\right) \tag{7.21}$$

whereby the trace runs over 'color' and orbifold indices. Written explicitly in terms of only a trace over color indices, it would spell as follows:

$$\begin{aligned} W_{\mathrm{Orb}} = {} & \mathrm{Tr}\Big(\boldsymbol{\alpha}^{(00)} \cdot \boldsymbol{\beta}^{(01)}\, w_1^{(10)}\Big) + \mathrm{Tr}\Big(\boldsymbol{\alpha}^{(11)} \cdot \boldsymbol{\beta}^{(10)}\, w_1^{(01)}\Big) \\ & + \mathrm{Tr}\Big(\boldsymbol{\beta}^{(10)} \cdot \boldsymbol{\alpha}^{(00)}\, w_2^{(01)}\Big) + \mathrm{Tr}\Big(\boldsymbol{\beta}^{(01)} \cdot \boldsymbol{\alpha}^{(11)}\, w_2^{(10)}\Big) \\ & + \frac{2}{k+1}\mathrm{Tr}\Big(\underbrace{w_1^{(0,1)} w_1^{(1,0)} \ldots w_1^{(1,0)}}_{k+1 \text{ terms}}\Big) \\ & - \frac{2}{k+1}\mathrm{Tr}\Big(\underbrace{w_2^{(0,1)} w_2^{(1,0)} \ldots w_2^{(1,0)}}_{k+1 \text{ terms}}\Big)\,. \end{aligned} \tag{7.22}$$

7.3 Geometry of the Moduli Space

The geometry of the threefold is defined by the vacuum moduli space of the theory. This corresponds to the set of holomorphic gauge-invariant operators (mesons) subject to the constraints imposed by the F-term equations.

7.3.1 The Determinantal Variety

We define the orbifold geometry by first determining the transformation properties of the parent coordinates u, v, z, w under the $H = \mathbb{Z}_2$ action. Recall the charge assignments from the orbifold construction:

- The base fields α are neutral.
- The fiber fields β and the adjoints w are charged.

Consequently, as it is clear from (7.12), all four affine coordinates of the parent Pagoda theory are odd under the orbifold action:

$$(u, v, w, z) \quad \longrightarrow \quad (-u, -v, -w, -z). \tag{7.23}$$

Since the coordinates flip sign, The ring of invariants is generated by all the monomials of degree two in u, v, z, w. There are ten such generators, which we arrange into a symmetric 4×4 matrix $\mathcal{M}$:

$$\mathcal{M} = \begin{pmatrix} u \\ v \\ z \\ w \end{pmatrix} \cdot \begin{pmatrix} u & v & z & w \end{pmatrix} = \begin{pmatrix} u^2 & uv & uz & uw \\ vu & v^2 & vz & vw \\ zu & zv & z^2 & zw \\ wu & wv & wz & w^2 \end{pmatrix} . \tag{7.24}$$

The geometry is defined by two conditions on this matrix:

1. **Rank Condition:** Since $\mathcal{M}$ is constructed from the outer product of the vector (u, v, z, w), it must have rank one. This implies the vanishing of all 2×2 minors, which are the defining equations of the orbifold singularity $\mathbb{C}^4/\mathbb{Z}_2$.

2. **Dynamical Constraint:** The parent Pagoda equation $uv - z^2 + w^{2k} = 0$ imposes the following constraint on the matrix entries:

$$\mathcal{M}_{12} - \mathcal{M}_{33} + (\mathcal{M}_{44})^k = 0\,. \tag{7.25}$$

The Orbifolded Pagoda is the intersection of these two conditions and it is a determinantal variety.

7.3.2 Resolution and the Hidden Surface

We can determine the topology of the compact 4-cycles by resolving the orbifold singularity. Our threefold will be defined as a hypersurface in the ambient space $\mathbb{C}^4/\mathbb{Z}_2$, which is resolved by a single blowup introducing an exceptional divisor $E \cong \mathbb{P}^3$. In toric language, this resolution is described by a Gauge Linear Sigma Model (GLSM) with a $U(1)$ gauge field corresponding to the

blow-up parameter λ.[2] The charge assignment is:

	u	v	z	w	λ
$\mathbb{C}^*$	1	1	1	1	-2

(7.26)

The D-term constraint implies that u, v, z, w cannot simultaneously vanish, defining a $\mathbb{P}^3$ base, while λ is a coordinate on the fiber of the line bundle $\mathcal{O}(-2)$. The exceptional divisor is located at $\lambda = 0$.

The geometry of the Calabi-Yau is the *proper transform* of the orbifolded hypersurface. Under the blowup with scaling parameter λ, the defining equation of homogeneous degree two is given by

$$uv - z^2 + w^{2k}\,\lambda^{k-1} = 0\,. \tag{7.27}$$

The exceptional divisor corresponds to the locus $\lambda = 0$:

- For $k = 1$, the equation is $uv - z^2 + w^2 = 0$. This defines a smooth quadric surface in $\mathbb{P}^3$, which is isomorphic to $\mathbb{P}^1 \times \mathbb{P}^1 \cong \mathbb{F}_0$.

- For $k > 1$, the higher-order term vanishes, leaving the equation $uv - z^2 = 0$. This defines a singular quadric cone in $\mathbb{P}^3$. The minimal resolution of this cone yields the Hirzebruch surface $\mathbb{F}_2$.

Thus, the geometry of the orbifolded Pagoda contains a compact divisor of type $\mathbb{F}_2$.

To see why the singular quadric in $\mathbb{P}^3$ corresponds to a partially blown-down $\mathbb{F}_2$, we describe the latter torically as $\mathbb{P}\left(\mathcal{O}_{\mathbb{P}^1}(0) \oplus \mathcal{O}_{\mathbb{P}^1}(-2)\right)$, which is the same as the following toric variety:

$\mathbb{F}_2$:

	x_1	x_2	y_1	y_2
$\mathbb{C}^*_1$	1	1	0	-2
$\mathbb{C}^*_2$	0	0	1	1

(7.28)

We can blow down the Kähler modulus associated to the first $\mathbb{C}^*$-action. This is achieved by

[2] Note that the GLSM is describing the toric variety resolving $\mathbb{C}^4/\mathbb{Z}_2$, while our nontoric threefold is described by an algebraic equation in this space.

writing its invariants. The resulting space is given by the ambient $\mathbb{P}^3$:

	$u := x_1^2 y_2$	$v := x_2^2 y_2$	$z := x_1 x_2 y_2$	$w := y_1$
$\mathbb{C}_2^*$	1	1	1	1

(7.29)

subject to the relation $u\,v = z^2$. So, this describes an $\mathbb{F}_2$ with its (-2)-curve blown down to an A_1-singularity. This singular surface will be a central character to our story.

The appearance of the compact surface $\mathbb{F}_2$ already indicates the existence of a rank-one Coulomb branch and, in an appropriate Kähler chamber, a low-energy gauge theory phase. In particular, when the exceptional divisor is a genuine $\mathbb{F}_2$, there will be an $SU(2)$ gauge theory phase where the Coulomb parameter will be described by the fiber class, while the volume of the base (-2)-curve plays the role of the inverse bare coupling. We now turn to the analysis of this curve.

7.3.3 The Pagodina Curve

The most critical physics lies in the *singularity* of this divisor itself, which is also a singularity of the threefold. To see the local geometry experienced by the BPS states, we analyze the local neighborhood of the "north pole" of the exceptional $\mathbb{P}^3$ (where $w \neq 0$). In the affine patch where we set $w = 1$, the proper transform equation becomes:

$$uv - z^2 + \lambda^{k-1} = 0\,. \tag{7.30}$$

Since we are focusing on odd values of k, this is precisely the defining equation of a Reid Pagoda of order $p = (k-1)/(2)$. We will affectionately refer to the associated curve as a *Pagodina*[3] curve. It will be our second main character, as it will host unconventional 5d matter.

This yields a striking structural observation: The $\mathbb{Z}_2$ orbifold of a Pagoda of order k contains, within its resolution, a local geometry equivalent to a Pagoda of order $(k-1)/2$.

Resolving the Pagodina singularity blows up a $\mathbb{CP}^1$, the Pagodina curve, and turns the exceptional divisor into a smooth Hirzebruch surface $\mathbb{F}_2$. It is straightforward to see that the Pagodina curve is precisely the rigid (-2)-curve of $\mathbb{F}_2$ (given by $y_2 = 0$ in (7.28)). We now do it explicitly.

[3] Given the composition of the author list, the use of the Italian diminutive was statistically inevitable.

Let us start from the equation (7.27) in the toric space (7.26) and perform the shift

$$z = t + w^k \, \lambda^{(k-1)/2} \, . \tag{7.31}$$

With this redefinition, the hypersurface equation becomes

$$uv = t \left(t + 2w^k \, \lambda^{(k-1)/2} \right) \, . \tag{7.32}$$

The singular locus is located at $u = v = t = \lambda = 0$. We can resolve this space by blowing up the ideal (u, t). The resulting space is given by the equation

$$uv = t \, \left(\sigma \, t + 2w^k \, \lambda^{(k-1)/2} \right) = 0 \tag{7.33}$$

in the toric space

	u	v	t	w	λ	σ
$\mathbb{C}^*$	1	1	1	1	-2	0
$\mathbb{C}^*$	1	0	1	0	0	-1

(7.34)

The divisor $\lambda = 0$ in the resolved space is a Hirzebruch surface $\mathbb{F}_2$. The map between this presentation and the standard toric description of $\mathbb{F}_2$ (see (7.28)) is given by

$$u = x_1^2, \qquad v = x_2^2 y_2, \qquad t = x_1 x_2, \qquad \sigma = y_2 \, . \tag{7.35}$$

Under this identification, the Pagodina curve corresponds to the locus $y_2 = 0$ in the standard toric presentation, which in the present coordinates is given by $v = \sigma = 0$.

Instead of resolving the singularity, one may consider deforming it. Working in the patch $w = 1$, where the singularity is located, the geometry is described by the Reid pagoda hypersurface

$$uv = z^2 - \lambda^{2p}, \tag{7.36}$$

with $p = \frac{k-1}{2}$. This singularity admits $2p - 1$ versal complex structure deformations. However, only p of them are 5d dynamical degrees of freedom in M-theory in the sense of [149, 150],[4]

[4]Let us review the counting of the dynamical modes: the singularity (7.36) is quasi-homogeneous. Normalizing its quasi-homogeneous weights q_u, q_v, q_z, q_λ so that the polynomial in (7.36) has weight one, we have $q_u = q_v = q_z = \frac{1}{2}, \quad q_\lambda = \frac{1}{2p}$. Now, define $\hat{c} = 4 - 2(q_u + q_v + q_z + q_\lambda) = \frac{p-1}{p}$, and $Q_j \equiv j q_\lambda$. Following [149, 150], if $Q_j \leq \frac{\hat{c}}{2}$ (or equivalently $j \leq p - 1$), The deformation is dynamical in M-theory. Recently, it was argued that the dynamical deformations must satisfy instead the strict inequality $Q_j < \frac{\hat{c}}{2}$ [151]. However, this does not alter our result in any

namely

$$uv = z^2 - \lambda^{2p} + \sum_{i=0}^{p-1} c_i \lambda^i \,. \tag{7.37}$$

In the five-dimensional theory obtained from M-theory on this threefold, The dynamical deformations correspond to giving vacuum expectation values to dynamical hypermultiplets. The fact that M-theory on the Reid pagoda exhibits a p-dimensional Higgs branch is well established in the literature [45, 96].[5]

Let us now return to the full threefold (7.32), restoring the coordinate w. In this case, the dynamical deformations take the form

$$uv = t\left(t + 2w^k \lambda^{(k-1)/2}\right) + \sum_{i=0}^{(k-3)/2} c_i\, w^{2i+2} \lambda^i \,. \tag{7.38}$$

Let us consider the $k = 3$ case first (meaning $p = 1$). The only dynamical deformation is the monomial w^2. The equation (7.38) becomes

$$uv = t\left(t + 2w^3\lambda\right) + c_0\, w^2 \,. \tag{7.39}$$

The exceptional divisor at $\lambda = 0$ is now a smooth quadric in $\mathbb{P}^3$, namely $\mathbb{F}_0 = \mathbb{P}^1 \times \mathbb{P}^1$.

Although the defining equation is formally similar to the deformation of the local $\mathbb{F}_2$ geometry to the local $\mathbb{F}_0$ considered by [41], the physical interpretation is different. In the construction of [41], the deformation corresponds to a non-normalizable complex structure deformation, which geometrically implements a Hanany-Witten transition. In contrast, in our case, the presence of the higher-degree term $w^6\lambda^2$ (equivalently $t\, w^3\lambda$ in (7.38)) renders the deformation normalizable in the sense of [149, 150]. This distinction is crucial: while the [41] deformation encodes a non-dynamical rearrangement of branes, our geometry describes a genuinely dynamical deformation of the five-dimensional theory.

significant way.

[5] Notice that in the gauge theory regime, the Pagodina curve is blown up and the corresponding Pagoda matter becomes massive.

An even more surprising phenomenon occurs for $k \geq 5$.[6] In this case, one can deform the Pagoda singularity of the threefold by switching on all deformations proportional to λ, while keeping only the w^2 deformation turned off. E.g. for $k = 5$ we can deform the Pagodina singularity as

$$uv = t\left(t + 2w^5\lambda^2\right) + c_1\, w^4\lambda\,. \tag{7.40}$$

The resulting threefold is completely smooth.[7] As a consequence, there is no remaining singular locus that could support a crepant resolution, and hence no exceptional $\mathbb{P}^1$ (notice that the exceptional divisor at $\lambda = 0$ is still singular). In other words, the Kähler modulus is frozen. Physically, this corresponds to *freezing the theory at infinite coupling*.

Summing up, while the singularity admits a small resolution at the undeformed point, generic normalizable deformations proportional to λ eliminate any crepant resolution, effectively freezing a Kähler modulus at infinite gauge coupling. The quadratic w^2 deformation is an exception, as it does not lead to such a freezing.

7.3.4 The Matrix Dictionary

To rigorously identify the geometric loci, we translate the affine coordinates u, v, w, z of the parent theory into the operator language of the orbifolded quiver. Under the orbifold map, the scalar coordinates lift to 2×2 matrices.

Using the matrix forms of the fields established in Section 3.2, we define the Coordinate Matrices. The base coordinates $\hat{\mathrm{U}}, \hat{\mathrm{V}}, \hat{\mathrm{Z}}$ are defined exactly as in the parent theory:

$$\hat{\mathrm{U}} \equiv 2\,\hat{\alpha}_1\,\hat{\beta}_1\,, \quad \hat{\mathrm{V}} \equiv 2\,\hat{\alpha}_2\,\hat{\beta}_2\,, \quad \hat{\mathrm{Z}} \equiv \hat{\alpha}_1\,\hat{\beta}_2 + \hat{\alpha}_2\,\hat{\beta}_1\,. \tag{7.41}$$

For the deformation coordinate, the quiver contains two adjoints w_1, w_2, we define two matrices $\hat{\mathrm{W}}_i$:

$$\hat{\mathrm{W}}_i = \begin{pmatrix} 0 & w_i^{(01)} \\ w_i^{(10)} & 0 \end{pmatrix}\,. \tag{7.42}$$

Note that all the matrices $\hat{\mathrm{U}}, \hat{\mathrm{V}}, \hat{\mathrm{Z}}, \hat{\mathrm{W}}_i$ transform in the sign representation of $\mathbb{Z}_2$ (odd parity),

[6] In this case, the Pagodina singularity is a genuine Reid Pagoda, while for $k = 3$ the pointlike singularity on the $w = 1$ patch is a conifold.

[7] This is manifest from the fact that the deformed hypersurface (7.38) no longer admits a factorized form that would allow for a small resolution.

consistent with their off-diagonal structure.

7.3.5 Geometric loci via nilpotent quiver representations

We can now identify the exceptional geometry by exploiting via quiver quantum mechanics the matrix structure of the orbifold coordinates, much like we did in the basic example of $\mathbb{C}^2/\mathbb{Z}_2 \times \mathbb{C}$, in Section 2.1. The singular point of the affine variety is the locus where all coordinate invariants vanish: $u = v = z = w = 0$. In our matrix formalism, this translates to the condition that all coordinate matrices $\hat{\mathrm{U}}, \hat{\mathrm{V}}, \hat{\mathrm{Z}}, \hat{\mathrm{W}}_i$ are nilpotent. Stability conditions prevent us from setting these matrices to zero; we *can* set all orbifold invariants to zero. These invariants are constructed analogously to (7.24), by defining the following *non-Abelian field valued matrix*:

$$\boldsymbol{\mathcal{M}} = \begin{pmatrix} \hat{\mathrm{U}} \\ \hat{\mathrm{V}} \\ \hat{\mathrm{Z}} \\ \hat{\mathrm{W}}_i \end{pmatrix} \cdot \begin{pmatrix} \hat{\mathrm{U}} & \hat{\mathrm{V}} & \hat{\mathrm{Z}} & \hat{\mathrm{W}}_j \end{pmatrix} = \begin{pmatrix} \hat{\mathrm{U}}^2 & \hat{\mathrm{U}} \cdot \hat{\mathrm{V}} & \hat{\mathrm{U}} \cdot \hat{\mathrm{Z}} & \hat{\mathrm{U}} \cdot \hat{\mathrm{W}}_j \\ \hat{\mathrm{V}} \cdot \hat{\mathrm{U}} & \hat{\mathrm{V}}^2 & \hat{\mathrm{V}} \cdot \hat{\mathrm{Z}} & \hat{\mathrm{V}} \cdot \hat{\mathrm{W}}_j \\ \hat{\mathrm{Z}} \cdot \hat{\mathrm{U}} & \hat{\mathrm{Z}} \cdot \hat{\mathrm{V}} & \hat{\mathrm{Z}}^2 & \hat{\mathrm{Z}} \cdot \hat{\mathrm{W}}_j \\ \hat{\mathrm{W}}_i \cdot \hat{\mathrm{U}} & \hat{\mathrm{W}}_i \cdot \hat{\mathrm{V}} & \hat{\mathrm{W}}_i \cdot \hat{\mathrm{Z}} & \hat{\mathrm{W}}_i \hat{\mathrm{W}}_j \end{pmatrix} . \tag{7.43}$$

Now, to find the exceptional locus of the resolution, we simply set $\boldsymbol{\mathcal{M}} = 0$. Crucially, nilpotency does *not* imply that the matrices themselves vanish. In a resolved phase, the D-term stability conditions (FI parameters) prevent the fields from vanishing identically.

$$\sum |Q_{\text{in}}|^2 - \sum |Q_{\text{out}}|^2 = \theta > 0 \, . \tag{7.44}$$

For our quiver quantum mechanics, we will choose the following FI parameters:

$$\theta_{L0} < \theta_{L1} < \theta_{R0} < \theta_{R1} \tag{7.45}$$

subject to $\theta_{L0} + \theta_{L1} + \theta_{R0} + \theta_{R1} = 0$.

Seeing that all matrices $\hat{\mathrm{U}}, \hat{\mathrm{V}}, \hat{\mathrm{Z}}, \hat{\mathrm{W}}_i$ are of the form

$$\begin{pmatrix} 0 & * \\ * & 0 \end{pmatrix}$$

the diagonal of $\boldsymbol{\mathcal{M}}$ tells us that all four must be nilpotent. Then, the fact that their products are all zero tells us that they are all simultaneously either upper or lower triangular. Our stability

choice is such that they must all be upper triangular. We can now explore the compact cycles of our geometry.

The $\mathbb{F}_2$ Surface

To find the $\mathbb{F}_2$ divisor, we search for a configuration where the coordinate matrices are nilpotent but non-zero. Repeating the matrices here for convenience:

$$\hat{\mathrm{U}} = 2\begin{pmatrix} 0 & \alpha_1^{(00)}\beta_1^{(01)} \\ \alpha_1^{(11)}\beta_1^{(10)} & 0 \end{pmatrix}, \qquad \hat{\mathrm{V}} = 2\begin{pmatrix} 0 & \alpha_2^{(00)}\beta_2^{(01)} \\ \alpha_2^{(11)}\beta_2^{(10)} & 0 \end{pmatrix},$$
$$\hat{\mathrm{Z}} = \begin{pmatrix} 0 & \alpha_1^{(00)}\beta_2^{(01)} + \alpha_2^{(00)}\beta_1^{(01)} \\ \alpha_1^{(11)}\beta_2^{(10)} + \alpha_2^{(11)}\beta_1^{(10)} & 0 \end{pmatrix}, \qquad \hat{\mathrm{W}}_i = \begin{pmatrix} 0 & w_i^{(01)} \\ w_i^{(10)} & 0 \end{pmatrix}. \tag{7.46}$$

We see that the minimal constraints we must impose to make them all upper triangular are achieved by setting the "return" arrows to zero, i.e.

$$\mathbb{F}_2: \qquad \boldsymbol{\beta}^{(10)} \equiv \begin{pmatrix} \beta_1^{(10)} \\ \beta_2^{(10)} \end{pmatrix} = 0 \quad \text{and} \quad \boldsymbol{w}^{(10)} \equiv \begin{pmatrix} w_1^{(10)} \\ w_2^{(10)} \end{pmatrix} = 0\,. \tag{7.47}$$

This forces all closed loops to vanish (nilpotency). The stability condition $\xi > 0$ ensures that we are on the resolved branch of the vacuum moduli space, meaning the fields parametrizing the cycle cannot all vanish simultaneously. The surviving fields $\boldsymbol{\alpha}^{(00)}$, $\boldsymbol{\alpha}^{(11)}$, $\boldsymbol{\beta}^{(01)}$ and $\boldsymbol{w}^{(01)}$ serve as homogeneous coordinates on the exceptional divisor.

It is easy to see that, upon restricting to this locus, we recover the quiver (see Figure 7.4) and F-term relations of the NCCR of the $\mathbb{F}_2$ surface [152]. The GLSM related to the quiver in Figure 7.4 describes the $\mathbb{F}_2$ surface as the moduli space of the abelian quiver with all $U(1)$ gauge groups[8]. It is given by

	$\alpha_1^{(00)}$	$\alpha_2^{(00)}$	$\alpha_1^{(11)}$	$\alpha_2^{(11)}$	$\beta_1^{(01)}$	$\beta_2^{(01)}$	$w_1^{(01)}$	$w_2^{(01)}$	FI
$\mathbb{C}_1^*$	1	1	0	0	0	0	1	0	ξ_1
$\mathbb{C}_2^*$	0	0	1	1	0	0	0	1	ξ_2
$\mathbb{C}_3^*$	1	1	1	1	-1	-1	0	0	ξ_3
$\mathbb{C}_4^*$	0	0	0	0	1	1	1	1	ξ_4

(7.48)

[8] Equivalently, the quiver representation with dimension vector $\vec{d} = (1,1,1,1)$.

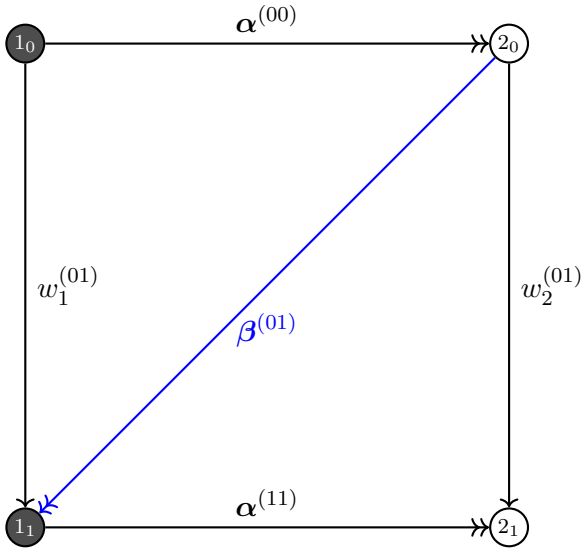

Figure 7.4: Subquiver with $\mathbb{F}_2$ as its moduli space.

where in the last column we have written the corresponding combinations of the stability parameters that are positive in the chamber we chose (i.e. $\theta_{L0} < \theta_{L1} < \theta_{R0} < \theta_{R1}$):

$$\xi_1 = -\theta_{L0}\,, \quad \xi_2 = \theta_{R1}\,, \quad \xi_3 = \theta_{R0} + \theta_{R1} = -\theta_{L0} - \theta_{L1}\,, \quad \xi_4 = \theta_{L1} + \theta_{R1} \tag{7.49}$$

The relations that survive after imposing (7.47) are

$$A \begin{pmatrix} \beta_1^{(01)} \\ \beta_2^{(01)} \end{pmatrix} = 0 \quad \text{and} \quad \begin{pmatrix} w_2^{(01)} & w_1^{(01)} \end{pmatrix} A = 0 \qquad \text{with} \quad A = \begin{pmatrix} \alpha_1^{(00)} & -\alpha_2^{(00)} \\ -\alpha_1^{(11)} & \alpha_2^{(11)} \end{pmatrix}\,. \tag{7.50}$$

The Pagodina via Vertical Quiver Fusion

Having established that the threefold contains a $\mathbb{F}_2$ divisor, and having isolated it in the quiver moduli space language, we will now show in quiver language that there is a patch in the moduli space where the threefold looks like an order $(k-1)/2$ Pagoda.

The Pagodina curve is obtained by setting $\boldsymbol{\beta}^{(01)} = 0$ in the space defined by (7.48) and (7.50). From the last row of (7.48), we see that $\boldsymbol{w}^{(01)} \neq (0,0)$. Together with the relations (7.50) and the stability conditions $\xi_1 > 0$ and $\xi_2 > 0$, this implies that both $w_1^{(01)} \neq 0$ and $w_2^{(01)} \neq 0$. We may

therefore gauge-fix them to 1 in a neighborhood of the curve. This gauge-fixing identifies pairs of nodes in the original quiver, yielding the quiver shown in Figure 7.5. After this identification, the GLSM describing the threefold in this local region takes the form

	$\alpha_1^{(00)}$	$\alpha_2^{(00)}$	$\alpha_1^{(11)}$	$\alpha_2^{(11)}$	$\beta_1^{(01)}$	$\beta_2^{(01)}$	$\beta_1^{(10)}$	$\beta_2^{(10)}$	$w_1^{(10)}$	$w_2^{(10)}$	FI
$\mathbb{C}^*$	1	1	1	1	-1	-1	-1	-1	0	0	$\xi_3 > 0$

(7.51)

The superpotential is obtained by inserting $w_1^{(01)} = w_2^{(01)} = 1$ into (7.22). This produces several quadratic terms, that allow us to eliminate some variables; in particular they force $\beta_i^{(10)} = \frac{1}{2}\beta_i^{(01)}(w_1^{(10)} - w_2^{(10)})$ and $\alpha_i^{(00)} = \alpha_i^{(11)}$. The resulting effective superpotential governing the remaining degrees of freedom is

$$W_{\text{eff}} = \text{Tr}\Big(\boldsymbol{\alpha}^{(11)} \cdot \boldsymbol{\beta}^{(01)}\, w_1^{(10)}\Big) + \text{Tr}\Big(\boldsymbol{\beta}^{(01)} \cdot \boldsymbol{\alpha}^{(11)}\, w_2^{(10)}\Big) + \frac{1}{p}\text{Tr}\left(\left(w_1^{(10)}\right)^{p+1} - \left(w_2^{(10)}\right)^{p+1}\right),$$

with the corresponding maps represented in the quiver of Figure 7.5. These are precisely the quiver and superpotential of the Reid pagoda of order $p = \frac{k-1}{2}$.

The geometry in a neighborhood of the Pagodina curve is therefore locally isomorphic to the Reid pagoda threefold. Shrinking this curve produces a point-like Pagoda singularity localized on the exceptional divisor. This sharply contrasts with the local $\mathbb{F}_2$ threefold, where collapsing the (-2)curve gives rise instead to a *line* of A_1 singularities.

We can identify the representation corresponding to a D2-brane wrapping this Pagodina curve. It would correspond to the Higgsed quiver Figure 7.5 with $U(0) \times U(1)$ gauge group. In terms of quiver representations, this is the $(0,1)$ representation, and it has a zero-dimensional moduli space corresponding to a fat point $\mathbb{C}[w_2^{(10)}]/\left(\left(w_2^{(10)}\right)^p\right)$. We can easily find the lift of this representation to the full orbifold quiver Figure 7.3: the 2_0 and 2_1 nodes have $U(1)$ gauge group each, and the other two are empty, i.e. the representation with dimension vector $(0,1,1,0)$ (starting from the top left node, moving clockwise). That subquiver has only two fields, $w_2^{(10)}$ and $w_2^{(10)}$, subject to the F-term and D-term conditions with the choice (7.45)

$$\left(w_2^{(01)}\right)^p \left(w_2^{(10)}\right)^p = 0 \tag{7.52}$$

$$|w_2^{(01)}|^2 - |w_2^{(10)}|^2 = \theta_{R1} - \theta_{R0} > 0\,. \tag{7.53}$$

This reduces the moduli space to $\mathbb{C}[w_2^{(10)}]/\left(\left(w_2^{(10)}\right)^p\right)$ as expected.

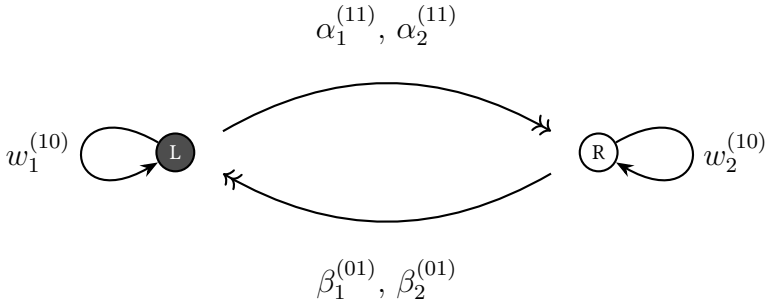

Figure 7.5: Quiver after Higgsing.

Having established this, we easily deduce that this state is a gauge singlet by noting that the dimension vector $(0,1,1,0)$ has Dirac pairing zero w.r.t. all other possible representations, since it sits in the kernel of the antisymmetric part of the adjacency matrix (7.75).

7.4 Higgsing Pagoda-matter: Coupling frozen at ∞

In this section, we discuss the physical significance of the class of geometries we have introduced. We claim that these give rise to 5d SCFTs that evade standard classifications, whether field-theoretic or geometric, such as those found in [38, 39, 41], among many more works.[9]

The root of their peculiar physical properties lies in their inherent non-toricity. The punch line is the following: We have found geometries yielding theories that, once their matter fields acquire a VEV, *do not admit any weak coupling regime.*

These geometries give rise to theories of arbitrarily high rank,[10] with an arbitrary amount of so-called *Pagoda-matter* fields. We recall that these are states arising from M2-branes wrapping $\mathcal{O}(0)\oplus\mathcal{O}(-2)$-curves whose moduli are obstructed at $k+1$-th order by a superpotential. In many respects, they behave as hypermultiplets, because their moduli space is zero-dimensional [153]. However, BPS quiver analysis identifies them as indecomposable representations whose moduli spaces are fat points, i.e. $\mathbb{C}[w]/(w^k)$. These uncharged hypers have a striking physical effect: their presence allows for a mechanism that freezes the gauge couplings to infinite value.

[9] Note that the possibility of coupling cDV matter to higher-rank theories was already pointed out in [45], Section 4.3.2, in a different example.

[10] Infinite families of theories with rank $r > 1$ will be introduced in Section 7.6.

To explain this, we revisit the relation between the geometry and the effective field theory. Although we presented our geometries as $\mathbb{Z}_2$-orbifolds of the Pagoda, they can equivalently be viewed as a deformation of the *local* $\mathbb{F}_2$ Calabi-Yau threefold, whereby the quivers are the same, but the superpotentials are deformations as follows:

$$W = W_{\text{local } \mathbb{F}_2} + W_k \,, \tag{7.54}$$

with the first term being the standard one for the toric variety

$$W_{\text{local } \mathbb{F}_2} = \text{Tr}\Big(\boldsymbol{\alpha}^{(00)} \cdot \boldsymbol{\beta}^{(01)}\, w_1^{(10)}\Big) + \text{Tr}\Big(\boldsymbol{\alpha}^{(11)} \cdot \boldsymbol{\beta}^{(10)}\, w_1^{(01)}\Big) \tag{7.55}$$

$$+ \text{Tr}\Big(\boldsymbol{\beta}^{(10)} \cdot \boldsymbol{\alpha}^{(00)}\, w_2^{(01)}\Big) + \text{Tr}\Big(\boldsymbol{\beta}^{(01)} \cdot \boldsymbol{\alpha}^{(11)}\, w_2^{(10)}\Big) \tag{7.56}$$

and the second one being the order $k+1$ deformation:

$$W_k = \frac{2}{k+1}\text{Tr}\Big(\underbrace{w_1^{(0,1)} w_1^{(1,0)} \dots w_1^{(1,0)}}_{k+1 \text{ terms}}\Big) - \frac{2}{k+1}\text{Tr}\Big(\underbrace{w_2^{(0,1)} w_2^{(1,0)} \dots w_2^{(1,0)}}_{k+1 \text{ terms}}\Big) \,.$$

The effective gauge coupling of a 5d theory on its Coulomb branch (parametrized by the scalar VEV ϕ) is given by the second derivative of the prepotential $\mathcal{F}(\phi)$. For the local $\mathbb{F}_2$ theory, the one-loop exact effective coupling is [38, 90]:

$$\frac{1}{g_{eff}^2(\phi)} = \frac{\partial^2 \mathcal{F}}{\partial \phi^2} = 2m_0 + 8|\phi| \,. \tag{7.57}$$

In a standard local $\mathbb{F}_2$ theory, m_0 is a tunable parameter. One can take the weak coupling limit by making the base curve very large ($m_0 \to \infty$), which decouples the instanton particles and recovers a perturbative $SU(2)$ gauge theory. For the local $\mathbb{F}_2$ theory, we identify the lhs of (7.57) with twice the volume of the curve in $\mathbb{F}_2$ of self-intersection $+2$. Consequently, the geometry dictates that the effective volume of the base is shifted by the fiber volume proportional to the twist $n = 2$ of the Hirzebruch surface [39]. Here, the two terms have distinct geometric interpretations:

- 2ϕ is the volume of the fiber $\mathbb{P}^1$ of the surface.
- m_0 is proportional to the inverse bare coupling squared ($m_0 = \frac{1}{2g_{YM,0}^2}$). Geometrically, it is the volume of the base (-2)-curve of the $\mathbb{F}_2$ surface.

However, the "Pagoda matter" changes this picture drastically once we activate the further normalizable deformations corresponding to giving VEVs to these fields. Turning on these deformations obstructs the Kähler modulus of the $\mathbb{F}_2$ base curve:

$$m_0 \longrightarrow 0\,. \tag{7.58}$$

Substituting this back into Eq. (7.57), the effective coupling in this Higgsed phase becomes simply:

$$\frac{1}{g^2_{eff}(\phi)} = 8|\phi|\,. \tag{7.59}$$

This has a profound consequence. In standard theories, one can keep ϕ small (near the SCFT point) while making g_{eff} small by dialing m_0 to be large. In the Higgsed Pagoda theories, this "buffer" is removed. As we approach the origin of the Coulomb branch ($\phi \to 0$), the effective coupling g_{eff} diverges immediately and unavoidably.

Thus, the activation of Pagoda matter VEVs freezes the bare coupling m_0 to zero. This implies that in this branch of the moduli space, there is no weakly coupled regime: the theory is intrinsically strongly coupled at the origin, and cannot be continuously deformed to a perturbative non-Abelian gauge theory.

7.5 Physical Interpretation: Non-constant flavor background

In this section, we provide a string-theoretic interpretation of the superpotential deformation W_k introduced in Eq. (7.21). This is a rather speculative section, based on upcoming work [57] by some of the present authors, building on a progression of ideas written in [19, 37, 56, 77]. We propose that the Pagoda theories should be viewed as deformations of the standard toric orbifold theories, such as the conifold or $\mathbb{C}^2/\mathbb{Z}_2 \times \mathbb{C}$, or in our main case, local $\mathbb{F}_2$, where the flavor symmetry parameters are promoted to *position-dependent background fields* for the $SU(2)$ global symmetry of the original 5d SCFT.

7.5.1 The 5d Perspective

The M-theory interpretation of this new phenomenon is the following: The toric parent geometry $K_{\mathbb{F}_2}$, contains a non-compact curve of A_1 singularities extending along the w-axis. In M-theory,

this singular locus supports 7d degrees of freedom (associated with vanishing 2-cycles) propagating along the entire w-line. This is the background $SU(2)$ vector multiplet.

The Pagoda geometry is defined by the deformation $uv - z^2 = -w^{2k}$. Geometrically, this describes an A_1 fiber whose deformation parameter μ varies over the base $\mathbb{C}_w$ as $\mu(w) \sim w^{2k}$. For any $w \neq 0$, the deformation is non-zero, the A_1 singularity is smoothed out, and the associated 2-cycles have finite volume. Consequently, the M2-branes wrapping these cycles become massive and non-BPS.

The physical effect of the term w^{2k} is therefore to *localize* the massless degrees of freedom. Unlike the toric parent, where states can propagate freely along the w-direction, the Pagoda geometry generates a "geometric potential" that confines the singular sector to the origin $w = 0$. The *Pagoda matter* consists of these localized states, trapped by the geometry itself. The background $SU(2)$ vector multiplet contains three real adjoint scalars. We pair two into a complex field Φ and keep the third, φ_3, real. Their VEVs correspond to the geometric moduli:

$$\langle \Phi \rangle \quad \longleftrightarrow \quad \text{Complex Structure (Smoothing)}\,, \tag{7.60}$$

$$\langle \varphi_3 \rangle \quad \longleftrightarrow \quad \text{Kähler Form (Resolution)}\,. \tag{7.61}$$

The Pagoda geometry is defined by the fixed background profile via the following spectral equation:

$$uv = \det\left(\mathbb{I}_2 \cdot z - \langle \Phi \rangle\right) \tag{7.62}$$

for the following choice of background:

$$\Phi(w) = \begin{pmatrix} w^k & 0 \\ 0 & -w^k \end{pmatrix}. \tag{7.63}$$

A background in Φ generates a potential for φ_3 of the form

$$V \sim |[\langle \Phi(w) \rangle, \varphi_3]|^2$$

A constant background for φ_3 corresponds to a real mass deformation of the 5d SCFT, i.e. $\langle \varphi_2 \rangle \sim m_0$. For the Pagoda background, we see that there is only one available background

$$\langle \varphi_3 \rangle = m_0 \cdot \begin{pmatrix} 1 & 0 \\ 0 & -1 \end{pmatrix}.$$

Now, following the analysis in [24, 25], we know that Φ for the Pagoda has k 5d dynamical fluctuations. In an appropriate gauge, they can be written as follows:

$$\delta\Phi = \begin{pmatrix} 0 & 1 \\ P_{k-1}(w) & 0 \end{pmatrix} ,$$

where $P_{k-1}(w)$ is an arbitrary polynomial of degree $k-1$, with k coefficients. These complex structure moduli coefficients are the projection of the full Higgs branch coordinates w.r.t. their $(\mathbb{C}^*)^k$ coordinates, which are realized as Wilson lines of the 11d supergravity C_3-form. The consequence of giving a vev to these deformations is that our background becomes:

$$\langle \Phi_{\text{new}}(w) \rangle = \begin{pmatrix} w^k & 1 \\ P_{k-1}(w) & -w^k \end{pmatrix} \tag{7.64}$$

and as a result the spectral equation changes drastically:

$$uv = \det\left(\mathbb{I}_2 \cdot z - \langle \Phi \rangle\right) \tag{7.65}$$

$$= z^2 - w^{2k} + P_{k-1}(w)\,. \tag{7.66}$$

These are precisely the dynamical deformations according to the analysis of [150]. Note now that we can no longer find a constant φ_3 that commutes with it, i.e.

$$[\langle \Phi_{\text{new}}(w) \rangle, \varphi_3] \neq 0\,.$$

Geometrically, this tells us that the small resolution of the CY threefold (which corresponds to blowing up the base curve of the $\mathbb{F}_2$) is obstructed, as advertised. For our orbifolded Pagodas, we actually apply this logic to the *Pagodina*, i.e., the resulting order $\frac{k-1}{2}$ Pagoda geometry that results from orbifolding the $K_{\mathbb{F}_2}$. It is in that geometry that the Kähler obstruction gives rise to an important physical phenomenon.

7.5.2 The view from D2-branes

We can further clarify the origin of the superpotential deformation W_k by considering the world-volume theory of a spacetime-filling D2-brane probing the Calabi-Yau threefold. This perspective, based on work in progress [57], utilizes 3d $\mathcal{N} = 4$ mirror symmetry to map geometric deforma-

tions to field-theoretic interactions.

The D2-brane probe admits two dual descriptions:

- The Quiver Frame: A D2-brane probing an A_1 singularity ($uv = z^2$). The theory is an affine A_1 quiver gauge theory where the $SU(2)$ flavor symmetry is realized via monopole operators and dual photons.
- The SQED Frame: The mirror dual theory, which is $\mathcal{N} = 4$ SQED with two hypermultiplets $(Q, \tilde{Q})$ coupled to a complex adjoint Φ of the $SU(2)$ flavor symmetry. Physically, this corresponds to a D2 probing a stack of two D6-branes in flat space. Φ is an adjoint of that stack.

In this setup, the Pagoda geometry (7.3) is realized by fibering the A_1 singularity over a complex plane $\mathbb{C}_w$. At the level of the probe D2-brane 3d theory, this corresponds to making the flavor symmetry background Φ depend on the field w controlling the position of the D2-brane on $\mathbb{C}_w$. In the SQED frame, this background enters the superpotential as a Yukawa-like interaction:

$$W_{\text{int}} = \text{Tr}\left(Q \cdot \langle \Phi(w) \rangle \cdot \tilde{Q}\right), \tag{7.67}$$

where for the k-Pagoda case, $\Phi(w)$ takes the form (7.63).

In the quiver frame, the superpotential term (7.67) becomes a w-dependent complex FI term [12],

$$W_{\text{int}} \sim \frac{1}{k+1} w^{k+1}. \tag{7.68}$$

This precisely matches the polynomial deformation terms $\frac{1}{k+1}\text{Tr}(w^{k+1})$ appearing in our BPS quivers. On the other hand, by analyzing the linearized fluctuations of the background Higgs field (7.63) using the techniques of [16], one finds that—unlike in the undeformed $\mathbb{C}^2/\mathbb{Z}_2 \times \mathbb{C}$ background—the theory now supports modes localized at $w = 0$. These localized degrees of freedom constitute what we refer to as *Pagoda matter*. Hence, these two observations are two sides of the same mechanism: the Φ-generated superpotential deformation both encodes the polynomial terms in the quiver description and is responsible for the appearance of localized Pagoda matter at $w = 0$.

We claim that this physical mechanism extends to all toric CY threefolds whose toric diagram has a side with points along the segment, i.e., anything that has a boundary segment as in Fig-

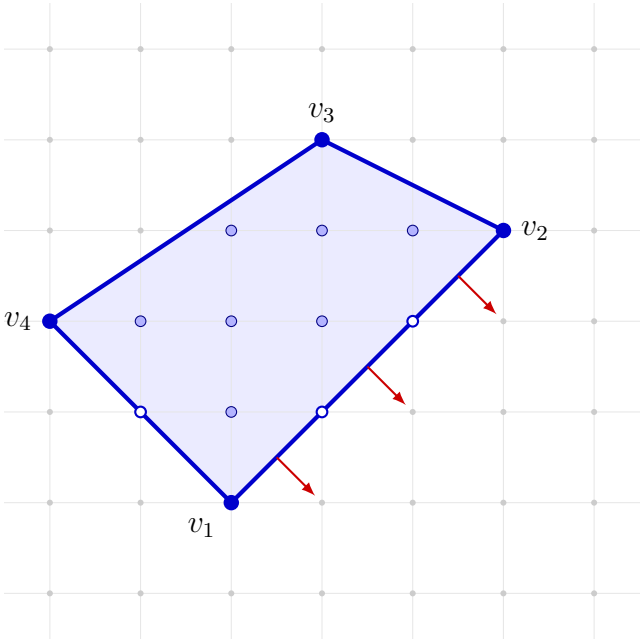

Figure 7.6: Toric polytope for a threefold with a highlighted $SU(3)$ global symmetry.

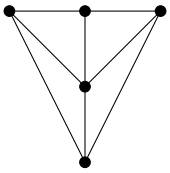

Figure 7.7: Toric diagram local $\mathbb{F}_2$.

ure 7.6. For such a theory, one can similarly introduce a position-dependent $SU(3)$ background, creating localized matter.

Now, we can apply this logic to local $\mathbb{F}_2$, see Figure 7.7. This theory has a global $SU(2)$ symmetry. By switching on a background Higgs vev (7.63), we claim that we end up with precisely the theory of the orbifolded Pagoda (7.55). The localized *Pagoda-matter* multiplets are fully accounted for by the analysis of linearized fluctuations of this vev.

7.6 More general orbifolds

We can apply the same procedure to much more general orbifolds and produce a wide class of new 5d theories. The ambient space coordinates (u, v, z, w) admit a larger group of symmetries

that preserve the structure of the Pagoda equation (7.3) and its holomorphic volume form.

The matrix formalism of Section 2.1 is directly generalized by choosing an appropriate matrix representation of the orbifold action: fields $\phi_\pm$ of charge ± 1 under an orbifold group $\mathbb{Z}_m$ are promoted to matrices of the form

$$\hat{\phi}_+ = \begin{pmatrix} 0 & \phi_+^{(0,1)} & 0 & \dots & 0 \\ 0 & 0 & \phi_+^{(1,2)} & \ddots & 0 \\ \vdots & \vdots & \ddots & \ddots & \vdots \\ 0 & 0 & \vdots & 0 & \phi_+^{(m-1,1)} \\ \phi_+^{(m,0)} & 0 & \cdots & 0 & 0 \end{pmatrix}, \quad \hat{\phi}_- = \begin{pmatrix} 0 & 0 & \cdots & 0 & \phi_-^{(0,m-1)} \\ \phi_-^{(1,0)} & 0 & \cdots & 0 & 0 \\ 0 & \phi_-^{(2,1)} & \ddots & \vdots & \vdots \\ \vdots & \ddots & \ddots & 0 & 0 \\ 0 & \cdots & 0 & \phi_-^{(m-1,m-2)} & 0 \end{pmatrix}, \tag{7.69}$$

while neutral (charge zero) fields will be promoted to diagonal matrices. In this notation, the superpotential for all cases is given by the master trace formula derived in Section 7.2:

$$W_{Orb} = \mathrm{Tr}\left(\hat{\boldsymbol{\alpha}} \cdot \hat{\boldsymbol{\beta}}\, \hat{w}_1\right) + \mathrm{Tr}\left(\hat{\boldsymbol{\beta}} \cdot \hat{\boldsymbol{\alpha}}\, \hat{w}_2\right) + \frac{1}{k+1}\mathrm{Tr}\left(\hat{w}_1^{k+1}\right) - \frac{1}{k+1}\mathrm{Tr}\left(\hat{w}_2^{k+1}\right). \tag{7.70}$$

For a general abelian orbifold, the D0-brane supersymmetric quantum mechanics is always described by the abelian quiver with $U(1)$ gauge group at every node. We highlight three distinct cases of interest.

7.6.1 $\mathbb{Z}_N$ orbifolds of the Pagoda: generalization of the $\mathbb{Z}_2$ case

We consider an orbifold group $H \cong \mathbb{Z}_N$, that generalizes the $\mathbb{Z}_2$ example of Section 7.2.1. Its action on the affine coordinates (u, v, z, w) is the following

	u	v	z	w
$\mathbb{Z}_N$	1	1	1	-1

(7.71)

where we require that N divides $k+1$, i.e. $k+1 = qN$.

Like in the $\mathbb{Z}_2$ case, we can understand the geometry of the orbifolded threefold by performing a partial resolution. First, we describe the $\mathbb{C}^4/\mathbb{Z}_N$ orbifold of the ambient space via the GLSM

	u	v	z	w	λ
$\mathbb{C}^*$	1	1	1	$N-1$	$-N$

(7.72)

The geometry of the Calabi-Yau is the proper transform of (7.3) under this blowup:

$$uv - z^2 + w^{2k}\lambda^{2(k-q)} = 0. \tag{7.73}$$

Setting $\lambda = 0$, we again obtain an exceptional divisor isomorphic to a degenerate $\mathbb{F}_2$, in which the (-2) curve has been shrunk. Moreover, upon restricting to the patch $w = 1$, we find a Pagodina singularity of order $k - q$.[11] Resolving the Pagodina curve via a small resolution, like in (7.33), yields an exceptional divisor isomorphic to the $\mathbb{F}_2$ surface. However, in contrast with the $\mathbb{Z}_2$ case, the resulting threefold now develops a $\mathbb{C}^2/\mathbb{Z}_{N-1}$ singularity at a point on the $\mathbb{F}_2$ fiber. This singularity is inherited from the $\mathbb{Z}_{N-1}$ orbifold singularity of the ambient space (7.72). Resolving it yields $N-1$ ruled surfaces, each fibered over a base isomorphic to the Pagodina curve. Altogether, the fully resolved geometry contains $r = N$ compact divisors.

We now study the orbifold action on the quiver. The induced action on the quiver maps follows from (7.72):

	α_1	α_2	β_1	β_2	w_1	w_2
$\mathbb{Z}_N$	0	0	1	1	-1	-1

(7.74)

Using the matrix formalism, we can explicitly determine the adjacency matrix A_{ab} of the resulting BPS quiver.[12] From it, one directly reads both the rank r of the Coulomb branch and the dimension f of the flavour lattice of BPS charges:

$$A_{ab} = \begin{cases} 2, & a = b+1 \pmod N, \\ 1, & a = b-1 \pmod N, \\ 0, & \text{otherwise}, \end{cases} \qquad r = N-1, \qquad f = 2\,. \tag{7.75}$$

The matrix representatives $\hat{\boldsymbol{\alpha}}$ are diagonal, while $\hat{\boldsymbol{\beta}}$ and $\hat{\boldsymbol{w}}$, that connect nodes $i \to i \pm 1$, have the form (7.69). The corresponding quivers for $N = 3, 4$ are shown in Figure 7.8.

[11] For $N = 2$ one has $q = \frac{k+1}{2}$, and we recover $p = k - q = \frac{k-1}{2}$.
[12] Results on the defect group of such theories will appear in [99].

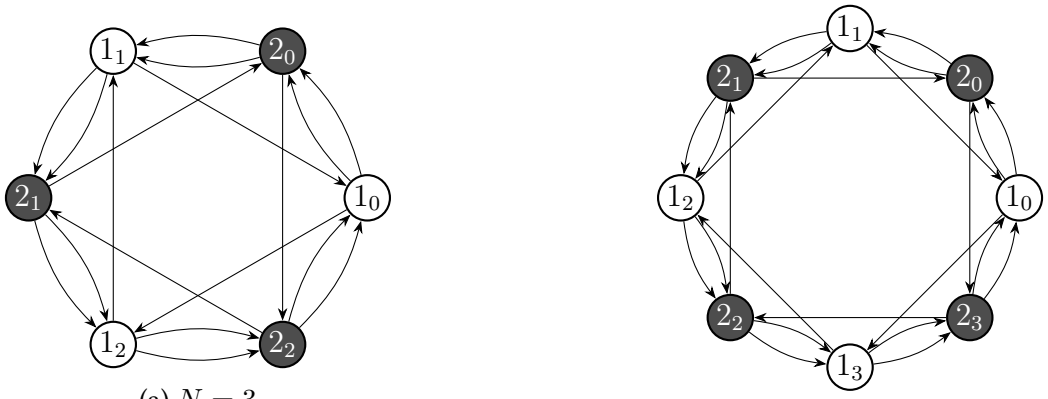

(a) $N = 3$ (b) $N = 4$

Figure 7.8: Antisymmetric BPS quivers for $\mathbb{Z}_3$ and $\mathbb{Z}_4$ orbifolds (7.74).

7.6.2 $\mathbb{Z}_m$ orbifolds leading to Conformal Matter

We now choose an orbifold that acts on u and v with opposite phases, leaving z and w invariant:

	u	v	z	w
$\mathbb{Z}_m$	1	-1	0	0

(7.76)

This action is valid for any order k of the Pagoda.

To understand the geometry, let us first consider the case $m = 2$. The additional $\mathbb{C}^2/\mathbb{Z}_2$ singularity created by the orbifold can be resolved by passing to the hypersurface

$$u\,e\,v = z^2 - w^{2k} \qquad \subset \qquad \begin{array}{c|ccccc} & u & e & v & z & w \\ \hline \mathbb{C}^* & 1 & -2 & 1 & 0 & 0 \end{array} \tag{7.77}$$

There are two Pagoda singularities of order k, located at the two poles of the blown-up $\mathbb{P}^1$. For generic m, the situation is analogous: resolving the ambient $\mathbb{C}^2/\mathbb{Z}_m$ singularity yields m Pagoda singularities, located at the $m-2$ intersections of the exceptional $\mathbb{P}^1$'s and at one point on each external $\mathbb{P}^1$. There are no exceptional divisors. The resulting 5d theory can be regarded as a new example of 5d conformal matter [154].

As regards the orbifold action on the Pagoda quiver, we have:

	α_1	α_2	β_1	β_2	w_1	w_2
$\mathbb{Z}_m$	-1	0	0	1	0	0

(7.78)

The quotient has the following adjacency matrix and values for r and f:

$$A_{ab} := \begin{cases} 1, & a = b \bmod 2m \\ 1, & a = b - 1 \bmod 2m \\ 1, & a = b + 1 \bmod 2m \\ 0, & \text{otherwise.} \end{cases} \qquad r = 0, \quad f = 2m\,. \tag{7.79}$$

The matrix fields $\hat{\alpha}_2$, $\hat{\beta}_1$, and $\hat{w}_i$ are diagonal, while $\hat{\alpha}_1$ and $\hat{\beta}_2$ have the form (7.69). The quivers for $m = 3, 4$ are in Figure 7.9.

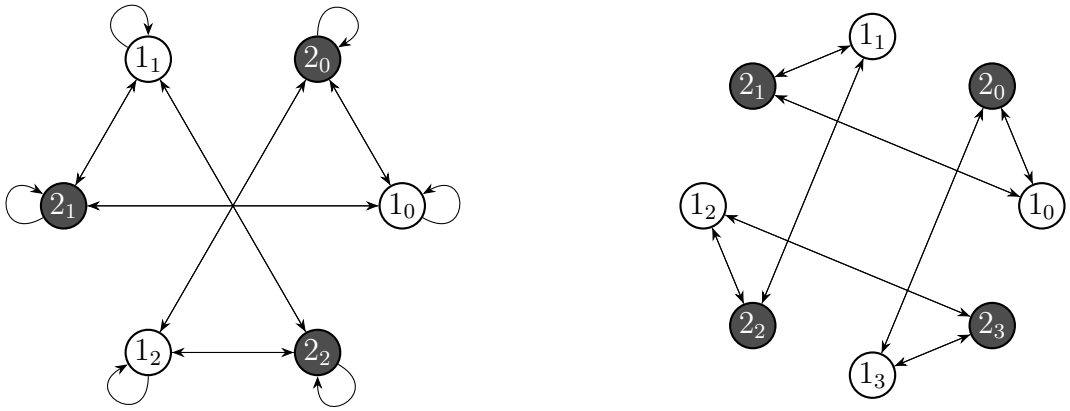

(a) $m = 3$

(b) $m = 4$

Figure 7.9: Symmetric BPS quivers for $\mathbb{Z}_3$ and $\mathbb{Z}_4$ orbifolds (7.78).

7.6.3 The General Abelian Orbifold $\mathbb{Z}_m \times \mathbb{Z}_N$

Finally, we combine the actions (7.71) and (7.76):

	u	v	z	w
$\mathbb{Z}_m$	1	-1	0	0
$\mathbb{Z}_N$	1	1	1	-1

(7.80)

The induced weights on the quiver fields are:

	α_1	α_2	β_1	β_2	w_1	w_2
$\mathbb{Z}_m$	-1	0	0	1	0	0
$\mathbb{Z}_N$	1	0	1	0	-1	-1

(7.81)

In the quotient, we have the $2mN \times 2mN$ adjacency matrix, r and f given by

$$A_{ab} := \begin{cases} 1, & a = b + 2m \bmod 2mN \\ 1, & a = b + 2m - 1 \bmod 2mN \\ 1, & a = b + 1 \bmod 2mN \\ 0, & \text{otherwise} \end{cases} \qquad \begin{aligned} r &= mN - f/2, \\ f &= 2m + N - 2 + GCD[N, 2m]\,. \end{aligned} \tag{7.82}$$

We can express the new maps as $N \times N$ block matrices, where each entry is itself an $m \times m$ matrix acting on the secondary orbifold index.

The resulting quivers for $N = m = 2$ and $N = m = 3$ are shown in Figure 7.10.

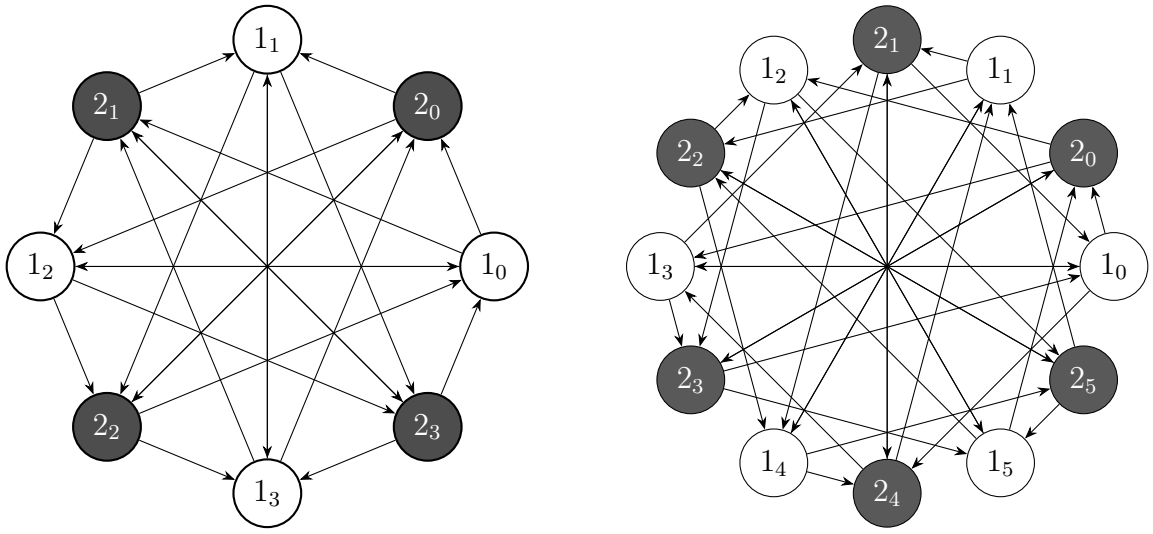

(a) $m = 2,\ N = 2$ (b) $m = 3,\ N = 2$

Figure 7.10: BPS quivers for the combined orbifold cases.

7.6.4 Orbifold of Reid Pagodas as deformations of toric orbifolds

We conclude with a unifying remark. As discussed above, the Reid Pagoda (7.3) can be viewed as a deformation of the toric orbifold

$$Y_{\text{toric}} \equiv \mathbb{C} \times \mathbb{C}^2/\mathbb{Z}_2,$$

with the defining equation

$$xy - z^2 = 0, \tag{7.83}$$

by the addition of a w-dependent term w^{2k}.[13] This realizes the Pagoda geometry as a family over w of deformed A_1 singularities.

Since all the orbifold actions considered above preserve Y_{toric}, the operations of quotient and deformation commute:

$$X = \frac{\text{Deform}\big(Y_{\text{toric}}\big)}{H} \;=\; \text{Deform}\left(\frac{Y_{\text{toric}}}{H}\right). \tag{7.84}$$

[13] For a discussion of abelian and non-abelian orbifolds of $\mathbb{C}^3$ and their BPS quiver we refer to [124].

The intermediate geometry Y_{toric}/H is a toric Calabi–Yau orbifold, while the final space X is a non-toric deformation thereof. The deformation does not modify the compact divisors, but it lifts the non-compact lines of singularities present in the toric model, leaving instead discrete "Pagodina" curves supporting the exotic matter.

To identify the toric model explicitly, we now construct $X_{\text{toric}} = Y_{\text{toric}}/H$. On the ambient space $\mathbb{C}^4$ of the Pagoda, the $\mathbb{Z}_N$ orbifold acts as

$$(x, y, w, z) \mapsto (\xi x, \xi y, \xi w, \xi^{-1} z), \qquad \xi^N = 1. \tag{7.85}$$

This action admits a natural lift to $\mathbb{C}^3$, from which the toric description follows.

1. Start from $\mathbb{C}^3 \ni (g_1, g_2, g_3)$.

2. Consider the group $\hat{\Gamma} \cong \mathbb{Z}_{2N} \subset SU(3)$ generated by

$$\epsilon = \begin{pmatrix} \zeta & 0 & 0 \\ 0 & \zeta & 0 \\ 0 & 0 & \zeta^{-2} \end{pmatrix}, \qquad \zeta^{2N} = 1. \tag{7.86}$$

3. First quotient by the subgroup $\Gamma' \cong \mathbb{Z}_2 \subset \mathbb{Z}_{2N}$ generated by ϵ^N, acting as

$$g_1 \mapsto -g_1, \qquad g_2 \mapsto -g_2, \qquad g_3 \mapsto g_3. \tag{7.87}$$

   The quotient $\mathbb{C}^3/\mathbb{Z}_2$ is isomorphic to Y_{toric}, with

$$x = g_1^2, \qquad y = g_2^2, \qquad z = g_1 g_2, \qquad w = g_3. \tag{7.88}$$

4. The residual group

$$\Gamma = \mathbb{Z}_{2N}/\mathbb{Z}_2 \cong \mathbb{Z}_N \tag{7.89}$$

   acts on Y_{toric} precisely as in (7.85), upon identifying $\xi = \zeta^2$.

5. Using the general identity $V/G \cong (V/N)/(G/N)$ for $N \triangleleft G$, we conclude

$$X_{\text{toric}} = \frac{Y_{\text{toric}}}{\Gamma} = \frac{\mathbb{C}^3}{\mathbb{Z}_{2N}}. \tag{7.90}$$

For $N = 2$, this $\mathbb{Z}_4$ orbifold of $\mathbb{C}^3$ is well known in the context of the McKay correspondence, and its crepant resolution yields

$$\hat{X}_{\text{toric}} \cong \text{Tot}(K_{\mathbb{F}_2}). \tag{7.91}$$

Conclusions

A central motivation of this work is the absence of a systematic framework for constructing quantum field theories from geometries that lie beyond the toric class. A fundamental object in this program is the quiver, a tool that bridges geometry and quantum field theory in a powerful and universal way.

This is apparent in two different but related contexts. The first is the context of probe brane dynamics, where quiver gauge theories emerge on D-branes probing the geometric background and encode how geometric data is translated into field-theoretic interactions. The second is geometric engineering, in which quivers provide access to the spectrum of BPS states of the theory across all dynamical regimes. A notable feature is that the quiver naturally embodies the duality between geometric and field-theoretic structures, making explicit the correspondence between BPS states in quantum field theory and stable sheaves on a complex variety.

Then, our first target is the systematic identification of quiver gauge theories for geometries that generalise toric cases. This leads us to consider compound Du Val (cDV) singularities, which are approachable thanks to the strong structural constraints arising from their connection to Lie algebra theory, while at the same time remaining non-trivial from the point of view of the physics that revolves around them. The realization of these geometries via non-constant Higgs backgrounds in M-theory [19, 25] has revealed the existence of not yet fully understood physical phenomena associated with the peculiar structure of these spaces.

In this work, we leverage this construction to propose a physically grounded interpretation of these exotic geometric features by analyzing the effects of the corresponding Higgs backgrounds on the dynamics of probe D2-branes. In particular, we show that Higgs field configurations induce superpotential deformations in the worldvolume theory. Following the RG flow that these deformations trigger, we are able to reconstruct the effective quiver gauge theory and show that its moduli space reproduces the probed geometry consistently.

A first main result is the identification of a concrete physical interpretation of constant but non-trivial Higgs field configurations Φ, in terms of their effects on the worldvolume theory of D2-branes. Through their coupling to moment map operators, these backgrounds induce monopole superpotential deformations and Fayet–Iliopoulos terms, which in turn deform the moduli space

of the theory. This provides a dynamical realization of how geometric data is encoded in field theory, allowing one to reconstruct families of singular geometries as families of moduli spaces of deformed gauge theories. In this framework, structures such as ADE families and universal flops naturally emerge, and geometric features such as singular loci and their resolutions admit a direct field-theoretic interpretation. In particular, the presence or absence of residual $U(1)$ gauge symmetry provides a diagnostic for the resolvability of singularities.

Building on this perspective, we have developed a systematic method for deriving three-dimensional $\mathcal{N} = 2$ quiver gauge theories associated with compound Du Val threefolds. The method applies to both non-monodromic and monodromic Higgs field configurations, and incorporates a reduction procedure based on ungauging and mirror symmetry that allows one to treat non-abelian backgrounds. Its validity is supported by agreement with known examples, and it is sufficiently general to be applied to a wide class of geometries, including cases for which the corresponding gauge theories are not yet known.

A second main contribution concerns the role of compound Du Val singularities in the context of five-dimensional superconformal field theories. In particular, we have constructed new infinite families of 5d SCFTs arising from abelian orbifolds of the Reid Pagoda geometry. General orbifold constructions give rise to theories of arbitrarily high rank, while, in the specific case of a $\mathbb{Z}_2$ orbifold, one obtains an infinite class of rank-one theories. These rank-one theories can be understood as non-toric deformations of the local $\mathbb{F}_2$ model and inherit a distinctive matter sector—referred to as Pagoda matter—from the parent geometry.

Like local $\mathbb{F}_2$, these theories admit a weakly coupled $SU(2)$ gauge theory phase, where the effective gauge coupling is controlled by the Kähler volumes of base and fiber curves in $\mathbb{F}_2$. The $M2$ branes wrapped on the base curve constitute the Pagoda matter. We have argued that these states are not charged under the gauge symmetry. However, they can't be considered fully decoupled since their vevs produce an effect that drastically alters the theory. We have described this phenomenon as the freezing of the gauge coupling. The Kähler volume of the base curve is the bare mass of Pagoda matter states, and the only tuning parameter for the inverse gauge coupling. Once we give a vev to these states, their mass is forced to zero, eliminating the weakly-coupled regime and rendering the theory intrinsically strongly coupled. This behavior is not observed in related geometries such as local $\mathbb{F}_2$ or local $\mathbb{P}^1 \times \mathbb{P}^1$, where the corresponding matter sector is absent.

We also provide a physical description of the mechanism responsible for the localization of the Pagoda matter sector. In the orbifold geometries under consideration, this matter is supported on the base of the $\mathbb{F}_2$ surface and arises from the structure of the Higgs field that engineers the Pagoda geometry. From the perspective of the probe D2-brane theory, this is captured by a field-dependent Higgs background which induces a superpotential deformation of the quiver gauge theory. This deformation can be interpreted as a non-constant Fayet–Iliopoulos term, which lifts part of the moduli space and leads to the confinement of fractional D2-branes at the origin of the w-plane. In this way, the localization of the Pagoda matter sector admits a direct field-theoretic interpretation.

This perspective furnishes a field-theoretic understanding of the obstruction to blowing up the Pagoda curve. Fluctuations of the Higgs field around the background that engineers the Pagoda geometry correspond to dynamical deformations of the geometry. When such deformations are turned on, they generate a potential for the field controlling the Kähler volume of the exceptional curve, forcing its vacuum expectation value, namely the Kahler modulus, to vanish. These dynamical deformations are parametrized by vacuum expectation values of the Pagoda matter sector, leading to the conclusion that such vevs obstruct the small resolution of the geometry.

We finally report preliminary evidence that this structure extends beyond the Pagoda case. In particular, orbifolds of higher-length flops, such as the Laufer threefold, appear to give rise to infinite families of 5d SCFTs of rank two and higher. While a systematic analysis of these constructions remains to be completed, these results suggest that the mechanism uncovered in the Pagoda case may be part of a more general pattern relating orbifolds of non-toric singularities to families of higher-rank theories.

An important aspect of this construction is that the origin of the Pagoda matter sector can be traced to an obstruction in the normal bundle of the exceptional curve. While the resolved geometry can locally be described as a $\mathbb{P}^1$ with normal bundle $\mathcal{O}(0) \oplus \mathcal{O}(-2)$, this local description does not capture the obstruction, which nevertheless has direct physical consequences. In particular, it is this obstruction that governs the emergence of the additional matter sector in orbifold constructions and ultimately leads to the freezing of the gauge coupling.

These observations point to a tension with the common expectation that local geometric data fully determine the interacting 5d SCFT. Although the local geometry of the curve is indistinguishable from that of similar toric models, the obstruction—being invisible at the level of the

naive local description—gives rise to physical effects that modify the interacting theory. This suggests that certain aspects of the geometry not captured by the standard notion of locality may nevertheless play a role in determining the physical content of the theory.

Taken together, the results of this thesis provide a physically grounded framework for extracting non-trivial consequences of Higgs field backgrounds, a systematic method for deriving quiver gauge theories beyond the toric regime, and new insights into the structure of five-dimensional superconformal field theories.

Outlook

The results of this thesis open several directions for further investigation.

Completing the cDV programme. The methods developed in this work apply to cDV singularities of type A and D, where the Higgs field takes values in classical Lie algebras, and the mirror duals remain abelian. The extension to E-type configurations presents a qualitatively new challenge: the colored Dynkin diagrams that arise involve non-abelian nodes, so that the mirror duals are themselves non-abelian gauge theories with non-perturbative monopole superpotentials. Developing a consistent treatment of these cases would complete the programme initiated here and, importantly, would give access to quiver gauge theories dual to non-Lagrangian 3d theories that are not reachable by other means. A complementary extension concerns non-abelian probe theories, obtained by considering stacks of $D2$-branes. This would promote the abelian quivers studied here to their non-abelian counterparts and provide access to the full path-algebraic structure, including the noncommutative crepant resolutions associated with higher-rank representations.

Higher-length flops and higher-rank 5d SCFTs. The orbifold construction applied in this thesis to the Reid Pagoda admits a natural generalization to simple flops of higher length, such as the Laufer threefold [17, 97, 127, 131]. Preliminary evidence suggests that abelian orbifolds of these geometries give rise to infinite families of 5d SCFTs of rank two and higher, in which the freezing mechanism identified here persists in a more intricate form. A systematic analysis of these constructions would clarify to what extent the phenomena uncovered in the Pagoda case are generic features of non-toric geometric engineering.

BPS spectra and wall-crossing. The BPS quivers constructed in this thesis encode the spectrum of stable BPS states, but a detailed determination of the spectrum across the Coulomb branch — including its wall-crossing behavior — remains to be carried out. A natural framework for this

analysis is provided by the cluster algebra structure associated with the BPS quiver [20, 106, 110, 111, 146, 147, 155–163] which gives a rigorous combinatorial description of the stable chambers and their mutations. This is currently a work in progress. It would also be interesting to understand whether the freezing of the gauge coupling, which constrains the Kähler moduli space, has consequences for the wall-crossing structure — for instance, by reducing the number of accessible chambers or by forcing the spectrum to be rigid in certain regions of parameter space.

Relation to magnetic quivers and generalized toric polygons. The approach developed in this thesis — extracting 5d physics from probe D2-branes and BPS quivers — is complementary to other recently developed frameworks for studying 5d SCFTs beyond the toric regime. The magnetic quiver programme [105, 164–171] provides an alternative route to the Higgs branch of 5d and 6d theories, one that has proven particularly effective for theories admitting a brane web description. For the non-toric geometries studied here, it is not clear whether a magnetic quiver description exists, and if so, how the Pagoda matter sector and the freezing mechanism would manifest in that language. Similarly, the generalized toric polygon (GTP) framework [14] incorporates certain non-toric deformations directly into the brane web formalism. Understanding the precise overlap between the GTP approach and the Higgs-field construction used here — in particular, whether the obstruction data responsible for the freezing has a GTP counterpart — would provide a valuable cross-check and could lead to a more unified picture.

Locality and classification. From a more conceptual standpoint, the observation that obstruction data in the normal bundle — invisible to the standard local description of the singularity — can have direct physical consequences raises a natural question: what is the minimal set of geometric data required to fully characterize the associated 5d SCFT The current classification programmes [22, 41, 42, 44, 45] rely, implicitly or explicitly, on the assumption that the local singularity type is sufficient. The results of this thesis suggest that this assumption may need to be refined for non-toric geometries, and that the relevant additional data may be of a cohomological nature — related to the obstruction classes governing the global structure of the exceptional locus. Clarifying this point could lead to a sharper formulation of the geometric conditions under which a canonical singularity defines a well-posed 5d fixed point.

Relation to the 6d classification. Finally, a natural and important question that remains to be addressed is whether the infinite family of SCFTs identified in this work can be realized via circle compactification of a six-dimensional theory. This question is closely tied to the broader classification program, where evidence suggests that five-dimensional SCFTs admit a six-dimensional

origin [42, 49]. From a geometric perspective, this amounts to asking whether the associated Calabi-Yau threefolds admit an elliptic or genus-one fibration structure, at least up to birational equivalence, as emphasized in the current literature [22, 40, 144, 172–174]. In the case of the orbifold Pagoda geometries studied here, the absence of a toric description and the non-trivial obstruction data in the normal bundle make it unclear whether such a fibration structure exists. Addressing this point would clarify the place of these theories within the classification of 5d SCFTs descending from 6d, systematically developed in [172] using the combined fiber diagram technology.

Appendix A

A.1 Supersymmetry in various dimensions

The structure of supersymmetric theories with eight supercharges across dimensions is summarized in Table A.1. While the number of supercharges is fixed, the realization of the algebra and the associated R-symmetry depend on the spacetime dimension. In five dimensions, $\mathcal{N} = 1$ supersymmetry is governed by the exceptional superconformal algebra $F(4)$, whose bosonic subalgebra is $SO(5,2) \times SU(2)_R$, and the supercharges transform as doublets of $SU(2)_R$. Upon reduction to four dimensions, one obtains $\mathcal{N} = 2$ supersymmetry with superconformal algebra $SU(2,2 \mid 2)$, where the R-symmetry enhances to $SU(2)_R \times U(1)_r$, and the supercharges carry both $SU(2)_R$ indices and $U(1)_r$ charge. In three dimensions, the superconformal algebra becomes $OSp(4 \mid 4)$, with bosonic subalgebra $SO(3,2) \times SU(2)_C \times SU(2)_H$, and the supercharges transform in the bifundamental representation, reflecting the symmetry between Coulomb and Higgs sectors. As shown in the table, this dimensional hierarchy is mirrored in the scalar content of vector multiplets, which increases from one real scalar in 5d to a complex scalar in 4d and three real scalars in 3d, while hypermultiplets universally contain four real scalars transforming in quaternionic representations of the R-symmetry.

Dim	SUSY	SConf Algebra	Bosonic Subalgebra	R-symmetry	Q repr.	Vector scalars	Hyper scalars
5d	$\mathcal{N}=1$	$F(4)$	$SO(5,2)\times SU(2)_R$	$SU(2)_R$	$\mathbf{2}$	1 real	4 real
4d	$\mathcal{N}=2$	$SU(2,2\mid 2)$	$SO(4,2)\times SU(2)_R\times U(1)_r$	$SU(2)_R\times U(1)_r$	$(\mathbf{2},\pm 1)$	1 complex	4 real
3d	$\mathcal{N}=4$	$OSp(4\mid 4)$	$SO(3,2)\times SU(2)_C\times SU(2)_H$	$SU(2)_C\times SU(2)_H$	$(\mathbf{2},\mathbf{2})$	3 real	4 real

Table A.1: Supersymmetric theories with eight supercharges.

A.2 Canonical singularities: Absolute VS relative MMP

When dealing with complex surfaces, there is a clear, rigorous way of classifying them. It involves the intersection theory of its curves inside the surface. Curves inside a surface qualify as divisors. In particular, inside a surface S, it makes sense to talk about the self-intersection of a curve C, $C\cdot C\equiv C^2\in\mathbb{Z}$. Then, one can prove that there are classes of curves for which $C^2=-1$ and others such that $C^2=-2$[1]. The former can be described as the blow-up of a smooth point. The latter are associated with a contraction map that produces a canonical singularity (i.e., a Du Val singularity). As a consequence, we can think of simplifying a given surface geometry further and further by shrinking all the (-1)-curves. Moreover, if the surface is singular, we have a well-defined minimal way to desingularize it, which is by blowing up the (-2)-curves alone (without introducing (-1)-divisors)[2]. Let us make a further comment.
It can be shown (See [126]) that given a singularity of generic type S and a resolution $f:\tilde{S}\to S$ we have:

$$K_{\tilde{S}}=f^*K_S+\sum_i a_iC_i \tag{A.1}$$

where a_i are the discrepancies (relative to the canonical divisor of S) introduced by the exceptional curves C_i in the canonical divisor of the resolved surface. If S is canonical, we have:

$$a_i\geq 0\quad\forall\, i \tag{A.2}$$

[1]Curves with negative self-intersections are the only contractible curves in the geometry.
[2]The minimal resolution in dimension 2 is the small resolution in higher dimensions.

The solution of a simple linear system for the a_i[3] shows that $a_i > 0$ when $C_i^2 = -1$ and $a_i \leq 0$ for $C_i^2 \leq -2$. In particular, the discrepancy is zero only for (-2)-curves. From this, we learn that minimal resolutions of canonical singularities are all crepant resolutions (and vice versa).
To summarize, in general, a minimal model over a surface is merely the result of smoothing out unnecessary divisors (i.e., (-1)-curves). When the surface is canonical, this requirement coincides with extracting only its crepant divisors.
When we go to higher dimensions, the notion of minimality becomes much less intuitive. Now, divisors and curves are different objects, and the self-intersection of a curve is not defined per se (only within a surface subspace of the total variety). The minimal model program was conceived to classify (normal) complex varieties in dimension greater than 2 by finding a suitable generalization of minimality. Mori identified the following condition as a measure of minimality in higher dimensions:

$$K_X \cdot C \geq 0 \quad \forall C \subset X \tag{A.5}$$

Here K_X is the canonical divisor of a threefold X and C is a generic effective curve, namely a curve in the convex cone generated by a basis of $H_2(X, \mathbb{Z})$. A theorem by Mori, known as the Cone Theorem, states that for any effective curve in X such that $K_X \cdot C < 0$ (extremal curve), there is a proper birational morphism that contracts the curve to a point. In surfaces, we just have rational (-1)-curves since positive self-intersection curves are non-contractible (and it follows from the adjunction formula that having $K_X \cdot C < 0$ and $C^2 < 0$ at the same time is only possible when the genus $g(C)$ is zero). Then the MM is easily obtained by contracting all such curves. In higher dimensions, it is not always simply a curve that gets contracted (this is a small contraction). Contractions can involve blowing down entire divisors containing the extremal curves. Moreover, performing these operations most often generates singularities, which may spoil the original properties of the variety. Therefore, starting from a generic smooth projective variety, it is no trivial task to land on its minimal model. The existence of the latter cannot even be granted. To define a universal procedure for producing an MM starting from a generic variety is precisely the scope of what is known as absolute MMP, which we define just below. There is, then,

[3] It just comes from computing the intersection:

$$K_{\tilde{S}} \cdot C_j = f^* K_S \cdot C_j + \sum_i a_i C_i \cdot C_j = \sum_i a_i C_i \cdot C_j \tag{A.3}$$

.
The last equality follows from:

$$f^* K_S \cdot C_j = K_S \cdot f(C_j) = 0 \tag{A.4}$$

.

a weaker notion of minimality that applies to resolutions of canonical and terminal singularities [126]. In this case, the idea is to study geometries whose singularities are not too severe (it is the case for canonical varieties) by constructing crepant maps to smoother versions (i.e., their relative minimal models). As in dimension two, the passage to the relative minimal model extracts exactly the crepant exceptional divisors and curves. The existence of a relative model for any canonical threefold singularity is proven by a theorem [126], but it is hardly ever explicit.

A.2.1 Absolute MMP

Let us start with the definition of absolute MM:

Definition A.2.1 (minimal model)**.** Given a variety X of dimension ≥ 2, the absolute minimal model on X is a variety S such that:

- S is $\mathbb{Q}$-factorial (i.e., any Weyl divisor $D \subset S$ is $\mathbb{Q}$-Cartier), and terminal
- $\exists$ birational morphism $f : S \to X$
- K_S is nef

Terminal means that S can still have singularities, but only of the terminal type. The last property is the condition of minimality for varieties of dimension $d \geq 3$.

Definition A.2.2 (nef divisor)**.** Given a variety Y of dimension $d \geq 3$. A divisor $D \in Y$ is nef if:

$$\forall \text{ effective curve } C,\ D \cdot C \geq 0 \tag{A.6}$$

Suppose we start from a generic variety X and want to obtain the MM on X. Running the MMP on X then means:

1. Identify the effective curves $C_i \in X$, such that $K_X \cdot C_i < 0$.
2. Identify the contraction maps f_i associated with each curve class. The contractions may be divisorial, small, or fiber-like (in the latter case, the dimensionsof X drop upon contraction).

3. If contraction f_i is small (no divisor involved in the contraction), perform a *flip*.

4. Process terminates once K_X becomes nef.

Step 3 is a modification of the geometry that one is forced to do each time the contraction is small. Small contractions spoil a condition that is fundamental to guarantee that the singularities introduced in the process are at most terminal. This condition is $\mathbb{Q}$-factoriality. A flip is an operation, similar to a flop (defined below), that shrinks the extremal curve C associated with the small contraction and replaces it with a new curve C^+ such that $K_{X^+} \cdot C^+ > 0$ and $K_X \simeq K_{X^+}$. Just like flops, flips are isomorphisms outside the locus of the involved curve, and preserve the canonical divisor. An important difference with flops is that flips can only go in one direction, as positive-degree curves cannot be contracted (they can, but with bad consequences on the global geometry). It is important to stress that both flips and divisor contractions introduce singularities that would spoil the desired properties of the MM without any possibility of avoiding them. Then, the MMP will not converge to a minimal model but to a different space (Mori fiber space or Mori fibration). For details, we refer to [23, 148].

A.2.2 Relative MMP

Again, let us start from the definition:

Definition A.2.3 (minimal model)**.** Given a singularity X of dimension ≥ 2, a minimal model over X is a variety S such that:

- S is $\mathbb{Q}$-factorial and terminal
- $\exists$ birational morphism $f : S \to X$ such that $K_S = f^* K_X$
- K_S is f-nef

Here S is a crepant partial resolution of X. Crepancy is guaranteed by the condition on the canonical divisor: $K_S = f^* K_X$. The definition here invokes a theorem (Reid [126]) which ensures the existence of a minimal model (also called by Reid partial terminal resolution) for any variety with canonical singularities. When we restrict to terminal singularities, minimal models are nothing but the partial simultaneous resolutions of the families of ADE surfaces described in section

4. A fundamental observation is that the relative MM always exists, but it is not unique. There is indeed no unique way of extracting crepant divisors (or performing small resolutions) in such a way that the outcome will have the desired properties ($\mathbb{Q}$-factoriality and terminality). However, for any given X canonical, all possible MMs will be related by some elementary transformations which preserve the canonical divisor. Such transformations are known as *flops*. To define them, we first introduce small contractions:

Definition A.2.4 (Small contraction). [4] Let f define a *small contraction* of Y to a variety Y', i.e., a birational morphism:

$$f : Y \to Y' \tag{A.7}$$

such that Y and Y' are isomorphic in codimension 1 and
for any curve in Y such that $f(C)$ is a point in Y', $K_Y \cdot C = 0$.

Definition A.2.5 (Flop). Let f and f^+ be two small contractions:

$$\begin{aligned} f : &\quad Y \to Y' \\ f^+ : &\quad Y^+ \to Y' \end{aligned} \tag{A.8}$$

Then, a flop from Y to Y^+ is a birational morphism defined by the diagram:

$$\begin{array}{ccc} Y & \dashrightarrow & Y^+ \\ f \downarrow & & \downarrow f^+ \\ Y' & & Y' \end{array} \tag{A.9}$$

Morally, the flop takes the space Y, contracts one of the K_Y-trivial curves C, and then replaces it with a new curve C^+. The outcome of this operation is a different space Y^+, on which $K_{X^+} \cdot C^+ = 0$. Y^+ and Y are isomorphic up to a codimension 2 subspace given by C and C^+, and the canonical divisors K_Y and K_{Y^+} are numerically equivalent (have the same intersections). Flops are the only surgical operations on the geometry that one can perform to move from one minimal model to another, as they preserve the relative nefness of the canonical divisor (the last condition in A.2.3). This corresponds to: $K_Y \cdot C = 0$, namely to the triviality of the canonical divisor on the contracted curves. Let us give the full definition:

[4] A small contraction is the same thing as a small resolution. When seen as a resolution, it is always crepant (in dimension ≥ 3) because it does not introduce divisors.

Definition A.2.6 (f-nef divisor)**.** Let f define a birational morphism of Y to a variety Y':

$$f : Y \to Y' \tag{A.10}$$

And let C be an (effective) curve in Y such that $f(C)$ is a point in Y'[5]
A divisor $D \in Y$ is f-nef if for any such curve:

$$D \cdot C \geq 0 \tag{A.11}$$

Clearly, this condition is weaker than the first one A.2.1, as it involves only the curves in Y that are vertical with respect to the base Y' (namely, the curves that get contracted by the f morphism). Note that f-nefness or relative nefness of the canonical divisor in A.2.3 is actually implied by the crepancy of f. Indeed, for any contracted curve C, the condition $K_S = f^*K_X$ implies:

$$K_S \cdot C = f^*K_X \cdot C = K_X \cdot f(C) = 0 \tag{A.12}$$

So, all the curves that are blown-up in a crepant partial resolution are those on which K_S has zero degree. These are the curves that give rise to the flopping transitions, which we have just described. The relative minimal program can thus be seen as the characterization of the flop structure over a canonical singularity. Each minimal model over a canonical singularity represents one of the most economical ways (in terms of the number of divisors and curves extracted) to make the variety terminal.

[5]Note that f need not be a small contraction when we talk about MM. It can be any crepant map.

Appendix B

B.1 Relation among A_1, A_2, A_3, B for $\ell = 2$ universal flop

Here we derive the relation (6.103), that we used in Section 5.2.2 for computing the universal flop of $\ell = 2$ equation.

We start by considering the identity:

$$A_2 A_1 A_3 = \text{tr}(\mathfrak{M}_0 \mathfrak{M}_2 \mathfrak{M}_0 \mathfrak{M}_1 \mathfrak{M}_0 \mathfrak{M}_3) \,. \tag{B.1}$$

We replace the red-colored $\mathfrak{M}_0$ with: $\mathfrak{M}_0 = \varrho_4 \mathbb{1} - \mathfrak{M}_1 - \mathfrak{M}_2 - \mathfrak{M}_3$, which comes from (5.54). Since $\text{tr}(\mathfrak{M}_0) = 2\varrho_4$ and $\mathfrak{M}_i^2 = \varrho_i \mathbb{1}$, we have:

$$A_2 A_1 A_3 = -\text{tr}(\mathfrak{M}_0 \mathfrak{M}_2 \mathfrak{M}_3 \mathfrak{M}_1 \mathfrak{M}_0 \mathfrak{M}_3) - \varrho_1 A_2 A_3 - \varrho_2 A_1 A_3 + \varrho_4 \text{Tr}(\mathfrak{M}_0 \mathfrak{M}_2 \mathfrak{M}_1 \mathfrak{M}_0 \mathfrak{M}_3).$$

Again, we use (5.54) to replace the colored $\mathfrak{M}_0$. As a result:

$$\begin{aligned} A_2 A_1 A_3 = &\,\text{tr}(\mathfrak{M}_0 \mathfrak{M}_2 \mathfrak{M}_3 \mathfrak{M}_1 \mathfrak{M}_2 \mathfrak{M}_3) - \varrho_1 A_2 A_3 - \varrho_2 A_1 A_3 + \varrho_1 \varrho_3 A_2 + \\ &+ \varrho_3 \text{Tr}(\mathfrak{M}_0 \mathfrak{M}_2 \mathfrak{M}_3 \mathfrak{M}_1) - \varrho_4 \text{Tr}(\mathfrak{M}_0 \mathfrak{M}_2 \mathfrak{M}_3 \mathfrak{M}_1 \mathfrak{M}_3) + \varrho_4 \text{Tr}(\mathfrak{M}_0 \mathfrak{M}_2 \mathfrak{M}_1) A_3 \,. \end{aligned} \tag{B.2}$$

Finally, we use again(5.54) to replace the $\mathfrak{M}_1$ in red as $\mathfrak{M}_1 \to \varrho_4 \mathbb{1} - \mathfrak{M}_0 - \mathfrak{M}_2 - \mathfrak{M}_3$, obtaining:

$$\begin{aligned} A_2A_1A_3 = & -\mathrm{tr}(\mathfrak{M}_0\mathfrak{M}_2\mathfrak{M}_3\mathfrak{M}_0\mathfrak{M}_2\mathfrak{M}_3) - \varrho_1 A_2A_3 - \varrho_2 A_1A_3 + \varrho_1\varrho_3 A_2 - \varrho_3\varrho_2(A_3+A_2) \\ & + \varrho_3 \mathrm{Tr}(\mathfrak{M}_0\mathfrak{M}_2\mathfrak{M}_3\mathfrak{M}_1) + \varrho_4 \mathrm{Tr}(\mathfrak{M}_0\mathfrak{M}_2\mathfrak{M}_3\mathfrak{M}_2\mathfrak{M}_3) - \varrho_4 \mathrm{Tr}(\mathfrak{M}_0\mathfrak{M}_2\mathfrak{M}_3\mathfrak{M}_1\mathfrak{M}_3) \\ & + \varrho_4 \mathrm{Tr}(\mathfrak{M}_0\mathfrak{M}_2\mathfrak{M}_1) A_3 \,. \end{aligned} \tag{B.3}$$

Now, let us compute

$$\begin{aligned} \mathrm{Tr}(\mathfrak{M}_0\mathfrak{M}_2\mathfrak{M}_1) &= -\mathrm{Tr}(\mathfrak{M}_0\mathfrak{M}_2\mathfrak{M}_3) - \varrho_4 A_2 - 2\varrho_4\varrho_2 \\ \mathrm{Tr}(\mathfrak{M}_0\mathfrak{M}_2\mathfrak{M}_3\mathfrak{M}_1) &= \varrho_4 \mathrm{Tr}(\mathfrak{M}_0\mathfrak{M}_2\mathfrak{M}_1) - \varrho_2 A_1 - \varrho_1 A_2 - A_2A_1 \\ &= -\varrho_4 \mathrm{Tr}(\mathfrak{M}_0\mathfrak{M}_2\mathfrak{M}_3) - \varrho_4^2 A_2 - 2\varrho_4^2\varrho_2 - \varrho_2 A_1 - \varrho_1 A_2 - A_2A_1 \\ \mathrm{Tr}(\mathfrak{M}_0\mathfrak{M}_2\mathfrak{M}_3\mathfrak{M}_1\mathfrak{M}_3) &= -\mathrm{Tr}(\mathfrak{M}_0\mathfrak{M}_2\mathfrak{M}_3\mathfrak{M}_2\mathfrak{M}_3) - (A_3+\varrho_3)\mathrm{Tr}(\mathfrak{M}_0\mathfrak{M}_2\mathfrak{M}_3) + \varrho_4\varrho_3 A_2 \\ &= -\left[\mathrm{Tr}(\mathfrak{M}_0\mathfrak{M}_2\mathfrak{M}_3\{\mathfrak{M}_2,\mathfrak{M}_3\}) - 2\varrho_4\varrho_3\varrho_2\right] - (A_3+\varrho_3)\mathrm{Tr}(\mathfrak{M}_0\mathfrak{M}_2\mathfrak{M}_3) + \varrho_4\varrho_3 A_2 \\ &= -\left[\mathrm{Tr}(\mathfrak{M}_0\mathfrak{M}_2\mathfrak{M}_3)(A_1+\varrho_4^2+\varrho_1-\varrho_3-\varrho_2) - 2\varrho_4\varrho_3\varrho_2\right] \\ &\quad - (A_3+\varrho_3)\mathrm{Tr}(\mathfrak{M}_0\mathfrak{M}_2\mathfrak{M}_3) + \varrho_4\varrho_3 A_2 \end{aligned} \tag{B.4}$$

where in the last line, we have applied $(\mathfrak{M}_2+\mathfrak{M}_3)^2 = (\mathbb{1}\varrho_4 - \mathfrak{M}_0 - \mathfrak{M}_1)^2$.

Using these relations and the fact that $\sum_i A_i = -2\varrho_4^2$ we can write

$$\begin{aligned} A_2A_1A_3 = & -\mathrm{tr}(\mathfrak{M}_0\mathfrak{M}_2\mathfrak{M}_3\mathfrak{M}_0\mathfrak{M}_2\mathfrak{M}_3) - (\varrho_1+\varrho_4^2)A_2A_3 - (\varrho_2A_3+\varrho_3A_2)(A_1+2\varrho_4^2) \\ & + 2\varrho_4\mathrm{Tr}(\mathfrak{M}_0\mathfrak{M}_2\mathfrak{M}_3)\left[A_1+\varrho_4^2+\varrho_1-\varrho_2-\varrho_3\right] - 4\varrho_4^2\varrho_3\varrho_2 \end{aligned} \tag{B.5}$$

Finally, using $\mathrm{tr}(\mathfrak{M}_0\mathfrak{M}_2\mathfrak{M}_3\mathfrak{M}_0\mathfrak{M}_2\mathfrak{M}_3) = [\mathrm{tr}(\mathfrak{M}_0\mathfrak{M}_2\mathfrak{M}_3)]^2$ and $B \equiv \mathrm{tr}(\mathfrak{M}_0\mathfrak{M}_2\mathfrak{M}_3)$, we obtain (6.103).

B.2 Universal flop of length 2 from $SU(2)$ with 4 flavors

Let us see what happens in the mirror dual of the D_4 quiver gauge theory, when a background for Φ is turned on. The mirror theory is a $SU(2)$ gauge theory with 4 flavors; it is realized by a D2-brane probing a stack of 4 D6-branes (plus their images) on top of an orientifold O6-plane.

Mirror symmetry maps the moment map μ (above (5.46)) into the meson matrix of the dual

theory ($SU(2)$ with 4 flavors):

$$\mathcal{M} = \begin{pmatrix} Q^T\tilde{Q}^T & Q^T\epsilon Q \\ -\tilde{Q}\epsilon^{-1}\tilde{Q}^T & -\tilde{Q}Q \end{pmatrix}$$
$$\updownarrow \tag{B.6}$$

Let us consider the Higgs field generating the universal flop of length $\ell = 2$, i.e. Φ given in (6.86). Turning on such a vev on the worldvolume of the D6-branes will induce the following mass term on the probe D2-brane:

$$\begin{aligned}\delta W = \frac{1}{2}\mathrm{Tr}(\Phi\mathcal{M}) = \tilde{Q}_1Q^2 + \tilde{Q}_3Q^4 - \tilde{Q}_4\epsilon^{-1}\tilde{Q}_3^T + \varrho_1\tilde{Q}_2Q^1 \\ + \varrho_2(Q^3)^T\epsilon Q^4 + \varrho_3\tilde{Q}_4Q^3 + \varrho_4(\tilde{Q}_1Q^1 + \tilde{Q}_2Q^2)\end{aligned} \tag{B.7}$$

Here we adopt the conventions: $\epsilon \equiv \epsilon_{ab}\,(\epsilon_{12} = -1), \epsilon^{-1} \equiv \epsilon^{ab}, \tilde{Q} \equiv \tilde{Q}_i^b, \quad Q = Q_a^j$. The deformed superpotential reads:

$$W = \tilde{Q}\Psi Q + \tilde{Q}_1Q^2 + \tilde{Q}_3Q^4 - \tilde{Q}_4\epsilon^{-1}\tilde{Q}_3^T + \varrho_1\tilde{Q}_2Q^1 + \varrho_2(Q^3)^T\epsilon Q^4 + \varrho_3\tilde{Q}_4Q^3 + \varrho_4(\tilde{Q}_1Q^1 + \tilde{Q}_2Q^2) \tag{B.8}$$

The mass terms in (B.8) deform the CB of the theory. To see this, let us analyze the mass spectrum of matter fields on a generic point of the CB. Here the gauge group is broken to its Cartan and $\Psi = \psi_3\sigma_3$ with σ_3 denoting the third Pauli matrix. The mass matrix is then given by

$$m = \begin{pmatrix} \psi_3\sigma_3 + \varrho_4\mathbb{1}_2 & \mathbb{1}_2 & 0 & 0 & 0 & 0 & 0 & 0 \\ \varrho_1\mathbb{1}_2 & \psi_3\sigma_3 + \varrho_4\mathbb{1}_2 & 0 & 0 & 0 & 0 & 0 & 0 \\ 0 & 0 & \psi_3\sigma_3 & \mathbb{1}_2 & 0 & 0 & 0 & \epsilon^{-1} \\ 0 & 0 & \varrho_3\mathbb{1}_2 & \psi_3\sigma_3 & 0 & 0 & -\epsilon^{-1} & 0 \\ 0 & 0 & 0 & 0 & -\psi_3\sigma_3 - \varrho_4\mathbb{1}_2 & -\varrho_1\mathbb{1}_2 & 0 & 0 \\ 0 & 0 & 0 & 0 & -\mathbb{1}_2 & -\psi_3\sigma_3 - \varrho_4\mathbb{1}_2 & 0 & 0 \\ 0 & 0 & 0 & -\varrho_2\epsilon & 0 & 0 & -\psi_3\sigma_3 & -\varrho_3\mathbb{1}_2 \\ 0 & 0 & \varrho_2\epsilon & 0 & 0 & 0 & -\mathbb{1}_2 & -\psi_3\sigma_3 \end{pmatrix}$$

and the mass term reads $W_m \equiv \frac{1}{2}(\tilde{Q}, Q^T)\cdot m \cdot (Q^T, \tilde{Q})^T$.

From it, we can deduce the monopole equation for the CB after turning on Φ [32]:

$$V_+V_- = \frac{\sqrt{\det(m)}}{\psi_3^4} = \frac{((-\psi_3^2+\varrho_1-\varrho_4^2)^2-4\varrho_4^2\psi_3^2)((-\psi_3^2+\varrho_3-\varrho_2)^2-4\varrho_2\psi_3^2)}{\psi_3^4} \tag{B.9}$$

At the denominator, we find the contribution from the W bosons' masses, which are left unchanged by the deformation. Out of $V_\pm, \psi_3$ we construct the Weyl invariant operators:

$$z \equiv -\psi_3^2, \quad y \equiv \frac{V_+ + V_-}{2} + \frac{(\varrho_2-\varrho_3)(\varrho_1-\varrho_4^2)}{\psi_3^2}, \quad x \equiv \psi_3\frac{V_+ - V_-}{2}. \tag{B.10}$$

Under such identifications, we have:

$$x^2 + z\left(y + \frac{(\varrho_2-\varrho_3)(\varrho_1-\varrho_4^2)}{z}\right)^2 = -\psi_3^2 V_+V_- \,. \tag{B.11}$$

The equation (B.9) then implies:

$$\begin{aligned} x^2 + zy^2 =& \frac{((z+\varrho_1-\varrho_4^2)^2+4\varrho_4^2 z)((z+\varrho_3-\varrho_2)^2+4\varrho_2 z) - (\varrho_2-\varrho_3)^2(\varrho_1-\varrho_4^2)^2}{z} \\ & - 2y(\varrho_2-\varrho_3)(\varrho_1-\varrho_4^2)\,. \end{aligned} \tag{B.12}$$

This is the expected equation (5.42) for the universal flop of length $\ell = 2$.

The computation of the universal flop equation on this side of the duality, gives the same result as computed with the mirror dual (5.66) (up to the coordinate change (5.43)). This is expected as we believe in mirror symmetry. Of course, the match is perfect if the duality map is settled appropriately, and this happens when the moment map M on this side is mapped by mirror symmetry to μ in the equation above (5.46) (moreover, we are also assuming that the abelian mirror maps as in Section 2.2.3 are correct). One can also prove that, up to a proper rescaling, the quantum monopole relations satisfied by the elements of μ reproduce the right relations the meson matrix M should fulfill.

Appendix C

C.1 Levi subalgebras

In this section, we will give two simple working definitions of Levi subalgebras, for reading convenience. The first definition is only valid for $sl_n\mathbb{C}$, the second is general. Both are equivalent, and are consequences of the more formal definition, which we will not give, in terms of parabolics and radicals.

Definition 1: Diagonal Blocks A Levi subalgebra of $sl_n\mathbb{C}$ consists in an algebra of block diagonal matrices, i.e. for $sl_5\mathbb{C}$, one possible Levi subalgebra is given by all matrices of the form:

$$A = \begin{pmatrix} * & * & 0 & 0 & 0 \\ * & * & 0 & 0 & 0 \\ 0 & 0 & * & * & 0 \\ 0 & 0 & * & * & 0 \\ 0 & 0 & 0 & 0 & * \end{pmatrix} \in sl_5\mathbb{C} \tag{C.1}$$

Defnition 2: Centralizers Given a *semi-simple* (diagonalizable) element $x \in \mathfrak{g}$ of a Lie algebra, the centralizer $\mathfrak{l} \subset \mathfrak{g}$, defined as

$$\mathfrak{l} := \{y \in \mathfrak{g} | [y, x] = 0\} \tag{C.2}$$

is a Levi subalgebra. For instance, in $sl_5\mathbb{C}$, the Levi subalgebra associated with the following element:

$$x = \begin{pmatrix} m_1 & 0 & 0 & 0 & 0 \\ 0 & m_1 & 0 & 0 & 0 \\ 0 & 0 & m_2 & 0 & 0 \\ 0 & 0 & 0 & m_2 & 0 \\ 0 & 0 & 0 & 0 & -2m_1 - 2m_2 \end{pmatrix} \tag{C.3}$$

consists in the subalgebra defined in the previous definition (C.1).

Appendix D

D.1 Quivers and path algebras

A quiver Q is a finite directed graph specified by the combinatorial data (Q_0, Q_1, h, t). Here, Q_0 is the set of vertices, Q_1 is the set of arrows, and the maps $h, t : Q_1 \to Q_0$ assign to each arrow its head and tail, respectively.

The path algebra $\mathbb{C}Q$ is the $\mathbb{C}$-vector space spanned by all oriented paths in Q, with multiplication given by concatenation of paths whenever this is defined. For arrows $a, b \in Q_1$, one sets

$$a \cdot b := \begin{cases} ab, & h(b) = t(a), \\ 0, & h(b) \neq t(a). \end{cases} \tag{D.1}$$

A representation $\rho_{\mathbf{d}}$ of Q with dimension vector $\mathbf{d} = (d_i)_{i \in Q_0}$ consists of a collection of vector spaces and linear maps

$$\rho_{\mathbf{d}} : \qquad \big\{ \rho_{\mathbf{d}}(i) = V_i \simeq \mathbb{C}^{d_i}, \qquad \rho_{\mathbf{d}}(a) : V_{t(a)} \to V_{h(a)} \big\}_{i \in Q_0,\, a \in Q_1} . \tag{D.2}$$

Quivers with potential. The category $\mathrm{Rep}(Q)$ of quiver representations is equivalent to the category of finitely generated left $\mathbb{C}Q$-modules. More generally, one may impose relations on the path algebra by specifying a superpotential W, whose formal derivatives generate a two-sided

ideal. One then defines the Jacobian algebra

$$\mathcal{A}(Q,W) := \mathbb{C}Q/\partial W, \qquad \partial W = \langle\langle \partial_a W : a \in Q_1 \rangle\rangle. \tag{D.3}$$

Representations of $\mathcal{A}(Q,W)$ are thus representations of the quiver subject to the F-term relations.

D.2 Quiver representations and θ-stability

To construct moduli spaces of quiver representations, one introduces a stability condition specified by a parameter

$$\theta = (\theta_i)_{i\in Q_0} \in \mathbb{Z}^{Q_0}, \tag{D.4}$$

subject to the constraint

$$\theta \cdot \mathbf{d} = \sum_{i\in Q_0} \theta_i d_i = 0. \tag{D.5}$$

A representation $\rho_{\mathbf{d}}$ is said to be θ-stable if for every proper nonzero subrepresentation $\rho_{\mathbf{d}'} \subset \rho_{\mathbf{d}}$ one has

$$\theta \cdot \mathbf{d}' > 0, \tag{D.6}$$

and θ-semistable if $\theta \cdot \mathbf{d}' \geq 0$.

For fixed $\mathbf{d}$, the space of representations of $\mathcal{A}(Q,W)$ carries a natural action of the complexified gauge group

$$G_{\mathbf{d}} = \prod_{i\in Q_0} GL(d_i,\mathbb{C}), \tag{D.7}$$

and the moduli space of θ-stable representations is obtained as a GIT quotient.

D.2.1 From GLSMs to stable quiver representations

The relation with gauged linear sigma models (GLSMs) is that both constructions produce moduli spaces as quotients depending on a stability parameter. In a GLSM, one obtains a space of the form

$$V/\!/_\theta G, \tag{D.8}$$

and varying θ produces different geometric phases, including singular varieties and their resolutions.

In the quiver setting, the same structure appears in the moduli space of θ-stable representations of the algebra $\mathcal{A}(Q, W)$ for fixed dimension vector $\mathbf{d}$. The data $(\mathbf{d}, \theta)$ therefore determine a moduli problem, but neither of them alone is sufficient: the dimension vector specifies the size of the representation, while θ selects which representations of that size are retained. For fixed $\mathbf{d}$, the condition $\theta \cdot \mathbf{d} = 0$ leaves a family of possible stability parameters, organized into chambers corresponding to different geometric phases.

Generation from a distinguished vertex. Let $0 \in Q_0$ be a distinguished vertex. A representation is said to be *generated by vertex* 0 if the smallest subrepresentation containing V_0 is the whole representation. Concretely, given a vector $v \in V_0$ and a path

$$p = a_k \cdots a_1, \qquad t(a_1) = 0,\ h(a_k) = i, \tag{D.9}$$

one obtains a vector in V_i by

$$\rho(p)(v) = \rho(a_k) \circ \cdots \circ \rho(a_1)(v). \tag{D.10}$$

The representation is generated by vertex 0 if every V_i is spanned by such vectors, for all possible paths starting at 0.

This condition is enforced by a suitable choice of stability parameter. For a given dimension vector $\mathbf{d} = (d_i)$, define

$$\theta_0 = -\sum_{i \neq 0} d_i, \qquad \theta_i = d_0 \quad (i \neq 0), \tag{D.11}$$

so that $\theta \cdot \mathbf{d} = 0$. The key feature is that $\theta_0 < 0$ while $\theta_i > 0$ for $i \neq 0$.

Consider now a subrepresentation $W \subset V$ with dimension vector $\mathbf{d}'$. There are two possibilities:

- If W contains V_0, then $d'_0 = d_0$ and one finds

$$\theta \cdot \mathbf{d}' < 0, \tag{D.12}$$

  so W is destabilizing.

- If W does not contain V_0, then $d'_0 < d_0$ and one finds

$$\theta \cdot \mathbf{d}' > 0, \tag{D.13}$$

  so W does not destabilize the representation.

Therefore, θ-stability is equivalent to requiring that no proper subrepresentation contains V_0, which is precisely the condition that the representation be generated by vertex 0.

Relation to geometry. From the physical point of view, the resulting moduli space is the vacuum moduli space of the quiver quantum mechanics describing a $D0$-brane probe. From the algebraic point of view, in favorable cases the algebra $\mathcal{A}(Q, W)$ is a non-commutative crepant resolution (NCCR) of the coordinate ring R of a singular variety [55, 175–179].

If

$$A \cong \mathrm{End}_R\Big(\bigoplus_{i=0}^{n} M_i\Big), \qquad M_0 \cong R, \tag{D.14}$$

one takes the dimension vector

$$\mathbf{d} = \big(\mathrm{rk}\, M_i\big)_{i=0}^{n}, \tag{D.15}$$

which is determined by the geometry. The corresponding moduli space depends on the choice of stability chamber, and the chamber described above selects representations generated from the distinguished vertex 0. For θ in this chamber, one obtains

$$Y \cong \mathcal{M}_\theta(A, \mathbf{d}), \tag{D.16}$$

where $Y \to \mathrm{Spec}R$ is a crepant resolution.

Thus GLSMs describe individual GIT quotients associated with particular stability parameters, while the non-commutative crepant resolution provides a single algebraic object whose moduli spaces of stable representations recover these quotients, with the resolved geometry arising for a specific choice of $(\mathbf{d}, \theta)$.
The first example we are going to discuss is the so-called Kronecker quiver (with two arrows). This will turn out to be very useful for the analysis of a class of unoriented quivers that includes the Conifold and the Reid Pagodas. The representation theory of these rather complex cases is, in fact, almost entirely reducible to the Kronecker's, as was pointed out in [106].

D.3 Kronecker quiver

This case is relatively simple to study due to the finiteness of the quiver's path algebra. Indeed, it has been worked out in full in the mathematical literature [180]. Anyway, it is instructive to examine it in detail.

We want to study the representation theory of a quiver shaped as:

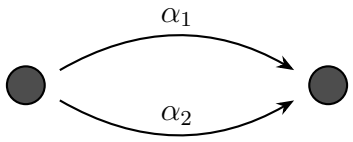

Figure D.1: Kronecker quiver.

A generic representation is given by vector spaces (V_L, V_R) of dimension $d = (d_L, d_R)$ and linear maps $(\alpha_1, \alpha_2) \in \mathcal{M}_{d_R \times d_L}(\mathbb{C})$.
We now define stability with respect to a parameter $\theta = (\theta_L, \theta_R)$, defined by:

$$d \cdot \theta = 0 \tag{D.17}$$

There are two independent choices:

$$\theta_1 = (-d_R, d_L), \quad \theta_2 = -\theta_1 = (d_R, -d_L) \tag{D.18}$$

To study the θ-stability of the representation, it is convenient to represent the dimension and the θ vectors as elements of a $\mathbb{Z}^2$ lattice in $\mathbb{R}^2$.

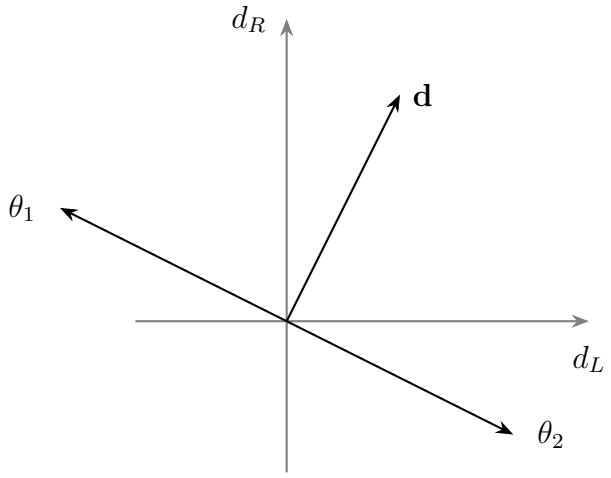

Figure D.2: xy-plane

The representation is unstable if at least a subrepresentation d' is such that $\theta \cdot d' < 0$. Then, θ_1-destabilizing subrepresentations are such that $\frac{d'_R}{d'_L} < \frac{d_R}{d_L}$. Similarly, for θ_2, we must have $\frac{d'_R}{d'_L} > \frac{d_R}{d_L}$. Let us first analyze θ_2-stability.

D.3.1 θ_2-stability

This is quite trivial. Indeed, in this case, representation $d' = (0, 1)$ is destabilizing, and it is a subrepresentation for any choice of dimension vector d and maps α_i. In other words, the following diagram is always commutative:

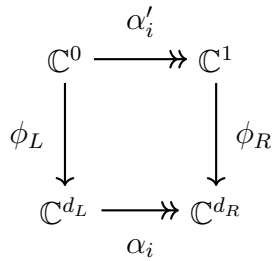

Figure D.3: Representation $(0, 1)$ is always a subrepresentation of (d_L, d_R).
Here, map $\Phi = (\phi_L, \phi_R)$ denotes a homomorphism of representations.

As a consequence, only $(1,0)$ and $(0,1)$ are θ_2-stable.

D.3.2 θ_1-stability

It is known that all θ-semistable representations of the Kronecker quiver with two inner arrows consist of [180]:

$$(k, k+1), \quad (k,k), \quad (k+1,k) \tag{D.19}$$

It is instructive to concretely see why this is the case.

$d_L < d_R$

The logic we are adopting is this: use the automorphism group of the quiver representations (namely $GL(d_L) \times GL(d_R)$, $GL(d'_L) \times GL(d'_R)$) to fix the maps α_i and α'_i. Then, look for a map $\Phi = (\phi_L, \phi_R)$, such that $\alpha_i \cdot \phi_L = \phi_R \cdot \alpha'_i$. If such a map exists and d' satisfies $d' \cdot \theta_1 < 0$, we can conclude that no stable (nor semistable) representation exists for the chosen d.
For clarity, let us set $d_L = k$ and $d_R = k + n$, with $k, n \in \mathbb{N}$.
First, we argue that all maps α_i must be injective.
Suppose α_1 were not injective. Namely:

$$\exists\, \mathbf{v} \in \mathbb{C}^k \quad \text{s.t.} \quad \alpha_1(\mathbf{v}) = \mathbf{0}, \quad \alpha_2(\mathbf{v}) = \mathbf{w} \in \mathbb{C}^{k+n}. \tag{D.20}$$

Then, the span of vectors $\mathbf{v}$ and $\mathbf{w}$ would be a $(1,1)$ (i.e. a destabilizing one) subrepresentation of $(k, k+n)$[1].
Another necessary condition for stability is:

$$\text{Im}\alpha_1 \oplus \text{Im}\alpha_2 \simeq \mathbb{C}^{k+n} \tag{D.21}$$

This implies: $2k \geq k + n > k$. When $k + n > 2k$ we can always construct a destabilizing subrepresentation by projecting away the cokernel of maps α_i via an apposite ϕ_R (in other words, we can map injectively $\oplus_i \text{Im}\alpha_i$ into $\mathbb{C}^{k+n}$).

[1] To see this we just need to take maps $\phi_L : \mathbb{C} \to \mathbb{C}^k$ and $\phi_R : \mathbb{C} \to \mathbb{C}^{n+k}$, such that: $\text{Im}\phi_L = \text{Span}\{\mathbf{v}\}, \quad \text{Im}\phi_R = \text{Span}\{\mathbf{w}\}$

From now on, we focus on the case: $k \geq n$. In this case, we can always write:

$$k = mn + l, \quad m \in \mathbb{N},\ l = 0, ..., n-1^{2} \tag{D.22}$$

We want to prove that, given a rep $(mn+l, (m+1)n+l)$, there is always a subrep with dimension vector $(m(n-1)+l, (m+1)(n-1)+l)$ that destabilizes it. Namely:

$$\forall\, \alpha_i : \mathbb{C}^{mn+l} \to \mathbb{C}^{(m+1)n+l} \quad \exists \quad \alpha_i', \phi_L, \phi_R \quad \text{s.t. the diagram:} \tag{D.23}$$

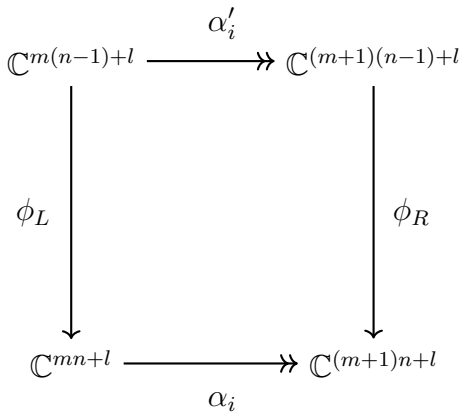

is commutative[3] Let us show this iteratively. We start by considering the case $m = 2$.
We want to prove that no matter how we choose the maps of the $(2n+l, 3n+l)$-representation, we can always identify a destabilizing subrep. To this end, we look for vectors $\mathbf{v} \in \mathbb{C}^k$ such that:

$$\alpha_1(\mathbf{v}) \notin \text{Im}\alpha_2, \quad \alpha_2(\mathbf{v}) \notin \text{Im}\alpha_1 \tag{D.25}$$

Indeed, if such a vector exists, by removing its Span from the domain $\mathbb{C}^k$, the dimension of $\text{Im}\alpha_1 \oplus \text{Im}\alpha_2$ decreases by a factor 2. As a result, we would get a $(k-1, k+n-2)$-subrep. Now, since the α's are injective we know that $\text{Im}\alpha_1 \cap \text{Im}\alpha_2 \simeq \mathbb{C}^{k-n}$. Given the dimensions of domain and

[2] Alternatively we can say: $(m+1)n > k \geq mn$ for some $m \in \mathbb{N}$.

[3] Look at the inequality:

$$\frac{d_R'}{d_L'} < \frac{k+n}{k}, \tag{D.24}$$

Inside the window $(m+1)n > k \geq mn$, the subvector (d_L', d_R') that satisfies the inequality while maximising the ratio $\frac{d_R'}{d_L'}$ is precisely of the form $(k-m, k+n-m-1)$.

codomain, and the fact that the maps are injective, it is clear that there is a set of vectors $\{\mathbf{v}_i\}_{i=1,...,n}$ in the domain such that $\alpha_1(\mathbf{v}_i) \notin \text{Im}\alpha_2 \, \forall \, i$[4].

What is not obvious is weather $\alpha_2(\mathbf{v}_i) \notin \text{Im}\alpha_1$ for at least one i. To avoid the existence of such vectors, we should choose α_1 and α_2 in such a way that $\alpha_2(\mathbf{v}_i) \in \text{Im}\alpha_1 \quad \forall \, i = 1, ..., n$. However, this is only possible if $k - n \geq n$.
In other words, when $k - n < n$, there is always at least one vector $\mathbf{v}$ in $\mathbb{C}^k$ s.t. $\alpha_1(\mathbf{v}) \notin \text{Im}\alpha_2$ and $\alpha_2(\mathbf{v}) \notin \text{Im}\alpha_1$. Any rep of this kind is destabilized by a subrep of dimension $(k-1, n+k-2)$[5]. It is convenient to decompose domain and codomain in the following way:

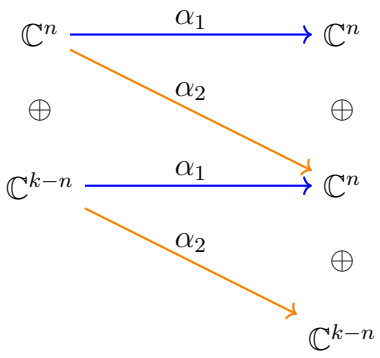

The domain is decomposed according to the action of α_1. Namely, the $\mathbb{C}^n$ is the span of vectors $\{\mathbf{v}_i\}_{i=1,...,n}$. In the codomain, the upper $\mathbb{C}^n$ is the span of $\alpha_1(\{\mathbf{v}_i\})$. The lower one is the span of $\alpha_2(\{\mathbf{v}_i\})$. When $k - n < n$, there are vectors in $Span < \alpha_2(\{\mathbf{v}_i\}) >$ which do not have a α_1 counterimage.

Now, let us consider the case $k \geq 2n$. The subvector of $d = (k, k+n)$ that maximises the ratio d'_R/d'_L is $(k-2, k+n-3)$. We want to find the necessary and sufficient conditions to avoid the existence of such a subrep. Along the lines of the previous reasoning, we must prohibit the existence of at least two linearly independent vectors in the domain whose elimination would

[4]We can always choose basis (using $GL_k(\mathbb{C})$ and $GL_{n+k}(\mathbb{C})$) such that:

$$\alpha_2 = \begin{pmatrix} A_{k,k} \\ \mathbf{0}_{n,k} \end{pmatrix}, \quad \alpha_1 = \begin{pmatrix} B_{k,k-n} & \mathbf{0}_{k,n} \\ \mathbf{0}_{n,k-n} & D_{n,n} \end{pmatrix} \tag{D.26}$$

Here A and D are nonsingular square matrices. With this choice, the set $\{\mathbf{v}_i\}$ is given by the last n vectors of the canonical basis $\{e_a\}$, $a = k - n + 1, ..., k$

[5]Note that our reasoning is perfectly symmetric under exchange of α_1 and α_2

make the dimension of $\text{Im}\alpha_1 \oplus \text{Im}\alpha_2$ decrease by a factor 3.[6] First, we impose that $Span < \alpha_2(\{\mathbf{v}_i\}) >_{\subset} \text{Im}\alpha_1$. Otherwise we would be in the previous situation. Schematically, we have:

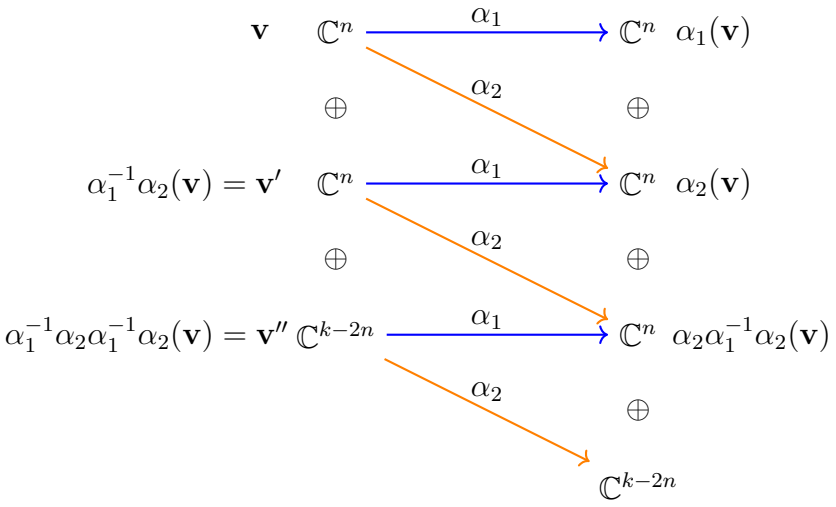

If $k - 2n < n$, then we can surely find at least two vectors $\mathbf{v}$, $\mathbf{v}'$, s.t. $\alpha_1(\mathbf{v}) \notin \text{Im}\alpha_2$, $\alpha_2(\mathbf{v}) = \alpha_1(\mathbf{v}')$, $\alpha_2(\mathbf{v}') \notin \text{Im}\alpha_1$.
If $k - 2n \geq n$, instead, for any pair $\mathbf{v}$, $\mathbf{v}'$, s.t. $\alpha_1(\mathbf{v}) \notin \text{Im}\alpha_2$, $\alpha_2(\mathbf{v}) = \alpha_1(\mathbf{v}')$ we'll always find a $\mathbf{v}''$, s.t. $\alpha_1(\mathbf{v}'') = \alpha_2(\mathbf{v}')$. Consequently, removing $\mathbf{v}$, $\mathbf{v}'$ will only decrease the dimension of the (union of the) α-images by a factor of 2. Iterating these steps, we can extract an answer for $k \geq mn$. We want to find m vectors:

$$\{\mathbf{v}_1, .., \mathbf{v}_m\} \in \mathbb{C}^k \quad \text{s.t.} \quad \alpha_1(\mathbf{v}_1) \notin \text{Im}\alpha_2, \tag{D.28}$$

$$\alpha_2(\mathbf{v}_1) = \alpha_1(\mathbf{v}_2) = \alpha_2(\mathbf{v}_3) = ... = \alpha_1(\mathbf{v}_m), \tag{D.29}$$

$$\alpha_2(\mathbf{v}_m) \notin \text{Im}\alpha_1 \tag{D.30}$$

[6] We are looking for vectors $\mathbf{v}$, $\mathbf{v}'$ s.t. :

$$\alpha_1(\mathbf{v}) \notin \text{Im}\alpha_2, \quad \alpha_2(\mathbf{v}) = \alpha_1(\mathbf{v}'), \quad \alpha_2(\mathbf{v}') \notin \text{Im}\alpha_1 \tag{D.27}$$

.

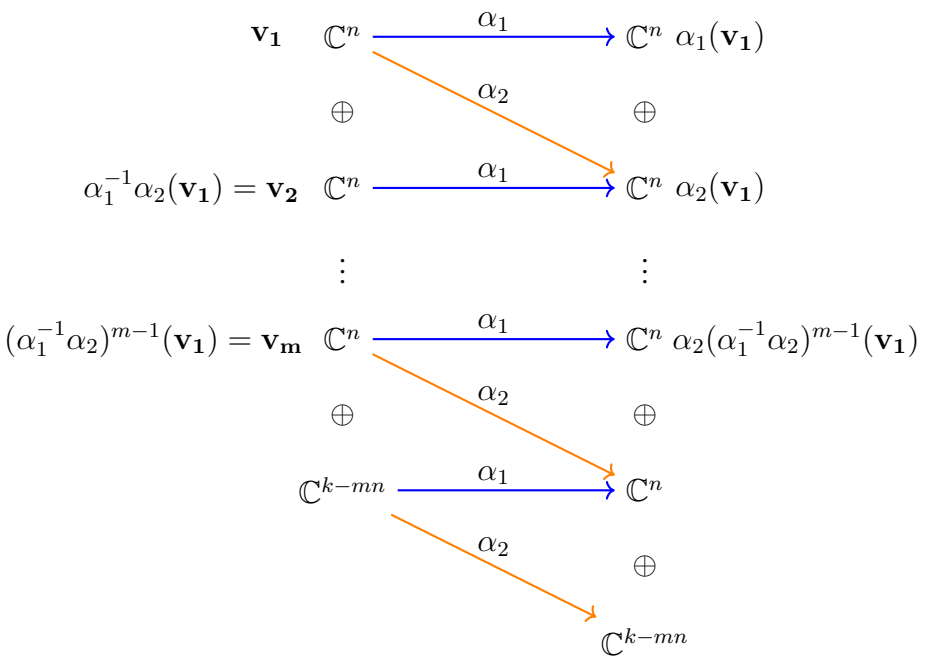

Again, this set of vectors exists only if $k - mn < n$. If this condition is met, as the m vectors are removed, the dimension of $\oplus \text{Im}\alpha_i$ decreases by $m+1$. We conclude that, for any $k = mn + l$, there is always a destabilizing subrep with dimension vector $(k-m, k+n-m-1)$. Note that, for $n = 1$, $k = m$ since $(m+1)n > k \geq mn$. This implies: $(k-m, k+n-m-1) = (0,0)$. Therefore, this argument doesn't tell us anything about the stability of the $x(k, k+1)$ reps.
Let us analyze them separately.

$(k, k+1)$ **representations:** We have to look for destabilizing subreps. So, first of all we require:

$$\mathbf{d} = (d'_L, d'_R) \quad : \quad \frac{d'_R}{d'_L} < \frac{k+1}{k} \tag{D.31}$$

Equivalently, we must have $d'_R \leq d'_L$. Trivially, we can exclude all subreps with: $\mathbf{d} = (k, k-l), \quad l = 1, .., k+1$, by imposing $\oplus_i \text{Im}\alpha_i \simeq \mathbb{C}^{k+1}$. The other possibilities are: $\mathbf{d} = (k-m, k+1-m')$ with $m' > m$[7]. The most restrictive case is for $m' = m+1$. But we know from the previous argument that no $(k-m, k+1-m-1)$-subrep exists unless $k = m$.
We conclude that finding stable $(k, k+1)$-representations is always possible.

[7] We have: $\frac{k+1-m'}{k-m} < \frac{k+1}{k} \quad \longrightarrow \quad m' > m\frac{k+1}{k}$

$d_L > d_R$

We now consider type $(k+n, k)$ representation vectors. Now, maps α_1, α_2 have a Kernel of dimension $\dim(\text{Ker}\alpha_i) \geq n$. Since the $(1,0)$-representation is destabilizing we must impose that $\cap_i \text{Ker}\alpha_i = \{0\}$. This requires that $k \geq \max_i \dim(\text{Ker}\alpha_i)$. The bound is minimized by $k \geq n$, which applies when both maps are surjective[8]. From now on, we will assume both α_i's to be surjective. As before, we look for destabilizing subreps, which can be defined for any choice of α's. First of all, note that subvectors (d'_L, d'_R) with $d'_L = d'_R$ are not destabilizing[9]. Then, take a vector $\mathbf{v} \in \text{Ker}\alpha_1$. For what we've just said, $\alpha_2(\mathbf{v}) \neq 0$. Since α_1 is surjective, there must be a vector $\mathbf{v}' \in \mathbb{C}^k$ such that $\alpha_1(\mathbf{v}') = \alpha_2(\mathbf{v})$. But then, if $\alpha_2(\mathbf{v}') = 0$ the two vectors and their α-image form a destabilizing $(2,1)$-subrep. At least a pair of such vectors exists only if $k - n < n$. We can visualize it in the following way:

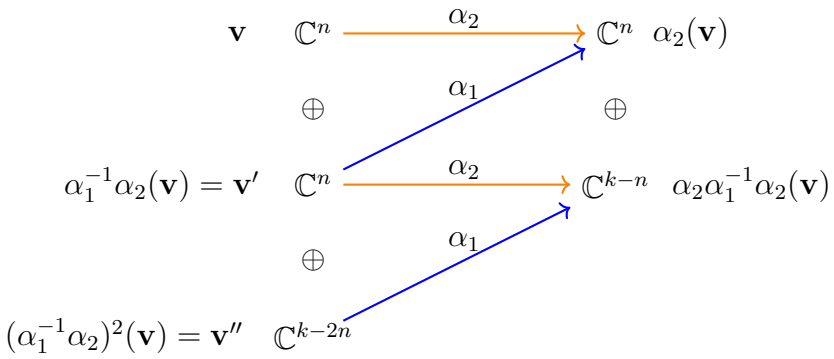

The upper $\mathbb{C}^n$ on the left is $\text{Ker}\alpha_1$. Summarizing, in the interval $2n > k \geq n$, it is always possible to identify a $(2,1)$-subrep, which makes the rep unstable. Iterating this procedure, we discover that, for $(m+1)n > k \geq mn$, there is always a destabilizing $(m+1, m)$ subrep.

[8] The bigger the Kernels, the easier it is to find destabilizing subreps. We have to look for destabilizing reps that exist as subreps no matter how we take the α_i.

[9] When $d'_L = d'_R$, $\quad 1 = \frac{d'_R}{d'_L} > \frac{k}{k+n}$.

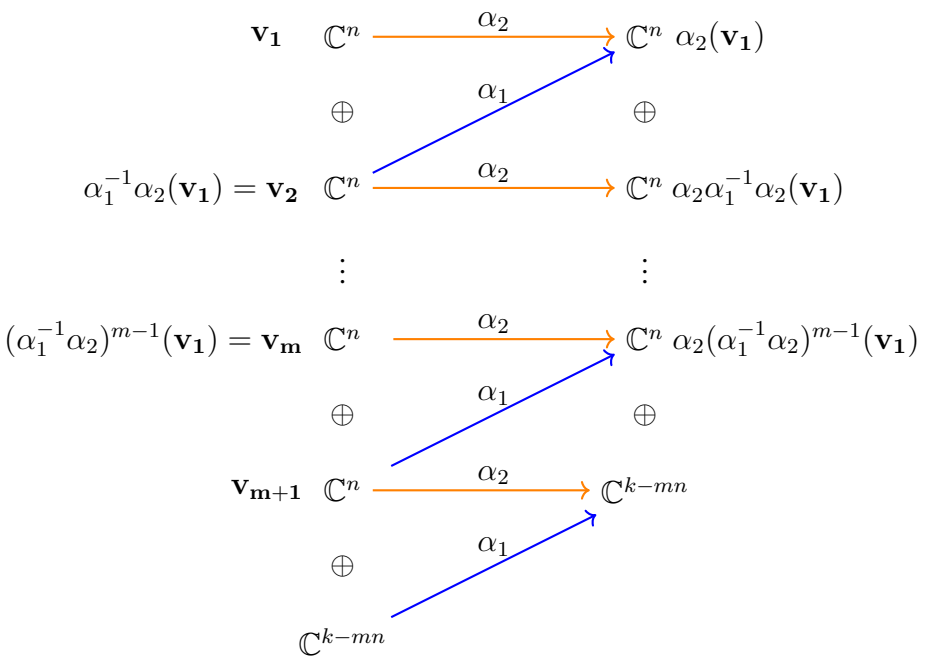

In the picture, we explicitly define a set of vectors $\{\mathbf{v}_J\}_{J=1,..,m+1}$ s.t.

$$\alpha_1(\mathbf{v}_1) = 0 \tag{D.32}$$

$$\alpha_2(\mathbf{v}_1) = \alpha_1(\mathbf{v}_2) = ... = \alpha_1(\mathbf{v}_{m+1}) \tag{D.33}$$

To have $\alpha_2(\mathbf{v}_{m+1}) = 0$ we need $k - mn < n$.

$(k+1, k)$ **representations** Again, when $n = 1$, the above argument doesn't identify any dangerous subrep[10]. So we discuss it separately. First, we observe that $d'_L > d'_R$. That means $(d'_L, d'_R) = (s, s-l)$, with $l = 1, .., s$, $s \leq k+1$. Surjectivity of α_1, α_2 already rules out subvectors $(s, s-l)$ with $l > 1$. Provided that $s \leq k$, we can always choose our maps in such a way as to avoid these reps. So the rep $(k+1, k)$ is stable by construction[11].

[10] It just tells me that $(k+n, k) = (m+1, m)$ is necessarily a subrep of itself

[11] We can always fix the sequence of vectors that interpolates between Kerα_1 and Kerα_2 to be as large as dim $= \mathbb{C}^{k+1}$

$d_L = d_R$

Explicit representatives for the stable maps of the $(k, k+1)$

Let us consider the representation

$$d_L = 1, \qquad d_R = 2. \tag{D.34}$$

Then, α_1, α_2 are two column vector with two entries. They can not have a kernel, since then the $(1,1)$ would be destabilizing, (the $(0,1)$ is always a subrep, so either one of the twos is in any case destabilizing). On top of that, the images must be linearly independent subspaces, else again the (1,1) destabilize. We can hence gauge-fix,

$$\alpha_1 = (a_1, 0), \qquad \alpha_2 = (0, a_2). \tag{D.35}$$

The residual gauge group, that we did not use to fix the gauge, is

$$\mathcal{G}_{res} = \mathbb{C}^*_{rel} \times \mathbb{C}^*_{\sigma_{3,right}}, \tag{D.36}$$

We notice that $a_1 \neq 0$ *and* $a_2 \neq 0$, and hence we can fix them both to one with (D.36)

D.4 The semistable representations of the Pagoda quiver

Let us recall the equation of the Reid Pagoda:

$$X_k : \qquad uv - (z - w^k)(z + w^k) = 0, \qquad (u, v, z, w) \in \mathbb{C}^4. \tag{D.37}$$

A noncommutative crepant resolution of X_k is described by the two-node quiver of fig. D.4, with loops w_1, w_2, arrows α_i from the left node to the right node, and arrows β_i in the opposite direction. Its Jacobian algebra is defined by the superpotential [18]

$$W = w_2(\alpha_1\beta_2 - \alpha_2\beta_1) + w_1(\beta_1\alpha_2 - \beta_2\alpha_1) - \frac{w_2^{k+1}}{k+1} + \frac{w_1^{k+1}}{k+1}, \tag{D.38}$$

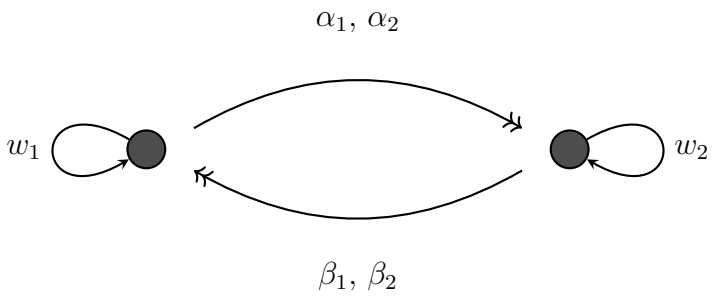

Figure D.4: Quiver of the Reid Pagoda.

whose F-term relations are

$$\alpha_1\beta_2 - \alpha_2\beta_1 - w_2^k = 0, \tag{D.39}$$
$$\beta_1\alpha_2 - \beta_2\alpha_1 - w_1^k = 0, \tag{D.40}$$
$$\alpha_i w_1 - w_2\alpha_i = 0, \tag{D.41}$$
$$\beta_i w_2 - w_1\beta_i = 0. \tag{D.42}$$

D.4.1 Center of the Jacobian algebra

A basic structural property of a noncommutative crepant resolution $\mathcal{A} \cong \mathrm{End}_{\mathcal{R}}(M)$ is that its center reproduces the coordinate ring of the singularity:

$$Z(\mathcal{A}) \cong \mathcal{R}. \tag{D.43}$$

In the present case, the relevant central elements are provided by the loops

$$\Theta_{ij} := (\beta_i\alpha_j, \alpha_j\beta_i), \qquad w := (w_1, w_2). \tag{D.44}$$

The fact that w is central follows immediately from (D.41)–(D.42). The elements Θ_{ij} are also central: the necessary commutation relations follow from the F-terms after suitable compositions with the arrows. In particular, one obtains the identities

$$\beta_i\alpha_i\beta_j = \beta_j\alpha_i\beta_i, \qquad i \neq j, \tag{D.45}$$
$$\alpha_i\beta_i\alpha_j = \alpha_j\beta_i\alpha_i, \qquad i \neq j, \tag{D.46}$$

which are sufficient to verify that the Θ_{ij} commute with the generators of the algebra.

For a Schur representation M, every central element acts by a scalar. Hence, one may write

$$\Theta_{ij} = \lambda_{ij}\,\mathbb{1}, \qquad w = \lambda_w\,\mathbb{1}, \qquad \lambda_{ij}, \lambda_w \in \mathbb{C}. \tag{D.47}$$

The scalars satisfy algebraic relations inherited from the path algebra. In particular,

$$\lambda_{12}\lambda_{21} = \lambda_{11}\lambda_{22}, \qquad \lambda_w^k = \lambda_{12} + \lambda_{21}, \tag{D.48}$$

and eliminating, for example, λ_{21} gives

$$\lambda_{12}(\lambda_w^k - \lambda_{12}) = \lambda_{11}\lambda_{22}. \tag{D.49}$$

This reproduces the defining equation of the Pagoda singularity, in agreement with (D.43). Thus the central scalars furnish a convenient coordinate system with which to organize the representations.

D.4.2 A remark on Schur representations

In the discussion below, it is convenient to restrict attention to Schur representations. This is justified for the analysis of stable points, since a stable representation has automorphism group equal to the scalars, and hence is Schur. The converse need not hold: a Schur representation need not be stable for a given choice of θ. Accordingly, Schur representations provide a useful class in which to analyze stability, but should not be identified *a priori* with the full stable locus.

D.4.3 Representations supported on the exceptional locus

We first consider the locus

$$\lambda_{ij} = 0, \qquad \forall\, i, j. \tag{D.50}$$

Geometrically, this corresponds to the fiber over the singular point of the threefold, and one expects it to capture representations supported on the exceptional locus of a small resolution.

Condition (D.50) implies that all composites $\beta_i\alpha_j$ and $\alpha_j\beta_i$ vanish. As in the conifold case, this

is achieved by setting one pair of arrows to zero. Choosing one chamber, we may impose

$$\beta_1 = \beta_2 = 0. \tag{D.51}$$

The opposite choice $\alpha_1 = \alpha_2 = 0$ corresponds to the other flop chamber.

After imposing (D.51), the quiver reduces to a two-node quiver with arrows α_1, α_2 and loops w_1, w_2. The F-term relations reduce to

$$w_1^k = 0, \qquad w_2^k = 0, \qquad w_2\alpha_i = \alpha_i w_1. \tag{D.52}$$

For a Schur representation, the central element $w = (w_1, w_2)$ acts by a scalar, so we may write

$$w_1 = \lambda_w \, \mathbb{1}_{d_1}, \qquad w_2 = \lambda_w \, \mathbb{1}_{d_2}. \tag{D.53}$$

Then (D.52) implies

$$\lambda_w^k = 0, \tag{D.54}$$

and therefore $\lambda_w = 0$ on such representations.

It follows that, on the Schur locus over the exceptional fiber, the loops do not introduce additional geometric moduli, although they do record a nonreduced structure of order k. In particular, the problem of determining which dimension vectors admit stable or semistable representations reduces to the corresponding question for the 2-Kronecker quiver. Hence the stable dimension vectors are the same as in the 2-Kronecker case:

$$(d_1, d_2) = (m, m+1), \qquad (m+1, m), \qquad (1, 1), \qquad m \in \mathbb{N}, \tag{D.55}$$

while strictly semistable representations occur for

$$(d_1, d_2) = (m, m). \tag{D.56}$$

The presence of the nilpotent parameter w should therefore be understood as a thickening of the exceptional-fiber locus rather than as a change in the list of admissible dimension vectors. For the purposes of stability, the reduced geometry is controlled by the same chamber structure as for the 2-Kronecker quiver.

D.4.4 Representations away from the exceptional locus

We now consider Schur representations for which the central scalars λ_{ij} are not all zero. In this regime, the central relations (D.45)–(D.46) imply proportionality conditions among the arrows. More precisely, using (D.47) one obtains

$$\beta_i \, \lambda_{ij} = \beta_j \, \lambda_{ii}, \tag{D.57}$$

$$\alpha_i \, \lambda_{ij} = \alpha_j \, \lambda_{ii}. \tag{D.58}$$

Whenever the relevant λ_{ii} are nonzero, these relations show that α_2 and β_2 are determined by α_1 and β_1. In this sense, away from the exceptional fiber the representation theory reduces to that of a simpler two-node quiver with one pair of arrows and the loops w_1, w_2.

Let us first consider the square dimension vector (m, m). In this case, if the corresponding central scalars are nonzero, the compositions $\alpha_1\beta_1$ and $\beta_1\alpha_1$ are nonzero scalar multiples of the identity. It follows that α_1 and β_1 are invertible. After a change of basis, one may set

$$\alpha_1 = \mathbb{1}_m, \tag{D.59}$$

and then β_1 is also forced to be a scalar multiple of the identity. Hence all arrows act by scalars, and the representation is a direct sum of copies of a one-dimensional representation. In particular, such representations are semistable but not stable.

For rectangular dimension vectors, such as $(m+1, m)$ or $(m, m+1)$, the same reduction suggests that any nonzero representation away from the exceptional locus contains a proper summand of square type, and is therefore decomposable. At the level of stable representations, this indicates that one does not obtain new stable objects away from the exceptional fiber. Since this step depends on a more detailed analysis of the ranks of α_1 and β_1, we state it here as the outcome suggested by the above reduction rather than as a separate theorem.

Summary

The center of the Pagoda Jacobian algebra provides a natural set of coordinates with which to organize its Schur representations. On the locus where the central composites Θ_{ij} vanish, the representation theory reduces to that of the 2-Kronecker quiver, with the additional nilpotent parameter w encoding a nonreduced thickening of order k. In particular, the stable and semistable dimension vectors are the same as in the 2-Kronecker case.

Away from the exceptional fiber, the nonvanishing of the central scalars forces proportionality relations among the arrows, reducing the representation to a simpler form. For square dimension vectors this yields only metastable representations, and the analysis strongly suggests that no genuinely new stable representations arise in the nonzero-central sector. Thus the stable BPS sector relevant for the small resolution is concentrated on the exceptional locus and is controlled, at the reduced level, by the same stability pattern as in the conifold case.

Bibliography

[1] Joseph Polchinski. "Dirichlet Branes and Ramond-Ramond charges". In: *Phys. Rev. Lett.* 75 (1995), pp. 4724–4727. DOI: 10.1103/PhysRevLett.75.4724. arXiv: hep-th/9510017.

[2] Michael R. Douglas and Gregory W. Moore. "D-branes, quivers, and ALE instantons". In: (Mar. 1996). arXiv: hep-th/9603167.

[3] Amihay Hanany and Edward Witten. "Type IIB superstrings, BPS monopoles, and three-dimensional gauge dynamics". In: *Nucl. Phys. B* 492 (1997), pp. 152–190. DOI: 10.1016/S0550-3213(97)00157-0. arXiv: hep-th/9611230.

[4] Ofer Aharony, Amihay Hanany, and Barak Kol. "Webs of (p,q) five-branes, five-dimensional field theories and grid diagrams". In: *JHEP* 01 (1998), p. 002. DOI: 10.1088/1126-6708/1998/01/002. arXiv: hep-th/9710116.

[5] Ofer Aharony and Amihay Hanany. "Branes, superpotentials and superconformal fixed points". In: *Nucl. Phys. B* 504 (1997), pp. 239–271. DOI: 10.1016/S0550-3213(97)00472-0. arXiv: hep-th/9704170.

[6] Amihay Hanany and Kristian D. Kennaway. "Dimer models and toric diagrams". In: (Mar. 2005). arXiv: hep-th/0503149.

[7] Amihay Hanany, Christopher P. Herzog, and David Vegh. "Brane tilings and exceptional collections". In: *JHEP* 07 (2006), p. 001. DOI: 10.1088/1126-6708/2006/07/001. arXiv: hep-th/0602041.

[8] Sebastian Franco et al. "Brane dimers and quiver gauge theories". In: *JHEP* 01 (2006), p. 096. DOI: 10.1088/1126-6708/2006/01/096. arXiv: hep-th/0504110.

[9] Sebastian Franco et al. "Gauge theories from toric geometry and brane tilings". In: *JHEP* 01 (2006), p. 128. DOI: 10.1088/1126-6708/2006/01/128. arXiv: hep-th/0505211.

[10] Bo Feng et al. "Dimer models from mirror symmetry and quivering amoebae". In: *Adv. Theor. Math. Phys.* 12.3 (2008), pp. 489–545. DOI: 10.4310/ATMP.2008.v12.n3.a2. arXiv: hep-th/0511287.

[11] Masahito Yamazaki. "Brane Tilings and Their Applications". In: *Fortsch. Phys.* 56 (2008), pp. 555–686. DOI: 10.1002/prop.200810536. arXiv: 0803.4474 [hep-th].

[12] F. Cachazo, S. Katz, and C. Vafa. "Geometric Transitions and N=1 Quiver Theories". In: (). eprint: hep-th/0108120. URL: https://arxiv.org/pdf/hep-th/0108120.pdf.

[13] Francesco Benini, Sergio Benvenuti, and Yuji Tachikawa. "Webs of five-branes and N=2 superconformal field theories". In: *JHEP* 09 (2009), p. 052. DOI: 10.1088/1126-6708/2009/09/052. arXiv: 0906.0359 [hep-th].

[14] Antoine Bourget, Andrés Collinucci, and Sakura Schafer-Nameki. "Generalized Toric Polygons, T-branes, and 5d SCFTs". In: *SciPost Phys.* 18 (2025), p. 079. DOI: 10.21468/SciPostPhys.18.3.079. arXiv: 2301.05239 [hep-th].

[15] Valery Alexeev, Hülya Argüz, and Pierrick Bousseau. "Non-toric Brane Webs, Calabi–Yau 3-Folds, and 5d SCFTs". In: *Commun. Math. Phys.* 406.11 (2025), p. 287. DOI: 10.1007/s00220-025-05461-9. arXiv: 2410.04714 [hep-th].

[16] Sergio Cecotti et al. "T-Branes and Monodromy". In: *JHEP* 1107 (2011), p. 030. DOI: 10.1007/JHEP07(2011)030. eprint: 1010.5780. URL: https://arxiv.org/pdf/1010.5780.pdf.

[17] Carina Curto and David Morrison. "Threefold Flops via Matrix Factorization". In: *Journal of Algebraic Geometry* 22 (Dec. 2006). DOI: 10.1090/S1056-3911-2013-00633-5.

[18] Paul S. Aspinwall and David R. Morrison. "Quivers from Matrix Factorizations". In: *Commun. Math. Phys.* 313 (2012), pp. 607–633. DOI: 10.1007/s00220-012-1520-1. arXiv: 1005.1042 [hep-th].

[19] Andrés Collinucci et al. "Flops of any length, Gopakumar-Vafa invariants, and 5d Higgs Branches". In: (Apr. 2022). arXiv: 2204.10366 [hep-th].

[20] Wu-yen Chuang and Guang Pan. "BPS State Counting in Local Obstructed Curves from Quiver Theory and Seiberg Duality". In: *J. Math. Phys.* 51 (2010), p. 052305. DOI: 10.1063/1.3364787. arXiv: 0908.0360 [hep-th].

[21] Andrés Collinucci et al. "High electric charges in M-theory from quiver varieties". In: *JHEP* 11 (2019), p. 111. DOI: 10.1007/JHEP11(2019)111. arXiv: 1906.02202 [hep-th].

[22] Fabio Apruzzi et al. "Fibers add Flavor, Part II: 5d SCFTs, Gauge Theories, and Dualities". In: *JHEP* 03 (2020), p. 052. DOI: 10.1007/JHEP03(2020)052. arXiv: 1909.09128 [hep-th].

[23] Miles Reid. "Young person's guide to canonical singularities". In: *Algebraic Geometry, Bowdoin 1985*. Ed. by Spencer J. Bloch. Vol. 46. Proc. Sympos. Pure Math. Providence, RI: Amer. Math. Soc., 1987, pp. 345–414.

[24] Andrés Collinucci, Andrea Sangiovanni, and Roberto Valandro. "Genus zero Gopakumar-Vafa invariants from open strings". In: *JHEP* 09 (2021), p. 059. DOI: 10.1007/JHEP09(2021)059. arXiv: 2104.14493 [hep-th].

[25] Andrés Collinucci et al. "Higgs branches of 5d rank-zero theories from geometry". In: *JHEP* 10.18 (2021), p. 018. DOI: 10.1007/JHEP10(2021)018. arXiv: 2105.12177 [hep-th].

[26] Mario De Marco, Andrea Sangiovanni, and Roberto Valandro. "5d Higgs branches from M-theory on quasi-homogeneous cDV threefold singularities". In: *JHEP* 10 (2022), p. 124. DOI: 10.1007/JHEP10(2022)124. arXiv: 2205.01125 [hep-th].

[27] Mario De Marco and Andrea Sangiovanni. "Higgs Branches of rank-0 5d theories from M-theory on (A_j, A_l) and (A_k, D_n) singularities". In: *JHEP* 03 (2022), p. 099. DOI: 10.1007/JHEP03(2022)099. arXiv: 2111.05875 [hep-th].

[28] Kenneth A. Intriligator and N. Seiberg. "Mirror symmetry in three-dimensional gauge theories". In: *Phys. Lett. B* 387 (1996), pp. 513–519. DOI: 10.1016/0370-2693(96)01088-X. arXiv: hep-th/9607207.

[29] Jan de Boer et al. "Mirror symmetry in three-dimensional theories, SL(2,Z) and D-brane moduli spaces". In: *Nucl. Phys. B* 493 (1997), pp. 148–176. DOI: 10.1016/S0550-3213(97)00115-6. arXiv: hep-th/9612131.

[30] Vadim Borokhov, Anton Kapustin, and Xin-kai Wu. "Topological disorder operators in three-dimensional conformal field theory". In: *JHEP* 11 (2002), p. 049. DOI: 10.1088/1126-6708/2002/11/049. arXiv: hep-th/0206054.

[31] Ofer Aharony et al. "Aspects of N=2 supersymmetric gauge theories in three-dimensions". In: *Nucl. Phys. B* 499 (1997), pp. 67–99. DOI: 10.1016/S0550-3213(97)00323-4. arXiv: hep-th/9703110.

[32] Mathew Bullimore, Tudor Dimofte, and Davide Gaiotto. "The Coulomb Branch of 3d $\mathcal{N} = 4$ Theories". In: *Commun. Math. Phys.* 354.2 (2017), pp. 671–751. DOI: 10.1007/s00220-017-2903-0. arXiv: 1503.04817 [hep-th].

[33] Stefano Cremonesi, Amihay Hanany, and Alberto Zaffaroni. "Monopole operators and Hilbert series of Coulomb branches of $3d$ $\mathcal{N} = 4$ gauge theories". In: *JHEP* 01 (2014), p. 005. DOI: 10.1007/JHEP01(2014)005. arXiv: 1309.2657 [hep-th].

[34] Hiraku Nakajima. "Instantons on ALE spaces, quiver varieties, and Kac-Moody algebras". In: *Duke Math. J.* 76.2 (1994), pp. 365–416. DOI: 10.1215/S0012-7094-94-07613-8.

[35] Francesco Benini, Sergio Benvenuti, and Sara Pasquetti. "SUSY monopole potentials in 2+1 dimensions". In: *JHEP* 08 (2017), p. 086. DOI: 10.1007/JHEP08(2017)086. arXiv: 1703.08460 [hep-th].

[36] Davide Gaiotto and Edward Witten. "S-Duality of Boundary Conditions In N=4 Super Yang-Mills Theory". In: *Adv. Theor. Math. Phys.* 13.3 (2009), pp. 721–896. DOI: 10.4310/ATMP.2009.v13.n3.a5. arXiv: 0807.3720 [hep-th].

[37] Andres Collinucci et al. "T-branes through 3d mirror symmetry". In: *JHEP* 07 (2016), p. 093. DOI: 10.1007/JHEP07(2016)093. arXiv: 1603.00062 [hep-th].

[38] Nathan Seiberg. "Five-dimensional SUSY field theories, nontrivial fixed points and string dynamics". In: *Phys. Lett. B* 388 (1996), pp. 753–760. DOI: 10.1016/S0370-2693(96)01215-4. arXiv: hep-th/9608111.

[39] Kenneth A. Intriligator, David R. Morrison, and Nathan Seiberg. "Five-dimensional supersymmetric gauge theories and degenerations of Calabi-Yau spaces". In: *Nucl. Phys. B* 497 (1997), pp. 56–100. DOI: 10.1016/S0550-3213(97)00279-4. arXiv: hep-th/9702198.

[40] Patrick Jefferson et al. "Towards Classification of 5d SCFTs: Single Gauge Node". In: (May 2017). arXiv: 1705.05836 [hep-th].

[41] Patrick Jefferson et al. "On Geometric Classification of 5d SCFTs". In: *JHEP* 04 (2018), p. 103. DOI: 10.1007/JHEP04(2018)103. arXiv: 1801.04036 [hep-th].

[42] Lakshya Bhardwaj. "On the classification of 5d SCFTs". In: *JHEP* 09 (2020), p. 007. DOI: 10.1007/JHEP09(2020)007. arXiv: 1909.09635 [hep-th].

[43] Lakshya Bhardwaj and Patrick Jefferson. "Classifying 5d SCFTs via 6d SCFTs: Arbitrary rank". In: *JHEP* 10 (2019), p. 282. DOI: 10.1007/JHEP10(2019)282. arXiv: 1811.10616 [hep-th].

[44] Dan Xie and Shing-Tung Yau. "Three dimensional canonical singularity and five dimensional $\mathcal{N}$ = 1 SCFT". In: *JHEP* 06 (2017), p. 134. DOI: 10.1007/JHEP06(2017)134. arXiv: 1704.00799 [hep-th].

[45] Cyril Closset, Sakura Schafer-Nameki, and Yi-Nan Wang. "Coulomb and Higgs Branches from Canonical Singularities: Part 0". In: *JHEP* 02 (2021), p. 003. DOI: 10.1007/JHEP02(2021)003. arXiv: 2007.15600 [hep-th].

[46] Jiahua Tian and Yi-Nan Wang. "5D and 6D SCFTs from $\mathbb{C}^3$ orbifolds". In: *SciPost Phys.* 12 (2022), p. 127. DOI: 10.21468/SciPostPhys.12.4.127. arXiv: 2110.15129 [hep-th].

[47] Fabio Apruzzi, Ling Lin, and Christoph Mayrhofer. "Phases of 5d SCFTs from M-/F-theory on Non-Flat Fibrations". In: *JHEP* 05 (2019), p. 187. DOI: 10.1007/JHEP05(2019)187. arXiv: 1811.12400 [hep-th].

[48] Lakshya Bhardwaj and Patrick Jefferson. "Classifying $5d$ SCFTs via $6d$ SCFTs: Rank one". In: *JHEP* 07 (2019). [Addendum: JHEP 01, 153 (2020)], p. 178. DOI: 10.1007/JHEP07(2019)178. arXiv: 1809.01650 [hep-th].

[49] Lakshya Bhardwaj. "Do all 5d SCFTs descend from 6d SCFTs?" In: *JHEP* 04 (2021), p. 085. DOI: 10.1007/JHEP04(2021)085. arXiv: 1912.00025 [hep-th].

[50] Lakshya Bhardwaj and Gabi Zafrir. "Classification of 5d $\mathcal{N}$ = 1 gauge theories". In: *JHEP* 12 (2020), p. 099. DOI: 10.1007/JHEP12(2020)099. arXiv: 2003.04333 [hep-th].

[51] Cyril Closset et al. "5d and 4d SCFTs: Canonical Singularities, Trinions and S-Dualities". In: *JHEP* 05 (2021), p. 274. DOI: 10.1007/JHEP05(2021)274. arXiv: 2012.12827 [hep-th].

[52] Hirotaka Hayashi et al. "More on 5d SCFTs from M-theory". In: *JHEP* 1810 (2018), p. 142. arXiv: 1805.09080 [hep-th].

[53] Miles Reid et al. "Minimal models of canonical 3-folds". In: *Adv. Stud. Pure Math* 1 (1983), pp. 131–180.

[54] M. Wemyss. "Lectures on Noncommutative Resolutions". In: (2014). arXiv: 1210.2564 [math.RT]. URL: https://arxiv.org/abs/1210.2564.

[55] Gwyn Bellamy et al. *Noncommutative Algebraic Geometry*. Mathematical Sciences Research Institute Publications. Cambridge University Press, 2016.

[56] Marina Moleti and Roberto Valandro. "Universal flops of length 1 and 2 from D2-branes at surface singularities". In: *JHEP* 01 (2025), p. 013. DOI: 10.1007/JHEP01(2025)013. arXiv: 2410.16767 [hep-th].

[57] Andrés Collinucci, Marina Moleti, and Roberto Valandro. "D2-branes at non-toric three-fold singularities with small resolution". Work in progress.

[58] Andrés Collinucci et al. "Non-toric 5d SCFTs from Reid's Pagoda". In: (Dec. 2025). arXiv: 2512.18778 [hep-th].

[59] Michael B. Green and John H. Schwarz. "Anomaly Cancellation in Supersymmetric D=10 Gauge Theory and Superstring Theory". In: *Phys. Lett. B* 149 (1984), pp. 117–122. DOI: 10.1016/0370-2693(84)91565-X.

[60] P. Candelas et al. "Vacuum configurations for superstrings". In: *Nuclear Physics B* 258 (1985), pp. 46–74. ISSN: 0550-3213. DOI: https://doi.org/10.1016/0550-3213(85)90602-9. URL: https://www.sciencedirect.com/science/article/pii/0550321385906029.

[61] Joseph Polchinski. "Tasi lectures on D-branes". In: *Theoretical Advanced Study Institute in Elementary Particle Physics (TASI 96): Fields, Strings, and Duality*. Nov. 1996, pp. 293–356. arXiv: hep-th/9611050.

[62] Edward Witten. "String theory dynamics in various dimensions". In: *Nucl. Phys. B* 443 (1995), pp. 85–126. DOI: 10.1016/0550-3213(95)00158-O. arXiv: hep-th/9503124.

[63] Christopher M. Hull and Paul K. Townsend. "Unity of superstring dualities". In: *Nucl. Phys. B* 438 (1995), pp. 109–137. eprint: hep-th/9410167.

[64] Sheldon H. Katz, Albrecht Klemm, and Cumrun Vafa. "Geometric engineering of quantum field theories". In: *Nucl. Phys. B* 497 (1997), pp. 173–195. DOI: 10.1016/S0550-3213(97)00282-4. arXiv: hep-th/9609239.

[65] Steven S. Gubser. "TASI lectures: Special holonomy in string theory and M theory". In: *Theoretical Advanced Study Institute in Elementary Particle Physics (TASI 2001): Strings, Branes and EXTRA Dimensions*. Jan. 2002, pp. 197–233. arXiv: hep-th/0201114.

[66] Bobby Samir Acharya. "M theory, Joyce orbifolds and superYang-Mills". In: *Adv. Theor. Math. Phys.* 3 (1999), pp. 227–248. DOI: 10.4310/ATMP.1999.v3.n2.a3. arXiv: hep-th/9812205.

[67] M. Bershadsky, C. Vafa, and V. Sadov. "D strings on D manifolds". In: *Nucl. Phys. B* 463 (1996), pp. 398–414. DOI: 10.1016/0550-3213(96)00024-7. arXiv: hep-th/9510225.

[68] Andrew Strominger. "Massless black holes and conifolds in string theory". In: *Nucl. Phys. B* 451 (1995), pp. 96–108. DOI: 10.1016/0550-3213(95)00287-3. arXiv: hep-th/9504090.

[69] Lara B. Anderson, Jonathan J. Heckman, and Sheldon Katz. "T-Branes and Geometry". In: *JHEP* 05 (2014), p. 080. DOI: 10.1007/JHEP05(2014)080. arXiv: 1310.1931 [hep-th].

[70] Lara B. Anderson et al. "T-Branes at the Limits of Geometry". In: *JHEP* 10 (2017), p. 058. DOI: 10.1007/JHEP10(2017)058. arXiv: 1702.06137 [hep-th].

[71] Rodrigo Barbosa et al. "T-branes and G_2 backgrounds". In: *Phys. Rev. D* 101.2 (2020), p. 026015. DOI: 10.1103/PhysRevD.101.026015. arXiv: 1906.02212 [hep-th].

[72] Iosif Bena, Johan Blåbäck, and Raffaele Savelli. "T-branes and Matrix Models". In: *JHEP* 06 (2017), p. 009. DOI: 10.1007/JHEP06(2017)009. arXiv: 1703.06106 [hep-th].

[73] Iosif Bena et al. "The two faces of T-branes". In: *JHEP* 10 (2019), p. 150. DOI: 10.1007/JHEP10(2019)150. arXiv: 1905.03267 [hep-th].

[74] Federico Carta, Simone Giacomelli, and Raffaele Savelli. "SUSY enhancement from T-branes". In: *JHEP* 12 (2018), p. 127. DOI: 10.1007/JHEP12(2018)127. arXiv: 1809.04906 [hep-th].

[75] Chan-Chi Chiou et al. "T-branes and Yukawa Couplings". In: *JHEP* 05 (2011), p. 023. DOI: 10.1007/JHEP05(2011)023. arXiv: 1101.2455 [hep-th].

[76] Michele Cicoli, Fernando Quevedo, and Roberto Valandro. "De Sitter from T-branes". In: *JHEP* 03 (2016), p. 141. DOI: 10.1007/JHEP03(2016)141. arXiv: 1512.04558 [hep-th].

[77] Andres Collinucci, Simone Giacomelli, and Roberto Valandro. "T-branes, monopoles and S-duality". In: *JHEP* 10 (2017), p. 113. DOI: 10.1007/JHEP10(2017)113. arXiv: 1703.09238 [hep-th].

[78] Falk Hassler et al. "T-Branes, String Junctions, and 6D SCFTs". In: *Phys. Rev. D* 101.8 (2020), p. 086018. DOI: 10.1103/PhysRevD.101.086018. arXiv: 1907.11230 [hep-th].

[79] Fernando Marchesano and Sebastian Schwieger. "T-branes and α'-corrections". In: *JHEP* 11 (2016), p. 123. DOI: 10.1007/JHEP11(2016)123. arXiv: 1609.02799 [hep-th].

[80] Fernando Marchesano, Raffaele Savelli, and Sebastian Schwieger. "Compact T-branes". In: *JHEP* 09 (2017), p. 132. DOI: 10.1007/JHEP09(2017)132. arXiv: 1707.03797 [hep-th].

[81] Fernando Marchesano, Raffaele Savelli, and Sebastian Schwieger. "T-branes and defects". In: *JHEP* 04 (2019), p. 110. DOI: 10.1007/JHEP04(2019)110. arXiv: 1902.04108 [hep-th].

[82] Fernando Marchesano, Ruxandra Moraru, and Raffaele Savelli. "A vanishing theorem for T-branes". In: *JHEP* 11 (2020), p. 002. DOI: 10.1007/JHEP11(2020)002. arXiv: 2007.02960 [hep-th].

[83] Noppadol Mekareeya, Tom Rudelius, and Alessandro Tomasiello. "T-branes, Anomalies and Moduli Spaces in 6D SCFTs". In: *JHEP* 10 (2017), p. 158. DOI: 10.1007/JHEP10(2017)158. arXiv: 1612.06399 [hep-th].

[84] Tomas Gomez and Eric R. Sharpe. "D-branes and scheme theory". In: (Aug. 2000). arXiv: hep-th/0008150.

[85] Ron Donagi, S. Katz, and E. Sharpe. "Spectra of D-branes with higgs vevs". In: *Adv. Theor. Math. Phys.* 8.5 (2004), pp. 813–859. DOI: 10.4310/ATMP.2004.v8.n5.a3. arXiv: hep-th/0309270.

[86] Andres Collinucci and Raffaele Savelli. "T-branes as branes within branes". In: *JHEP* 09 (2015), p. 161. DOI: 10.1007/JHEP09(2015)161. arXiv: 1410.4178 [hep-th].

[87] Cyril Closset and Michele Del Zotto. "On 5d SCFTs and their BPS quivers. Part I: B-branes and brane tilings". In: (Dec. 2019). arXiv: 1912.13502 [hep-th].

[88] Igor R. Klebanov and Edward Witten. "Superconformal field theory on three-branes at a Calabi-Yau singularity". In: *Nucl. Phys. B* 536 (1998), pp. 199–218. DOI: 10.1016/S0550-3213(98)00654-3. arXiv: hep-th/9807080.

[89] F. Cachazo, K. Intriligator, and C. Vafa. "A Large N Duality via a Geometric Transition". In: *Nucl.Phys.B* 603 (2001), pp. 3–41. DOI: 10.1016/S0550-3213(01)00228-0. eprint: hep-th/0103067. URL: https://arxiv.org/pdf/hep-th/0103067.pdf.

[90] David R. Morrison and Nathan Seiberg. "Extremal transitions and five-dimensional supersymmetric field theories". In: *Nucl. Phys. B* 483 (1997), pp. 229–247. DOI: 10.1016/S0550-3213(96)00592-5. arXiv: hep-th/9609070.

[91] Cyril Closset, Sakura Schäfer-Nameki, and Yi-Nan Wang. "Coulomb and Higgs branches from canonical singularities. Part I. Hypersurfaces with smooth Calabi-Yau resolutions". In: *JHEP* 04 (2022), p. 061. DOI: 10.1007/JHEP04(2022)061. arXiv: 2111.13564 [hep-th].

[92] Michael R. Douglas, Brian R. Greene, and David R. Morrison. "Orbifold resolution by D-branes". In: *Nucl. Phys. B* 506 (1997), pp. 84–106. eprint: hep-th/9704151.

[93] Nathan Seiberg. "IR dynamics on branes and space-time geometry". In: *Phys. Lett. B* 384 (1996), pp. 81–85. DOI: 10.1016/0370-2693(96)00819-2. arXiv: hep-th/9606017.

[94] Davide Gaiotto and Edward Witten. "Supersymmetric Boundary Conditions in N=4 Super Yang-Mills Theory". In: *J. Statist. Phys.* 135 (2009), pp. 789–855. DOI: 10.1007/s10955-009-9687-3. arXiv: 0804.2902 [hep-th].

[95] Denis Bashkirov and Anton Kapustin. "Supersymmetry enhancement by monopole operators". In: *JHEP* 05 (2011), p. 015. DOI: 10.1007/JHEP05(2011)015. arXiv: 1007.4861 [hep-th].

[96] Andrea Sangiovanni and Roberto Valandro. "M-theory geometric engineering for rank-0 3d $\mathcal{N}$ = 2 theories". In: *JHEP* 03 (2025), p. 160. DOI: 10.1007/JHEP03(2025)160. arXiv: 2410.13943 [hep-th].

[97] Andrés Collinucci, Marco Fazzi, and Roberto Valandro. "Geometric engineering on flops of length two". In: *JHEP* 04 (2018), p. 090. DOI: 10.1007/JHEP04(2018)090. arXiv: 1802.00813 [hep-th].

[98] Mario De Marco and Shani Nadir Meynet. "Symmetries Beyond Branes: Geometric Engineering and Isometries". In: (Mar. 2025). arXiv: 2503.19022 [hep-th].

[99] Darius Dramburg, Shani Nadir Meynet, and Andrea Sangiovanni. "On the Orbifold origin of Higher Form Symmetries in Geometric Engineering". In: (Dec. 2025). arXiv: 2512.19797 [hep-th].

[100] Vivek Saxena. "Rank-two 5d SCFTs from M-theory at isolated toric singularities: a systematic study". In: *JHEP* 04 (2020), p. 198. DOI: 10.1007/JHEP04(2020)198. arXiv: 1911.09574 [hep-th].

[101] Amihay Hanany and Rak-Kyeong Seong. "Brane Tilings and Reflexive Polygons". In: *Fortsch. Phys.* 60 (2012), pp. 695–803. DOI: 10.1002/prop.201200008. arXiv: 1201.2614 [hep-th].

[102] Marieke van Beest et al. "(Symplectic) Leaves and (5d Higgs) Branches in the Poly(go)nesian Tropical Rain Forest". In: *JHEP* 11 (2020), p. 124. DOI: 10.1007/JHEP11(2020)124. arXiv: 2008.05577 [hep-th].

[103] Marieke Van Beest et al. "(5d RG-flow) Trees in the Tropical Rain Forest". In: *JHEP* 03 (2021), p. 241. DOI: 10.1007/JHEP03(2021)241. arXiv: 2011.07033 [hep-th].

[104] Martin Bender and Sergey Mozgovoy. *Crepant resolutions and brane tilings II: Tilting bundles*. 2009. arXiv: 0909.2013 [math.AG]. URL: https://arxiv.org/abs/0909.2013.

[105] Antoine Bourget et al. "Magnetic Quivers from Brane Webs with O5 Planes". In: *JHEP* 07 (2020), p. 204. DOI: 10.1007/JHEP07(2020)204. arXiv: 2004.04082 [hep-th].

[106] Cyril Closset, Michele Del Zotto, and Vivek Saxena. "Five-dimensional SCFTs and gauge theory phases: an M-theory/type IIA perspective". In: *SciPost Phys.* 6.5 (2019), p. 052. DOI: 10.21468/SciPostPhys.6.5.052. arXiv: 1812.10451 [hep-th].

[107] Tom Bridgeland, Alastair King, and Miles Reid. "The McKay correspondence as an equivalence of derived categories". In: *Journal of the American Mathematical Society* 14.3 (2001), pp. 535–554.

[108] {A. D.} King. "Moduli of representations of finite dimensional algebras". English. In: *Quarterly Journal of Mathematics* 45.4 (Dec. 1994), pp. 515–530. ISSN: 0033-5606. DOI: 10.1093/qmath/45.4.515.

[109] Tom Bridgeland, Fabrizio Del Monte, and Luca Giovenzana. "Invariant Stability Conditions on Certain Calabi-Yau Threefolds". In: (Dec. 2024). arXiv: 2412.08531 [math.AG].

[110] Fabrizio Del Monte and Pietro Longhi. "Quiver Symmetries and Wall-Crossing Invariance". In: *Commun. Math. Phys.* 398.1 (2023), pp. 89–132. DOI: 10.1007/s00220-022-04515-6. arXiv: 2107.14255 [hep-th].

[111] Fabrizio Del Monte. "BPS Spectra and Algebraic Solutions of Discrete Integrable Systems". In: *Commun. Math. Phys.* 405.6 (2024), p. 147. DOI: 10.1007/s00220-024-05016-4. arXiv: 2306.01626 [hep-th].

[112] Yang-Hui He. "On algebraic singularities, finite graphs and D-brane gauge theories: A string theoretic perspective". In: (). eprint: hep-th/0209230.

[113] Yang-Hui He. "Lectures on D-branes, gauge theories and Calabi-Yau singularities". In: (). eprint: hep-th/0408142.

[114] Paul S. Aspinwall, Brian R. Greene, and David R. Morrison. "Calabi-Yau moduli space, mirror manifolds and spacetime topology change in string theory". In: *Nucl. Phys. B* 416 (1994), pp. 414–480. eprint: hep-th/9309097.

[115] John McKay. "Graphs, singularities, and finite groups". In: *Finite Groups*. Vol. 37. Proc. Sympos. Pure Math. Amer. Math. Soc., 1980, pp. 183–186.

[116] Igor R. Klebanov and Matthew J. Strassler. "Supergravity and a confining dual". In: *JHEP* 08 (2000), p. 052. eprint: hep-th/0007191.

[117] Rajesh Gopakumar and Cumrun Vafa. "On the gauge theory / geometry correspondence". In: *Adv. Theor. Math. Phys.* 3 (1999). Ed. by Cumrun Vafa and S. T. Yau, pp. 1415–1443. DOI: 10.4310/ATMP.1999.v3.n5.a5. arXiv: hep-th/9811131.

[118] Philip Candelas and Xenia C. de la Ossa. "Comments on conifolds". In: *Nucl. Phys. B* 342 (1990), pp. 246–268.

[119] Philip Candelas, Paul S. Green, and Tristan Hübsch. "Rolling among Calabi-Yau vacua". In: *Nucl. Phys. B* 330 (1990), pp. 49–102.

[120] Brian R. Greene, David R. Morrison, and Andrew Strominger. "Black hole condensation and the unification of string vacua". In: *Nucl. Phys. B* 451 (1995), pp. 109–120. eprint: hep-th/9504145.

[121] Sheldon Katz and David R. Morrison. "Gorenstein Threefold Singularities with Small Resolutions via Invariant Theory for Weyl Groups". In: *J. Alg. Geom.* 1 (1992), pp. 449–530. eprint: alg-geom/9202002. URL: https://arxiv.org/pdf/alg-geom/9202002.pdf.

[122] János Kollár and Shigefumi Mori. *Birational Geometry of Algebraic Varieties*. Vol. 134. Cambridge Tracts in Mathematics. Cambridge University Press, 1998.

[123] Shigefumi Mori. "On 3-dimensional terminal singularities". In: *Nagoya Mathematical Journal* 98 (1985), 43–66. DOI: 10.1017/S0027763000021358.

[124] Michele Del Zotto et al. "Higher Symmetries of 5d Orbifold SCFTs". In: (Jan. 2022). arXiv: 2201.08372 [hep-th].

[125] H. Clemens, J. Kollár, and S. Mori. "Higher-dimensional complex geometry". In: *Astérisque* (1989).

[126] M. Reid. “Minimal models of canonical 3-folds”. In: *North-Holland, Amsterdam* (1983).

[127] H. Laufer. “On CP1 as an exceptional set”. In: *Ann. of Math. Stud. Vol. 100, Princeton Univ. Press, Princeton, NJ* (1981).

[128] Henry C. Pinkham. “Factorization of birational maps in dimension 3”. In: *Amer. Math. Soc., Providence, RI* 40 (1983), pp. 343–371.

[129] Gavin Brown and Michael Wemyss. “Gopakumar-Vafa invariants do not determine flops”. In: *Commun. Math. Phys.* 361.1 (2018), pp. 143–154. DOI: 10.1007/s00220-017-3038-z. arXiv: 1707.01150 [math.AG].

[130] Joseph Karmazyn. *The length classification of threefold flops via noncommutative algebras*. 2017. arXiv: 1709.02720 [math.AG]. URL: https://arxiv.org/abs/1709.02720.

[131] Joseph Karmazyn. “The length classification of threefold flops via noncommutative algebras”. In: *Advances in Mathematics* 343 (2019), pp. 393–447. ISSN: 0001-8708. DOI: https://doi.org/10.1016/j.aim.2018.11.023. URL: https://www.sciencedirect.com/science/article/pii/S0001870818304870.

[132] Will Donovan and Michael Wemyss. “Noncommutative deformations and flops”. In: *Duke Mathematical Journal* 165.8 (June 2016). ISSN: 0012-7094. DOI: 10.1215/00127094-3449887. URL: http://dx.doi.org/10.1215/00127094-3449887.

[133] David R. Morrison and Daniel S. Park. “F-Theory and the Mordell-Weil Group of Elliptically-Fibered Calabi-Yau Threefolds”. In: *JHEP* 10 (2012), p. 128. DOI: 10.1007/JHEP10(2012)128. arXiv: 1208.2695 [hep-th].

[134] Kazunobu Maruyoshi and Jaewon Song. “Enhancement of Supersymmetry via Renormalization Group Flow and the Superconformal Index”. In: *Phys. Rev. Lett.* 118.15 (2017), p. 151602. DOI: 10.1103/PhysRevLett.118.151602. arXiv: 1606.05632 [hep-th].

[135] Kazunobu Maruyoshi and Jaewon Song. “$\mathcal{N} = 1$ deformations and RG flows of $\mathcal{N} = 2$ SCFTs”. In: *JHEP* 02 (2017), p. 075. DOI: 10.1007/JHEP02(2017)075. arXiv: 1607.04281 [hep-th].

[136] D. H. Collingwood and W. M. McGovern. “Nilpotent Orbits In Semisimple Lie Algebra: An Introduction”. In: *Chapman and Hall/CRC* (1993).

[137] Amihay Hanany and Kristian D. Kennaway. “Dimer models and toric diagrams”. In: *unpublished* (2005). arXiv: hep-th/0503149.

[138] Bo Feng, Amihay Hanany, and Yang-Hui He. "D-brane gauge theories from toric singularities and toric duality". In: *Nucl. Phys. B* 595 (2001), pp. 165–200. DOI: 10.1016/S0550-3213(00)00699-4. arXiv: hep-th/0003085.

[139] Sergio Benvenuti et al. "Planar Abelian mirror duals of N=2 SQCD3". In: *Phys. Rev. D* 112.10 (2025), p. L101703. DOI: 10.1103/k5b3-lrnz. arXiv: 2411.05620 [hep-th].

[140] Sergio Benvenuti et al. "A chiral-planar dualization algorithm for 3d $\mathcal{N}$ = 2 Chern-Simons-matter theories". In: *JHEP* 10 (2025), p. 211. DOI: 10.1007/JHEP10(2025)211. arXiv: 2505.02913 [hep-th].

[141] Edward Witten. "Branes and the dynamics of QCD". In: *Nucl. Phys. B* 507 (1997), pp. 658–690. DOI: 10.1016/S0550-3213(97)00648-2. arXiv: hep-th/9706109.

[142] Shamit Kachru et al. "Open string instantons and superpotentials". In: *Phys. Rev. D* 62 (2000), p. 026001. DOI: 10.1103/PhysRevD.62.026001. arXiv: hep-th/9912151.

[143] Mina Aganagic and Cumrun Vafa. "Mirror symmetry, D-branes and counting holomorphic discs". In: (Dec. 2000). arXiv: hep-th/0012041.

[144] Lakshya Bhardwaj et al. "Twisted Circle Compactifications of 6d SCFTs". In: *JHEP* 12 (2020), p. 151. DOI: 10.1007/JHEP12(2020)151. arXiv: 1909.11666 [hep-th].

[145] Lakshya Bhardwaj. "Flavor symmetry of 5d SCFTs. Part I. General setup". In: *JHEP* 09 (2021), p. 186. DOI: 10.1007/JHEP09(2021)186. arXiv: 2010.13230 [hep-th].

[146] Sergio Cecotti and Cumrun Vafa. "Classification of complete N=2 supersymmetric theories in 4 dimensions". In: (Mar. 2011). arXiv: 1103.5832 [hep-th].

[147] Murad Alim et al. "BPS Quivers and Spectra of Complete N=2 Quantum Field Theories". In: *Commun. Math. Phys.* 323 (2013), pp. 1185–1227. DOI: 10.1007/s00220-013-1789-8. arXiv: 1109.4941 [hep-th].

[148] Miles Reid. "Minimal Models of Canonical 3-Folds". In: *Algebraic Varieties and Analytic Varieties*. Ed. by Shigeru Iitaka. Vol. 1. Advanced Studies in Pure Mathematics. Proceedings of the conference "Algebraic Varieties and Analytic Varieties" (Tokyo, 1981). Tokyo & Amsterdam: Kinokuniya / North-Holland, 1983, pp. 131–180. DOI: 10.2969/aspm/00110131. URL: https://projecteuclid.org/10.2969/aspm/00110131.

[149] Sergei Gukov, Cumrun Vafa, and Edward Witten. "CFT's from Calabi-Yau four folds". In: *Nucl. Phys. B* 584 (2000). [Erratum: Nucl.Phys.B 608, 477–478 (2001)], pp. 69–108. DOI: 10.1016/S0550-3213(00)00373-4. arXiv: hep-th/9906070.

[150] Alfred D. Shapere and Cumrun Vafa. "BPS structure of Argyres-Douglas superconformal theories". In: (Oct. 1999). arXiv: hep-th/9910182.

[151] Bobby Samir Acharya. "Confinement in Five Dimensions". In: (July 2024). arXiv: 2407.03171 [hep-th].

[152] Alastair Craw and Gregory G Smith. "Projective toric varieties as fine moduli spaces of quiver representations". In: *American journal of mathematics* 130.6 (2008), pp. 1509–1534.

[153] Edward Witten. "Phase transitions in M theory and F theory". In: *Nucl. Phys. B* 471 (1996), pp. 195–216. DOI: 10.1016/0550-3213(96)00212-X. arXiv: hep-th/9603150.

[154] Mario De Marco et al. "Conformal matter". In: *JHEP* 05 (2024). [Erratum: JHEP 08, 067 (2024)], p. 306. DOI: 10.1007/JHEP05(2024)306. arXiv: 2311.04984 [hep-th].

[155] Giulio Bonelli, Fabrizio Del Monte, and Alessandro Tanzini. "BPS Quivers of Five-Dimensional SCFTs, Topological Strings and q-Painlevé Equations". In: *Annales Henri Poincare* 22.8 (2021), pp. 2721–2773. DOI: 10.1007/s00023-021-01034-3. arXiv: 2007.11596 [hep-th].

[156] Sergio Cecotti and Cumrun Vafa. "BPS Wall Crossing and Topological Strings". In: *Commun. Math. Phys.* (2010). arXiv: 0910.2615 [hep-th].

[157] Davide Gaiotto, Gregory W. Moore, and Andrew Neitzke. "Wall-Crossing, Hitchin Systems, and the WKB Approximation". In: *Adv. Math.* (2013). arXiv: 0907.3987 [hep-th].

[158] Sibasish Banerjee, Pietro Longhi, and Mauricio Romo. "Exploring 5d BPS Spectra with Exponential Networks". In: *Annales Henri Poincare* 20.12 (2019), pp. 4055–4162. DOI: 10.1007/s00023-019-00851-x. arXiv: 1811.02875 [hep-th].

[159] Maxim Kontsevich and Yan Soibelman. "Stability structures, motivic Donaldson-Thomas invariants and cluster transformations". In: (Nov. 2008). arXiv: 0811.2435 [math.AG].

[160] Daniel L. Jafferis and Gregory W. Moore. "Wall crossing in local Calabi Yau manifolds". In: (Oct. 2008). arXiv: 0810.4909 [hep-th].

[161] Sergio Cecotti and Michele Del Zotto. "Galois covers of $\mathcal{N} = 2$ BPS spectra and quantum monodromy". In: *Adv. Theor. Math. Phys.* 20 (2016), pp. 1227–1336. DOI: 10.4310/ATMP.2016.v20.n6.a1. arXiv: 1503.07485 [hep-th].

[162] Piotr Kucharski et al. "BPS states, knots and quivers". In: *Phys. Rev. D* 96.12 (2017), p. 121902. DOI: 10.1103/PhysRevD.96.121902. arXiv: 1707.02991 [hep-th].

[163] Davide Gaiotto, Gregory W. Moore, and Andrew Neitzke. "Framed BPS States". In: *Adv. Theor. Math. Phys.* 17.2 (2013), pp. 241–397. DOI: 10.4310/ATMP.2013.v17.n2.a1. arXiv: 1006.0146 [hep-th].

[164] Antoine Bourget et al. "The Higgs mechanism — Hasse diagrams for symplectic singularities". In: *JHEP* 01 (2020), p. 157. DOI: 10.1007/JHEP01(2020)157. arXiv: 1908.04245 [hep-th].

[165] Santiago Cabrera and Amihay Hanany. "Quiver Subtractions". In: *JHEP* 09 (2018), p. 008. DOI: 10.1007/JHEP09(2018)008. arXiv: 1803.11205 [hep-th].

[166] Santiago Cabrera, Amihay Hanany, and Marcus Sperling. "Magnetic quivers, Higgs branches, and 6d N=(1,0) theories". In: *JHEP* 06 (2019). [Erratum: JHEP 07, 137 (2019)], p. 071. DOI: 10.1007/JHEP06(2019)071. arXiv: 1904.12293 [hep-th].

[167] Antoine Bourget et al. "Brane Webs and Magnetic Quivers for SQCD". In: *JHEP* 03 (2020), p. 176. DOI: 10.1007/JHEP03(2020)176. arXiv: 1909.00667 [hep-th].

[168] Antoine Bourget et al. "Magnetic quivers for rank 1 theories". In: *JHEP* 09 (2020), p. 189. DOI: 10.1007/JHEP09(2020)189. arXiv: 2006.16994 [hep-th].

[169] Antoine Bourget et al. "S-fold magnetic quivers". In: *JHEP* 02 (2021), p. 054. DOI: 10.1007/JHEP02(2021)054. arXiv: 2010.05889 [hep-th].

[170] Antoine Bourget et al. "Branes, Quivers, and the Affine Grassmannian". In: *Adv. Stud. Pure Math.* 88 (2023), pp. 331–435. DOI: 10.2969/aspm/08810331. arXiv: 2102.06190 [hep-th].

[171] Antoine Bourget, Marcus Sperling, and Zhenghao Zhong. "Higgs branch RG flows via decay and fission". In: *Phys. Rev. D* 109.12 (2024), p. 126013. DOI: 10.1103/PhysRevD.109.126013. arXiv: 2401.08757 [hep-th].

[172] Fabio Apruzzi et al. "Fibers add Flavor, Part I: Classification of 5d SCFTs, Flavor Symmetries and BPS States". In: *JHEP* 11 (2019), p. 068. DOI: 10.1007/JHEP11(2019)068. arXiv: 1907.05404 [hep-th].

[173] Craig Lawrie, Sakura Schafer-Nameki, and Jin-Mann Wong. "F-theory and All Things Rational: Surveying U(1) Symmetries with Rational Sections". In: *JHEP* 09 (2015), p. 144. DOI: 10.1007/JHEP09(2015)144. arXiv: 1504.05593 [hep-th].

[174] Hirotaka Hayashi et al. "Box Graphs and Singular Fibers". In: *JHEP* 05 (2014), p. 048. DOI: 10.1007/JHEP05(2014)048. arXiv: 1402.2653 [hep-th].

[175] Michel Van den Bergh. “Non-commutative crepant resolutions”. In: *The Legacy of Niels Henrik Abel: The Abel Bicentennial, Oslo, 2002*. Springer, 2004, pp. 749–770.

[176] Michel Van den Bergh. *Non-commutative crepant resolutions*. 2009. arXiv: math/0211064 [math.RA]. URL: https://arxiv.org/abs/math/0211064.

[177] Robin Hartshorne. *Algebraic Geometry*. 1st ed. Vol. 52. Graduate Texts in Mathematics. New York, NY: Springer, 1977. ISBN: 978-0-387-90244-9. DOI: 10.1007/978-1-4757-3849-0.

[178] Michael R. Douglas, Bartomeu Fiol, and Christian Romelsberger. “The Spectrum of BPS branes on a noncompact Calabi-Yau”. In: *JHEP* 09 (2005), p. 057. DOI: 10.1088/1126-6708/2005/09/057. arXiv: hep-th/0003263.

[179] Hannah Dell. “Stability conditions on free abelian quotients”. In: *Épijournal de Géométrie Algébrique* 9 (2025).

[180] M. Gross and R. Pandharipande. *Quivers, curves, and the tropical vertex*. 2009. arXiv: 0909.5153 [math.AG]. URL: https://arxiv.org/abs/0909.5153.